The Dissertation Committee for Meghal Kanaiyalal Gandhi Certifies that this is the approved version of the following dissertation:

Genetic interactors of the Cdc42 GTPase effectors Gic1 and Gic2: their identification and functions in budding yeast cell polarity

Committee:

Clarence S. M. Chan, Supervisor

Makkuni Jayaram

Arlen Johnson

Arturo De Lozanne

Vishwanath Iyer

Genetic interactors of the Cdc42 GTPase effectors Gic1 and Gic2: their identification and functions in budding yeast cell polarity

by

Meghal Kanaiyalal Gandhi, B.S., M.S.

Dissertation

Presented to the Faculty of the Graduate School of

The University of Texas at Austin

in Partial Fulfillment

of the Requirements

for the Degree of

Doctor of Philosophy

The University of Texas at Austin

August, 2004

Dedication

To my parents

Acknowledgements

This dissertation has been an enlightening journey, both professionally and personally. I take this opportunity to thank all who have contributed on the way. I express my gratitude to Dr. Clarence Chan, my advisor, for introducing me to the 'awesome power of yeast genetics'. I am positive that the critical and meticulous scientific training I have received from him over these years will take me a long way in the future. I sincerely appreciate my dissertation committee members Dr. Makkuni Jayaram, Dr. Arlen Johnson, Dr. Arturo De Lozanne and Dr. Vishwanath Iyer for their helpful input and encouragement. I also thank Dr. Rasika Harshey for her incredible support as a graduate advisor.

I acknowledge all members of the Jayaram lab, former and present, for their ever welcoming and friendly attitude. In particular, I thank Shailja for her moral support throughout these years, Velu for teaching me to look at the positive aspect of every negative experience and Shwetal for being extremely helpful and encouraging, always. I appreciate Jungseog, John, Changwon, Rashmi, Jun and Patrick for their friendship. I also thank Ruth, Kavita and Shital for lending me their ears and can't appreciate enough my best friends Sanjay and Sneha for being there for me. Finally, I thank my mom and brother Jatin for teaching me the importance of perseverance and ambition in life and appreciate my sister-in-law Nita and nieces Rajvee and Harshvee for all their love.

Genetic interactors of the Cdc42 GTPase effectors Gic1 and Gic2: their identification and functions in budding yeast cell polarity

Publication No._____

Meghal Kanaiyalal Gandhi, Ph.D.
The University of Texas at Austin, 2004

Supervisor: Clarence S. M. Chan

Gic1 and Gic2 are structurally and functionally related effectors of the evolutionarily conserved Cdc42 GTPase in *Saccharomyces cerevisiae*. Like many other effectors of Cdc42, Gic1 and Gic2 function in the process of polarized cell growth. In the absence of both Gic1 and Gic2, yeast cells exhibit depolarized actin cytoskeleton and polarized growth defects at elevated temperatures. To obtain further insight into the biological role of Gic1 and Gic2, genetic approaches were used to identify functionally interacting partners of these proteins.

A screen for multi-copy suppressors of the temperature-sensitivity of *gic1 gic2* cells identified many genes (including *AXL2*, *BNI1*, *CLN2*, *MSB1*, *MSB2*, *RSR1* and *STE20*) that have known roles in polarized cell growth. In addition, two pairs of structurally related genes - *VHS2* and *MLF3*, *MGC1* and *TOS2* - with no previously reported functions were also identified. Functional characterization of *VHS2* and *MLF3* revealed their role in a pathway that affects

the actin cytoskeleton organization and cell wall integrity. This pathway is functionally redundant to that mediated by *GIC1* and *GIC2*. Functional characterization of *MGC1* and *TOS2* indicated that these genes function in the process of polarized growth, particularly in the process of cytokinesis.

A genome-wide Synthetic Genetic Analysis identified more than 30 non-essential genes as those whose function overlaps with that of *GIC1* and *GIC2*. Mutation in each of these genes exacerbates the growth defect of *gic1 gic2* cells. As expected, some of these genes are involved in polarity-related functions, such as actin cytoskeleton organization, bud-site selection and cell wall biosynthesis. Others participate in a variety of biological processes, including organelle biogenesis, secretion and vesicular transport. The latter finding suggests that *GIC1* and *GIC2* may have function outside the scope of actin cytoskeleton organization.

Taken together, the work presented here has uncovered the function of four previously uncharacterized genes in polarized cell growth. It has also provided hints to additional potential functions of *GIC1* and *GIC2*. Further exploration of these functions might provide important links between Cdc42 signaling and cellular processes such as organelle biogenesis, secretion and vesicular transport, all of which need to be executed coordinately during polarized cell growth.

Table of Contents

List of Tables

List of Figures

CHAPTER 1

Introduction

1.1 POLARITY AS A UNIVERSAL CELLULAR TRAIT

Cell polarity is defined as an asymmetry in cell shape, protein distributions and cell functions. The establishment of cell polarity is an important component of the overall process of cellular morphogenesis and is fundamental to differentiation and diversity of functions in most, if not all cells (Drubin and Nelson, 1996; Johnson, 1999; Nelson, 2003). Single cell organisms such as bacteria are often highly polarized, exhibiting specialized structures at or near the ends of the cell. Among such structures are actin-organizing centers, which mediate the movement of certain pathogenic bacteria (e.g., *Shigella* and *Listeria*) within the cytoplasm of an animal host cell; organized array of membrane receptors, which govern the chemosensory behavior in swimming bacteria such as *E. coli*; and asymmetrically positioned septa, which generate specialized progeny in differentiating bacteria, as seen in the sporulating *B. subtilis* (Shapiro et al., 2002). Unicellular eukaryotes such as budding yeast *Saccharomyces cerevisiae* and fission yeast *Schizosaccharomyces pombe* also undergo well-defined programs of polarized growth during their cell division cycle (Chang and Peter, 2003). In multicellular eukaryotes, polarity is established to encompass many aspects of cellular behavior (e.g., in a *Caenorhabditis elegans* zygote to define the anterior-posterior axis; in a *Drosophila melanogaster* oocyte to localize specific mRNAs and proteins during early stages of oogenesis (Wodarz, 2002); and in mammalian epithelial cells to generate the apical/basolateral asymmetry (Etienne-Manneville and Hall, 2002)).

1.2 EVENTS LEADING TO POLARIZATION ARE CONSERVED

Although polarity is portrayed in a wide variety of cell shape and functions amongst various organisms, the core mechanism involved in its establishment appears to be evolutionarily conserved in eukaryotes. The process of polarization is conceptualized as a hierarchy of sequential events. Feedback regulation at each step coordinates and reinforces the proper ordering of events, resulting in the maintenance of cell polarity (Drubin and Nelson, 1996).

The first step in the process of polarization involves breaking the symmetry of cells that are otherwise isotropic, and selection of a site on the cell surface in order to define an axis of polarization (e.g., mother-daughter axis in yeast cells and the apicobasal axis in epithelial cells (Nelson, 2003)). This step typically occurs in response to an internal spatial cue, such as the point of cytokinesis in budding and fission yeasts, or is triggered by an external stimuli, such as entry of a sperm into an egg or cell (-cell) adhesion in worm, fly and mammalian epithelial cells (Macara, 2004; Nelson, 2003). Recent evidence, however, suggests that a polarized pattern can emerge spontaneously even in the absence of an asymmetric cue in initially symmetric but unstable systems (Wedlich-Soldner et al., 2003). Ensuing this, the second step in the process of polarization is marked by the deposition of 'landmark' proteins on the cell surface. In the third step in polarization, these landmark proteins recruit a set of small GTPases to their vicinity. These GTPases are subsequently activated to initiate and maintain localized assembly of modular protein scaffolds that in turn direct the assembly and orientation of the cytoskeleton and stabilize it so as to enable the cell to assume an asymmetric shape (Nelson, 2003). Cellular polarization, however, can happen also at the level of signaling molecules, without any detectable change in the morphology of the cell (Sohrmann and Peter, 2003).

In yeast, polarized growth and organelle segregation are mediated by the actin cytoskeleton whereas in larger eukaryotic cells, it involves the cooperation between both the actin- and microtubule-based cytoskeletons (Bretscher, 2003).

1.3 YEAST AS A MODEL SYSTEM TO UNDERSTAND POLARIZED MORPHOGENESIS

Yeast and mammalian cells are separated by large phylogenetic distances (Drubin and Nelson, 1996). Yet, many features of polarized growth between the two cell-types are highly similar, including regulation by both intrinsic and extrinsic cues, involvement of conserved molecules like the Cdc42 GTPase, and asymmetric rearrangement of the cytoskeleton at its centerpiece (Chant, 1999). In light of such similarity, both budding and fission yeast cells have been extensively studied to understand how cells generate cell polarity and couple it to a specific function, namely cell cycle and cell division. These systems are simple because yeast cells are single cell organisms and they are well understood because of their genetic tractability (Nelson, 2003). The research described in this thesis has exploited the budding yeast system to elucidate functions and interactions of several proteins involved in polarized morphogenesis. In this introductory chapter, I will focus on the present state of knowledge on how polarized growth is initiated and maintained during budding to coordinate with cell cycle progression in *S. cerevisiae*. This review will provide background for the experiments detailed in the subsequent chapters and the context for the interpretation of my results.

1.4 CELL POLARITY IN YEAST

Laboratory *S. cerevisiae* strains typically exist as either *MATa* or *MATα* haploid cells or *MATa/α* diploid cells. They demonstrate several forms of polarized growth (Madden and Snyder, 1998; Figure 1.1). In the presence of ample nutrients, they grow by budding, where the position of the bud ultimately

determines the plane of cell division (Chant and Pringle, 1995). However, when access to specific nutrients such as nitrogen is decreased, a second type of polarized growth occurs whereby cells elongate, bud primarily from one pole of the cell and thus form chains of connected cells that can spread across a substrate and invade a solid medium. This form of polarized growth is called pseudohyphal growth in *a*/α diploids (Gimeno et al., 1992) and invasive growth in haploids (Roberts and Fink, 1994).

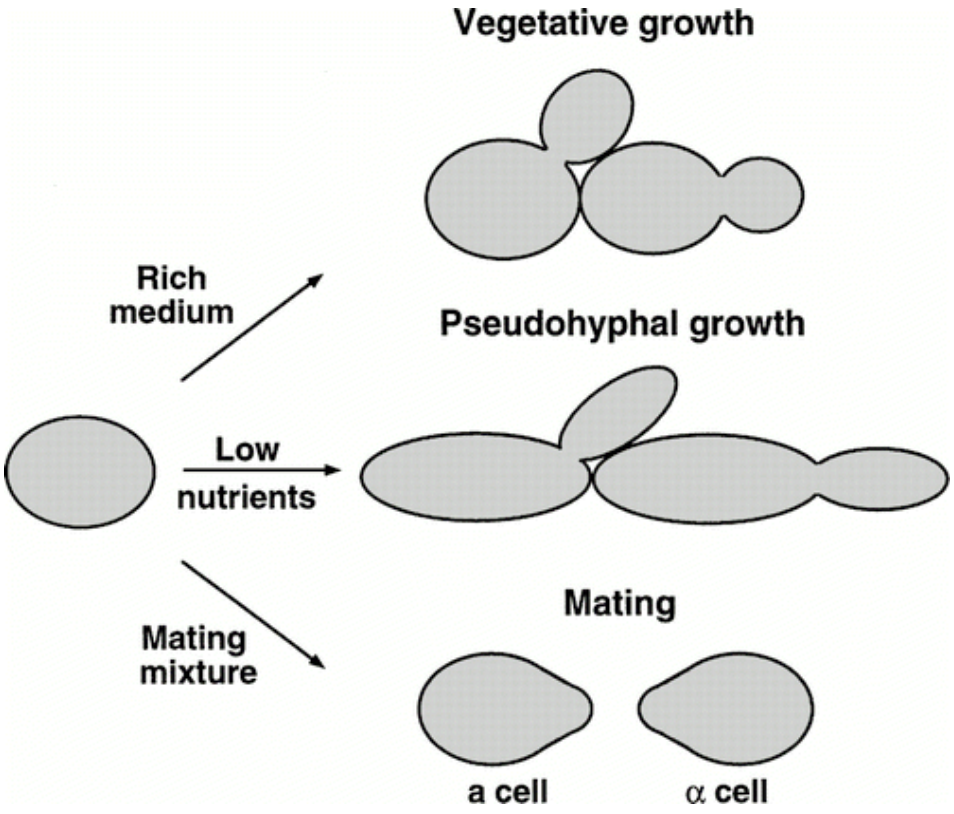

Figure 1.1 Three forms of polarized cell growth in *S. cerevisiae*. Cells grown in a rich medium are round (haploid) or oval (diploid) and have defined budding patterns. When exposed to a low-nutrient medium, cells elongate and bud from the distal end to form pseudohyphae. Haploid cells exposed to pheromone from cells of the opposite mating-type arrest in G1 and extend a projection toward their mating partner. This figure originally appeared in a review article by Madden and Snyder (1998).

A third form of polarized growth in haploid yeast cells occurs during the mating response to form a mating projection, which is often referred to as a 'shmoo' (Cross et al., 1988).

Regardless of the form in which polarized growth is manifested, the molecular framework underlying the polarized growth consists of two steps: First, choosing the direction of polarization and second, building an axis of polarization in the chosen direction. These two steps unfold in a temporal sequence and can be distinguished genetically (Chant, 1999).

Choosing a direction of polarization

Budding cells use intrinsic spatial landmarks from the previous cell division to select a new bud-site. The pattern of bud-site selection is determined by the mating-type of the cell (Chant and Pringle, 1995; Figure 1.2). Haploid *MATa* and *MATα* cells exhibit an axial budding pattern, where a new bud-site is constructed adjacent to the previous bud-site. Such a pattern is possible due to the function of cortical tag proteins such as Bud3, Bud4, Bud10/Axl2 and Axl1, which provide a landmark for axial bud-site selection (Chant et al., 1995; Fujita et al., 1994; Roemer et al., 1996; Sanders and Herskowitz, 1996). Diploid *MATa/α* cells, in contrast, exhibit a bipolar bud-site selection pattern, where the new bud is formed either adjacent or opposite to the previous bud-site. This pattern is regulated by the cortical tag proteins Bud8 and Bud9 (Chant and Pringle, 1995). Although both *bud8* and *bud9* mutant diploids exhibit unipolar budding, *bud8* mutant buds almost exclusively at the proximal pole, whereas *bud9* mutant buds almost exclusively at the distal pole (Zahner et al., 1996). In the absence of appropriate cortical cues, haploid cells display a bipolar budding pattern, suggesting that bipolar sites are used by default and haploid cells have a mechanism to preferentially select axial sites (Madden and Snyder, 1998).

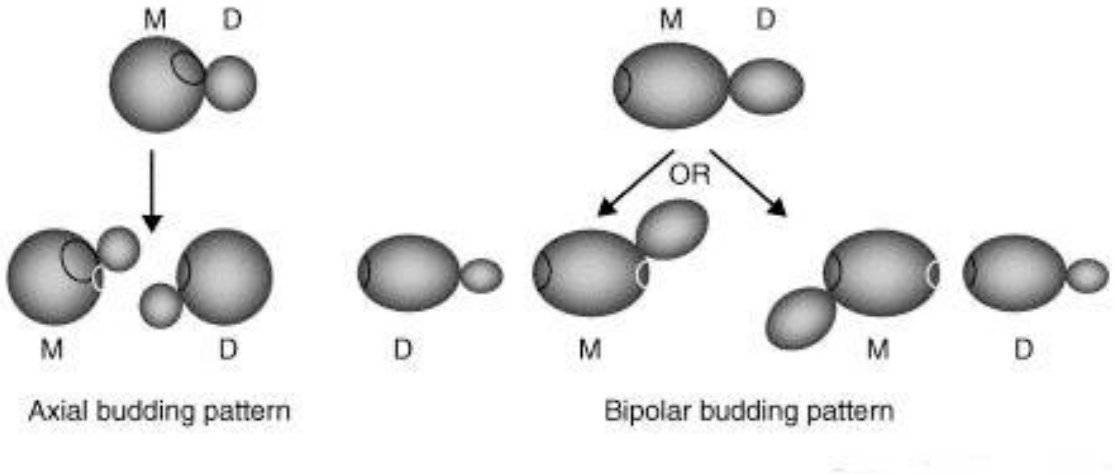

Figure 1.2 Axial and bipolar budding patterns in yeast cells. The scar marking the place where the cell was initially attached to its mother (M) cell is called the birth scar (curved black line), whereas smaller scars that originated by cytokinesis of the daughter (D) cells are named bud scars (curved white lines). Examination of bud and/or birth scars by calcofluor white staining reveals the budding pattern. The axial budding seen typically in haploid cells is characterized by budding adjacent to the birth scar in the daughter cell and adjacent to the bud scar in the mother cell. Diploid cells exhibit bipolar budding in which daughter cells usually bud distally (that is, at the pole opposite to the birth scar), and the mother cell buds at either pole. This figure appeared in a review article by Casamayor and Snyder (2002).

Placement of cortical cues for the budding patterns described above is dependent on one of the two cytoskeletal proteins, septin and actin. Septins are cytoskeletal proteins that are required for cytokinesis (described in detail later). They are arranged in a ring at the bud neck and are important for the localization of the Bud3 and Bud4 proteins and thus, for axial bud-site selection (Flescher et al., 1993). Partial loss-of-function mutations in septins can cause defects in the axial budding of *MATa* or *MATα* cells. Actin, on the other hand, is important for generation of the bipolar budding pattern (Drubin and Nelson, 1996). Mutations in many genes (e.g., *ACT1*, *AIP3/BUD6*, *BNI1*, *PEA2*, *PHO85, RVS161*, *RVS167*, *SAC6*, *SEC3*, *SEC4*, *SEC9, SPA2*, and *VRP1*) that affect the actin cytoskeleton or the secretory pathways shift the bipolar pattern to a random pattern (Chant, 1999).

Contrary to the intrinsic cue that guides polarity during budding, external factors such as gradients of mating pheromones determine the direction of polarization during mating (Chant, 1999).

Building an axis of polarization

Following the integration of spatial cue from the bud-site selection machinery, the cell builds an axis of polarization that is reflected in the asymmetrical rearrangement of the actin cytoskeleton. As in most other eukaryotes, the actin cytoskeleton provides the structural basis for polarized growth in *S. cerevisiae* (Pruyne and Bretscher, 2000a; Figure 1.3 for an overview) Actin rearrangement is coupled with the positioning of the secretory machinery, leading to cell membrane insertion and new cell wall synthesis at the site of polarized secretion and growth. Rho-type GTPases, including Rho1-Rho4 and most importantly Cdc42, play crucial roles in this process (Chant, 1999).

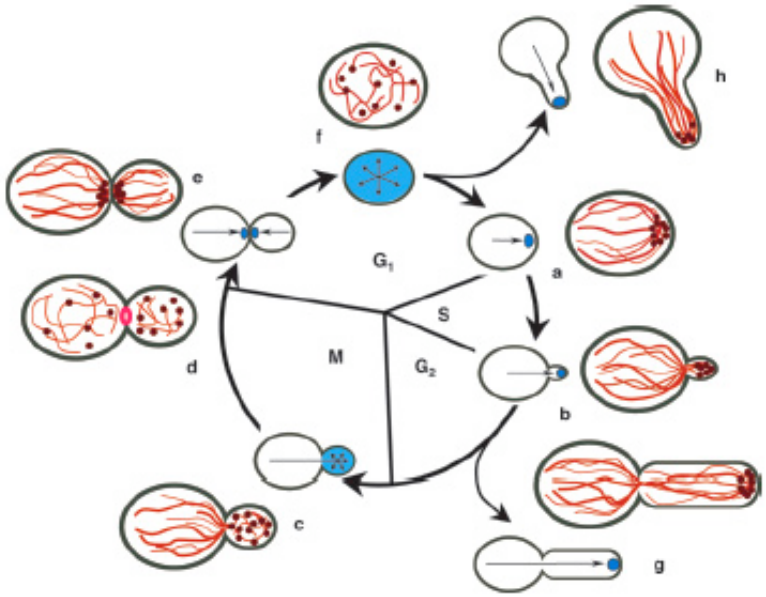

Figure 1.3 Cell polarity in budding yeast during cell cycle. Polarity is established by the localized plasma membrane recruitment of the Rho GTPase Cdc42p (blue) and proteins related to its function. These proteins orient the actin cytoskeleton, which consists of actin cables (pink) and cortical patches (brown). In turn, the actin cytoskeleton guides secretory vesicles to the cell surface, where they accumulate (also blue) and fuse, thus polarizing growth (arrows). **(a)** The cell cycle begins in G1 with establishment of a nascent bud site. **(b)** Clustering of Cdc42p directs early bud growth toward the tip. **(c)** Redistribution of Cdc42p over the bud surface during G2-M redirects bud growth isotropically, and results in an ellipsoidal shaped bud. **(d)** With the completion of bud growth, cables and patches disorganize, and a cytokinetic ring forms, then contracts and disassembles after mitosis. **(e)** Cdc42p reorients actin and growth between the two new cells to generate new cell walls. The mother cell resumes budding immediately. **(f)** The new daughter undergoes a period of undirected growth. **(g)** Under certain growth conditions, some strains of *S. cerevisiae* differentiate into a filamentous state that forgoes the transition in G2-M from tip-directed to isotropic growth. The resulting cells are highly elongated. **(h)** Mating pheromones arrest haploid yeast in G1 and polarize Cdc42p toward potential mating partners to generate a mating projection (shmoo). (Source: Pruyne and Bretscher, 2000).

1.5 RHO-TYPE GTPases

Rho-type GTPases belong to the Ras superfamily of small monomeric GTPases (Etienne-Manneville and Hall, 2002). These GTPases assume different conformations (and thus have different biochemical properties) upon binding to GTP or GDP. To date, 20 genes encoding Rho-type GTPases have been described

in humans. Based on the primary sequence and known functions of some of these proteins, Rho-type GTPases can be divided into the Rho-like, Rac-like, Cdc42-like, Rnd, and RhoBTB subfamilies (Burridge and Wennerberg, 2004). The first Rho gene was identified in 1985, but it was not until 1992 when insight into the cellular function of these GTPases was provided (Etienne-Manneville and Hall, 2002). When introduced into serum-starved Swiss 3T3 fibroblasts, constitutively activated (GTPase-deficient) mutant RhoA was found to induce the assembly of contractile actin and myosin filaments (stress fibers). Likewise, constitutively active Rac mutant induced actin-rich surface protrusions/membrane ruffles (lamellipodia) (Ridley and Hall, 1992; Ridley et al., 1992). Later, Cdc42 was shown to promote the formation of actin-rich, finger-like membrane extensions (filopodia) (Kozma et al., 1995; Nobes and Hall, 1995). The conclusion that Rho, Rac and Cdc42 regulate three separate signal transduction pathways linking plasma membrane receptors to the assembly of distinct filamentous actin structures has since been confirmed in a wide variety of mammalian cell-types as well as in yeast, flies and worms (Etienne-Manneville and Hall, 2002).

In addition to their functional link with the actin cytoskeleton, Rho-type GTPases are also known to participate in the regulation of cell polarity, gene expression, G1 cell cycle progression, microtubule dynamics, vesicular transport, and a variety of enzymatic activities ranging from glucan synthase in yeast to an NADPH oxidase in phagocytes (Etienne-Manneville and Hall, 2002).

Guanine nucleotide exchange factors (GEFs), GTPase-activating proteins (GAPs) and guanine nucleotide dissociation inhibitors (GDIs) are the three families of proteins that regulate the activities of Rho proteins. These proteins regulate the ability of Rho-type GTPases to cycle between an active GTP-bound state and an inactive GDP-bound state (Figure 1.4). Once GTP-loaded, Rho-type

GTPases interact with specific downstream effectors that process the information and propagate the signal within the cell (Aznar et al., 2004).

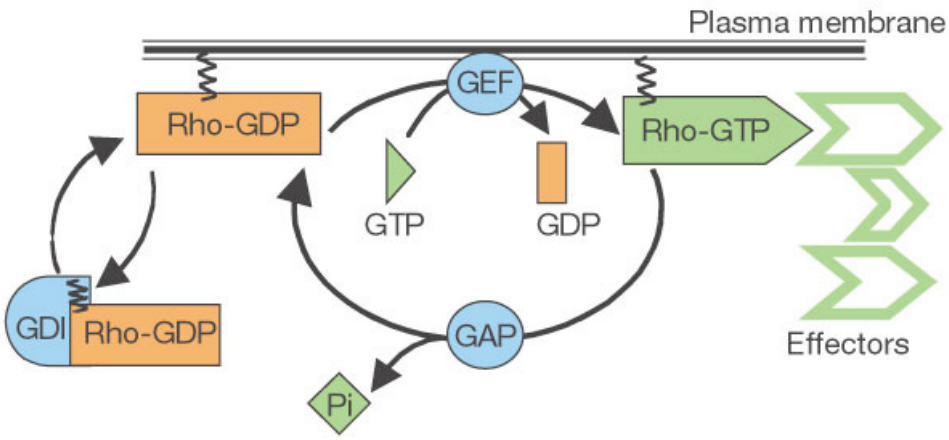

Figure 1.4 The Rho-type GTPase cycles between an active (GTP-bound) and an inactive (GDP-bound) conformation. The cycle is regulated by three classes of protein: guanine nucleotide exchange factors (GEFs) catalyze nucleotide exchange and mediate activation; GTPase-activating proteins (GAPs) stimulate GTP hydrolysis, leading to inactivation; and guanine nucleotide exchange inhibitors (GDIs) extract the inactive GTPase from membranes. All Rho-type GTPases are prenylated at C-terminus, and prenylation is required for their GTPase function. Activated Rho-type GTPases interact with diverse downstream effectors to manifest their cellular functions. (Source: Etienne-Manneville and Hall, 2002).

Budding yeast contains the Rho1-4 and Cdc42 Rho-type GTPases. Rho1 and Rho2 primarily function in the process of cell wall biosynthesis and maintenance (described later). Rho3 and Rho4 are partially redundant and function positively in actin cytoskeleton polarization and regulation of actin cable-based vesicular transport (Imai et al., 1996; Matsui and Toh-e, 1992; Matsui and Toh-e, 1992). The key player in the establishment of polarity in yeast is the Cdc42 GTPase. Its recruitment at the presumptive bud-site is of paramount importance and it leads to changes in the organization of the actin cytoskeleton (Ziman et al., 1993).

1.6 Cdc42

The Cdc42 GTPase was first identified in *S. cerevisiae* through the study of the temperature-sensitive *cdc42-1* mutant. Bud formation was blocked in *cdc42-1* cells but cell mass and volume continued to increase, resulting in greatly enlarged, unbudded cells (Adams et al., 1990). Although cell division was arrested in these cells at the restrictive temperature, DNA replication and nuclear division continued into the next cycle, resulting in multinucleate cells. Additionally, the actin cytoskeleton was depolarized in these cells, and chitin and other cell surface materials were deposited uniformly throughout the cell wall, in contrast to their normal polarized patterns of deposition. Taken together, it was understood that Cdc42 functioned in the organization of the actin cytoskeleton, which in turn is necessary for polarized cell growth (Johnson and Pringle, 1990). Consistent with its role in polarized growth and more specifically in the organization of the actin cytoskeleton, localization of Cdc42 is under temporal and spatial control during the cell cycle and mirrors that of the actin cytoskeleton network. Cdc42 is localized at the site of bud emergence, at the tip of growing buds (the tip of mating projections in pheromone-arrested cells) and at the mother-bud neck region in cells undergoing cytokinesis (Ziman et al., 1991; Ziman et al., 1993). This localization pattern of Cdc42 is independent of actin polarization since incubation of cells with the actin-depolymerizing drug latranculin-A does not affect Cdc42 localization (Ayscough et al., 1997). Together with the observation that Cdc42 can stimulate actin polymerization in permeabilized *S. cerevisiae* cells (Li et al., 1995), it is now known that the position of Cdc42 on the cell cortex defines the axis of actin cytoskeletal polariztion.

In addition to its role in actin organization, study on the *cdc42-6* mutant has revealed that Cdc42 also participates in the docking and fusion of secretory vesicles at the plasma membrane in an actin-independent manner (Adamo et al.,

2001; Eitzen et al., 2001; Muller et al., 2001). Furthermore, a role for Cdc42 in polarized secretion and exocytosis has been demonstrated by direct *in vitro* interaction between Cdc42 and Sec3, a member of the exocyst complex (Zhang et al., 2001).

CDC42 is an essential gene (Johnson and Pringle, 1990), and the Cdc42 protein is evolutionarily conserved. Furthermore, the phenotypic defect of the budding yeast *cdc42-1* mutant can be complemented by expression of the Cdc42 protein from *S. pombe*, *Drosophila*, *C. elegans* and human, thus suggesting that yeast Cdc42 has conserved functions in all these other eukaryotes (Johnson, 1999). In all organisms examined, Cdc42 is post-translationally prenylated at a C-terminal cysteine residue and attached to the plasma membrane. The association between Cdc42 and the plasma membrane is essential for the function of Cdc42, since $Cdc42^{C188S}$, which lacks the membrane anchor, cannot support polarized growth (Ziman et al., 1993).

Analyses of gain-of-function, loss-of-function and dominant negative mutations of Cdc42 have provided most of the information we know today about its functional domains. As mentioned above for Rho-type GTPases, Cdc42 is regulated by its GEFs, GAPs and GDI (Johnson, 1999). However, instead of functioning as a simple on/off switch, the optimal function of Cdc42 in polarization requires it to cycle between its GTP- and GDP-bound forms (Irazoqui et al., 2003). Cdc42 function is also regulated by its subcellular localization, which in turn, depends on its prenylation state and interactions with its GDI (Johnson, 1999).

How is Cdc42 activity restricted to one site on the plasma membrane?

The enrichment of Cdc42 at the presumptive bud-site ultimately depends on the landmark proteins deposited by the bud-site selection machinery. A schematic representation of the molecular pathway leading to an asymmetric

activation of Cdc42 at the polarized growth site is depicted in Figure 1.5. Bud5 and Bud2, the GAP and GEF respectively, for the Rsr1/Bud1-GTPase, colocalize with the cortical tags of the bud-site selection machinery at the presumptive bud-site, and at least the localization of Bud5 depends on the landmark proteins (Bender, 1993; Kang et al., 2001; Marston et al., 2001).

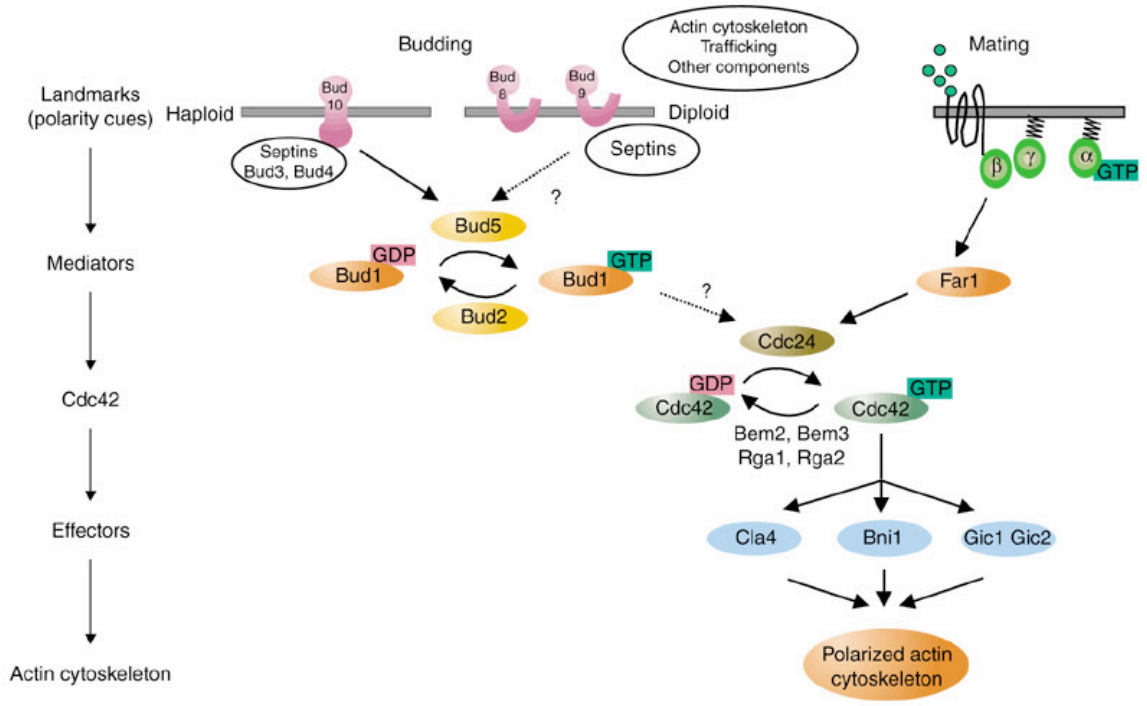

Figure 1.5 Molecular pathways leading to a polarized organization of the actin cytoskeleton in response to internal cues during budding and external signals during mating. Common to both pathways is the asymmetric activation of Cdc42 at the site determined by the landmarks. In turn, activated Cdc42 triggers the polarized assembly of the actin cytoskeleton by binding to various effectors. The mediators Bud1 and Far1 are thought to recruit and activate the GEF Cdc24 downstream of the specific landmark proteins. Far1 interacts directly with activated Gβγ at activated receptors, whereas the Bud1 GTPase is regulated at landmarks by the GEF Bud5 and the GAP Bud2. This figure appeared in a review published by Chang and Peter (2003).

Upon recruitment, Bud5 locally activates the uniformly distributed Rsr1/Bud1 GTPase (Marston et al., 2001). *In vitro* studies show that GTP-bound

Bud1/Rsr1 binds to Cdc24 (Zheng et al., 1995), the GEF for Cdc42 that restricts the Cdc42 activity to the site of bud emergence. Activation of Cdc24 at the incipient bud site thus leads to a local enrichment of active Cdc42, which then recruits the adaptor protein Bem1 to the bud emergence site. Bem1 in turn interacts with Cdc24 and this interaction contributes to a positive feedback loop stabilizing the active GEF at the cortex, and thereby further increasing the local concentration of activated Cdc42 (Butty et al., 2002). Thus, the bud-site selection cues and the Rsr1/Bud1-GTPase module are necessary to restrict the Cdc42 activity to a specific site on the plasma membrane. However, cells lacking any of the landmark genes or the Rsr1/Bud1 machinery do form buds, albeit randomly, in a process that requires activated Cdc42 (Chant and Herskowitz, 1991; Zahner et al., 1996). Together with the observation that constitutively activated mutant Cdc42 causes the formation of multiple buds in the same cell cycle, often at random sites on the cell surface, a new model has recently been proposed. In this model, the concentration of Cdc42 at the cell surface occurs through a 'stochastic process' rather than a deterministic process involving landmarks (Wedlich-Soldner et al., 2003).

Upon being loaded with GTP at the bud emergence site, activated Cdc42 interacts with a myriad of downstream effectors (Figure 1.5) and unleashes global changes in cytoskeletal organization within the bud. These changes include the assembly of a cap of actin filaments and the organization of actin cables that extend into the mother cell (Nelson, 2003), the organization of septin ring, regulation of membrane traffic, and the formation of membrane compartments (Chang and Peter, 2003). The interactions of Cdc42 with its effectors are regulated temporally and spatially within the cell cycle. Figure 1.6 depicts different molecular scaffolds that recruit and maintain Cdc24-Cdc42 cluster at the cell surface during various stages of polarized growth.

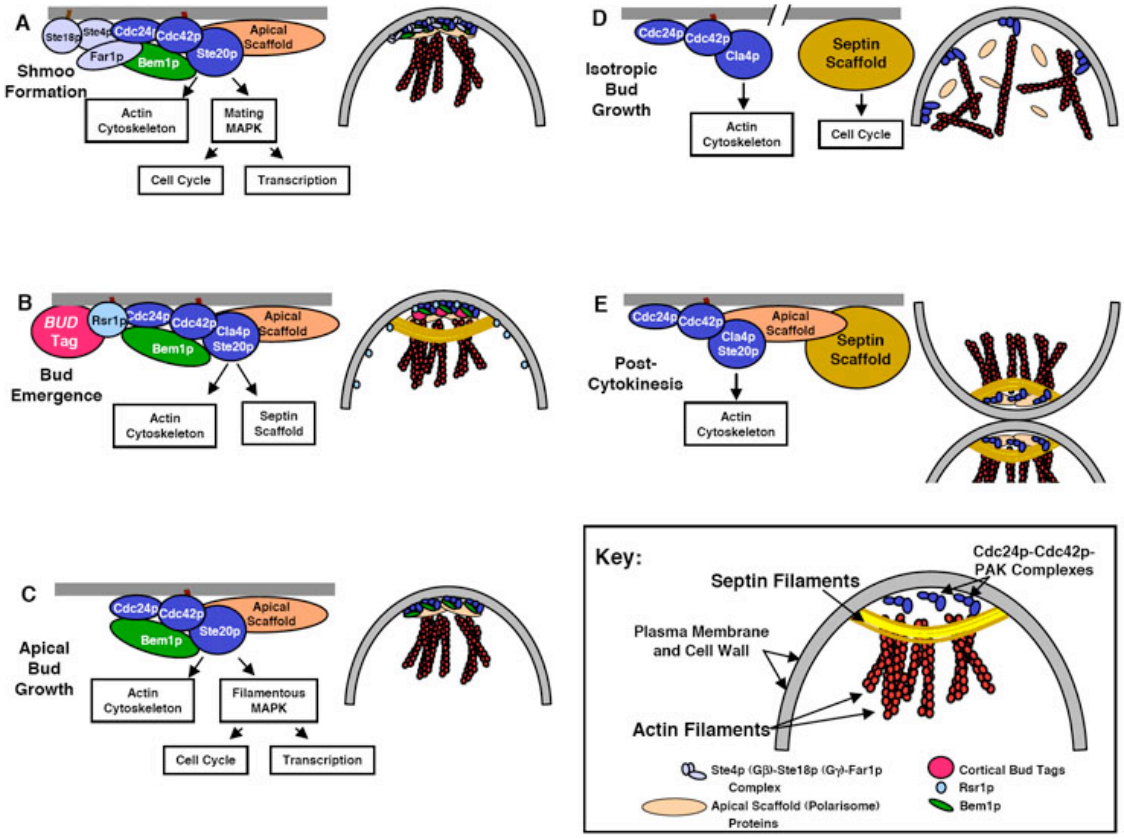

Figure 1.6 Clustering of Cdc24-Cdc42-effector complexes (dark blue) at the cell surface requires factors that form putative scaffolds. The Cdc42-activated effectors, such as Ste20, Cla4, Gic1 and Gic2, orient the actin cytoskeleton (red) from these signaling clusters. **(A)** Shmoo formation. Cdc24-Cdc42-Ste20 assembles at the cell surface into a pheromone-induced complex with Bem1 (green), Far1 (purple) and free Gβγ (Ste4, Ste18; purple). This complex polarizes the actin cytoskeleton to guide shmoo growth. Tight clustering of this complex for proper shmoo morphogenesis also requires polarisome proteins (Spa2, Sph1, Bud6, Bni1 and Pea2) as a putative apical scaffold (tan). Finally, the mating complex recruits a MAPK cascade to promote signaling of Cdc42 through Ste20 to trigger MAPK-dependent transcriptional changes and cell cycle arrest. **(B)** Bud emergence. A tight patch of Cdc24-Cdc42 on the plasma membrane establishes the nascent bud site. Bem1 strongly facilitates bud emergence, possibly as a scaffold to assist clustering of Cdc24-Cdc42. Cortical cues (pink) established by *BUD* gene products and the Rsr1 (Bud1) GTPase (light blue) normally guide bud emergence, but are non-essential. Cdc42 probably functions through several effectors during bud emergence, including Gic1, Gic2, Ste20 and Cla4, to both polarize the actin cytoskeleton and to direct assembly of a ring of septin proteins (yellow). **(C)** Apical bud growth. Early apical bud growth and filamentous bud elongation require polarisome proteins, possibly as a scaffold for Cdc42-containing complexes and MAPK cascade proteins. Ste20 is the primary Cdc42-effector during sustained apical growth, signaling to the actin cytoskeleton and a MAPK cascade. **(D)** Isotropic bud growth. During isotropic bud growth, accessory scaffolds are apparently not required. Inactivation of these scaffolds depends at least

indirectly upon Cla4, and Cla4 is the primary Cdc42 effector that signals to the actin cytoskeleton during isotropic growth. **(E)** Post-cytokinesis. After contraction of the cytokinetic ring, Cdc24, Cdc42 and polarisome proteins re-polarize to the former mother-bud neck site in order to redirect the actin cytoskeleton to the mother-bud junction. This guides the formation of a new cell wall between the mother and daughter, and in the absence of a contractile ring, this directed wall synthesis provides a secondary mechanism of cytokinesis. The septin scaffolds at the former mother-bud neck site are required to reorient the actin cytoskeleton, perhaps acting in part through direct recruitment of polarisome proteins (e.g. Spa2). This figure appeared in a review article by Pruyne and Bretscher (2000).

Cdc42 effectors

Ste20 and Cla4, the p21-activated kinase (PAK) homologs, and Gic1 and Gic2 are four well-known effectors of the Cdc42 GTPase in yeast. All of these proteins interact with Cdc42 via their N-terminal Cdc42/Rac-interactive binding (CRIB) domain, which is conserved amongst many effectors of Cdc42 (Johnson, 1999). Binding of Cdc42-GTP to the CRIB domain of Ste20 and Cla4 relieves the intramolecular inhibition on the C-terminal kinase domain of these proteins, which are then rendered active (Vojtek and Cooper, 1995). Analogous activation mechanism for the Gic1 and Gic2 proteins is not known so far but it has been shown that the Gic2 protein is present in the cell only at the time of bud emergence, after which it is degraded via ubiquitination and proteolysis (Jaquenoud et al., 1998). It is possible to speculate that recruitment of Gic1 and Gic2 proteins at sites of polarization during specific periods of the cell cycle may be the mode by which their activity is regulated.

Ste20 and Cla4

These two Cdc42-activated kinases are essential to Cdc42-actin signaling at all stages of growth. Simultaneous absence of both Ste20 and Cla4 blocks initial bud emergence, bud growth and cytokinesis (Cvrckova et al., 1995; Eby et al., 1998; Holly and Blumer, 1999). Ste20 appears to mediate apical growth not only at the time of bud emergence and G1-S transition but is also involved in the

mating and filamentous growth pathways (Eby et al., 1998; Madhani and Fink, 1998). The role of Ste20 in actin polarization is strengthened by the observation that continuous Ste20 activation prolongs apical growth. Cla4, on the other hand, is involved in the apical-isotropic growth switch that occurs during G2-M phase of the cell cycle and it also functions in cytokinesis. Consequently, cells lacking *CLA4* or bearing a $cdc42^{V44A}$ allele, whose product binds poorly to Cla4, generate highly elongated buds and exhibit defect in cytokinesis (Cvrckova et al., 1995; Richman et al., 1999).

Although Ste20 and Cla4 perform distinct roles in polarized growth at different stages of the cell cycle, *ste20 cla4* double mutants are inviable, suggesting that some of their functions must overlap (Eby et al., 1998). This idea is supported by the ability of both Ste20 and Cla4 to phosphorylate common cytoskeletal substrates such as the class I myosins, Myo3 and Myo5 (Wu et al., 1997). These molecular motors localize to actin patches and function in proper cytoskeleton organization. Further, there is also additional genetic data to speculate the existence of as yet unidentified signaling pathways from Ste20 and Cla4 to the cytoskeleton (Pruyne and Bretscher, 2000b).

The stable states of either highly polarized or isotropic growth need to be synchronized with cell cycle progression. This is achieved by a reciprocal regulation between the PAK and Cdk-cyclin activities. The function of Cdc42-Ste20 is regulated by Cdc28-Cln1 and Cdc28-Cln2, the G1 Cdk-cyclin complexes, possibly by direct phosphorylation of Ste20 (Oda et al., 1999). Such phosphorylation at the G1-S transition allows the Ste20 kinase to direct early apical bud growth. On the other hand, Ste20, via its indirect activation of the Fus3 and Kss1 MAP kinases, participates in feedback loops to regulate Cdc28-cyclin states and thereby sustained apical growth during mating and filamentous cell growth, respectively (Madhani et al., 1999; Oehlen and Cross, 1994). In the former scenario, the inhibition of Cdc28-Cln1 and Cdc28-Cln2 by mating

pheromone signaling allows Ste20 to direct shmoo growth rather than bud emergence. In the latter scenario, continuous Cdc28-Cln1 activity and inhibition of G2 cyclins prolong the period of apical growth.

Likewise, the function of Cla4 requires Cdc28-Clb1 and Cdc28-Clb2, the G2 Cdk-cyclin complexes. Cla4 appears to promote the apical-isotropic switch indirectly through the Nim1-related kinases (Gin4, Hsl1 and Kcc4), which are activated by Cdc28-Clb1/Clb2 in the presence of septins. In the absence of these partially redundant kinases, and septins, yeast generates elongated buds similar to *cla4* mutant cells (Altman and Kellogg, 1997; Barral et al., 1999; Carroll et al., 1998; Longtine et al., 1998a).

Skm1

In addition to Ste20 and Cla4, another PAK homolog called Skm1 is also present in *S. cerevisiae*. *skm1* deletion cells, however, do not exhibit any apparent phenotypic defects. Also, combination of *skm1* mutation with either *ste20* or *cla4* mutation does not lead to a synthetic phenotype. Thus, the normal function of Skm1 is not clear so far (Martin et al., 1997).

Gic1 and Gic2

Gic1 and Gic2 are structurally and functionally related proteins that were identified in our laboratory as high-copy suppressors of the temperature-sensitive growth defect of *bem2-101* mutant (Bem2 is a GAP for Cdc42- and Rho1-GTPase) (Chen et al., 1997). They were simultaneously identified in Matthias Peter's and John Chant's laboratories as CRIB domain-containing yeast proteins (Brown et al., 1997). The Gic1 and Gic2 proteins interact with Cdc42-GTP via their CRIB domain. Both these proteins colocalize with Cdc42 at sites of

polarized growth as cell polarity is established during bud emergence and during mating in response to pheromones. Although neither *GIC1* nor *GIC2* is

essential, the Gic1 and Gic2 proteins together are required for cell size and shape control, bud-site selection, bud emergence, actin cytoskeletal organization and mitotic spindle orientation/positioning. Thus, the Gic1 and Gic2 proteins define a novel class of Cdc42 effectors that are specifically required for normal actin cytoskeleton. However, the exact molecular mechanism by which they mediate the polarization of the actin cytoskeleton remains to be elucidated.

DNA microarray analysis has revealed that both *GIC1* and *GIC2*, like many other genes that are predominantly involved in budding and in membrane and cell wall biosynthesis, are targets of the SBF transcription factor. They are expressed in the cell specifically during the G1/S transition of the cell cycle (Iyer et al., 2001). The Gic1 and Gic2 proteins are present at the time of bud emergence but Gic2 is rapidly degraded thereafter in a process that requires the SCF^{Grr1} components Cdc34, Cdc53, Skp1 and Grr1 (Jaquenoud et al., 1998). Whether Gic1 is similarly regulated via ubiquitin-mediated proteolysis is not known. Proteolysis of the Gic2 protein may be part of a regulatory mechanism that either restricts the cytoskeleton polarization to the G1 phase of the cell cycle or allows Cdc42-GTP to interact with other effectors like the Cla4 kinase, thus preparing the polarized cell for later events such as isotropic bud growth and cytokinesis (Jaquenoud et al., 1998).

The actin polarization defect of *gic1 gic2* cells resembles that of *cdc42* mutants but is less severe. *gic1 gic2* cells are viable at 26°C but exhibit polarized growth defect at elevated temperatures. Synthetic lethality and multi-copy suppression analyses suggest that Gic1 and Gic2 function in parallel with Msb3 and Msb4 to mediate the function of Cdc42 in the organization of the actin cytoskeleton (Bi et al., 2000). Msb3 and Msb4 constitute a pair of structurally related proteins that interact genetically with Cdc42. They display a GAP activity for the Rab GTPase Sec4 (Albert and Gallwitz, 1999; Albert and Gallwitz, 2000). The GAP activity of Msb3 and Msb4 is required for efficient polarization of the

actin patches and for the ability of multiple copies of *MSB3/4* to suppress the actin-organization defects in *cdc42* mutants (Gao et al., 2003). While the Msb3/4-mediated pathway appears to be more important in diploids and at low temperatures, the Gic1/2-mediated pathway appears to be more important in haploids and at high temperatures (Bi et al., 2000).

Although the involvement of Gic1 and Gic2 in actin cytoskeleton organization is quite clear, it is not understood how these proteins interact with the actin cytoskeleton. Cdc24 and Cdc42 continue to remain clustered for apical growth during shmoo formation, early vegetative bud growth and filamentous bud elongation. The 12S polarisome complex, comprising of Bni1, Sph1, Spa2, Pea2 and Bud6/Aip3 (Sheu et al., 1998), is reported to function as an apical scaffold for Cdc24-Cdc42 during these processes (Figure 1.6). Protein-protein interactions involving polarisome components suggest that under the regulation of Rho-type GTPases, the polarisome assembles and participates in the nucleation of actin filament via the formin protein Bni1 (Evangelista et al., 1997; Sagot et al., 2002). In this manner, the polarisome links Rho-type GTPase signaling to the process of actin filament assembly (Pruyne and Bretscher, 2000b). Interestingly, the *gic2* mutation exhibits synthetic genetic interaction with the *bni1*, *bud6* and *spa2* mutations (Jaquenoud and Peter, 2000). In addition, overexpression of the Gic2 protein is lethal in *bni1*, *bud6* and *spa2* deletion cells, suggesting that Gic2 may regulate the function of polarisome proteins *in vivo*. In support of this idea, Gic2 co-fractionates with Bud6 and Spa2, and it interacts with Bud6 in coimmunoprecipitation and two-hybrid analyses. The localization of Bni1 and Bud6 to the incipient bud-site is dependent on active Cdc42 and the Gic proteins but not on intact actin cytoskeleton (Jaquenoud and Peter, 2000). Taken together, it appears that Gic2 functions as an adaptor to link together activated Cdc42 to the components involved in actin organization and polarized growth at the time of bud emergence. Additionally, the synthetic lethal

interactions between *rsr1* and *gic1 gic2*, but not other Cdc42 effector mutations suggest that the Gic proteins may have a role in stabilizing or maintaining a complex consisting of Cdc42p-GTP and its effectors at the budding site, which are assembled by the action of the Rsr1-Cdc24 system (Kawasaki et al., 2003; Figure 1.5). Localization of both Gic1 and Gic2 with Cdc42 at growth sites before bud emergence bolsters this hypothesis (Chen et al., 1997).

The Gic proteins may also participate in the process of cytokinesis. This idea is based on the two-hybrid interactions displayed by both Gic1 and Gic2 with Cla4 and the Cdc12 septin (Drees et al., 2001) as well as the synthetic lethal interaction between the *gic1 gic2* and *cla4* mutations (Chen et al., 1997). However, the mechanism by which the Gic proteins function in cytokinesis is not clear.

Comparing yeast to other eukaryotic systems, it is noteworthy that some of the yeast proteins that are counterparts of mammalian Cdc42 effectors have little or no measurable affinity for yeast Cdc42 (Chant, 1999). Among these are Las17/ Bee1 (the yeast homolog of mammalian WASP), which functions in modulating actin dynamics (Karpova et al., 1998; Li, 1997), and Iqg1/Cyk1 (the yeast homologue of mammalian IQGAP), which is involved in cytokinesis rather than the establishment of cell polarity (Epp and Chant, 1997; Lippincott and Li, 1998b).

1.7 CYTOKINESIS

Cytokinesis is fundamental to the successful completion of the cell cycle. In animal cells, the position of the spindle mid-zone at the time of anaphase determines the site of cleavage furrow formation (Satterwhite and Pollard, 1992). In contrast, the site for cell division in budding yeast is determined at the beginning of the cell cycle and it is the same as the site of bud emergence (Drubin and Nelson, 1996). Time-lapse analysis has shown that cell division in budding yeast normally occurs through the contraction of the actomyosin ring, followed

closely by septum (including primary and secondary cell wall) formation and subsequent cell separation (removal of the primary septum) (Bi et al., 1998). The actomyosin ring is formed at the mother-bud neck and undergoes a contraction-like size change during cytokinesis. This process requires actin (Act1), the type II myosin Myo1, and the IQGAP homolog Cyk1, which is crucial for the recruitment of actin filaments to the Myo1 ring (Lippincott and Li, 1998b). Bni1 also functions in cytokinesis, most likely in the same process as that requiring the function of Myo1 (Kohno et al., 1996; Vallen et al., 2000).

Unlike in fission yeast or mammalian cells, the action of the actomyosin contractile ring is not absolutely essential for cytokinesis in budding yeast. In fact, septum formation can drive the cell division process (Vallen et al., 2000). The Bni1-related protein Bnr1 and the Cyk2/Hof1 protein (described below) participate in a linear pathway leading to septum formation. Mutations that abolish Bnr1 or Cyk2/Hof1 function do not block cytokinesis completely. However, when loss of Bni1 and Cyk2/Hof1 or Bnr1 is combined, cells demonstrate a synthetic phenotype and arrest with morphology indicative of a total failure in cytokinesis (Kamei et al., 1998; Vallen et al., 2000), thus suggesting that the actomyosin contractile ring system and the septum formation system function in a redundant manner to result in cytokinesis.

Although capable of independent function, the actomyosin ring contraction and septum formation pathways are coordinated in that the actomyosin contraction ring provides the directionality to septum formation. Thus, *bni1* mutants display a delay in septum formation and cell separation. Also cells with little or no actomyosin ring contraction exhibit an asymmetric and/or misaligned septum that often deviates from the neck axis. Both mechanisms of cytokinesis depend on septins because mutations in the septin-encoding genes completely block cytokinesis (Vallen et al., 2000).

Cyk2

CYK2 is a budding yeast homolog of *CDC15* in *S. pombe* and is often referred to as *HOF1* (homolog of fifteen). Homologs of this protein are also present in multicellular organisms, including *C. elegans*, mouse, and human. In *S. pombe*, Cdc15 is involved in the assembly of the actomyosin ring and is essential for cytokinesis (Fankhauser et al., 1995). In *S. cerevisiae*, Cyk2 is proposed to function as an adapter that links the primary septum synthesis machinery to the actomyosin system (Vallen et al., 2000).

Cyk2 localizes at the bud neck as a ring structure. The assembly and maintenance of the Cyk2 ring structure at the bud neck require septins. During most part of the cell cycle, the Cyk2 double rings colocalize with septin rings. However, during anaphase, Cyk2 becomes phosphorylated. The two rings of Cyk2 merge into a single ring that becomes sandwiched between the septin rings (Lippincott and Li, 1998a; Vallen et al., 2000). During this time, the Cyk2 ring colocalizes with the actomyosin ring and contracts slightly (Lippincott and Li, 1998a). Following cytokinesis and septum formation, the Cyk2 ring splits into two rings that spread around the neck area and extend toward the future bud site. It is at this site, a new Cyk2 ring structure is formed as the new bud emerges (Vallen et al., 2000).

Cells carrying *cyk2* deletion exhibit a temperature-sensitive growth phenotype. At elevated temperatures, these cells are multinucleate with large and elongated bud, and they show deposition of chitin throughout the entire cell surface. They accumulate as chains or clumps of cells with connected cytoplasm and fail to form septum between two cell bodies. Additionally, these cells show cortical actin patches at the bud tip but not at the mother-bud neck. Taken together, the phenotype of *cyk2* cells suggests a defect in cytokinesis. Both genetic and biochemical experiments suggest that Cyk2 is not involved directly in the actomyosin contraction system (Kamei et al., 1998; Lippincott and Li, 1998a;

Vallen et al., 2000). Instead, together with the formin protein Bnr1, it functions in the septum formation process, where it restricts the septal and bud-scar chitin to the bud neck (Vallen et al., 2000). However, Cyk2 may also function in modulating the stability of the actomyosin ring during contraction since inactivation of Cyk2 results in a rapid disassembly of the myosin ring during the contractile phase (Lippincott and Li, 1998a), thus interfering with the completion of cytokinesis. In this manner, Cyk2 functions as an adapter linking the primary septum synthesis machinery to the actomyosin system (Vallen et al., 2000).

The Septins

Septins belong to a family of evolutionarily conserved GTPases that were discovered over three decades ago in budding yeast. They form a unique cytoskeletal structure at the cleavage apparatus in yeast and animal cells, and are required for cytokinesis (Moffat and Andrews, 2003). The domain structure of septins is conserved, with an N-terminal region of variable length, a central GTP-binding region, and a C-terminal region that is predicted to form a coiled-coil structure. Septins form heteromeric septin-septin complexes as well as bind and hydrolyze GTP. Both of these properties are important for septin function (Longtine and Bi, 2003).

The budding yeast genome encodes seven septins, five of which (Cdc3, Cdc10, Cdc11, Cdc12 and Shs1/Sep7) are coexpressed and colocalize during mitotic growth. Based on electron microscopy studies, they seem to be organized as ~10 nm filaments that spiral around the mother-bud neck just beneath the plasma membrane. During sporulation, Cdc3, Cdc10, Cdc11 and two sporulation-specific septins (Spr3 and Spr28) are expressed and localized at the leading edge of the forespore membrane. The function of septins in sporulation, however, is unclear (Longtine and Bi, 2003).

Localization of septins during the cell cycle

Septins retain fluid-dynamic properties during their recruitment and assembly. In early G1 phase, septins are recruited as a cap-like structure at the incipient bud site and are subsequently assembled into a ring. Once this cortical ring is formed, the septin structure gets stabilized and develops into an hourglass structure (often appearing as two closely apposed rings) during bud emergence (Moffat and Andrews, 2003). This septin collar remains at the bud neck until cytokinesis, when its hourglass structure splits into two distinct rings, which move further apart and away from the bud neck (Longtine and Bi, 2003). Figure 1.7 depicts the dynamics of septin structure during the cell cycle.

The partitioning of the septin rings at the time of cytokinesis might occur for at least two reasons. First, since the septin hourglass structure is stable and possibly even rigid, the removal of septins from the middle of the hourglass might be required to permit contraction of the actomyosin ring and septum formation. This idea is consistent with the localization of the actomyosin ring to the region between the two separated septin rings. Second, upon splitting, each septin ring can localize to the respective cortex of the mother and daughter cells. Subsequent to cell separation, these individual septin rings elongate at one end and mark the new bud site by guiding the localization of 'cortical tag' proteins as part of the bud-site selection machinery during the next cell cycle. Subsequently, the septin rings completely delocalize from the old site as the new bud emerges (Longtine and Bi, 2003).

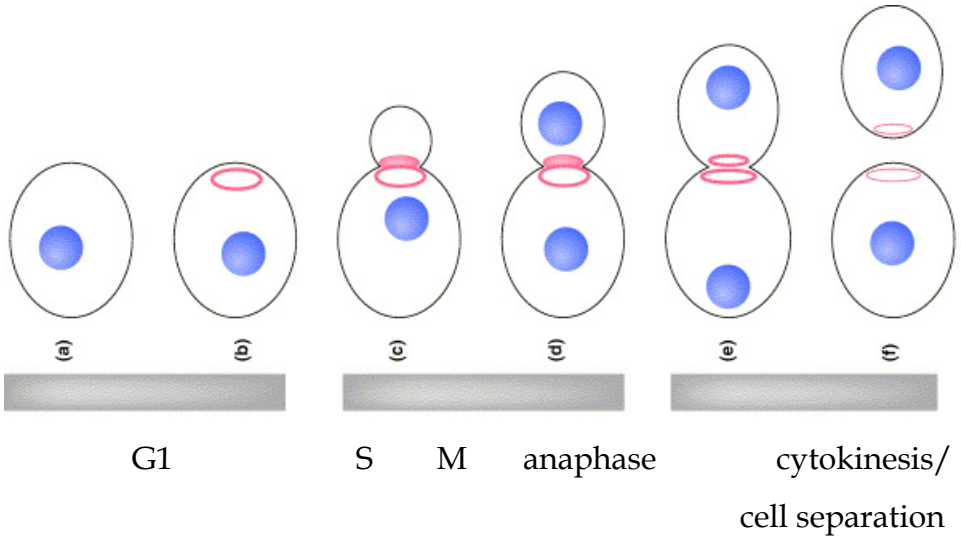

Figure 1. 7 Septin dynamics during the cell cycle. **(a)** Early in G1 in unbudded cells, septins show no specific organization. **(b)** Late in G1, septins localize to the incipient bud site as a cortical ring. **(c)** As the bud emerges, the septins are organized into a cortical hourglass structure, which often appears as two closely apposed rings. **(e)** The septin hourglass is maintained until the time of cytokinesis, when it is split into two distinct rings. **(f)** Cortical septin rings remain at the division site after cell separation where they mark the old division sites. (Source: Longtine and Bi, 2003).

Regulation of the septin structure and assembly

Assembly of septin ring is dependent on Cdc28-G1 cyclin-mediated cell cycle signals and the signaling of the Cdc42 GTPase to Cla4 (Cvrckova et al., 1995; Holly and Blumer, 1999). Both loss-of-function and hyperactivation of *CDC42* have negative effect on the integrity of the septin cytoskeleton. Recently, Gladfelter et al. proposed that hydrolysis of Cdc42-bound GTP has a direct role in guiding the formation of septin rings, without any intermediate steps (Gladfelter et al., 2002). This function of Cdc42 in septin ring assembly is independent of its signaling to the actin cytoskeleton. Although the assembly of septin ring structure requires Cdc42, maintenance of the septin hourglass structure later in the cell cycle does not require the presence of Cdc42. However, deletion of *GIN4*, *ELM1* or *CLA4* results in aberrant 'septin bar' formation,

suggesting that Gin4, Elm1 and Cla4 kinases might function to crosslink septin bundles and thereby to stabilize the septin hourglass structure (Cvrckova et al., 1995; Lee et al., 2002; Longtine et al., 1998a). Finally, the splitting of septin hourglass structure at cytokinesis is dependent on the function of the mitotic exit network GTPase, Tem1 (Lippincott et al., 2001).

The proposed models for septin function

Originally identified as a protein family involved in cytokinesis in yeast, septins are now clearly known to have diverse roles in eukaryotic cells. Recent advances in mammalian systems have implicated septins in vesicle trafficking and possibly even in oncogenesis (Moffat and Andrews, 2003). The current literature describes the function of septins in terms of two models.

The scaffold model: According to this model, septins form a scaffold at discrete cortical regions, such as the mother-bud neck in *S. cerevisiae*, and direct the localization of other proteins that are involved in diverse processes (Longtine and Bi, 2003). In support of this hypothesis, the neck localization of Myo1, F-actin and Cyk1 (all required for actomyosin ring), and of chitin synthase II components (required for primary septum formation) depends on the localization of septins at the bud neck (Bi et al., 1998; Lippincott and Li, 1998b; Schmidt et al., 2002). Furthermore, the reorientation of cortical actin patches and actin cables to the bud neck after cytokinesis also depends on the presence of septins (Adams and Pringle, 1984). Besides cytokinesis, the role of septins in the localization of cortical landmark proteins for bud-site selection (Flescher et al., 1993) also reinforces their role as *in vivo* molecular scaffolds.

The diffusion-barrier model: This model proposes that the neck localization of septins allows for the asymmetric distribution of several proteins, either

preferentially or exclusively, to the daughter cell at specific stages of the cell cycle. These include the integral membrane protein Ist2 (Takizawa et al., 2000), the mitotic exit network regulator Lte1 (Jensen et al., 2002; Seshan et al., 2002), the exocyst complex components Sec3 and Sec5, the polarisome protein Spa2 as well as and other factors that regulate actin stability (Barral et al., 2000). Both higher-order septin structures and direct or indirect interactions of septins with plasma membrane appear to be important in this function of septin as a diffusion barrier (Longtine and Bi, 2003), which is analogous to the diffusion barrier function of the tight junction in epithelial cells (Casamayor and Snyder, 2002).

1.8 Role of CDK-cyclin complexes in polarized cell growth

As shown in Figure 1.6, the distribution of Cdc42 changes from being polarized at the bud tip during apical growth to being depolarized in the bud during isotropic growth, and to being polarized again at the mother-bud neck during cytokinesis. Consequently, the actin cytoskeleton also undergoes rearrangement. Cdk-cyclin complexes play a significant role in regulating such changes (Pruyne and Bretscher, 2000b). Cyclins originally came to our attention as cell-cycle regulatory proteins that oscillate in abundance through the cell cycle and function by activating a kinase partner, the Cdk (cyclin-dependent kinase). However, as more cyclins are being studied in various eukaryotic cells, it is becoming clear that not all of them fluctuate in abundance during the cell cycle, and their function extends beyond the regulation of cell cycle progression (Andrews and Measday, 1998).

Cdc28-cyclin complexes

Cdc28 is the major Cdk in budding yeast. As mentioned earlier, the G1 Cdk-cyclin complexes such as Cdc28-Cln1 and Cdc28-Cln2 act through the p21-activated kinase Ste20 to regulate apical bud growth. In accordance with this

role, Cln1-, Cln2- and Cln3-depleted cells arrest in G1 as unbudded cells, and overexpression of *CLN1* or *CLN2*, or delaying the activation of the Cdc28-G2 cyclin complexes prolongs the apical growth phase and produces cells with elongated buds due to hyperpolarized actin cytoskeleton (Cross, 1990; Lew and Reed, 1993; Richardson et al., 1989). Likewise, the G2 Cdk-cyclin complexes such as Cdc28-Clb1 and Cdc28-Clb2 promote entry into the isotropic growth phase during which actin is distributed throughout the bud. Hence, cells overexpressing *CLB1* or *CLB2* accelerate the isotropic switch and are unable to initiate a new bud. It is unclear whether Cdc28-G2 cyclin complexes simply inactivate the Cdc28-G1 cyclin complexes or whether they also have direct roles in promoting the isotropic growth. Finally, cyclin degradation at the end of anaphase inactivates Cdc28. This triggers a transient repolarization of Cdc42 and the actin cytoskeleton to the bud neck, thus facilitating cytokinesis and cell separation (Lew and Reed, 1993). In this manner, polarized growth undergoes dynamic changes during the cell cycle in yeast and Cdc28-cyclin complexes control distinct aspects of cell polarization and morphogenesis. Since these kinase complexes also regulate nuclear progression, they coordinate bud formation and growth with other aspects of the cell cycle.

Pho85-Pcl complexes

Pho85 is a non-essential Cdk that is 51% identical in sequence to Cdc28. Like its mammalian counterpart Cdk5, it has emerged as an important model in *S. cerevisiae* for the study of Cdks in processes beyond cell cycle control. Pho85 can associate with ten different cyclin partners that are collectively referred to as Pcls. Based on the sequence similarity within their cyclin box regions, Pcls are grouped into two subfamilies (Andrews and Measday, 1998). One subfamily is called the Pho80 family, consisting of Pho80, Pcl6, Pcl7, Pcl8 and Pcl10. These Pcls participate in phosphate, carbon source and glycogen metabolism pathways.

The second subfamily is called the Pcl1/2 family and it is comprised of Pcl1, Pcl2, Pcl5, Pcl9 and Clg1. These Pcls have cell cycle and morphogenesis-related functions.

Like Cdc28-Cln1 and Cdc28-Cln2 complexes, Pho85-Pcl1 and Pho85-Pcl2 complexes appear to regulate cell cycle progression at START. The function of Pho85 or Pcl1 and Pcl2 becomes essential in *cln1 cln2* mutants as *pho85 cln1 cln2* triple mutant and *cln1 cln2 pcl1 pcl2* quadruple mutant cells arrest in G1 as unbudded cells (Espinoza et al., 1994; Measday et al., 1994). These genetic interactions suggest that the function of Pcl1 and Pcl2 at least partially overlaps with that of Cln1 and Cln2. Accordingly, Pcl1 and Pcl2 cyclins, like Cln1 and Cln2 cyclins, are expressed specifically during G1 stage of the cell cycle and their associated kinase activities peak during G1 (Measday et al., 1997, Moffat, 2004 #63).

G1 Cdk-cyclin complexes function beyond cell cycle progression

Current models for cell cycle commitment invoke phosphorylation (and subsequent degradation) of Sic1 (a B-type Cdk-cyclin inhibitor) by the G1 Cdk-cyclin complexes as a critical event that promotes passage through START. Both Cdc28-Cln1/2 and Pho85-Pcl1 complexes can phosphorylate Sic1 and thus promote its degradation and subsequent initiation of DNA replication (Nishizawa et al., 1998). However, if this is the only function of Cln1, Cln2 and Pcl1 in regulating cell cycle progression, then removal of Sic1 should rescue the phenotype of *pho85 cln1 cln2* triple mutants. Indeed, deletion of *SIC1* in *pho85 cln1 cln2* cells eliminates the growth arrest in G1 stage. However, such cells remain inviable, suggesting that G1 cyclin kinases have additional roles in cell growth (Nishizawa et al., 1998). Moreover, the suppression of the G1 arrest of *cln1 cln2 pcl1 pcl2* cells by sorbitol suggests that these mutant cells do not have an

absolute defect in G1 progression but rather a defect in a morphogenesis- or cell wall biogenesis-related function (Lenburg and O'Shea, 2001).

Recently, it has been suggested that in *S. cerevisiae*, a burst of G1 Cdk-cyclin activity is essential for bud emergence and hence cellular morphogenesis. This burst of Cdk activity is not essential for other landmark events associated with the G1-S phase transition, including initiation of DNA replication (Moffat and Andrews, 2004). Cdc28-Cln1/2 as well as Pho85-Pcl1/2 complexes have been shown to phosphorylate Cdc24 *in vitro* and it appears that the activity of these complexes at the bud site at START is required for the *in vivo* phosphorylation of Cdc24, which in turn polarizes growth. This activity is also required for the assembly of septin ring and thus the development of the cleavage apparatus. Consequently, actin patches and chitin are delocalized in cells lacking the aforementioned Cdk activity (Moffat and Andrews, 2004). Consistent with the role of Pho85 and Pcl1/2 in cellular morphogenesis, Pcl1 and Pcl2 are localized at sites of polarized growth (Moffat and Andrews, 2004). Furthermore, the *pho85*, *pcl1* and *pcl2* mutations interact genetically with several mutations in the cell integrity and actin organization pathways (Lenburg and O'Shea, 2001; Moffat and Andrews, 2004).

The synthetic growth phenotypes observed between *pho85-9* and mutations (e.g., *bck1* or *mpk1*) in the Pkc1-MAP kinase pathway (also called cell integrity pathway, described below) can be rescued by the presence of 1M sorbitol. In contrast, the synthetic growth phenotypes observed between *pho85-9* (or *pcl1 pcl2*) and mutations (e.g., *bem2*, *cdc42-1*, *cla4*, *ste20* and *gic1 gic2*) in the polarity establishment pathway are not alleviated by osmotic stabilization (Huang et al., 2002; Lenburg and O'Shea, 2001; Moffat and Andrews, 2004). Functional genomics approaches using Synthetic Genetic Array (SGA) and transcriptional profiling revealed that amongst *pho85* synthetic lethal interactors, ~32% (including *BCK1*, *FKS1*, *GSC2*, *RGD1*, *ROM2*, *SLT2*, *SWI4*, *WSC1* and

WSC4) are involved in cell wall maintenance and/or integrity and ~17% (including *BEM1*, *BEM2*, *BEM4*, *BNI1* and *CLA4*) are involved in bud emergence and spatial regulation of polarity establishment (Huang et al., 2002). Taken together, it indicates that Pho85, together with the Pcl1 and Pcl2 cyclins, functions in ensuring cell wall integrity through regulation of the actin cytoskeleton and cell polarity. Such regulation of the actin cytoskeleton appears to be mediated at least partly via the Rvs161 and Rvs167 proteins (Lee et al., 1998).

1.9 THE RVS PROTEINS

The Rvs161 and Rvs167 proteins of *S. cerevisiae* belong to a conserved family of BAR proteins (Bin1-Amphiphysin-Rvs) that also include the amphiphysins in mammals, fly and nematode. All these proteins contain a conserved N-terminal BAR domain. In addition to the BAR domain, Rvs167 also contains a glycin-, proline- and alanine-rich central GPA domain and a C-terminal SH3 domain (Sivadon et al., 1997a).

Rvs proteins regulate the actin cytoskeleton

Like mammalian amphiphysins, which are involved in controlling endocytosis and actin cytoskeleton function, yeast Rvs proteins also participate in the regulation of the actin cytoskeleton (Bon et al., 2000). Their cytoskeleton-related function is reflected by several phenotypes that are exhibited by *rvs161* and *rvs167* mutants, including salt-sensitivity, delocalized actin distribution, defect in endocytosis, poor sporulation, and randomized budding in diploids (Bauer et al., 1993; Desfarges et al., 1993; Munn et al., 1995; Sivadon et al., 1995; Sivadon et al., 1997a). Based on both two-hybrid and coimmunoprecipitation experiments, it appears that Rvs161 and Rvs167 form functional heterodimers with each other and each Rvs protein contributes to the stability of the other. This conclusion supports the similar spectrum of phenotypes observed in each *rvs*

single mutant, which in effect could be due to a combined loss of both proteins (Bon et al., 2000; Lombardi and Riezman, 2001).

Consistent with a function of the Rvs proteins in regulating the actin cytoskeleton, Rvs161 localizes at the cell cortex during bud emergence and Rvs167 colocalizes with actin patches, which also polarize at the cell cortex during bud emergence. In fact, cortical actin patches are mislocalized in *rvs167* mutant but not vice-versa, suggesting that Rvs167 may be instrumental in the proper localization of cortical actin complex (Balguerie et al., 1999). Further, two-hybrid screens and phage-display screens have identified several physical interactors of Rvs167 that have known roles in the actin cytoskeleton. These include Acf2, Act1 (Drees et al., 2001), Las17 (Bon et al., 2000; Colwill et al., 1999), Abp1, Sla1, Sla2 and Srv2 (Tong et al., 2002). In addition, various synthetic lethal or negative growth synergistic genetic interactions have been identified between *RVS167* and actin cytoskeleton genes, such as *ACT1, MYO1* and *MYO2* (Breton and Aigle, 1998), *SLA1*, *SLA2*, *SAC6*, *SRV2* (Lila and Drubin, 1997) and *VPS21* (Singer-Kruger and Ferro-Novick, 1997). Based on these observations, it is believed that Rvs167 may function as an adaptor to congregate several proteins that are involved in the process of actin rearrangement process at specific places or times in the yeast life cycle. Thus, Rvs167 (and Rvs161) plays an important but perhaps redundant role in organizing the actin cytoskeleton (Friesen et al., 2003).

Rvs167 is a phosphorylation target of Pho85-Pcl1/2 kinase

The function of Rvs167 appears to be regulated by phosphorylation. Rvs167 is phosphorylated *in vivo* at several sites near or within its C-terminal SH3 domain. Phosphorylation of three major sites of Rvs167 is mediated by the Pho85-Pcl2 complex (Friesen et al., 2003). In fact, Rvs167 is the first substrate identified for the Pho85-Pcl1/2 Cdk-cyclin complex, and both two-hybrid and direct interactions of Rvs167 with Pcl2 and Pcl9 have been demonstrated. It was

suggested that phosphorylation of Rvs167 by the Pho85-Pcl1/2 complex may influence either the association of Rvs167 with Abp1, Rvs161 and Sla2/End4 or the subcellular localization of these Rvs167-interacting proteins (Lee et al., 1998). Consistent with the importance of phosphorylation of Rvs167 for its actin cytoskeleton function, cells lacking Pho85 or Pcl1/2 subfamily cyclins display many phenotypes similar to those of *rvs167* mutant and other mutants with defects in actin function. These phenotypes include abnormalities in actin cytoskeleton, fluid-phase endocytosis and bud-site selection in diploids (Lee et al., 1998). The function of Rvs167 in actin cytoskeleton described above and its regulation by G1 Pho85-Pcl1/2 complexes provide a potential mechanistic link to synchronize actin cytoskeleton organization with cell cycle progression.

1.10 THE CELL WALL

Cell wall biosynthesis and the actin cytoskeleton

During polarized growth of the bud or mating projection, the cell wall undergoes dynamic remodeling, which involves weakening of the existing cell wall by digestive enzymes to allow cell expansion, insertion of the new plasma membrane at the cell surface, and synthesis of new cell wall by biosynthetic enzymes (Pruyne and Bretscher, 2000b). Actin patches provide sites where deposition of new cell wall material occurs (Mulholland et al., 1994) and actin cables serve as tracks for the translocation of vesicles containing new plasma membrane and cell wall material to the sites of polarized growth (Pruyne et al., 1998). Consistent with the role of these actin cytoskeleton structures in the process of cell wall biosynthesis, high concentrations of membrane vesicles are present in the buds of small-budded cells (Madden and Snyder, 1998).

The cell wall in *S. cerevisiae* is a complex structure of cross-linked chitin, β-(1,3) D-glucan, β-(1,6) D-glucan and mannoproteins. It serves as a rigid but dynamic structure that maintains the shape of the cell and it also affords

mechanical protection to the cell (Raclavsky, 1998). Additionally, cell wall also contributes to yeast cell polarity through the asymmetric deposition of structural components such as chitin and septin, and also by allowing proper polarization of bud-site selection components and actin organization machinery. Mutations that affect cell wall synthesis lead to defects in bud-site selection, and removal of the cell wall results in actin delocalization (Madden and Snyder, 1998). The Rho1 and Rho2 GTPases and the Pkc1-MAP kinase pathway described below regulate the synthesis and maintenance of the cell wall during budding and environmental stress conditions.

Cell wall biosynthesis and Rho1/Rho2 GTPases

RHO1 is an essential gene whereas *RHO2* is not. Both genes encode partially redundant Rho-type GTPases and overexpression of *RHO2* can suppress the defects of *rho1* mutant (Madaule et al., 1987). When activated by its GEFs Rom1 and Rom2 (Ozaki et al., 1996), Rho1-GTP can stimulate cell wall synthesis directly by functioning as a regulatory subunit of the β-1,3-glucan synthase complex that contains Fks1 or Fks2 as its catalytic subunit (Drgonova et al., 1996; Qadota et al., 1996). Rho1 also partakes in cell wall synthesis indirectly by activating protein kinase C (Pkc1) (Kamada et al., 1996), which in turn upregulates wall-enzyme transcription through the Mpk1 MAPK cascade (also called the cell integrity pathway) (Cabib et al., 1998; Schmidt and Hall, 1998; Figure 1.8). Consistent with its role in cell wall biosynthesis, Rho1 is localized at growth sites (Drgonova et al., 1996). Expansion of the growing buds in *rho1* cells outpaces the synthesis of cell wall material at the bud tip, resulting in a cell wall defect. Consequently, small-budded *rho1* mutants lyse at their bud tips (Yamochi et al., 1994).

Although the Rho1 and Rho2 GTPases function primarily in the process of cell wall biosynthesis, the Rho1 GTPase also participates in the processes of actin

cytoskeleton organization and cell cycle progression. The role of Rho1 in actin cytoskeleton organization is evident from the phenotype of some *rho1* mutants that exhibit depolarized actin cytoskeleton. Rho1 mediates its actin cytoskeleton function either via Pkc1 (Helliwell et al., 1998) or the formin Bni1 (Kohno et al., 1996). Bni1 interacts with several actin-binding proteins (profilin, tropomyosins, and Bud6/Aip3) and it functions in the nucleation of actin filaments (Evangelista et al., 1997; Pruyne et al., 2002; Sagot et al., 2002).

The role of Rho1 in modulating G1 Cdk-cyclin activity and cell cycle progression is inferred from the phenotype of a class of *rho1* mutants that arrest as unbudded cells and exhibit a defect in progressing through START (Drgonova et al., 1999).

The cell integrity pathway

This pathway operates during periods of polarized growth to facilitate proper construction of the cell wall, thus preventing cell lysis (Figure 1. 8). Multiple stimuli - including mating pheromone, heat shock, hypo-osmotic shock, actin depolymerization, as well as treatment of cells with chlorpromazine, caffeine, vanadate, zymolyase, congo red, calcofluor and rapamycin - have been shown to activate this stress response pathway (Harrison et al., 2004). Several plasma membrane glycoproteins, including Wsc1, Wsc2, Wsc3 and Mid2, act as 'stress sensors' and transduce a signal to activate Rom1 and Rom2, the nucleotide exchange factors for the Rho1 GTPase (Rajavel et al., 1999; Verna et al., 1997). GTP-bound Rho1 in turn activates Pkc1, the critical protein kinase C component of this signaling pathway (Kamada et al., 1996). Activated Pkc1 then initiates sequential activation of the MAP kinase cascade of the pathway, which comprises of Bck1 (the MAP kinase kinase kinase), Mkk1 and Mkk2 (the two redundant MAP kinase kinases) and Mpk1/Slt2 (the terminal MAP kinase).

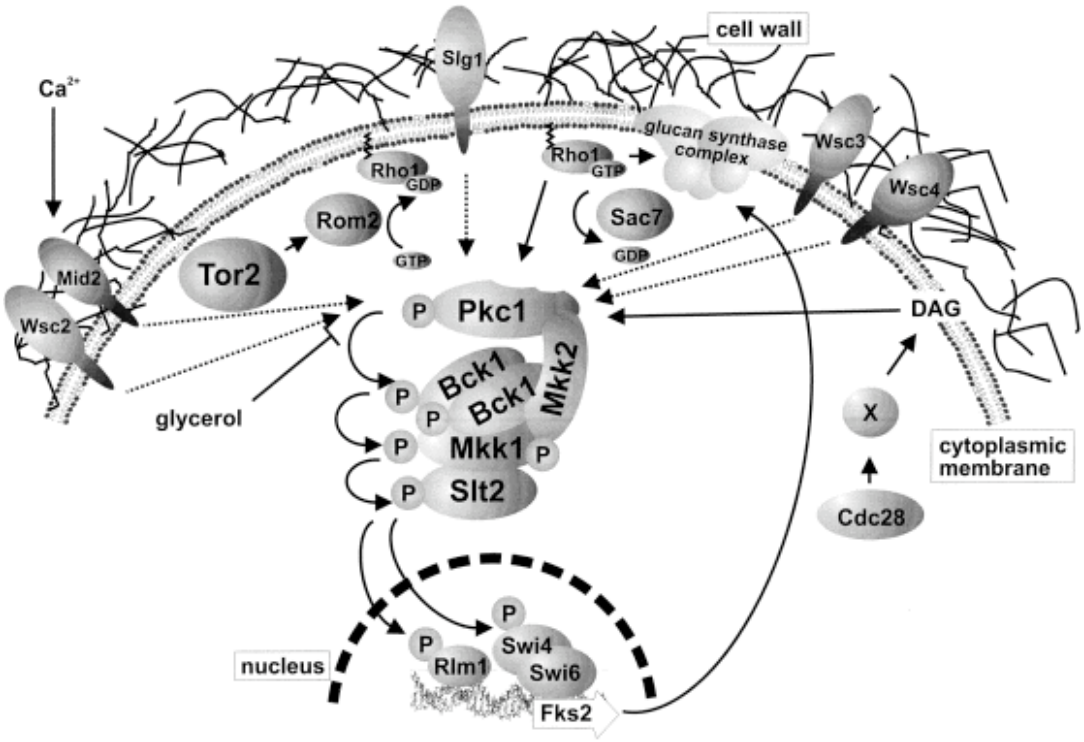

Figure 1.8 The schematic of the yeast Pkc1 pathway. Shown here are the major components of the pathway. Dotted arrows indicate activation of the Pkc1p pathway in which the detailed mechanisms of signal transmission are not yet known. Component 'X' reflects the fact that the connection between cell cycle regulation and DAG levels remains to be elucidated (Heinisch et al., 1999).

Upon activation, Mpk1 phosphorylates Rlm1, a MADS box family transcription factor that regulates the expression of several genes that are involved in cell wall biosynthesis and maintenance (Watanabe et al., 1997). Mpk1 also activates the SBF and MBF transcription factor complexes via phosphorylation of their components Swi4 and Swi6 (Heinisch et al., 1999). Expression profiling results have shown that ~27% of SBF target genes are involved in budding and cell wall biogenesis-related processes. These targets include G1 cyclin genes such as *CLN1*, *CLN2*, *PCL1* and *PCL2*, and cell wall biosynthesis genes such as *CHS3*, *FKS1* and *MNN1* (Iyer et al., 2001). Thus, the

function of the Pkc1-MAP kinase pathway is to upregulate the expression of G1 cyclin genes and cell wall biosynthesis genes, all of which encode proteins that have important roles in polarized cell growth.

Mutants in each component of the cell integrity pathway (from Rho1 to Mpk1) exhibit a similar phenotype. They lyse as small-budded cells and this lysis defect that can be rescued by an osmotically stabilized medium. The observation that *PKC1* (and *RHO1*) is essential at all temperatures whereas the other downstream kinases are only essential at 37°C suggests that Pkc1 may regulate additional downstream targets important for cell integrity (Heinisch et al., 1999). Consistent with the role of Pkc1 in cell wall biogenesis, the cell wall ultrastructure in Pkc1-depleted cells shows an ~60% reduction in thickness compared to that of wild-type cells (Levin et al., 1994).

Until recently, it was believed that the cell integrity pathway operates in a linear 'top-down' manner. However, recent work has suggested that depending upon the nature of the stress, at least three different kinases acting between Rho1 and Mpk1 can feed the signal into the pathway, and thereby provide 'lateral' inputs into the pathway (Harrison et al., 2004). Another pathway constituting the Bck2 kinase and the Ppz1/2 protein phosphatases is also proposed to operate downstream of Pkc1 but parallel to the Bck1-Mkk1/2-Mpk1 mediated pathway. This pathway also participates in regulating the expression of genes that are under the control of the SBF and MBF transcription factors (Di Como et al., 1995; Lee et al., 1993).

Rvs proteins and cell wall biosynthesis/integrity

In addition to their role in the actin cytoskeleton organization, the Rvs161 and Rvs167 proteins are also implicated to function in the cell wall biosynthesis/integrity pathway. Synthetic genetic interactions observed between *mpk1* and each *rvs* mutation, together with the rescue of this lethal phenotype by

an osmotic stabilizer such as sorbitol, suggest that the Rvs proteins function in a pathway that is parallel to the Pkc1-MAP kinase pathway to control the integrity of the cell. Further, the synthetic phenotype of *rvs161 mpk1* cells and *rvs167 mpk1* cells is very similar to the phenotype of *pkc1* mutants, thus suggesting that the function of the Rvs proteins in cell wall biosynthesis/integrity may be under direct or indirect control of Pkc1 (Breton et al., 2001). In this capacity, Mpk1 is proposed to monitor the production of cargoes required for cell wall organization via Rlm1, whereas the Rvs proteins might be required for proper delivery of those cargoes at the plasma membrane (Breton et al., 2001). The accumulation of late secretory vesicles at sites of membrane and cell wall construction in *rvs* mutants as well as the two-hybrid interactions between Rvs167 and the exocyst complex components Sec8 and Exo70 (Bon et al., 2000) further support the role for the Rvs proteins in late targeting of vesicles whose cargoes are required for cell wall construction.

In summary, polarized morphogenesis in budding yeast requires the essential Cdc42 GTPase, which enables the establishment of the actin organization machinery at sites of polarized growth. The asymmetric rearrangement of actin cytoskeleton in turn directs the secretion and the cell wall biosynthesis machineries to regions of active growth. Cross talk between the Rho1-4 GTPases, Cdc42, Cdk-cyclin complexes and actin organization machinery is critical for the coordination of spatial regulation of budding and cytokinesis with the temporal execution of the cell cycle.

1.11 RESEARCH OBJECTIVE AND CHAPTERS TO FOLLOW

As mentioned earlier, the recruitment and activation of the Cdc42 GTPase at sites of polarization is of critical significance for both the establishment and maintenance of cell polarity. Based on genetic and biochemical evidences that demonstrate the interaction between activated Cdc42 and Gic1/2 as well as the

mutant phenotypes of *gic1 gic2* cells, it is clear that the Gic proteins function as downstream effectors of Cdc42 in mediating asymmetric arrangement of the actin cytoskeleton. However, the mechanism by which they mediate this function is poorly understood. The main objective of this research has been to obtain greater insights into the function of the Gic1/Gic2 proteins. I have attempted to address this question by genetically identifying proteins that functionally interact with the Gic proteins and participate in the process of polarized morphogenesis. Following Chapter 2 that outlines the strains, plasmids and experimental techniques employed in this study, Chapter 3 delves into the details of high-copy suppressors of *gic1 gic2* mutant cells. Included in this chapter are two sections, describing the characterization of two structurally and functionally related pairs of genes – *VHS2/MLF3* and *MGC1/TOS2*. Chapter 4 entails the study on synthetic lethal interactors of *gic1 gic2* cells. Lastly, Chapter 5 includes the concluding remarks highlighting the major findings of this investigation.

CHAPTER 2

Materials and Methods

2.1 Strains, Media, and Genetic techniques

The yeast strains used in this study are listed in Table 2.1. Yeast cultures were grown in rich medium YEPD (1% yeast extract, 2% peptone, and 2% glucose) unless otherwise stated. Synthetic minimal medium (SD; 0.17% yeast nitrogen base without amino acids and ammonium sulfate, 0.5% ammonium sulfate, and 2% glucose) supplemented with appropriate nutrients (Rose et al., 1990) was used to select for plasmid maintenance. Cells were routinely grown at 26°C unless otherwise specified. Yeast transformation was carried out by the lithium acetate method (Gietz et al., 1992). Standard genetic methods such as complementation analysis, mating, and tetrad dissection were performed as described by Rose et al. (Rose et al., 1990).

Deletions and modifications of chromosomal genes (C- or N- terminal epitope tagging and placement of full-length gene under regulatable *GAL1* promoter) by homologous recombination technique were carried out using a one-step PCR method as described by Longtine et al. (1998b).

Table 2.1 Yeast strains used in this study.

Strain	Genotype	
1064	α	*cdc3-3 leu2 ura3*
CCY471-13C	*a*	*ade2 his3Δ-200 leu2-3,112 ura3-52 bem2-101*
CCY1024-3A	*a*	*lys2-801 his3-Δ200 leu2-3,112 trp1-1 ura3-52 gic1-Δ1::LEU2 gic2-1::HIS3*
CCY1024-19C	α	*his3-Δ200 leu2-3,112 trp1-1 ura3-52 gic1-Δ1::LEU2 gic2-1::HIS3*

CCY1137-3B	*a*	*ade2 his3-Δ200 leu2-3,112 ura3-52 trp1-1 cyk2-Δ101::spHIS5* with pCC1368 (CEN, *URA3, CYK2*)
CCY1145-1B	*a*	*lys2-801 lys2-801 his3-Δ200 leu2-3,112 trp1-1 ura3-52 tos2-Δ1::spHIS5*
CCY1145-9D	α	*ade2 lys2-801 his3-Δ200 leu2-3,112 trp1-1 ura3-52 tos2-Δ1::spHIS5*
CCY1145-12D	α	*lys2-801 his3-Δ200 leu2-3,112 trp1-1 ura3-52 tos2Δ1::spHIS5*
CCY1147-3A	*a*	*ade2 his3-Δ200 leu2-3,112 ura3-52 trp1-1 TOS2-3HA::spHIS5*
CCY1151-1B	*a*	*lys2-801 his3-Δ200 leu2-3,112 trp1-1 ura3-52 mgc1-Δ1::kan*
CCY1151-1D	α	*ade2 lys2-801 his3-Δ200 leu2-3,112 trp1-1 ura3-52 mgc1-Δ1::kan*
CCY1152-3B	*a*	*ade2 his3-Δ200 leu2-3,112 trp1-1 ura3-52 mgc1-Δ1::kan tos2-Δ1::spHIS5*
CCY1152-5C	α	*lys2-801 his3-Δ200 leu2-3,112 trp1-1 ura3-52 mgc1-Δ1::kan tos2-Δ1::spHIS5*
CCY1152-8B	*a*	*lys2-801 his3-Δ200 leu2-3,112 trp1-1 ura3-52 mgc1-Δ1::kan tos2Δ1::spHIS5*
CCY1154-2D	α	*lys2-801 his3-Δ200 leu2-3,112 trp1-1 ura3-52 MGC1-GFP::spHIS5*
CCY1165-1C	*a*	*lys2-801 his3-Δ200 leu2-3,112 ura3-52 trp1-1 MGC1-3HA::spHIS5*
CCY1176-1B	*a*	*ade2 his3-Δ200 leu2-3,112 trp1-1 ura3-52 mgc1-Δ1::kan tos2-Δ2::URA3*
CCY1176-10B	α	*lys2-801 his3-Δ200 leu2-3,112 trp1-1 ura3-52 mgc1-Δ1::kan*
CCY1176-11A	α	*lys2-801 his3-Δ200 leu2-3,112 trp1-1 ura3-52 mgc1-Δ1::kan tos2Δ2::URA3*
CCY1244-4D	α	*his3-Δ200 leu2-3,112 trp1-1 ura3-52 cyk2-Δ101::spHIS5*
CCY1244-7C	α	*his3-Δ200 leu2-3,112 trp1-1 ura3-52 cyk2-Δ101::spHIS5 mgc1-Δ1::kan*
CCY1244-10D	α	*his3-Δ200 leu2-3,112 trp1-1 ura3-52 cyk2-Δ101::spHIS5*

		tos2-Δ2::URA3
CCY1244-17C	α	*his3-Δ200 leu2-3,112 trp1-1 ura3-52 cyk2-Δ101::spHIS5 mgc1-Δ1::kan tos2-Δ2::URA3*
CCY1292-1A	*a*	*lys2-801 his3-Δ200 leu2-3,112 trp1-1 ura3-52*
CCY1292-1D	*a*	*lys2-801 his3-Δ200 leu2-3,112 trp1-1 ura3-52 mlf3-Δ1::kan*
CCY1292-4B	*a*	*lys2-801 his3-Δ200 leu2-3,112 trp1-1 ura3-52 vhs2-Δ1::TRP1*
CCY1292-5B	*a*	*lys2-801 his3-Δ200 leu2-3,112 trp1-1 ura3-52 vhs2-Δ1::TRP1 mlf3-Δ1::kan*
CCY1292-10C	α	*lys2-801 his3-Δ200 leu2-3,112 trp1-1 ura3-52 vhs2-Δ1::TRP1 mlf3-Δ1::kan*
CCY1338	*a*/α	*ade2/+ lys2-801/+ his3-Δ200/his3-Δ200 leu2-3,112/leu2-3,112 trp1-1/trp1-1 ura3-52/ura3-52 vhs2-Δ1::TRP1/ vhs2-Δ1::TRP1 mlf3-Δ1::kan/mlf3-Δ1::kan*
CCY1368-4C	α	*lys2-801 his3-Δ200 leu2-3,112 trp1-1 ura3-52 cla4- Δ101::URA3*
CCY1368-8C	α	*lys2-801 his3-Δ200 leu2-3,112 trp1-1 ura3-52 vhs2-Δ1::TRP1 mlf3-Δ1::kan cla4-Δ101::URA3*
CCY1368-12A	α	*lys2-801 his3-Δ200 leu2-3,112 trp1-1 ura3-52 vhs2-Δ1::TRP1 mlf3-Δ1::kan*
CCY1380-1C	*a*	*his3Δ1 leu2Δ0 ura3Δ0 lys2Δ0 met15Δ0 gic1-Δ2::kan*
CCY1380-1C-1	*a*	*his3Δ1 leu2Δ0 ura3Δ0 lys2Δ0 met15Δ0 gic1-Δ3::natR*
CCY1446-1A	α	*his3Δ1 leu2Δ0 ura3Δ0 lys2Δ0 met15Δ0 gic1-Δ3::natR gic2-Δ3::URA3 can1Δ::MFApr-HIS3-MFα1pr-LEU2*
CCY1447	α	*his3Δ1 leu2Δ0 ura3Δ0 lys2Δ0 met15Δ0 can1Δ::MFApr-HIS3-MFα1pr-LEU2 gic2-Δ3::URA3*
CCY1456-4B	*a*	*ade2 his3-Δ200 leu2-3,112 trp1-1 ura3-52 mlf3-Δ2::spHIS5 rvs161-Δ::kan*
CCY1456-7A	α	*ade2 his3-Δ200 leu2-3,112 trp1-1 ura3-52 vhs2-Δ1::TRP1 mlf3-Δ2::spHIS5 rvs161-Δ::kan*

CCY1456-10D	α	*lys2-801 his3-Δ200 leu2-3,112 trp1-1 ura3-52 vhs2-Δ1::TRP1 rvs161-Δ::kan*
CCY1456-11B	*a*	*lys2-801 his3-Δ200 leu2-3,112 trp1-1 ura3-52 rvs161-Δ::kan*
CCY1457-2C	*a*	*lys2-Δ0 his3-Δ200 leu2-3,112 trp1-1 ura3-52 mlf3-Δ2::spHIS5 rvs167-Δ::kan*
CCY1457-6C	*a*	*lys2-Δ0 his3-Δ200 leu2-3,112 trp1-1 ura3-52 vhs2-Δ1::TRP1 rvs167-Δ::kan*
CCY1457-7C	*a*	*lys2-Δ0 his3-Δ200 leu2-3,112 trp1-1 ura3-52 vhs2-Δ1::TRP1 mlf3-Δ2::spHIS5 rvs167-Δ::kan*
CCY1457-8B	*a*	*lys2-Δ0 his3-Δ200 leu2-3,112 trp1-1 ura3-52 rvs167-Δ::kan*
CCY1502-1D	*a*	*lys2-801 his3-Δ200 leu2-3,112 trp1-1 ura3-52 MGC1-GFP::spHIS5 gic1-Δ1::LEU2 gic2-Δ2::TRP1*
CCY1516-1D	α	*his3Δ1 leu2Δ0 ura3Δ0 lys2Δ0 cap1Δ::kan*
CCY1517-2C	α	*his3Δ1 leu2Δ0 ura3Δ0 lys2Δ0 cap2Δ::kan*
CCY1518-1A	α	*his3Δ1 leuΔ0 ura3Δ0 lys2Δ0*
CCY1523-1D	α	*his3Δ1 leu2Δ0 ura3Δ0 lys2Δ0 ilm1Δ::kan*
CCY1525-3C	α	*his3Δ1 leu2Δ0 ura3Δ0 las21Δ::kan*
CCY1530-8A	α	*his3Δ1 leu2Δ0 ura3Δ0 ric1Δ::kan*
CCY1532-1A	α	*his3Δ1 leu2Δ0 ura3Δ0 lys2Δ0 smi1Δ::kan*
CCY1533-3C	α	*his3Δ1 leu2Δ0 ura3Δ0 sur7Δ::kan*
CCY1542-1C	α	*his3Δ1 leu2Δ0 ura3Δ0 ygr228wΔ::kan*
CCY1546-4A	α	*his3Δ1 leu2Δ0 ura3Δ0 lys2Δ0 ylr374cΔ::kan*
CCY1547-4A	α	*his3Δ1 leu2Δ0 ura3Δ0 lys2Δ0 vam10Δ::kan*
CCY1548-2C	α	*his3Δ1 leu2Δ0 ura3Δ0 ypl144wΔ::kan*

CCY1551-11B	*a*	*his3Δ1 leu2Δ0 ura3Δ0 met15Δ0 gic1-Δ3::natR gic2-Δ3::URA3*
CCY1551-12A	*a*	*his3Δ1 leu2Δ0 ura3Δ0 met15Δ0 gic1-Δ3::natR gic2-Δ3::URA3 can1Δ::MFApr-HIS3-MFα1pr-LEU2*
CCY1551-1B	α	*his3Δ1 leu2Δ0 ura3Δ0 gic1-Δ3::natR gic2-Δ3::URA3 can1Δ::MFApr-HIS3-MFα1pr-LEU2*
CCY1551-2D	*a*	*his3Δ1 leu2Δ0 ura3Δ0 lys2Δ0 gic1-Δ3::natR gic2-Δ3::URA3*
CCY1551-3B	α	*his3Δ1 leu2Δ0 ura3Δ0 lys2Δ0 gic1-Δ3::natR gic2-Δ3::URA3*
CCY1551-3C	*a*	*his3Δ1 leu2Δ0 ura3Δ0 met15Δ0 gic1-Δ3::natR gic2-Δ3::URA3 can1Δ::MFApr-HIS3-MFα1pr-LEU2*
CCY1551-5C	α	*his3Δ1 leu2Δ0 ura3Δ0 gic1-Δ3::natR gic2-Δ3::URA3 can1Δ::MFApr-HIS3-MFα1pr-LEU2*
CCY1551-8B	α	*his3Δ1 leu2Δ0 ura3Δ0 lys2Δ0 gic1-Δ3::natR gic2-Δ3::URA3*
CCY1554-4A	α	*lys2Δ0 his3Δ1 leu2Δ0 ura3Δ0 gic1Δ::natR gic2Δ::URA3 ilm1Δ::kan*
CCY1556-5A	α	*his3Δ1 leu2Δ0 ura3Δ0 gic1Δ::natR gic2Δ::URA3 las21Δ::kan*
CCY1559-1C	α	*lys2Δ0 his3Δ1 leu2Δ0 ura3Δ0 gic1Δ::natR gic2Δ::URA3 pre9Δ::kan*
CCY1559-21B	α	*lys2Δ0 his3Δ1 leu2Δ0 ura3Δ0 pre9Δ::kan*
CCY1561-8B	α	*his3Δ1 leu2Δ0 ura3Δ0 gic1Δ::natR gic2Δ::URA3 sur7Δ::kan*
CCY1567-1C	*a*	*his3Δ1 leu2Δ0 ura3Δ0 gic1Δ::natR gic2Δ::URA3 ypl144wΔ::kan*
CCY1569-5D	α	*his3Δ1 leu2Δ0 ura3Δ0 gic1Δ::natR gic2Δ::URA3 smi1Δ::kan*
CCY1571-5D	α	*lys2Δ0 his3Δ1 leu2Δ0 ura3Δ0 gic1Δ::natR gic2Δ::URA3 ypt6Δ::kan*
CCY1571-14A	α	*met15Δ0 his3Δ1 leu2Δ0 ura3Δ0 ypt6Δ::kan*
CCY1574-6B	α	*lys2Δ01 his3Δ1 leu2Δ0 ura3Δ0 gic1Δ::natR gic2Δ::URA3 ygr228wΔ::kan*
CCY1575-2B	α	*lys2Δ0 his3Δ1 leu2Δ0 ura3Δ0 gic1Δ::natR gic2Δ::URA3 ylr374cΔ::kan*
CCY1585-4B	α	*lys2Δ0 his3Δ1 leu2Δ0 ura3Δ0 gic1Δ::natR gic2Δ::URA3 cap1Δ::kan*

CCY1586-6C	α	*lys2Δ0 his3Δ1 leu2Δ0 ura3Δ0 gic1Δ::natR gic2Δ::URA3 cap2Δ::kan*
CCY1587-7C	α	*lys2Δ0 his3Δ1 leu2Δ0 ura3Δ0 gic1Δ::natR gic2Δ::URA3 vam10Δ::kan*
CCY1590-3B	α	*lys2Δ0 his3 Δ1 leu2Δ0 ura3Δ0 axl2Δ::kan*
CCY1594-3B	α	*lys2Δ0 his3Δ1 leu2Δ0 ura3Δ0 cla4Δ::kan*
CCY1595-3B	α	*his3Δ1 leu2Δ0 ura3Δ0 msb3Δ::kan*
CCY1596-4A	α	*met15Δ his3Δ1 leu2Δ0 ura3Δ0 pea2Δ::kan*
CCY1598-1D	α	*his3Δ1 leu2Δ0 ura3Δ0 spa2Δ::kan*
CCY1599-1A	α	*lys2Δ0 his3Δ1 leu2Δ0 ura3Δ0 ssd1Δ::kan*
CCY1601-10C	α	*lys2Δ0 his3Δ1 leu2Δ0 ura3Δ0 bni1Δ::kan*
CCY1601-11C	α	*lys2Δ0 his3Δ1 leu2Δ0 ura3Δ0 gic1Δ::natR gic2Δ::URA3 bni1Δ::kan*
CCY1602-1C	α	*lys2Δ0 met15Δ0 his3Δ1 leu2Δ0 ura3Δ0 bud6Δ::kan*
CCY1602-5A	α	*lys2Δ0 met15Δ0 his3Δ1 leu2Δ0 ura3Δ0 gic1Δ::natR gic2Δ::URA3 bud6Δ::kan*
CCY1603-7A	α	*lys2Δ01 his3Δ1 leu2Δ0 ura3Δ0 gic1Δ::natR gic2Δ::URA3 cla4Δ::kan*
CCY1604-6D	α	*lys2Δ0 met15 Δ0 his3Δ1 leu2Δ0 ura3Δ0 gic1Δ::natR gic2Δ::URA3 msb3Δ::kan*
CCY1605-3A	α	*lys2Δ0 his3Δ1 leu2Δ0 ura3Δ0 gic1Δ::natR gic2Δ::URA3 pea2Δ::kan*
CCY1606-11A	*a*	*lys2Δ0 his3Δ1 leu2Δ0 ura3Δ0 gic1Δ::natR gic2Δ::URA3 rsr1Δ::kan*
CCY1606-5B	α	*lys2Δ0 his3Δ1 leu2Δ0 ura3Δ0 rsr1Δ::kan*
CCY1607-2D	α	*met15Δ0 his3Δ1 leu2Δ0 ura3Δ0 gic1Δ::natR gic2Δ::URA3 ssd1Δ::kan*
CCY1608-6A	α	*lys2Δ0 his3Δ1 leu2Δ0 ura3Δ0 gic1Δ-3::natR gic2Δ-3::URA3 axl2Δ::kan*
CCY1609-5A	α	*his3Δ1 leu2Δ0 ura3Δ0 gic1Δ::natR gic2Δ::URA3 spa2Δ::kan*

CCY1617-1B	α	*met15Δ0 his3 Δ1 leu2Δ0 ura3Δ0 est2Δ::kan*
CCY1618-2B	*a*	*lys2Δ0 his3 Δ1 leu2Δ0 ura3Δ0 nbp2Δ::kan*
CCY1625-1C	α	*his3Δ1 leu2Δ0 ura3Δ0 erv14Δ::kan*
CCY1627-1D	α	*lys2Δ0 his3 Δ1 leu2Δ0 ura3Δ0 ymr124wΔ::kan*
CCY1635-1B	α	*his3Δ1 leu2Δ0 ura3Δ0 swi4Δ::kan*
CCY1642-8D	α	*met15Δ0 his3Δ1 leu2Δ0 ura3Δ0 gic1Δ::natR gic2Δ::URA3 est2Δ::kan*
CCY1643-4B	α	*his3Δ1 leu2Δ0 ura3Δ0 gic1Δ::natR gic2Δ::URA3 erv14Δ::kan*
CCY1649-13B	α	*lys2Δ0 his3Δ1 leu2Δ0 ura3Δ0 gic1Δ::natR gic2Δ::URA3 nem1Δ::kan*
CCY1649-16C	α	*lys2Δ0 his3Δ1 leu2Δ0 ura3Δ0 nem1Δ::kan*
CCY1651-2A	α	*his3Δ1 leu2Δ0 ura3Δ0 gic1Δ::natR gic2Δ::URA3 swi4Δ::kan*
CCY1652-2A	*a*	*his3Δ1 leu2Δ0 ura3Δ0 gic1Δ::natR gic2Δ::URA3 ymr124wΔ::kan*
CCY1654-4B	α	*lys2Δ0 his3Δ1 leu2Δ0 ura3Δ0 gic1Δ::natR gic2Δ::URA3 ric1Δ::kan*
CCY1661-3A	α	*his3Δ1 leu2Δ0 ura3Δ0 gic1Δ::natR gic2Δ::URA3 nbp2Δ::kan*
CCY1662-1A	α	*his3Δ1 leu2Δ0 ura3Δ0 gic1Δ::natR gic2Δ::URA3 sur4Δ::kan*
CCY1662-1C	α	*his3Δ1 leu2Δ0 ura3Δ0 sur4Δ::kan*
CCY1663-3C	α	*ade2 his3-Δ200 leu2-3,112 trp1-1 ura3-52 VHS2-3HA-kanMX6 MLF3-13MYC-spHIS5*
CCY1664	*a*/α	*ade2/+ his3-Δ200/his3-Δ200 leu2-3,112/leu2-3,112 trp1-1/ trp1-1 ura3-52/ ura3-52 VHS2-3HA-kanMX6/ VHS2-3HA-kanMX6 MLF3-13MYC-spHIS5/MLF3-13MYC-spHIS5*
CCY1708-1A	*a*	*ade2 his3-Δ200 leu2-3,112 lys2-801 ura3-52 spHIS5-PGAL1-3HA-MGC1*
CCY1709-2B	*a*	*his3-Δ200 leu2-3,112 lys2-801 ura3-52 spHIS5-PGAL1-3HA-TOS2*
CCY1710-3C	*a*	*ade2 his3-Δ200 leu2-3,112 lys2-801 ura3-52*

CCY1710-7B	*a*	*his3-Δ200 leu2-3,112 lys2-801 ura3-52 spHIS5-PGAL1-3HA-MGC1 spHIS5-PGAL1-3HA-TOS2*
CCY1720	*a/α*	*ade2/+ lys2-801/+ his3-Δ200/his3-Δ200 leu2-3,112/leu2-3,112 trp1-1/trp1-1 ura3-52/ura3-52 vhs2-Δ1::TRP1/vhs2-Δ1::TRP1*
CCY1721	*a/α*	*ade2/+ lys2-801/+ his3-Δ200/his3-Δ200 leu2-3,112/leu2-3,112 trp1-1/trp1-1 ura3-52/ura3-52 mlf3-Δ1::kan/mlf3-Δ1::kan*
CCY1726-18C	*α*	*lys2-801 his3-Δ200 leu2-3,112 trp1-1 ura3-52 gic1-Δ1::LEU2 gic2-1::HIS3*
CCY1726-2B	*α*	*lys2-801 his3-Δ200 leu2-3,112 trp1-1 ura3-52 gic1-Δ1::LEU2 gic2-1::HIS3 vhs2-Δ1::TRP1*
CCY1726-4D	*α*	*lys2-801 his3-Δ200 leu2-3,112 trp1-1 ura3-52 gic1-Δ1::LEU2 gic2-1::HIS3 vhs2-Δ1::TRP1 mlf3-Δ1::kan*
CCY1726-5B	*α*	*lys2-801 his3-Δ200 leu2-3,112 trp1-1 ura3-52 gic1-Δ1::LEU2 gic2-1::HIS3 mlf3-Δ1::kan*
CCY1746-3A	*α*	*cdc3-3 leu2 ura3 MGC1-GFP::spHIS5*
CCY1830-51-1-4	*a/α*	*ade2/+ lys2-801/+ his3-Δ200/his3-Δ200 leu2-3,112/leu2-3,112 trp1-1/trp1-1 ura3-52/ura3-52 gic1-Δ1::LEU2/+ gic2-1::HIS3/+ vhs2-Δ1::TRP1/+*
CCY1830-51-1-5	*a/α*	*ade2/+ lys2-801/+ his3-Δ200/his3-Δ200 leu2-3,112/leu2-3,112 trp1-1/trp1-1 ura3-52/ura3-52 gic1-Δ1::LEU2/+ gic2-1::HIS3/+ vhs2-Δ1::TRP1/+*
CCY1830-67	*a/α*	*ade2/+ lys2-801/+ his3-Δ200/his3-Δ200 leu2-3,112/leu2-3,112 trp1-1/trp1-1 ura3-52/ura3-52 tos2-Δ1::spHIS5/+*
CCY1830-72	*a/α*	*ade2/+ lys2-801/+ his3-Δ200/his3-Δ200 leu2-3,112/leu2-3,112 trp1-1/trp1-1 ura3-52/ura3-52 mgc1-Δ1::kan /+*
CCY1830-74	*a/α*	*ade2/+ lys2-801/+ his3-Δ200/his3-Δ200 leu2-3,112/leu2-3,112 trp1-1/trp1-1 ura3-52/ura3-52 MGC1-GFP::spHIS5/+*
DBY1828	*α*	*ade2 his3-Δ200 leu2-3,112 trp1-1 ura3-52*
DBY1829	*α*	*lys2-801 his3-Δ200 leu2-3,112 trp1-1 ura3-52*

DBY1830	*a/α*	*ade2/+ lys2-801/+ his3-Δ200/his3-Δ200 leu2-3,112/leu2-3,112 trp1-1/trp1-1 ura3-52/ura3-52*
EGY48	*α*	*his3 ura3-52 trp1 leu2::3Lexop-LEU2*
Y3656	*α*	*his3Δ1 leu2Δ0 ura3Δ0 lys2Δ0 met15Δ0 can1Δ::MFApr-HIS3-MFα1pr-LEU2*

Most of the strains were constructed specifically for this study, with the following exceptions:

- Strains DBY1828, DBY1829 and DBY1830 are from D. Botstein's laboratory collection.
- Strain EGY48 is from R. Brent's laboratory collection.
- Strain 1064 is a gift from J. Pringle.
- Strains CCY471-13C, CCY1024-3A, CCY-1024-19C and CCY1137-3B are from C. Chan's laboratory collection.

2.2 DNA MANIPULATION

The plasmids used in this study are listed in Table 2.2. Standard procedures were used for recombinant DNA manipulations (Sambrook, 1989). DNA fragments were eluted from TAE (40 mM Tris-acetate, 1 mM EDTA [pH 8.0]) agarose gels using the Geneclean II kit as recommended by the manufacturer (BIO 101 Inc., La Jolla, CA). Polymerase chain reactions (PCRs) were performed in 50 μl of a reaction containing 100 μM dNTP, 1 mM $MgCl_2$, ~0.5 μM of primers, 100-250 ng of template DNA, 5 μl 10x cloned *Pfx* buffer and 2.5 U cloned *Pfx* DNA polymerase (Invitrogen, Carlsbad, CA). The PCR thermocycler was programmed as follows: one cycle of 5 min. at 94°C, 1 min. at 50°C, 3 min. at 68°C; 25 cycles of 1 min. at 94°C, 1 min. at 50°C, 3 min. at 68°C; and one cycle of 1 min. at 94°C, 1 min. at 50°C, 10 min. at 68°C. PCR products were purified using the QIAquick PCR purification kit according to the instruction of the manufacturer (Qiagen Inc., Valencia, CA).

The *E. coli* strain DB1142 (*leu pro thr hsdR hsdM recA*) was routinely used as host for plasmids. These cells were grown at 37°C in LB medium (1% tryptone,

0.5% yeast extract, 0.5% NaCl) or LB medium supplemented with ampicillin (100 μg/ml).

Table 2.2 Plasmids used in this study.

Plasmid	Relevant Features	Reference or Source
AB440	2μ, *URA3, SIT4*	A. Adam
ACT5/pRS426	2μ, *URA3, ACT5*	J. Cooper
B305	2μ, *URA3, SLT2 (MPK1)*	M. Snyder
B309	2μ, *URA3, BCK1*	M. Snyder
B327	2μ, *URA3, SWI4*	M. Snyder
BK64	2μ, *LEU2, SWI6*	M. Snyder
p167	2μ, *URA3, WSC1^{HA}*	D. Levin
p200	2μ, *URA3, PKC1*	D. Levin
p366	2μ, *LEU2, CLG1*	B. Andrews
p582	2μ, *URA3, MPK1*	D. Levin
p594	2μ, *URA3, MKK1*	D. Levin
p636	CEN, *URA3, BCK1-20*	D. Levin
p669	2μ, *URA3, PPZ2*	D. Levin
p1245	2μ, *URA3, MID2^{HA}*	D. Levin
p4339	pFA6::natRMX4	C. Boone
p2μ-SHM	2μ, *URA3, BEM1*	A. Bender

pAJ181	2μ, *URA3, TUP1*	A. Johnson
pBA531	2μ, *URA3, PCL1*	B. Andrews
pBA623	2μ, *URA3, PCL2*	B. Andrews
pBH124	2μ, *URA3, BCK2*	B. Haarer
pCC75	CEN, *URA3, SSD1-v(1)*	(Kim et al., 1994)
pCC251	2μ, *URA3, BEM2*	Chan Lab
pCC693	2μ, *URA3, RGA1*	Chan Lab
pCC854	2μ, *URA3, LRG1*	Chan Lab
pCC904	2μ, *URA3, GIC1*	(Chen et al., 1997)
pCC933	*2μ, HIS3, LexA-CDC42*	(Simon et al., 1995)
pCC934	*2μ, HIS3, LexA-cdc42* ^{C188S}	(Simon et al., 1995)
pCC935	*2μ, HIS3, LexA-cdc42* $^{G12V, C188S}$	(Simon et al., 1995)
pCC936	*2μ, HIS3, LexA-cdc42* $^{Q16L, C188S}$	(Simon et al., 1995)
pCC937	*2μ, HIS3, LexA-cdc42* $^{D118A, C188S}$	(Simon et al., 1995)
pCC939	*2μ, HIS3, LexA-rho1* ^{C206S}	(Simon et al., 1995)
pCC941	*2μ, HIS3, LexA-rho2* $^{C206S, C189S}$	(Simon et al., 1995)
pCC943	*2μ, HIS3, LexA-rho3* ^{C228S}	(Simon et al., 1995)
pCC945	2μ, *HIS3, LexA-rho4* ^{C228S}	(Simon et al., 1995)
pCC946	2μ, *HIS3, LexA-RSR1*	(Simon et al., 1995)
pCC952	2μ, *HIS3, LexA-rsr1* ^{G12V}	Chan Lab
pCC967	2μ, *URA3, GIC2*	(Chen et al., 1997)
pCC973	2μ, *URA3, SAC7*	Chan Lab
pCC984	2μ, *TRP1, B42* ^{AD} *-GIC1*	(Chen et al., 1997)

pCC985	2μ, *TRP1, B42^{AD}-GIC2*	(Chen et al., 1997)
pCC1044-1	2μ, *TRP1, B42^{AD}-gic1-2*	Chan Lab
pCC1050-1	2μ, *TRP1, B42^{AD}-gic1-3*	Chan Lab
pCC1066-1	2μ, *TRP1, B42^{AD}-gic1-Δ4*	Chan Lab
pCC1079	2μ, *URA3, CLA4*	Chan Lab
pCC1081-1	2μ, *HIS3, LexA-cdc42$^{T35A, C188S}$*	Chan Lab
pCC1107	2μ, *URA3, MSB3*	E. Bi
pCC1108	2μ, *URA3, MSB4*	E. Bi
pCC1215	2μ, *URA3, RPI1*	Chan Lab
pCC1284	2μ, *URA3, MSB2*	This study
pCC1290	2μ, *URA3, RSR1*	This study
pCC1291	2μ, *URA3, AXL2*	This study
pCC1293	2μ, *URA3, SSN6*	This study
pCC1294	2μ, *URA3, NΔ118-STE20*	This study
pCC1295	2μ, *URA3, CLN2*	This study
pCC1333	2μ, *URA3, CYK2*	Chan Lab
pCC1347	2μ, *URA3, SSN6*	Chan Lab
pCC1368	CEN, *URA3, CYK2*	Chan Lab
pCC1478	2μ, *URA3, MGC1*	This study
pCC1492	2μ, *TRP1, TOS2*	This study
pCC1551	2μ, *HIS3, lexA-MGC1* under *pADH1*	This study
pCC1552	2μ, *HIS3, lexA-TOS2* under *pADH1*	This study

pCC1574	2μ, *URA3, TOS2*	This study
pCC1580	2μ, *TRP1, B42^{AD}-MGC1* under *pGAL1*	This study
pCC1581	2μ, *TRP1, B42^{AD}-TOS2* under *pGAL1*	This study
pCC1606	2μ, *URA3, VHS2*	This study
pCC1635	2μ, *URA3, MLF3*	This study
pCC1644	2μ, *URA3, VHS2, MLF3*	This study
pCC1658	CEN, *URA3, GFP^{S65T}-VHS2* under *pACT1*	This study
pCC1659	CEN, *URA3, GFP^{S65T}-MLF3* under *pACT1*	This study
pCC1691	*2μ, URA3, gic2-Δ3::URA3*	This study
pCC1870	2μ, *URA3, RVS161*	This study
pCC1871	2μ, *URA3, RVS167*	This study
pCC1872	CEN, *HIS3, HO*	This study
pDD3	2μ, *URA3, ABP1*	B.Andrews
pEG202	2μ, *HIS3, lexA^{BD}*, under *pADH1*	(Gyuris et al., 1993)
pEG202-BEM3	2μ, *HIS3, LexA-BEM3*	J. Pringle
pEG202-BNI1	2μ, *HIS3, LexA-BNI1*	J. Pringle
pEG202-CDC10	2μ, *HIS3, LexA-CDC10*	J. Pringle
pEG202-CDC11	2μ, *HIS3, LexA-CDC11*	J. Pringle
pEG202-CDC12	2μ, *HIS3, LexA-CDC12*	J. Pringle
pEG202-CDC3	2μ, *HIS3, LexA-CDC3*	J. Pringle

pEG202-RHO1	2μ, *HIS3, LexA-RHO1*	J. Pringle
pEG202-RHO2	2μ, *HIS3, LexA-RHO2*	J. Pringle
pEG202-RHO3	2μ, *HIS3, LexA-RHO3*	J. Pringle
pEG202-RHO4	2μ, *HIS3, LexA-RHO4*	J. Pringle
pJG4-5	2μ, *TRP1, B42^{AD}*, under *pGAL1*	(Gyuris et al., 1993)
pJG4-5-BNI1	2μ, *TRP1, B42^{AD}-BNI1*	J. Pringle
pJG4-5-CDC10	2μ, *TRP1, B42^{AD}-CDC10*	J. Pringle
pJG4-5-CDC11	2μ, *TRP1, B42^{AD}-CDC11*	J. Pringle
pJG4-5-CDC12	2μ, *TRP1, B42^{AD}-CDC12*	J. Pringle
pJG4-5-CDC3	2μ, *TRP1, B42^{AD}-CDC3*	J. Pringle
pJG4-5-CLA4	2μ, *TRP1, B42^{AD}-CLA4*	D. Lew
pJG4-5-SKM1	2μ, *TRP1, B42^{AD}-SKM1*	D. Lew
pJJ244	*URA3*	(Jones and Prakash, 1990)
pOPR3	2μ, *URA3, RHO3*	Y. Matsui
pPB191	2μ, *URA3, MSB1*	A. Bender
pPB207	2μ, *URA3, MSB2*	A. Bender
pPB547	2μ, *LEU2, BEM3*	A. Bender
pRS316-CDC3-GFP	CEN, *URA3*, *CDC3-GFP*	(Caviston et al., 2003)
pRS426	2μ, *URA3*	(Christianson et al., 1992)
pS7	2μ, *URA3, BUD5*	J. Chant
pSH18-34	2μ, *URA3, lexOp-lacZ*	(Gyuris et al., 1993)
SPA2/2u	2μ, *URA3, SPA2*	M. Snyder

YEp103-CDC24	2μ, *URA3, CDC24*	E. Bi
YEp13-ZDS2	2μ, *LEU2, ZDS2*	E. Bi
YEp181-ZDS1	2μ, *LEU2, ZDS1*	E. Bi
YEp24-CDC28	2μ, *URA3, CDC28*	F. Cross
YEp24-CLN1	2μ, *URA3, CLN1*	F. Cross
YEp24-CLN2	2μ, *URA3, CLN2*	F. Cross
YEp352-BNI1	2μ, *URA3, BNI1*	M. Longtine
YEp352-ERF2	2μ, *URA3, ERF2*	R. Deschenes
YEp352-FKS2	2μ, *URA3, FKS2*	
YEp352-SKM1	2μ, *URA3, SKM1*	H. Martin
YEp420-PFY	2μ, *URA3, PFY1*	
YEp420-SLA1	2μ, *URA3, SLA1*	
YEpSMY1	2μ, *URA3, SMY1*	
YEpU-CDC42	2μ, *URA3, CDC42*	
YEpU-RHO1	2μ, *URA3, RHO1*	Y. Ohya
YEpU-RHO2	2μ, *URA3, RHO2*	Y. Ohya
YEpU-RSR1	2μ, *URA3, RSR1*	Y. Ohya

2.3 ISOLATION OF HIGH-COPY SUPPRESSORS OF *gic1-Δ1::LEU2 gic2-1::HIS3* MUTATIONS

Two former students of the laboratory, Guang-Chao Chen and Liaoteng Wang, performed the screen. Briefly, *gic1-Δ1::LEU2 gic2-1::HIS3 ura3-52* cells (CCY1024-19C, Ts^- at ≥33°C) were transformed with a yeast genomic library (pRB112 and pRB113), that was constructed in the high-copy number *URA3*-

containing plasmid YEp24 (Carlson and Botstein, 1982). Ura^+ transformants were selected by plating the cells on supplemented SD lacking uracil. After 20-24 h at 26°C, plates containing Ura^+ transformants were shifted to 35°C. Three more days later, Ts^+ Ura^+ transformants were identified. Out of ~100,000 library transformants screened, 426 transformants were able to grow at 35°C. Plasmids from such transformants were recovered into *E. coli*. In order to screen out previously known multi-copy suppressors of *gic1 gic2* mutation, these *E. coli* strains were then colony hybridized against such known multi-copy suppressors, including *BNI1, CDC42*, *GIC1*, *GIC2*, *MSB1*, *MSB3*, and *SSD1-v(1)*. 232 out of 426 candidates contained known suppressor genes.

Restriction enzyme digestion and partial sequencing of the remaining 194 candidates revealed that they represented 11 classes of plasmids, two of which contained *GIC2* and *BEM1*, which somehow escaped our detection by colony hybridization. Sequence analyses of the inserts present within the remaining nine classes of plasmids revealed the presence of four to six genes on each of the inserts. Subcloning experiments were carried out where possible, in order to attribute the suppression effect to a single gene on each class of plasmid. In cases where subcloning of the single putative ORF from the library plasmid was not easy, either that ORF was deleted or disrupted by the insertion of random DNA sequence and the ability of such plasmids to suppress the growth defects of *gic1 gic2* cells was tested.

2.4 CYTOLOGICAL TECHNIQUES

Phase-contrast and fluorescence microscopy were performed using a Zeiss Axioscope (Carl Zeiss, Oberkochen, Germany). Images were captured using a MicroMax CCD camera (Princeton Instruments, Trenton, NJ) and processed using IPLab spectrum (Scanalytics Inc., Fairfax, VA) and Photoshop 5.0 (Adobe Systems Inc., San Jose, CA) software.

For examining the morphological features of cells cultured at restrictive growth temperatures, aliquots of cells from different time points were fixed with formaldehyde (3.7% final concentration; EM Sciences, Gibbstown, NJ) for 30 min-1 h at room temperature. This was followed by 1-2 washes with PBS (Phosphate Buffered Saline, containing 0.15 M NaCl and 50 mM sodium phosphate [pH7.4]). Cells were scored immediately or stored at 4°C.

Bud scar staining and actin staining were carried out essentially as previously described (Pringle et al., 1989) except for some minor modifications. For bud scar staining, exponentially growing cells were fixed as above, stained with calcofluor white (0.2 mg/ml final concentration; Fluorescent Brightner 28 from Sigma-Aldrich Co., St. Louis, MO) for 10 minutes and washed with water for up to five times.

For F-actin staining, ~1 X 10^7 cells were fixed, washed once with PBS and resuspended in 500 µl of PBS. 200 µl aliquot of these cells was then concentrated in 45 µl of PBS and 5 µl of rhodamine-conjugated phalloidin (6.6 µM stock concentration, stored at -70°C; Molecular Probes, Eugene, OR) was added. Cells were incubated in the dark in a rotary shaker at room temperature for 1 h and washed with PBS for three to four times.

For trypan blue staining, equal volumes of yeast cells and trypan blue solution (4% [w/v] stock, Sigma-Aldrich Co., St. Louis, MO) were mixed and allowed to sit on a bench-top for five minutes. Cells appearing blue or bluish-purple upon examination by light microscopy were considered as trypan blue-positive.

For determining the subcellular localization of GFP-tagged proteins in wild-type cells, cells were cultured at 26°C and were examined live without fixing them with formaldehyde. However, for examining GFP-tagged protein in cells cultured at higher temperatures and in time-course experiments, cells were

fixed with 1% formaldehyde on ice for 10 minutes and washed once with ice-cold PBS.

2.5 PREPARATION OF YEAST CELL LYSATE AND IMMUNOBLOTTING

Cells were cultured in an appropriate growth media to a density of ~1 X 10^7 cells/ml, and 2 OD_{600} equivalent of cells were harvested by centrifugation in a table-top centrifuge at 4,000 rpm for 3 min. Cells were resuspended in 1 ml of a pre-chilled (4°C) solution containing 10 mM sodium azide, 25 mM Tris-HCl [pH 7.5]. After centrifugation, the cell pellets were incubated in a boiling water bath for 3 min. and resuspended in 20 µl of ESB (2% SDS, 10% glycerol, 80 mM Tris-HCl [pH 6.8], 10 mM dithiothreitol [Sigma-Aldrich Co., St. Louis, MO], and 0.002% bromophenol blue [Bio-Rad, Hercules, CA]), containing protease inhibitors that were added just before use from frozen stocks of cocktail 1 (0.5 mg/ml of antipain, leupeptin, pepstatin A, chymostatin, and aprotinin) and cocktail 2 (1 mg/ml of phenanthroline, phenylmethylsulfonyl fluoride and benzamidine, dissolved in ethanol) at 1:500 and 1:100 dilutions, respectively. Acid-washed glass beads (0.45-0.55 mm diameter; Sigma-Aldrich Co., St. Louis, MO) were added and cells were disrupted by vortexing for 4 min. in a multi-tube vortexer (VWR Scientific, Bridgeport, NJ) at setting 9. An additional 80 µl of ESB buffer (with protease inhibitors) was added to the cell lysate, mixed and centrifuged for 1 min. The supernatant was boiled for 3 min. and fractionated by SDS-PAGE.

Proteins separated by electrophoresis were then transferred to a nitrocellulose membrane (0.45 µm; Schleicher & Schuell Bioscience, Inc., Keene, NH). Following transfer, the nitrocellulose membrane was stained with 0.5% Ponceau S (Sigma-Aldrich Co., St. Louis, MO) to monitor the efficiency of transfer. The membrane was then destained with the western buffer (10 mM Tris-HCl [pH 7.5], 150 mM NaCl, 0.05% Tween 20 [v/v]) and blocked for 1 h at room

temperature in western buffer containing non-fat dry milk (5% w/v). Incubation with primary antibody (mouse anti-HA or anti-Myc at 1:1,1000 dilutions [both from Molecular Probes Inc., Eugene, OR]; or rabbit anti-G6PDH at 1:100,000 dilution [Sigma-Aldrich Co., St. Louis, MO]) was carried out for 2 h with constant agitation, followed by three rounds of washing (10 min. each) with western buffer without non-fat dry milk. Incubation with secondary antibody (anti-mouse or anti-rabbit IgG conjugated with horse-radish peroxidase at 1:5,000 dilution; Amersham Biosciences Corp., Piscataway, NJ) was carried out for 1 h with constant agitation, followed by three rounds of washing as above. Finally, antibodies bound to the protein of interest were visualized using the enhanced chemiluminescence detection system (Amersham Biosciences Corp., Piscataway, NJ).

2.6 Flow cytometric Analysis

1 ml of cells at OD_{600} of ~0.5 was harvested from cultures at each time point. Cells were washed once with PBS and resuspended in 0.5 ml of PBS. 1 ml of 100% ethanol was added and cells were fixed by incubating overnight at 4°C in a rotary shaker. After washing once with 50 mM Tris-HCl, cells were subjected to pancreatic RNAse treatment (1 mg/ml in 10 mM Tris-Cl for 2 h at 37°C), followed by proteinase K treatment (10 μg/ml for 60 min. at 55°C). Cells were washed once with PBS, and resuspended in 1 ml of PBS by sonicating them for 5 seconds in a Sonics Vibra cell sonicator, using the microtip set at 25% amplitude. Following sonication, cells were collected by centrifugation, resuspended in 200 μl of propidium iodide (100 μg/ml), incubated in the dark for at least 1 h and then subjected to flow cytometric analysis. The DNA content of ~20,000 cells per sample was determined by a FACSCalibur Systems (BD Bioscience, San Jose, CA) using the Cellquest software.

2.7 FLUID-PHASE ENDOCYTOSIS

Lucifer Yellow (LY) uptake assay was carried out as previously described (Dulic et al., 1991). Cells were cultured to log phase in YEPD at 26°C or 37°C. 1 X 10^7 cells were harvested, resuspended in 80 µl of YEPD, and transferred to a 1.5 ml Eppendorf tube. 20 µl of Lucifer Yellow CH-dilithium salt (8 mg/ml final concentration; Sigma-Aldrich Co., St. Louis, MO) was added. Cells were incubated at 26°C or 37°C in a rotary shaker for 1 h. Cultures were then centrifuged in a table-top microfuge at 4,000 rpm for 1 minute, followed by three rounds of washing with 1 ml of ice-cold succinate-sodium hydroxide buffer (50 mM succinic acid, adjusted to pH 5.0 with 10 M NaOH/20 mM sodium azide). Cells were then resuspended in 10 µl of the same buffer and immediately kept on ice until visualization using fluorescein isothiocyanate (FITC) optics for the accumulation of LY in the vacuoles.

2.8 α-FACTOR-SENSITIVITY ASSAY

Two approaches were used to measure α-factor-sensitivity of cells. In the first approach, a log phase culture was spread on a YEPD agar plate and then a sterile 3 mM paper disk saturated with 10 µl of α-factor (1 mg/ml stock concentration) was placed in the centre of the petri dish. After incubation at 26°C for 2 days, the diameter of the zone of growth inhibition formed around the paper disk was measured. In the second approach, a similar paper disk saturated with α-factor was placed in the center of a YEPD agar plate and 10 µl of log phase cultures of different strains were streaked radially away from the paper disk and towards the periphery of the petri plate. The size of the zone of growth inhibition around the α-factor source reflects the degree of α-factor-sensitivity.

2.9 TWO-HYBRID INTERACTION TRAP ASSAY

The protocol previously described by Finley and Brent (1994) was modified. EGY48 cells (carrying a *LEU2* reporter gene integrated in the

chromosome and a lacZ reporter gene on the plasmid pSH18-34) were co-transformed with pEG202-based (encoding LexA-binding domain fusion proteins) and pJG4-5-based (encoding B42-activation domain fusion proteins) plasmids. Transformants were selected on SD + Leu agar and then analyzed for the reporter gene activities.

For assaying the *LEU2* reporter activity, transformants were spotted on supplemented synthetic minimal medium that lacked leucine and contained dextrose (2%; SD agar) or galactose and raffinose (2% and 1%, respectively; SGal/Raff agar) as carbon source. Growth of cells on SGal/Raff agar but not on SD agar indicated positive 2-hybrid interactions.

For assaying the lacZ reporter activity, transformants were first spotted on SD + Leu agar master plate and then replica plated onto buffered (20 mM sodium phosphate, pH7.0) SD + Leu and SGal/Raff + Leu agar, both containing 40 μg/ml of XGal (chromogenic compound 5-bromo-4-chloro-3 indolyl-β-D-galactopyranoside; United States Biological, Swampscott, MA). Blue coloration of cell growth at 30°C on SGal/Raff + Leu but not SD + Leu agar indicated positive 2-hybrid interactions.

2.10 CONSTRUCTION OF *gic1-Δ3::natR gic2-Δ3::URA3* STRAIN

gic1-Δ3::natR gic2-Δ3::URA3 strain (CCY1446-1A) was obtained as a haploid segregant from a heterozygous diploid strain (CCY1446), which was obtained by crossing a *gic1-Δ3::natR* strain (CCY1380-1C-1) with a *gic2-Δ3::URA3* strain (CCY1447).

To construct CCY1380-1C-1 strain, a haploid *gic1-Δ2::kanR* strain (CCY1380-1C) was first obtained from a heterozygous *gic1-Δ::kanR* diploid strain (Research Genetics deletion strain collection). Disruption at the *GIC1* locus in the strain CCY1380-1C was confirmed by PCR using oligonucleotides MIP23.1P and MIP23.2P, which gave a *GIC1* amplification product (0.9-kb) in the wild-type

control strain but not in the CCY1380-1C strain. The kanamycin-resistance marker in strain CCY1380-1C was then replaced by a naurseothricin-resistance marker (*natR*; Goldstein and McCusker, 1999) by transforming CCY1380-1C with an ~1.2-kb *EcoR*I fragment of p4339 (containing natR marker; gift from Amy Tong, University of Toronto, Canada). Transformants were selected on YEPD + cloNAT (100 mg/L; Werner BioAgents, Jena-Cospeda, Germany) agar. A successful replacement of the *kanR* marker with the *natR* marker in the resulting strain (CCY1380-1C-1) was confirmed by its inability to grow on G418-containing agar, which selects for kanamycin-resistance.

To construct strain CCY1447, strain Y3656 (gift from Amy Tong, University of Toronto, Canada) was transformed with an ~3.1-kb *Xba*I/*Kpn*I fragment containing the *GIC2* disruption cassette (Figure 2.1). Transformants were selected on SD + casamino acids agar. Ura^+ transformants were then examined for their ability to grow on SD + His + Met + Lys agar containing canavanine (50 mg/L; Sigma Chemical Co.; St. Louis, MO). The Can^r Ura^+ Leu^+ (i.e., *MAT*α) strain was selected as the *gic2-Δ3::URA3* strain. The disruption at the *GIC2* locus in this strain (CCY1447) was confirmed by PCR using oligonucleotides MIP23H.1P and MIP23H.2P, which gave a *GIC2* amplification product (~1.1-kb) in the wild-type control strain but not in CCY1447.

Construction of the *GIC2* disruption (*gic2Δ3::URA3)* cassette

Plasmid pCC1691, containing *gic2Δ3::URA3*, was constructed using a 3-way ligation technique. Briefly, plasmid pCC967 (2μ, *GIC2*) was digested with *Avr*II/*Kpn*I and the resulting ~5.3-kb fragment (containing 305 bp upstream of the start codon of and the first 147 bp of the *GIC2* ORF) was simultaneously ligated to an ~1.6-kb *URA3*-containing *Xba*I/*Aat*II fragment (obtained from pJJ244) and a 1-kb *Aat*II/*Kpn*I PCR fragment containing sequence immediately downstream of the *GIC2* ORF. This latter fragment was obtained by restriction

enzyme digestion of the product of a PCR using the primers Gic2-dF and Gic2-dR, which bear *Aat*II and *Kpn*I sites at their 5′ ends, respectively.

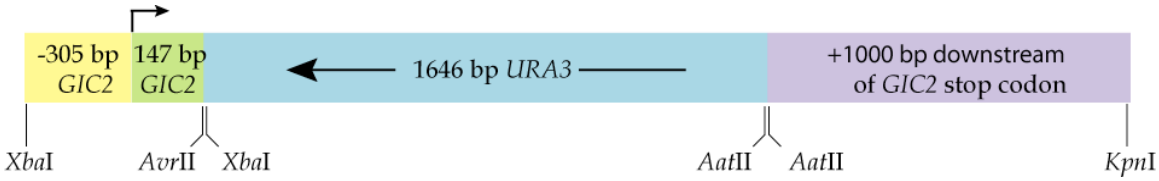

Figure 2.1 *GIC2* disruption cassette present in pCC1691.

2.11 SYNTHETIC GENETIC ARRAY

The *gic1-Δ3::natR gic2-Δ3::URA3* strain used for the synthetic genetic array was sent to Amy Tong (in Dr. Charlie Boone's laboratory at the University of Toronto, Canada), who performed the screen. Schematics of the synthetic genetic array methodology and analysis are shown in Figures 4.1 and 4.2, respectively. Validation of the synthetic interactors (obtained from the screen) was performed by routine tetrad analysis.

CHAPTER 3

Isolation and characterization of dosage-dependent suppressors of *gic1 gic2* mutations

3.1 BACKGROUND

The structurally related Gic1 and Gic2 proteins associate with Cdc42-GTP through their CRIB motif. As effectors of Cdc42, they play important roles in the process of cellular morphogenesis (Brown et al., 1997; Chen et al., 1997). During polarized cell growth, Cdc42 localizes to the plasma membrane at sites of active cell growth (Ziman et al., 1993). The interaction of GTP-bound Cdc42 with its effectors at these sites initiates signaling pathways that regulate organization of the actin cytoskeleton. For example, Cdc42-GTP stimulates the p21-activated kinases Ste20 and Cla4 (Eby et al., 1998), which phosphorylate the actin-based motor proteins Myo3 and Myo5 (Wu et al., 1997). Both Myo3 and Myo5 are implicated in the activation of the Arp2/3 complex, which is involved in the process of actin filament assembly (Evangelista et al., 2000; Lechler et al., 2000).

Several lines of evidence suggest a functional link between Gic1, Gic2, and the 12S polarisome complex (comprising of Bni1, Bud6, Spa2 and Pea2), which is involved in the organization of the actin cytoskeleton (Sheu et al., 1998). First, *gic2* mutation exhibits synthetic interaction with *bni1*, *bud6* and *spa2* mutations (Jaquenoud and Peter, 2000). Second, Gic2 co-fractionates with Bud6 and Spa2, and it also physically interacts with Bud6 in co-immunoprecipitation and two-hybrid interaction assays (Jaquenoud and Peter, 2000). Third, the localization of Bni1 and Bud6 at the incipient bud-site depends on active Cdc42 and the Gic proteins (Jaquenoud and Peter, 2000). In light of the direct roles of Bni1 and Bud6 in the process of actin filament nucleation (Evangelista et al., 1997; Moseley et al., 2004; Sagot et al., 2002), these evidences suggest that Gic1 and Gic2 may

function as adapters that link Cdc42 signaling to the actin cytoskeleton organization machinery. Interestingly, *gic1 gic2* mutants exhibit temperature-sensitive growth defect whereas none of the single mutants of the polarisome complex show a similar growth defect, suggesting that Gic1 and Gic2 function in polarized cell growth may not be exclusively restricted to the context of polarisome function.

Neither *GIC1* nor *GIC2* is an essential gene. When both *GIC1* and *GIC2* are absent, yeast cells exhibit several phenotypes associated with the loss of polarity, including defects in bud-site selection and organization of the actin cytoskeleton (Chen et al., 1997). Although viable at 26°C, *gic1 gic2* cells display a temperature-sensitive growth defect at ≥33°C (in yeast cells carrying the *ssd1-d* allele). Using this property of *gic1 gic2* cells, previous students in our laboratory isolated a large number of multi-copy suppressors of the Ts^- growth defect of *gic1 gic2* cells. In brief, *gic1-Δ1::LEU2 gic2-1::HIS3* cells (CCY1024-19C) were transformed with a yeast genomic library that was constructed in the 2μ-based high copy-number plasmid YEp24 (Carlson and Botstein, 1982). Ts^+ (at 37°C or 35°C) transformants were selected. The plasmid-borne suppressor genes could theoretically function either downstream of Gic1 and Gic2 or in a pathway functionally redundant to that mediated by Gic1 and Gic2. Functional analyses of these suppressors will be the subject of inquiry in this chapter.

3.2 RESULT

3.2.1 Analysis of multi-copy suppressors of *gic1 gic2* mutations

Suppression of the Ts^- growth defect of gic1 gic2 cells

The multi-copy suppressor plasmids previously isolated in our laboratory complemented the Ts^- growth defect of *gic1-Δ1::LEU2 gic2-1::HIS3* mutant cells to varying degrees (Figure 3.1). Sequencing and subcloning experiments led to my

identification of the genes responsible for suppression on each plasmid. Several of these suppressor genes - including *AXL2, BNI1, CLN2*, *MSB1, MSB2, RSR1,* and *STE20* - are known to participate in the process of polarized growth (see Introduction). It is noteworthy, however, that the suppressor plasmid bearing *STE20* lacks sequence upstream of nucleotide 355 of the *STE20* ORF (and hence the clone is referred to as *NΔ118-STE20*). If expressed, this truncated form of *STE20* should produce a mutant Ste20 kinase that lacks the N-terminal 118 residues that may contribute to the auto-inhibition of the kinase activity (Lamson et al., 2002). *NΔ118-STE20* rescued the growth defect of *gic1 gic2* cells reasonably well. In contrast, a full-length *STE20*-bearing plasmid (pVTU-STE20, CEN, *ACT1* promoter) failed to show such suppression effect (not shown), thus suggesting that activated Ste20 may be responsible for suppression.

In addition to the polarity-related genes, we isolated *SSN6* as one of the multi-copy suppressors of *gic1 gic2* cells. Increased dosage of *SSN6* alleviated the growth defect of *gic1 gic2* cells at 33°C. Ssn6 is a conserved protein that functions in a complex with Tup1 (Keleher et al., 1992) to repress the transcription of ~3% of all yeast genes of diverse functions (Smith and Johnson, 2000). Coincidentally, our laboratory has also identified a two-hybrid interaction between Gic1 and Ssn6 (unpublished). Both these results imply that at least some function mediated by the Gic proteins and the Ssn6/Tup1 complex must closely intersect. To further support this assumption, I examined whether increased dosage of *TUP1* could complement the growth defect of *gic1 gic2* cells. Indeed, a multi-copy plasmid bearing *TUP1* did raise the permissive growth temperature of *gic1 gic2* cells, albeit slightly less efficiently than the *SSN6* plasmid.

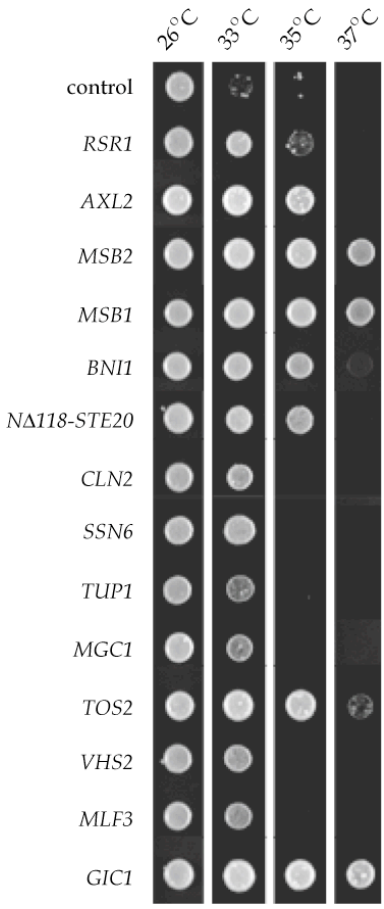

Figure 3.1 Complementation of the Ts- growth defect of *gic1 gic2* cells by multi-copy suppressor plasmids. Suspensions of haploid *gic1-Δ1::LEU2 gic2-1::HIS3* cells (CCY1024-19C) carrying different 2μ-based plasmids were spotted on YEPD agar and allowed to grow at the indicated temperatures for 2 days. The plasmids used were pRS426 (empty vector, negative control), pCC1290 (*RSR1*), pCC1291 (*AXL2*), pCC1284 (*MSB2*), pPB191 (*MSB1*), YEp352-BNI1 (*BNI1*), pCC1294 (*NΔ118-STE20*), pCC1295 (*CLN2*), pCC1293 (*SSN6*), pAJ181 (*TUP1*), pCC1529 (*MGC1*), pCC1574 (*TOS2*), pCC1606 (*VHS2*), pCC1635 (*MLF3*) and pCC904 (*GIC1*, positive control). Plasmids carrying *BNI1, CDC42*, *GIC1*, *GIC2*, *MSB1*, *MSB3*, and *SSD1-v(1)* were also isolated from the screen but they were eliminated by *E. coli* colony hybridization (see Materials and Methods). However, the *BNI1* and *MSB1* plasmids are included in this figure because this result has not been published in the literature so far. Note that *TUP1* and *MLF3* were not originally identified from the screen (see text for details).

The multi-copy suppressor screen also identified three ORFs of previously unknown function. These were *YHR149C* (which I have named *MGC1* for multi-

copy suppressor of Gic), *TOS2* (*YGR221C*) and *VHS2* (*YIL135C*). Database searches for sequence homology revealed that *MGC1* and *TOS2* are structurally related and *VHS2* is homologous to another yeast gene named *MLF3* (*YNL074C)*. To investigate whether *VHS2* and *MLF3* are related in structure as well as function, I cloned *MLF3* into a 2μ plasmid and found that this plasmid also could partially suppress the growth defect of *gic1 gic2* cells. However, simultaneous increase in the dosage of *VHS2* and *MLF3* (from the same 2μ plasmid pCC1644) or *MGC1* and *TOS2* (from two separate 2μ plasmids, pCC1478 and pCC1492) did not result in an additive effect on the suppression of the growth phenotype of *gic1 gic2* cells (not shown).

Suppression of the bud-site selection defect of gic1 gic2 cells

Since haploid *gic1 gic2* cells exhibit a moderate bud-site selection defect at 26°C (Chen et al., 1997), I next examined whether the multi-copy suppressors that I identified also rescued this defect of *gic1 gic2* cells. While ~21% of haploid *gic1 gic2* cells carrying an empty vector showed deviation from the normal axial budding pattern, only 5% of *gic1 gic2* cells carrying a 2μ *GIC1* plasmid showed such a defect (Table 3.1 and Figure 3.2). Consistent with the role of Axl2 in axial bud-site selection (Roemer et al., 1996), only 4% of haploid *gic1 gic2* cells carrying a 2μ *AXL2* plasmid exhibited non-axial budding, whereas the other suppressor plasmids rescued this defect of *gic1 gic2* cells to varying degrees (Table 3.1 and Figure 3.2). Overall, no strict correlation was observed between the ability of these suppressors to rescue the bud-site selection defect and the temperature-sensitive growth defect of *gic1 gic2* cells.

Table 3.1 Budding patterns of *gic1 gic2* cells carrying different multi-copy plasmids.

Plasmid	Gene	Bud scar pattern (%)		
		I	II	III
pRS426	-	79	2	19
pCC1290	*RSR1*	90	0	10
pCC1291	*AXL2*	96	0	4
pCC1284	*MSB2*	92	2	6
pPB191	*MSB1*	89	2	9
YEp352-BNI1	*BNI1*	86	3	11
pCC1294	*NΔ118-STE20*	82	4	14
pCC1295	*CLN2*	77	4	19
pCC1293	*SSN6*	89	0	11
pAJ181	*TUP1*	92	0	8
pCC1529	*MGC1*	92	1	7
pCC1574	*TOS2*	91	3	6
pCC1606	*VHS2*	92	2	6
pCC1635	*MLF3*	87	2	11
pCC904	*GIC1*	95	1	4

Haploid *gic1-Δ1::LEU2 gic2-1::HIS3 ura3-52* (CCY1024-19C) cells carrying different 2μ plasmids (same as in Figure 3.1) were cultured at 26°C in SD medium supplemented with amino acids (allowing selection for the *URA3* marker present on different plasmids) to a density of 1 x 10^7 cells/ml, fixed and stained with calcofluor white. For each sample, ≥200 cells with two or more bud scars were examined. For scoring purposes, each mother cell body was divided into three equal sectors along its length. Cells with pattern I showed bud scars adjacent to each other only in one terminal sector; cells with pattern II showed bud scars located at both the terminal, but not in the middle, sectors; and cells with pattern III showed bud scars in the middle (and terminal) sector(s).

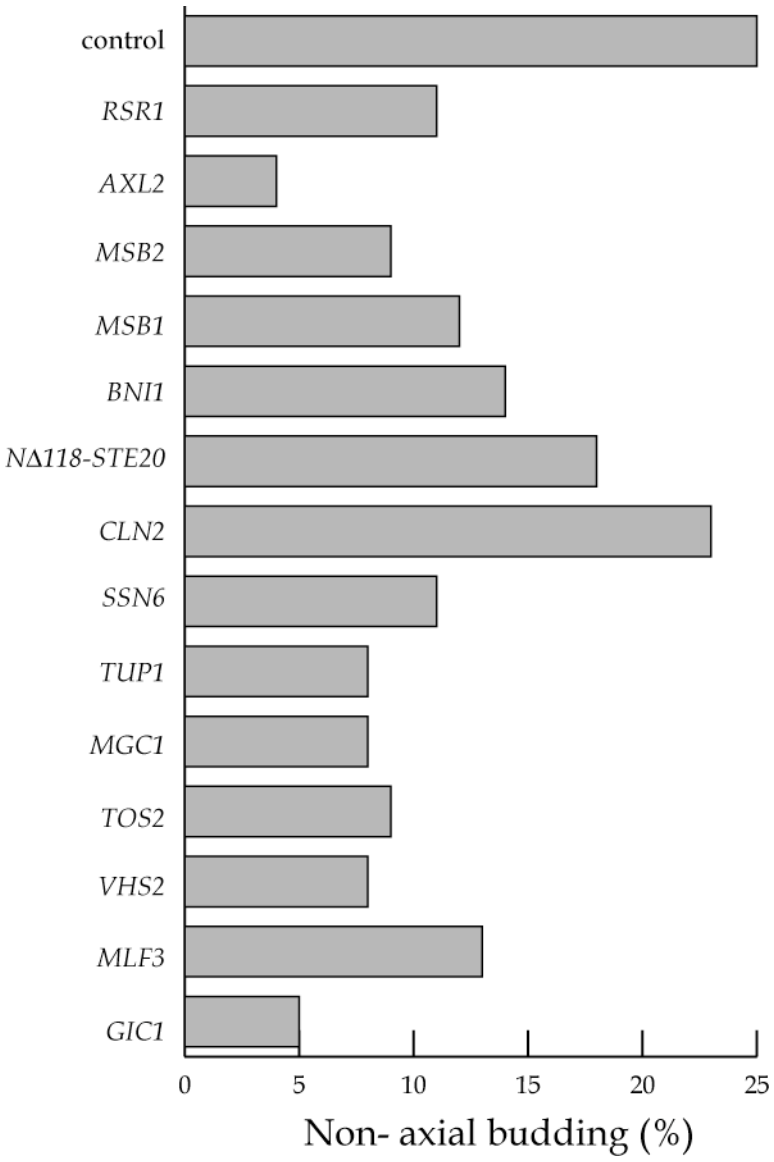

Figure 3.2 Graphical representation of the bud-site selection defect of haploid *gic1-Δ1::LEU2 gic2-1::HIS3* cells (CCY1024-19C) carrying different multi-copy suppressors. Values for pattern II and pattern III from Table 3.1 were combined to obtain the fraction of cells displaying non-axial budding pattern.

Suppression of the actin organization defect of gic1 gic2 cells

At elevated temperatures, *gic1 gic2* cells exhibit *cdc42* mutant-like phenotype and arrest as unbudded cells due to a failure in the polarization of the actin cytoskeleton. After 4 h of incubation at 37°C, ~80% of *gic1 gic2* cells are reported to demonstrate a defect in actin organization (Chen et al., 1997). I therefore examined whether the multi-copy suppressors could alleviate the actin organization defect of *gic1 gic2* cells. Since some of the suppressors complemented the growth defect of *gic1 gic2* cells only at 33°C but not at 35°C (Figure 3.1), the *gic1 gic2* cells carrying multi-copy suppressor plasmids were incubated at 33°C for 4 h and then examined for their ability to polarize actin cytoskeleton.

The result of this experiment suggested that most suppressor plasmids were competent in suppressing the actin polarization defect of *gic1 gic2* cells (Table 3.2). In all but *TUP1*-overexpressing cells, the fraction of unbudded cells was reduced to varying degrees. Except in the case of *CLN2*-overexpressing cells, this drop in the fraction of unbudded cells was generally accompanied by a corresponding decrease in the percentage of unbudded cells that have depolarized actin cytoskeleton (Figure 3.3). Overall, the ability of these suppressors to rescue the actin polarization defect roughly correlated with their ability to suppress the temperature-sensitive growth defect of *gic1 gic2* cells (Figure 3.1).

Since the multi-copy suppressors *VHS2*, *MLF3*, *MGC1* and *TOS2* suppressed not only the temperature-sensitive growth defect but also the bud-site selection and the actin organization defects of *gic1 gic2* cells, I was intrigued by the potential role of these genes in polarized cell growth. I therefore decided to undertake the functional characterization of these two pairs of genes.

Table 3.2 Cortical actin polarization in *gic1 gic2* cells carrying genes on multi-copy plasmids.

Plasmid	Gene	Total (%)		Depolarized (%)	
		Unbudded	Budded	Unbudded	Budded
pRS426	-	70	30	81	13
pCC1290	*RSR1*	52	48	65	15
pCC1291	*AXL2*	49	51	65	0
pCC1284	*MSB2*	47	53	57	4
pPB191	*MSB1*	49	51	73	6
YEp352-BNI1	*BNI1*	52	48	65	2
pCC1294	*NΔ118-STE20*	53	47	64	6
pCC1295	*CLN2*	57	43	81	40
pCC1293	*SSN6*	62	38	77	16
pAJ181	*TUP1*	72	28	75	18
pCC1529	*MGC1*	66	34	71	21
pCC1574	*TOS2*	44	56	57	4
pCC1606	*VHS2*	48	52	60	23
pCC1635	*MLF3*	58	42	74	21
pCC904	*GIC1*	36	64	42	8

Haploid *gic1-Δ1::LEU2 gic2-1::HIS3* (CCY1024-19C) cells carrying different 2μ plasmids (same as in Figure 3.1) were incubated at 33°C for 4 h in SD medium supplemented with amino acids (allowing selection for the *URA3* marker present on different plasmids) to a density of 1 x 10^7 cells/ml, fixed, stained with rhodamine-phalloidin and examined by fluorescent microscopy. For each sample, ~200 cells were examined. For scoring purposes, budded cells were considered polarized as long as the actin organization pattern was appropriate for the bud-size and thus cell cycle stage (as shown in Figure 1.3).

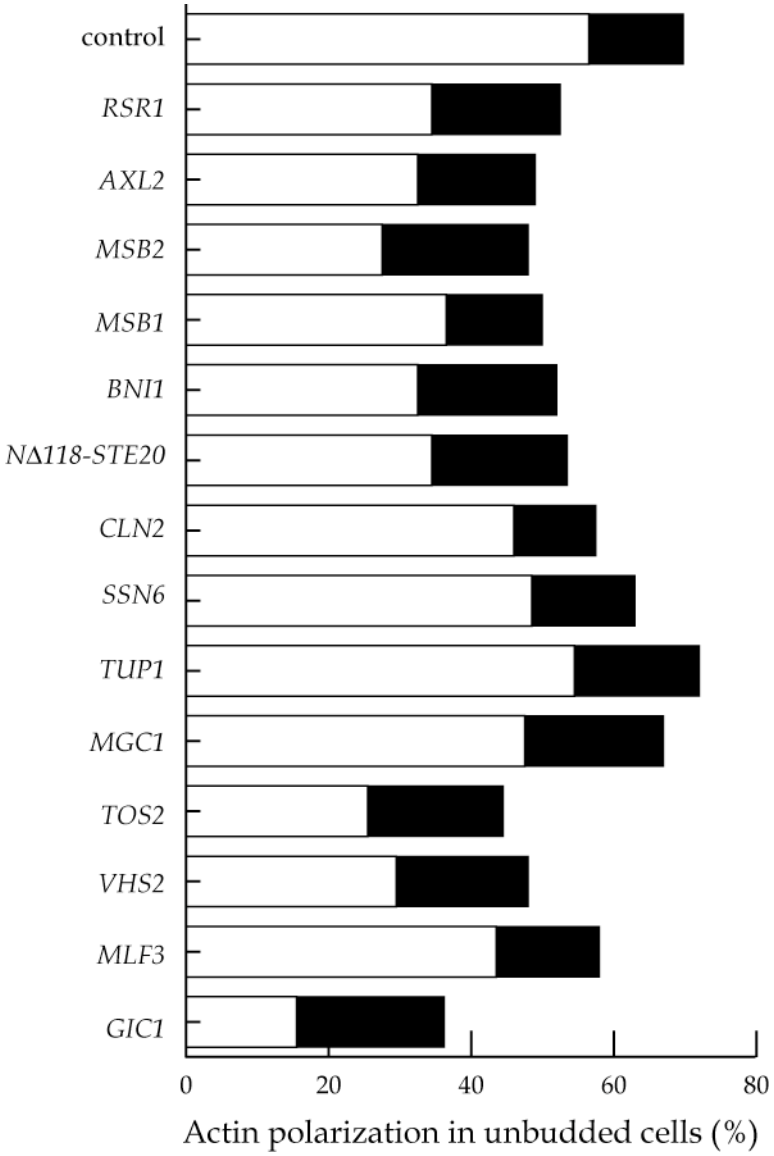

Figure 3.3 Graphical representation of the complementation of actin polarization defects of haploid *gic1-Δ1::LEU2 gic2-1::HIS3* cells (CCY1024-19C) by multi-copy suppressors. Shown here is the total fraction of cells that appeared unbudded, including those that have depolarized (open) or polarized (filled) actin organization. The values are derived from Table 3.2.

3.2.2 Functional Characterization of *VHS2* and *MLF3*

VHS2 encodes a protein of 436 residues, with a predicted molecular mass of ~48 kDa; and *MLF3* encodes a protein of 452 amino acids, with a predicted molecular mass of ~49 kDa. Vhs2 and Mlf3 are 30% identical and 36% similar in sequence. The sequence homology between Vhs2 and Mlf3 extends through the entire amino acid sequence of these proteins (Figure 3.4). Further, these two proteins are not conserved in other non-fungal species and there are no obvious and predictable functional motifs within these proteins. During the course of this study, Muñoz et al. reported that overexpression of *VHS2* suppressed the lethality of the *hal3 sit4* mutant and suggested that Vhs2 may have a role in G1 to S transition (Muñoz et al., 2003). It has also been reported that increased dosage of *MLF3* suppresses the sensitivity of yeast cells to the immuno-suppressive drug leflunomide (Fujimura, 1998). However, based on the ability of *VHS2* and *MLF3* to function as multi-copy suppressors of the various phenotypic defects of *gic1 gic2* mutants (Figures 3.1, 3.2 and 3.3), I surmised that Vhs2 and Mlf3 might be functionally related and have roles in polarized cell growth.

Phenotypic consequences of vhs2 and mlf3 mutations

Simultaneous loss of Vhs2 and Mlf3 results in a temperature-sensitive growth defect

To understand the cellular functions of *VHS2* and *MLF3*, I used a PCR-mediated deletion technique (Longtine et al., 1998b) to delete one of the two chromosomal copies of *VHS2* in a diploid strain. Similarly, one of the two chromosomal copies of *MLF3* was deleted in a diploid strain. Tetrad analyses of the resulting heterozygous diploid strains carrying the *vhs2-Δ1::TRP1* (CCY1830-51-1-4) or *mlf3-Δ1::Kan* mutation (CCY1830-51-1-5) produced four viable spore colonies, indicating that neither *VHS2* nor *MLF3* is essential for viability.

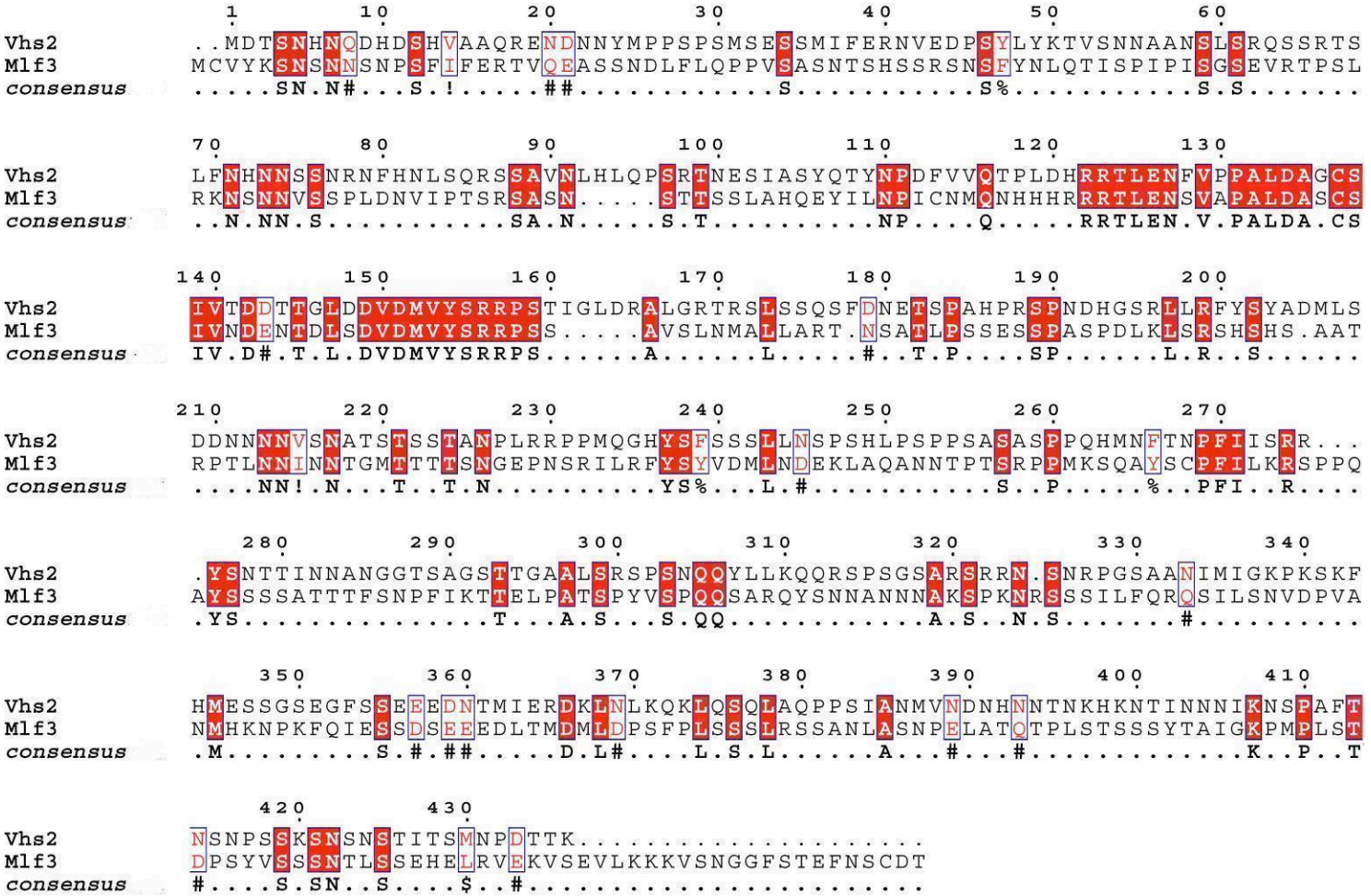

Figure 3.4 Alignment of the predicted sequences of Vhs2 (*YIL135C*) and Mlf3 (*YNL074C*) using Multalin software (Corpet, 1988). Gaps are introduced for alignment purposes. Sequence identity and similarity are shown in red background and boxed, respectively.

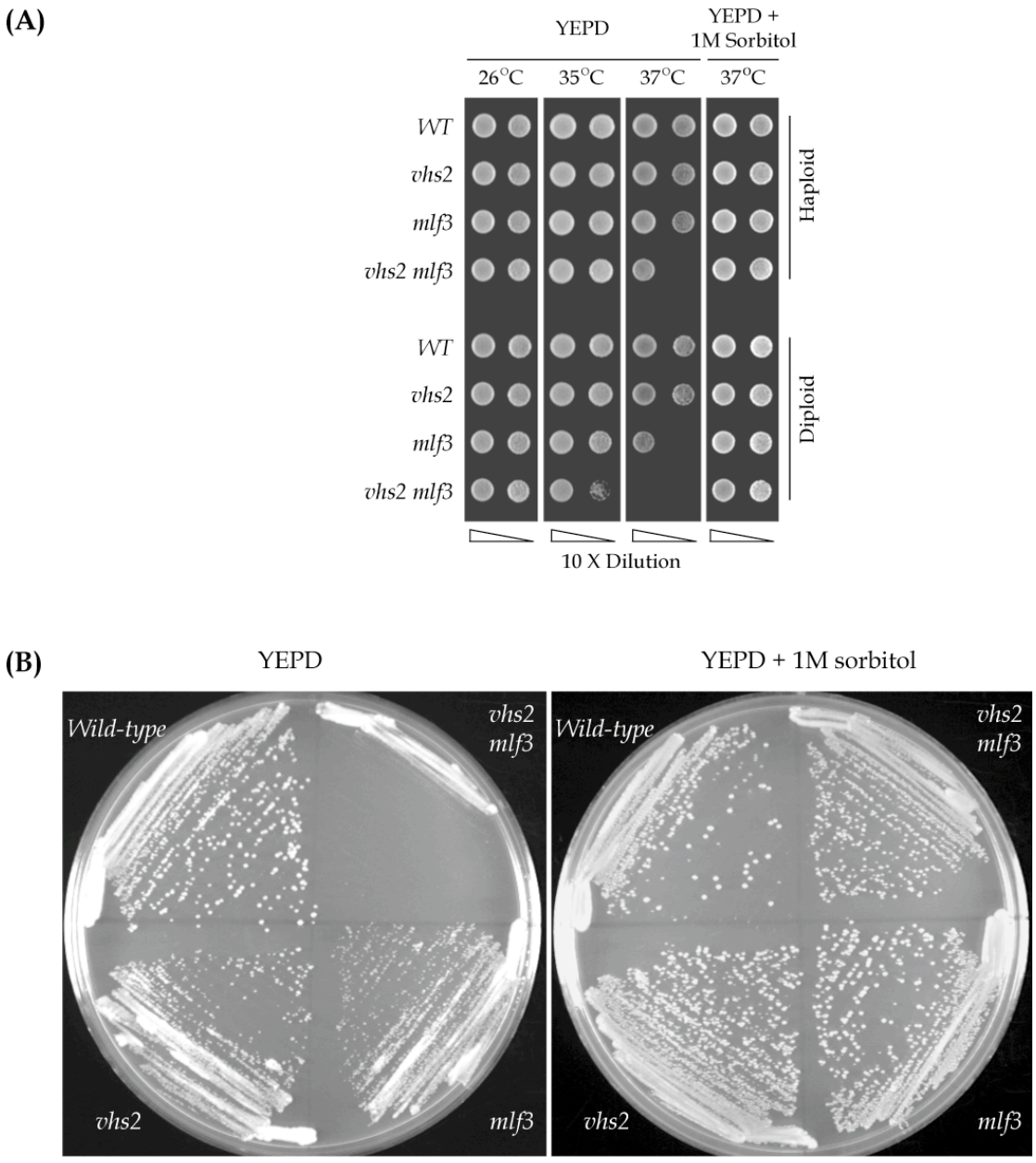

Figure 3.5 Simultaneous deletion of *VHS2* and *MLF3* results in a growth defect that can be rescued by the presence of an osmotic support in the growth medium. **(A)** Suspensions (at OD_{600} = 1 and OD_{600} = 0.1) of congenic haploid and homozygous diploid wild-type (CCY1292-1A and DBY1830), *vhs2* (CCY1292-4B and CCY1720), *mlf3* (CCY1292-1D and CCY1721) and *vhs2 mlf3* (CCY1292-5B and CCY1338) cells were spotted on YEPD agar (with or without 1M sorbitol) and incubated at the indicated temperatures for 2 days. **(B)** Wild-type (CCY1292-1A), *vhs2* (CCY1292-4B), *mlf3* (CCY1292-1D) and *vhs2 mlf3* (CCY1292-5B) haploid cells were streaked on YEPD agar (with or without 1M sorbitol) and incubated at 37°C.

Additionally, neither *vhs2* nor *mlf3* single mutant cells showed any major growth defect at temperatures ranging from 13°C to 37°C, although they produced slightly smaller colonies when streaked out on YEPD agar at 37°C (Figure 3.5B). Next, I questioned whether simultaneous deletion of both *VHS2* and *MLF3* was deleterious to the growth of yeast cells. Indeed, haploid *vhs2 mlf3* double mutant cells displayed a mild temperature-sensitive growth defect at 37°C (Figure 3.5A), indicating that the combined absence of Vhs2 and Mlf3 compromise a function that is essential for optimal cell growth at 37°C. This idea was further confirmed by the inability of *vhs2 mlf3* cells to form single colonies on YEPD agar at 37°C (Figure 3.5B). Instead, *vhs2 mlf3* cells formed microcolonies, each consisting of ~50-150 cells as observed on a dissection microscope, thereby indicating that these double mutant cells had ceased to grow after 6-8 population doublings. Consistent with this growth defect, liquid YEPD cultures of haploid *vhs2 mlf3* cells showed a drop in optical density at 600 nm after an 8-10 h incubation at 37°C (not shown).

Many polarity-related mutations result in more severe phenotypes in diploid cells. Therefore, I next examined the growth property of homozygous *vhs2*, *mlf3* and *vhs2 mlf3* diploid mutants. While the growth property of *vhs2* cells was similar to that of wild type cells, *mlf3* cells exhibited a noticeable growth defect at 37°C (Figure 3.5A). Furthermore, diploid *vhs2 mlf3* cells showed a growth defect that was more pronounced than that of its haploid counterpart (Figure 3.5A). These results are consistent with the reduced growth rate (measured as an increase in the cell number over a period of time) of liquid cultures of the diploid *mlf3* and *vhs2 mlf3* mutant cells at 37°C (Figure 3.6). The optical density, cell number and viability of diploid wild-type and *vhs2 mlf3* liquid YEPD cultures were also measured after incubation at 37°C (Figure 3.7). These results consistently showed that diploid *vhs2 mlf3* cells are defective in

growth at 37°C. Since diploid *vhs2 mlf3* double mutants exhibited the most pronounced growth phenotype, I decided to use the homozygous diploid *vhs2 mlf3* mutant cells for further phenotypic analyses.

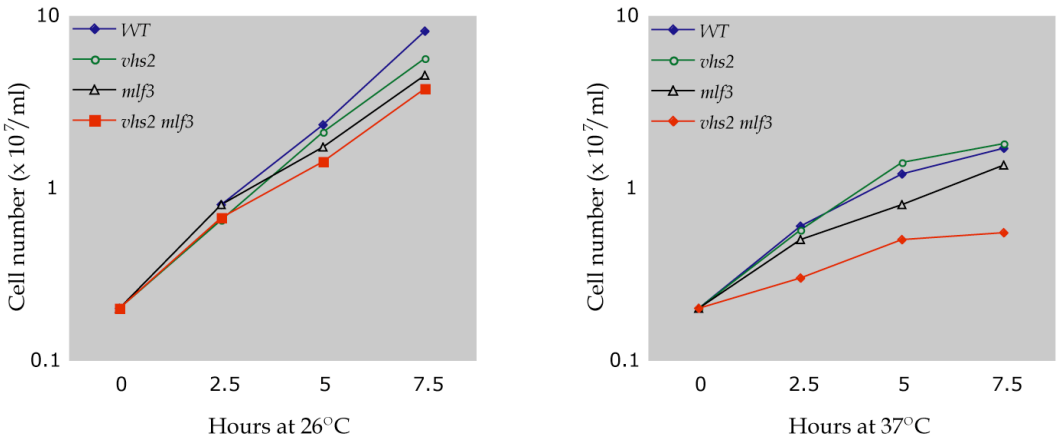

Figure 3.6 Growth curves of homozygous diploid wild-type (DBY1830), *vhs2* (CCY1720), *mlf3* (CCY1721) and *vhs2 mlf3* (CCY1338) cells in YEPD medium at 26°C **(A)** or 37°C **(B)**. Saturated cultures were diluted and incubated overnight at 26°C such that cell density would be ~1 X 10^7/ml the following morning. These actively growing cultures were then diluted (at 0 h) to a cell density of ~0.2 X 10^7/ml and incubated at 26°C or 37°C for different periods of time. Cells were counted using a hemocytometer.

vhs2 mlf3 mutant cells become large, round and wrinkled

Accumulation of large, unbudded cells is a characteristic morphological phenotype of *cdc42-1*, *gic1 gic2* and many other polarity mutants that fail to organize their actin cytoskeleton for budding (Drubin and Nelson, 1996; Pruyne and Bretscher, 2000b). To investigate if the loss of *VHS2* and *MLF3* resulted in similar cytological changes, exponentially growing cultures of diploid wild-type and homozygous *vhs2*, *mlf3* and *vhs2 mlf3* cells were shifted from 26°C to 37°C, and the morphology of these cells was examined by phase-contrast microscopy

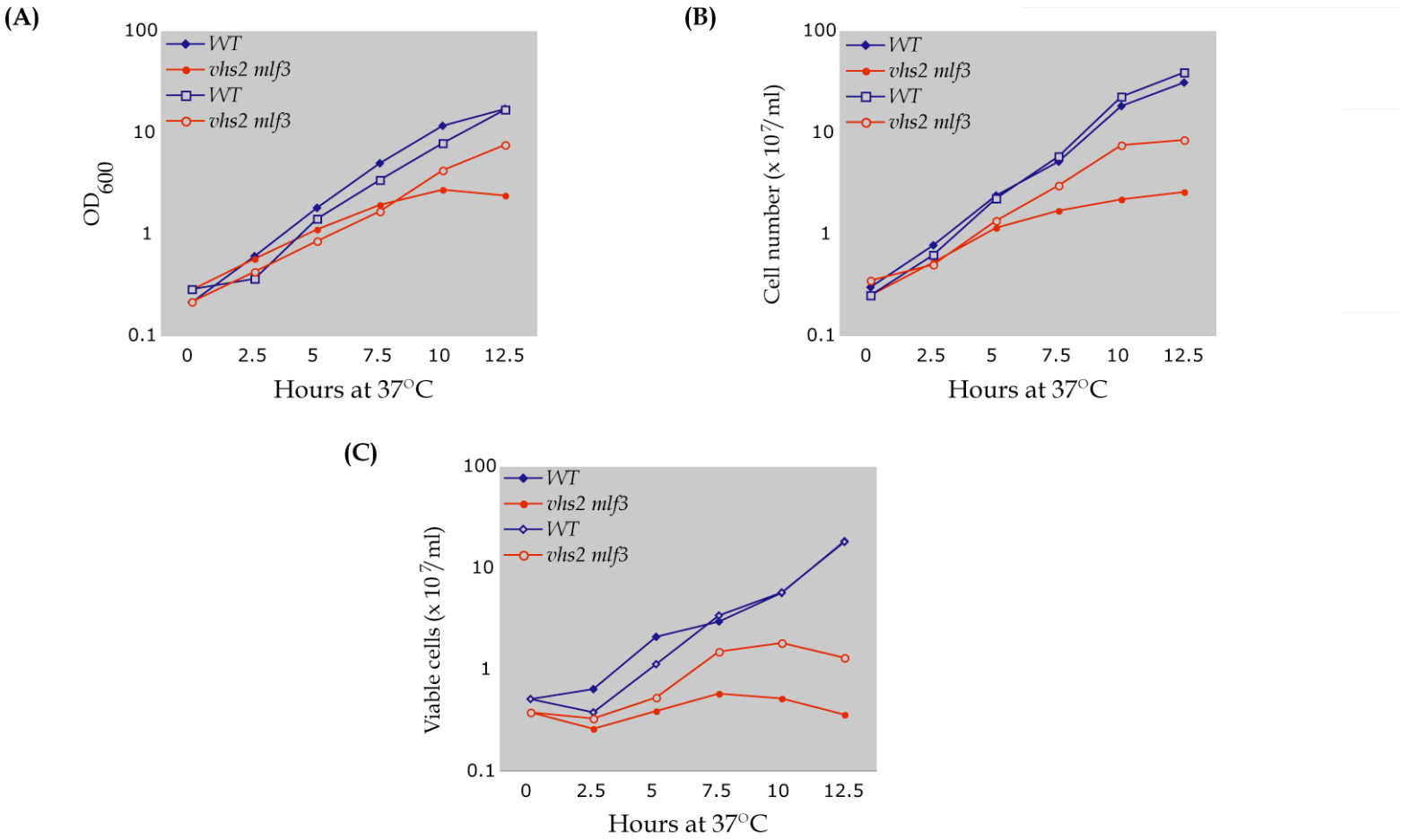

Figure 3.7 The optical density **(A)**, cell number **(B)** and viability **(C)** of diploid wild-type (DBY1830) and *vhs2 mlf3* (CCY1338) cells cultured at 37°C in liquid YEPD with (open diamonds and circles) or without 1M sorbitol (filled diamonds and circles) were monitored for different time periods.

at different time points (Figure 3.8). At 26°C, none of the mutant cells differed significantly from wild-type cells in their size and shape. At 37°C, both *vhs2* and *mlf3* cells exhibited clumpiness. However, *vhs2* cells retained the ellipsoidal shape of normal diploid cells whereas *mlf3* cells were slightly enlarged and more spherical in shape.

vhs2 mlf3 cells, on the other hand, showed several pronounced changes. First, the culture containing *vhs2 mlf3* cells became flocculent after 5 h at 37°C, whereas wild-type cultures became slightly flocculent only after 10-12 h at 37°C. One possible explanation for an early onset of flocculation observed in *vhs2 mlf3* cells is that the cell wall structure of these cells might be altered, thus allowing them to clump together. Indeed, *vhs2 mlf3* cells appeared as small clumps of cells and these clumps were not separable upon mild sonication treatment. The clumpiness observed in the *vhs2 mlf3* cells was much more severe than that observed in either *vhs2* or *mlf3* cells. Second, *vhs2 mlf3* double mutant cells became large and round, suggesting a loss of cell polarity. However, unlike *cdc42-1* or *gic1 gic2* cells, these *vhs2 mlf3* cells did not completely arrest as unbudded cells. Instead, they existed as a heterogeneous population of budded and unbudded cells, with an enrichment of unbudded cells occurring over a period of time (Figures 3.8 and 3.9B; Table 3.3). Third, *vhs2 mlf3* cells with a wrinkled morphology began to appear at 5 h and this phenotype became more severe with further incubation at 37°C. Such a morphological change implied that the cell wall integrity of *vhs2 mlf3* cells might have been compromised. Most of the wrinkled cells were large and unbudded, suggesting that the wrinkled-cell phenotype might have occurred preferentially in those *vhs2 mlf3* cells that had suffered loss of polarity. Taken together, the morphological abnormalities of *vhs2 mlf3* cells reveal that they may have a growth polarization defect, which culminates in a loss of structural integrity.

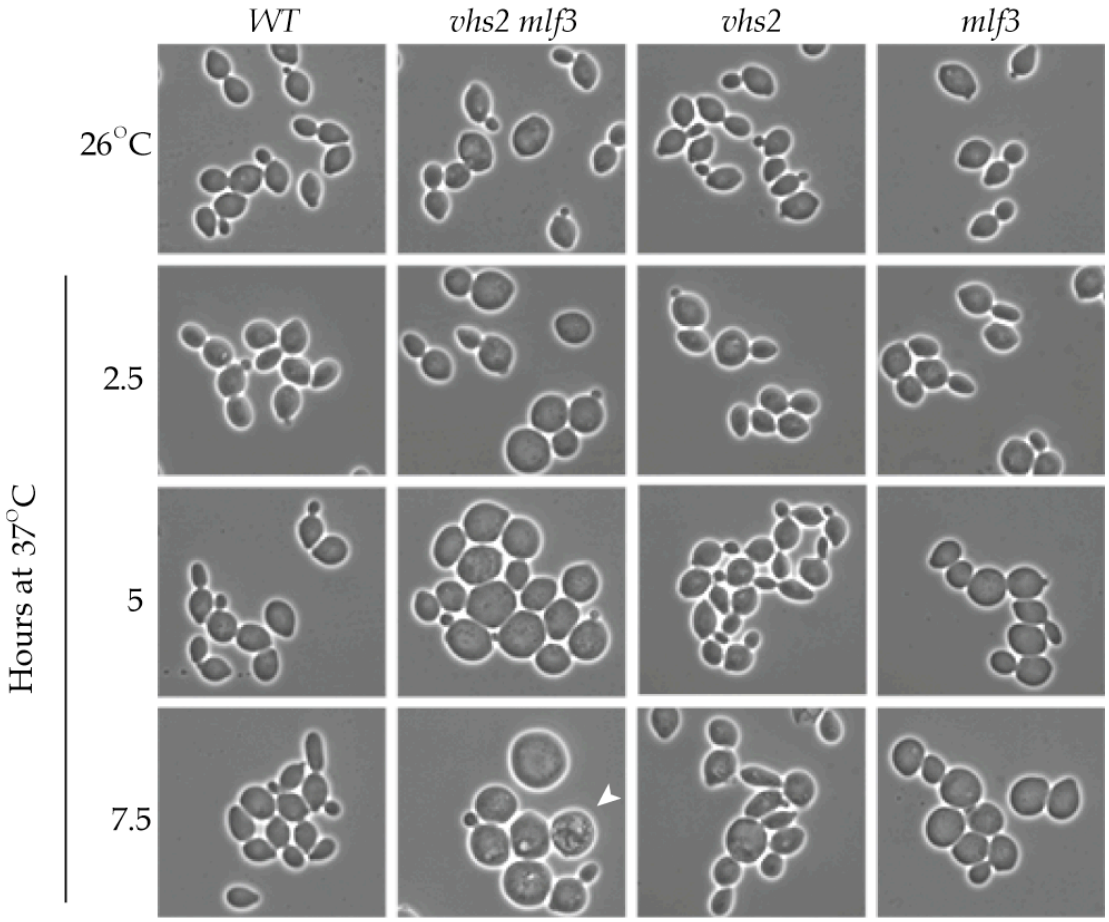

Figure 3.8 Morphology of diploid congenic wild-type (DBY1830), *vhs2 mlf3* (CCY1338), *vhs2* (CCY1720) and *mlf3* (CCY1721) cells. Cells were grown to logarithmic phase in YEPD medium at 26°C, shifted to 37°C for the indicated time periods and fixed with 3.7% formaldehyde. Cells were imaged by phase-contrast microscopy and all cells are shown at the same magnification. The filled arrowhead in the *vhs2 mlf3* panel highlights a wrinkled cell.

Table 3.3 Budding indices of diploid wild-type (DBY1830) and homozygous *vhs2 mlf3* (CCY1338) cells that had been incubated in liquid YEPD medium at 37°C for different time periods.

Time (h) at 37°C	Genotype	Unbudded (%)	Budded (%)		
			Small	Medium	Large
0	WT	43	21	28	8
	vhs2 mlf3	37	26	26	11
2.5	WT	42	33	18	7
	vhs2 mlf3	49	21	12	18
5	WT	39	28	20	13
	vhs2 mlf3	56	27	8	9
7.5	WT	46	26	16	12
	vhs2 mlf3	67	12	7	14

For scoring purposes, the length of the bud was ≤30% that of the mother in small-budded cell, ~30-70% that of that of the mother in medium-budded cells, and ≥70% that of the mother in large-budded cells. 200 cells from each sample were scored.

Absence of VHS2 and MLF3 results in an actin organization defect

The morphological changes in the diploid *vhs2 mlf3* cells observed at 37°C suggested a potential defect in the polarization of the actin cytoskeleton in these cells. To address this possibility, diploid wild-type and homozygous *vhs2 mlf3* cells were cultured in YEPD medium at 37°C for different periods of time, fixed and stained with rhodamine-phalloidin. The F-actin structures in these cells were examined using fluorescent microscopy (Figure 3.9).

The cortical actin organization pattern of wild-type and *vhs2 mlf3* cells at different stages of budding is summarized in Table 3.4. In an asynchronous culture of diploid wild-type cells, roughly half of the unbudded cells had a highly polarized pattern of cortical actin patches that was characteristic of cells that were about to bud. In small- and medium-budded cells, almost all of the cortical actin patches were concentrated in the bud (or at the bud tip). In large-budded cells, cortical actin patches were more evenly distributed between the mother and bud, and a fraction of such cells also had actin patches concentrated at the bud neck.

In contrast, many diploid *vhs2 mlf3* cells had depolarized patterns of cortical actin patches. Upon incubation at 37°C, an increasing fraction of unbudded *vhs2 mlf3* cells became depolarized. By 5 h, >80% of such cells had a depolarized pattern of cortical actin patches (Table 3.4 and Figure 3.9C). Many small-budded *vhs2 mlf3* cells were abnormal in that their buds were devoid of cortical actin patches (and possibly also actin cables) (Table 3.4; Figures 3.9A and 3.9D). By 5 h, ~22% of small-budded *vhs2 mlf3* cells had this phenotype. Interestingly, this abnormal pattern was typically found in cells that were abnormally round, with the mother-half also being unusually large (Figure 3.9A) The medium- and large-budded *vhs2 mlf3* cells had relatively normal patterns of cortical actin patches (Table 3.4), suggesting that small-budded cells that had

Table 3.4 Cortical actin polarization patterns in diploid *vhs2 mlf3* cells.

Time (h) at 37°C	Genotype	Unbudded (%)		Small-budded (%)						Medium-budded (%)				Large-budded (%)		
		I	II	I	II	III	IV	V	VI	I	II	III	IV	I	II	III
		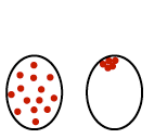		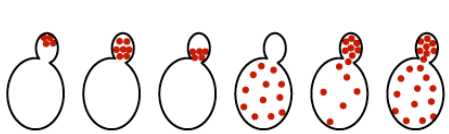						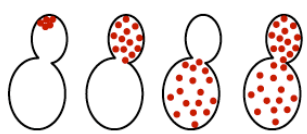				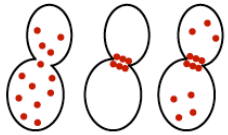		
0	WT	15	28	20	1	0	0	0	0	2	26	0	0	3	4	1
	vhs2 mlf3	13	24	19	6	0.5	0	0	0.5	2	23	0	1	4	5	2
2.5	WT	22	20	31	2	0	0	0	0	3	14	0	1	2	3	2
	vhs2 mlf3	36	13	16	1	0	3	0.5	0.5	2	7	0	3	4	6	8
5	WT	21	18	25	2	0	0	1	0	0	19	0	1	6	4	3
	vhs2 mlf3	46	10	18	2	0	6	1	0	1	6	0	1	2	2	5
7.5	WT	24	22	22	3	0	0	1	0	2	13	0	1	1	5	6
	vhs2 mlf3	65	2	6	1	0	3	2	0	0	3	2	2	1	2	11

Diploid wild-type (DBY1830) and homozygous *vhs2-Δ1::TRP1 mlf3-Δ1::kan* (CCY1338) cells were cultured in YEPD medium at 26°C to a cell density of ~1 –2 X 10^6 cells/ml and then shifted to 37°C for the indicated periods of time. At each time point, ~1 X 10^7 cells were fixed with formaldehyde and stained with rhodamine-phalloidin to visualize actin. ~200-250 cells were counted for each sample.

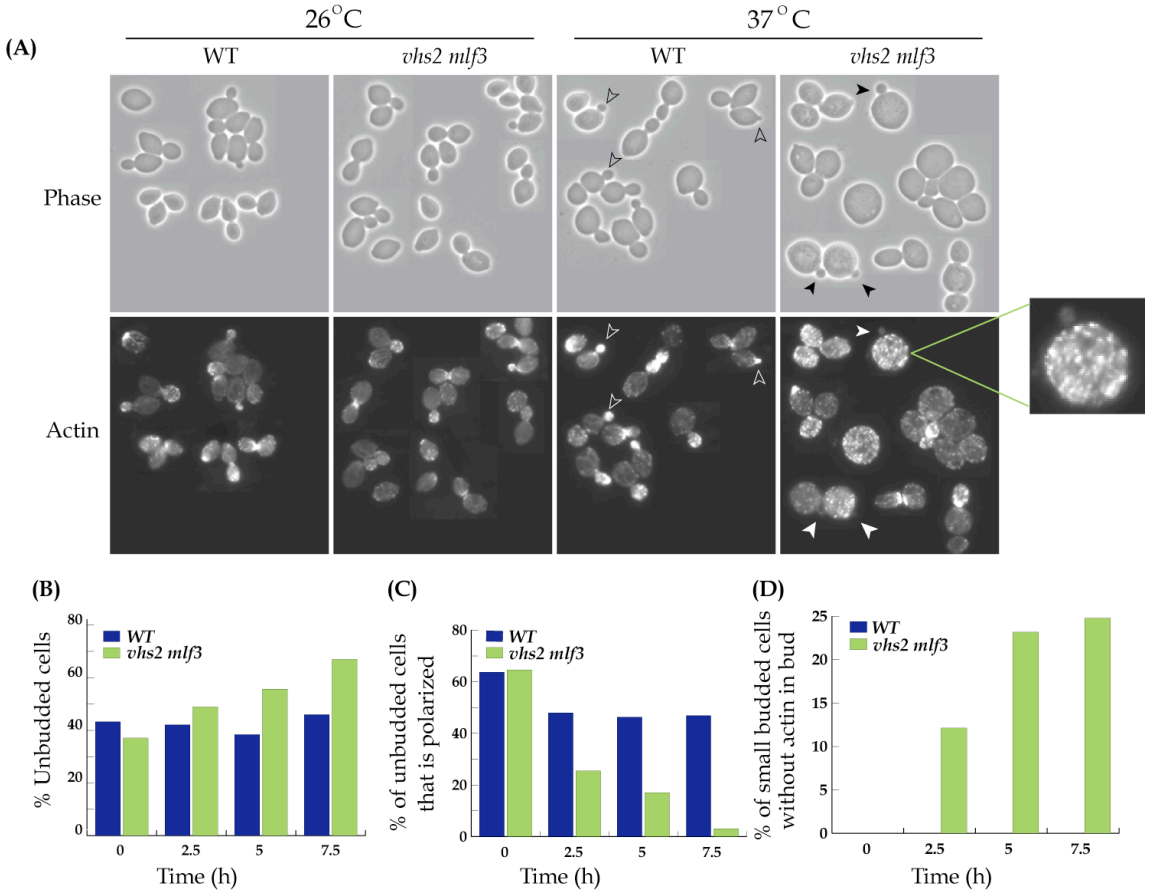

Figure 3.9 Actin polarization defect in *vhs2 mlf3* cells. Diploid wild-type (DBY1830) and homozygous *vhs2 mlf3* (CCY1338) cells incubated at 37°C for the indicated time periods were fixed and stained with rhodamine-phalloidin to reveal F-actin structures. **(A)** Phase and actin-staining images of the same cells. Open arrowheads show small-budded wild-type cells with F-actin concentrated in the bud. Filled arrowheads show small-budded *vhs2 mlf3* cells lacking actin in the bud. All cells are shown at the same magnification except in the inset. Summaries of the distribution of diploid wild-type and *vhs2 mlf3* cells that were unbudded **(B)**, unbudded and with polarized actin **(C)**, and small-budded lacking actin in the bud **(D)**.

depolarized actin patches failed to increase the size of their buds and directed growth to the mother-half instead.

In addition to the drastic actin polarization defects described above, the majority of *vhs2 mlf3* cells that I considered polarized had an abnormally large number of cortical actin patches in the mother cell, indicating that the actin cytoskeleton in these cells may not be totally polarized. Taken together, the data presented here suggested that the combined absence of Vhs2 and Mlf3 results in a defect in actin cytoskeleton organization, particularly in the localization of cortical actin patches.

Mating projection formation in vhs2 mlf3 mutant cells

Polarized organization of actin cytoskeleton in yeast cells is not only required during budding but also for the formation of mating projection in cells that are exposed to mating pheromone (Figure 1.1). I therefore examined if the actin organization defect of *vhs2 mlf3* cells was reflected in the inability of *vhs2 mlf3* cells to form mating projections. As shown in Figure 3.10, at 26°C haploid *vhs2 mlf3* cells responded to α-factor treatment in a manner similar to wild-type cells and initiated the formation of mating projections. However, unlike the wild-type cells, *vhs2 mlf3* cells failed to elongate these mating projections when incubated at 37°C.

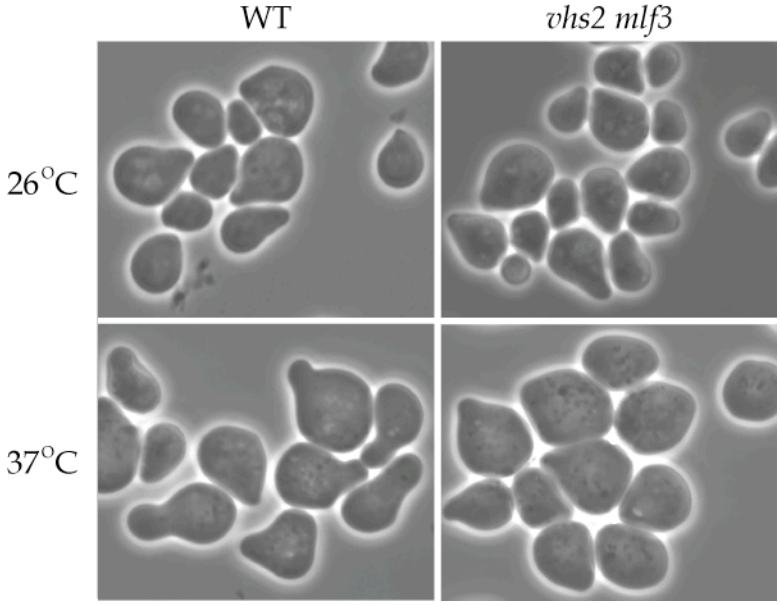

Figure 3.10 *vhs2 mlf3* cells exhibit defect in the formation of elongated mating projections at 37°C. Wild-type (CCY1292-1A) and *vhs2 mlf3* (CCY1292-5B) haploid cells were cultured in acidic YEPD (containing 0.1M citrate, pH 4.5) medium at 26°C and arrested as unbudded cells with α-factor (10 μg/ml final concentration). When more than 90% cells were arrested (26°C sample), a second dose of α-factor was added to continue the cell cycle arrest and cultures were shifted to 37°C for 4 h (37°C sample). Cells were then fixed with 3.7% formaldehyde and their morphology was determined. While most wild-type cells formed elongated mating projections, the majority of *vhs2 mlf3* cells appeared rounder and larger, with pointed structure restricted to one site on the cell surface that apparently failed to elongate as mating projection.

Bud-site selection in vhs2 mlf3 mutant cells

In budding yeast, the site at which the daughter cell separates from its mother cell is marked by a 'birth scar'. This region is also referred to as the proximal pole of the cell. Sites on the cell surface where subsequent buds are formed are marked by 'bud scars'. Because of their axial budding pattern, bud scars are normally seen in the vicinity of the proximal pole in wild-type haploid cells. Because of the bipolar budding pattern of diploids, bud scars can be present at the proximal pole or at the distal pole (the end opposite to the proximal pole) in diploid cells. However, the initial 2-3 rounds of budding in diploid cells preferentially occur at the distal pole, and this bias decreases

thereafter, resulting in a more random selection of the subsequent bud sites at either the proximal or distal pole (Zahner et al., 1996).

Since the bud-site selection defect of *gic1 gic2* cells could be complemented partially by an increased dosage of *VHS2* or *MLF3* (Figure 3.2), I tested whether Vhs2 and Mlf3 were required for proper bud-site selection. The budding patterns of *vhs2 mlf3* cells at 26°C were examined after staining their birth and bud scars with calcofluor white.

Analysis of the budded cells with two or more bud scars revealed that haploid *vhs2 mlf3* cells, like wild-type cells, predominantly had the axial budding pattern (Table 3.5). However, 23% of diploid *vhs2 mlf3* cells demonstrated randomized bud-site selection compared to 9% of diploid wild-type cells (Table 3.6). To examine whether diploid *vhs2 mlf3* cells demonstrated any deviation from the normal pattern of preference for the selection of the first, second or the

Table 3.5 Budding pattern of haploid *vhs2 mlf3* cells.

Genotype	Bud scar pattern (%)		
	I	II	III
WT	95	2.5	2.5
vhs2 mlf3	95	1	4

Haploid wild-type (CCY1292-1A) and *vhs2-Δ1::TRP1 mlf3-Δ1::kan* (CCY1292-5B) cells were cultured in YEPD at 26°C to a density of 1 x 10^7 cells/ml, fixed and stained with calcofluor white. For each sample, more than 200 cells with two or more bud scars were examined. The scoring criteria were identical to those described in Table 3.1.

Table 3.6 Budding patterns of diploid *vhs2 mlf3* cells.

Genotype	Bud scar pattern (%)							
	I	II	III	IV	V			VI
	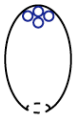		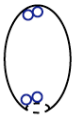	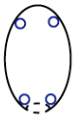	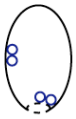	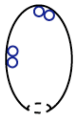	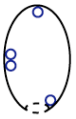	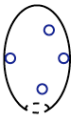
Wild-type	7	0	83	1	0	1	7	1
vhs2 mlf3	0	0	74	3	0	5	8	10

Diploid wild-type (DBY1830) and homozygous *vhs2-Δ1::TRP1 mlf3-Δ1::kan* (CCY1338) cells were cultured in YEPD at 26°C to a density of 1 X 10^7 cells/ml, fixed and stained with calcofluor white. Since budding from both proximal and distal poles is normal in diploid cells, only those cells with four or more bud scars were scored to assess if bud-site selection was randomized in *vhs2 mlf3* mutant cells. Although cartoons show only 4 bud scars, cells that were scored had four or more bud scars in different combination of numbers at the sites shown. For category V, the bud scars were present at either one (proximal or distal) or both poles of the cells as well as at other sites on the cell surface. A dotted ring (black) represents the birth scar whereas solid rings (blue) represent bud scars. ~200 cells were counted for each sample. Categories V and VI are considered abnormal.

third bud site, wild-type and *vhs2 mlf3* diploid cells with one, two or three bud scars were examined (Table 3.7). While the preference for the selection of the first and the third bud sites remained normal in *vhs2 mlf3* cells, a greater fraction (50%) of *vhs2 mlf3* cells chose the proximal instead of the distal pole for their second round of budding (Figure 3.11).

Table 3.7.1 Selection of the first bud-site in homozygous diploid *vhs2 mlf3* cells.

	Bud scar pattern (%)					
	I	II	III	IV	V	VI
Genotype	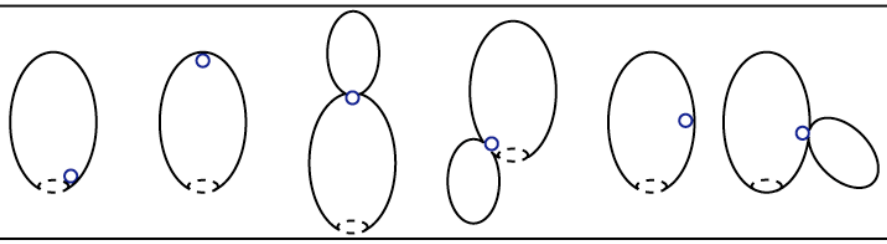					
Wild-type	2	15	82	1	0	0
vhs2 mlf3	0	26	73	1	0	0

Table 3.7.2 Selection of the second bud-site in homozygous diploid *vhs2 mlf3* cells.

	Bud scar pattern (%)					
	I	II	III	IV	V	VI
Genotype	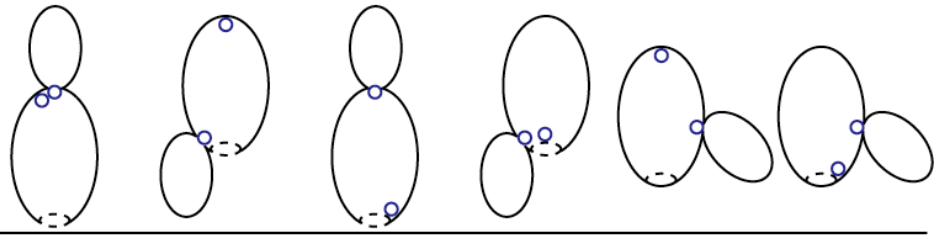					
Wild-type	66	21	9	0	4	0
vhs2 mlf3	46	50	2	0	2	0

Table 3.7.3 Selection of the third bud-site in homozygous diploid *vhs2 mlf3* cells.

	Bud scar pattern (%)										
	I	II	III	IV	V	VI	VII	VIII	IX	X	XI
Genotype	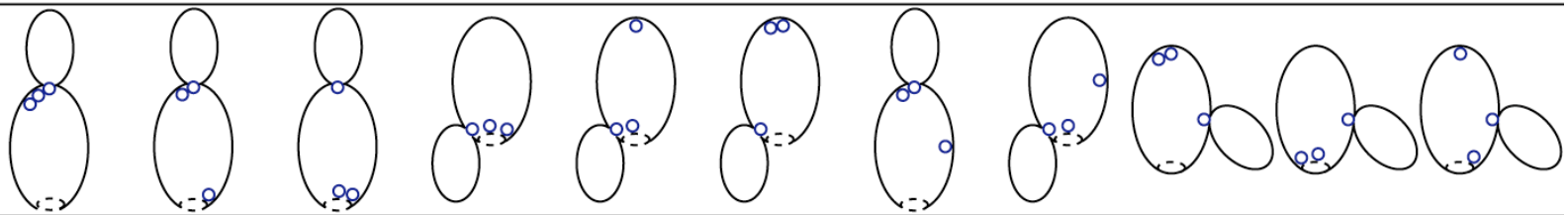										
Wild-type	36	19	0	1	12	30	1	0	1	0	0
vhs2 mlf3	25	37	1	0	12	24	0	0	1	0	0

Diploid wild-type (DBY1830) and homozygous *vhs2-Δ1::TRP1 mlf3-Δ1::kan* (CCY1338) cells were cultured in YEPD at 26°C to a density of 1 x 10^7 cells/ml, fixed and stained with calcofluor white. For scoring the selection preference of the first bud-site, unbudded or budded cells with only one bud scar were scored. For scoring the selection preference for the second and third bud-sites, budded cells with only two and three bud scars, respectively, were scored. The dotted ring (black) represents the birth scar whereas solid rings (blue) represent bud scars. ~200 cells were counted for each sample.

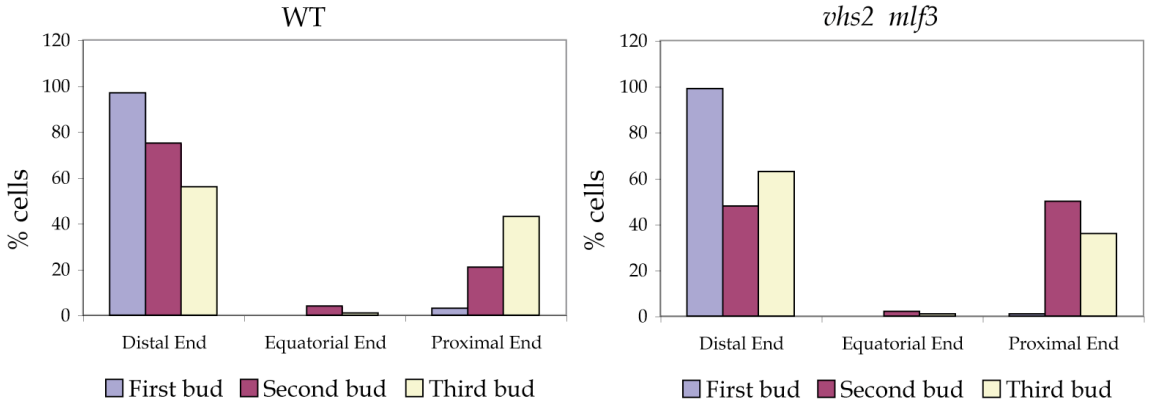

Figure 3.11 Compared to wild-type (DBY1830) cells, homozygous diploid *vhs2 mlf3* (CCY1338) cells show a greater usage of the proximal end of the cell for the second round of bud emergence. This figure summarizes the data from Tables 3.7.1, 3.7.2 and 3.7.3.

In summary, at 26°C, haploid *vhs2 mlf3* cells displayed normal axial budding pattern, whereas diploid *vhs2 mlf3* cells showed some degree of randomized budding and a modest decrease in their bias in the selection for the second bud-site. This diploid-specific defect in bud-site selection is a characteristic of many mutants that have an actin cytoskeletal defect.

vhs2 mlf3 mutant cells exhibit cell lysis defect

The flocculation of cultures containing homozygous diploid *vhs2 mlf3* cells at 37°C, the clumpiness of these cells as observed under the microscope, and the wrinkled morphology of such cells together suggested that the cell wall structure of *vhs2 mlf3* cells might be compromised. To examine the potential cell wall defect of *vhs2 mlf3* cells, I tested the calcofluor white-sensitivity of these cells. Many mutants with defective cell wall have been identified in genetic screens based on their increased calcofluor white-sensitivity (Ram et al., 1994). Growth of haploid and diploid cells lacking *VHS2* and *MLF3*, either singly or in combination, was evaluated at 30°C on YEPD agar containing

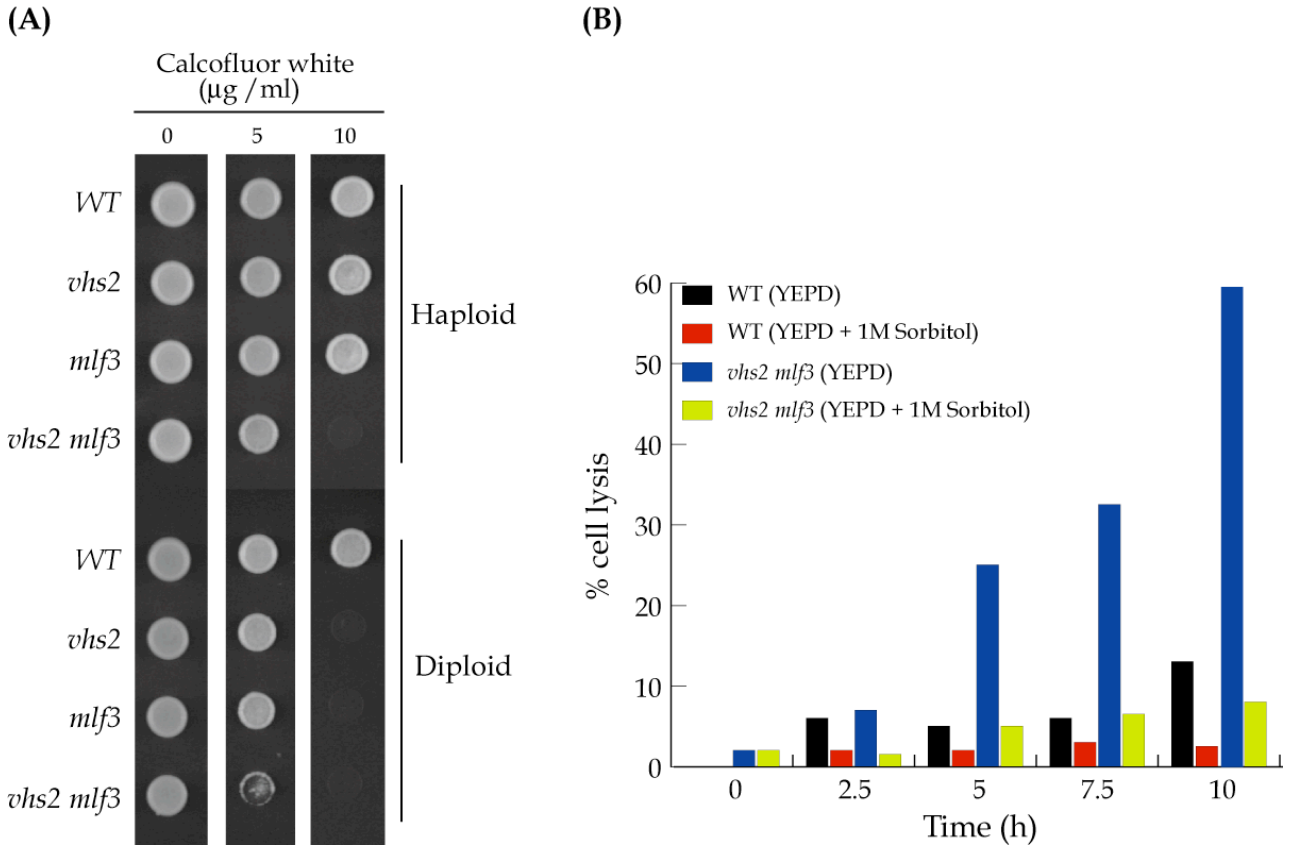

Figure 3.12 *vhs2 mlf3* cells exhibit a defect in cell integrity. **(A)** Hypersensitivity of *vhs2 mlf3* cells to calcofluor white. Suspensions (OD_{600} = 1) of congenic haploid and diploid wild-type (CCY1292-1A and DBY1830), *vhs2* (CCY1292-4B and CCY1720), *mlf3* (CCY1292-1D and CCY1721) and *vhs2 mlf3* (CCY1292-5B and CCY1338) cells were spotted on YEPD agar containing 0, 5 or 10 µg/ml of calcofluor white and incubated at 30°C for 2 days. **(B)** *vhs2 mlf3* cells undergo cell lysis that can be partially rescued by including 1M sorbitol in the growth medium. Diploid wild-type (DBY1830) and *vhs2 mlf3* (CCY1338) cells were cultured at 26°C to ~0.5-0.7 X 10^7 cells/ml and shifted to 37°C. After indicated time periods at 37°C, equal volumes of cell culture and trypan blue solution (0.4% stock concentration) were mixed and allowed to sit on the bench-top for 5 minutes. Cells that appeared blue (as observed by light microscopy) were considered lysed.

0, 5 or 10 μg/ml of calcofluor white (Figure 3.12A). Like wild-type cells, haploid *vhs2* and *mlf3* single mutant cells proliferated in the presence of 10 μg/ml of calcofluor white. However, growth of haploid *vhs2 mlf3* double mutant cells was inhibited by this concentration of calcofluor white. Similar to the pattern observed for the growth of haploid and diploid mutants at 37°C (Figure 3.5A), the diploid mutants appeared to be more sensitive to calcofluor white than their haploid counterparts (Figure 3.12A). These results were consistent with a potential cell wall defect in *vhs2 mlf3* cells.

To address whether wrinkled *vhs2 mlf3* cells (Figure 3.8) might be the result of cell lysis, diploid homozygous *vhs2 mlf3* cells were cultured in YEPD medium at 37°C for varying periods of time and stained with trypan blue, which is not excluded from cells that are lysed and dead. As shown in Figure 3.12B, after 5 h at 37°C, ~25% of *vhs2 mlf3* cells lysed and the percentage of lysed cells increased with further incubation at 37°C. Furthermore, the cell lysis phenotype of *vhs2 mlf3* cells was rescued by the presence of an osmotic stabilizer (1 M sorbitol) in the growth medium (Figure 3.12B). Correspondingly, the growth defect of *vhs2 mlf3* cells at 37°C was also rescued by sorbitol (Figures 3.5 and 3.7). Taken together, the data demonstrate that *vhs2 mlf3* mutant cells suffer from sub-optimal cell integrity at higher temperatures and as a consequence, undergo cell lysis and yield wrinkled cells. Since the onset of the actin polarization defect in these cells appears to precede that of cell lysis (Figures 3.9C, 3.9D, and 3.12B), the cell wall integrity defect might occur as a consequence of the defect in actin cytoskeleton polarization.

Is the abundance of Vhs2 and Mlf3 affected by elevated temperatures?

Since the mutant phenotype of *vhs2 mlf3* cells was most apparent at 37°C, I examined if Vhs2 and Mlf3 were more abundant at 37°C. For this purpose, haploid and homozygous diploid strains expressing both chromosomally tagged Vhs2-3HA and Mlf3-13Myc fusion proteins were cultured in YEPD media at 26°C or at 37°C for 2, 4 and 6 h. Immunoblotting of the protein extracts obtained from these cells with anti-Myc antibodies showed that comparable amounts of Mlf3-13Myc protein were present when cells were incubated at 26°C or at 37°C for 6 h (Figure 3.13).

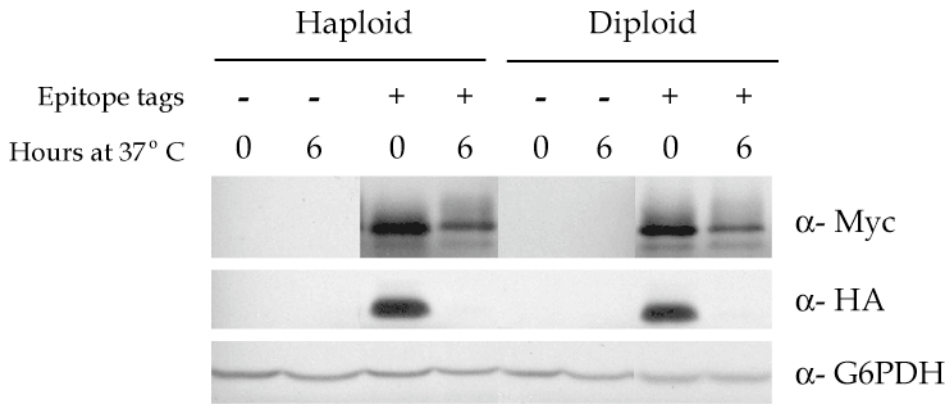

Figure 3.13 Abundance of Vhs2 and Mlf3. Haploid (CCY1663-3C) and homozygous diploid (CCY1664) cells expressing chromosomally tagged *VHS2-3HA* and *MLF3-13MYC* together were cultured at 26°C (0 h lanes) or 37°C (6 h lanes). Haploid strain DBY1828 and diploid strain DBY1830 were used as untagged controls. Proteins were separated by SDS-PAGE and immunoblotted with α-HA and α-Myc antibodies for detecting Vhs2-3HA and Mlf3-13Myc proteins, respectively. Equal amount of protein loading between lanes was confirmed by probing the filter with α-G6PDH antibody. The amounts of Vhs2-3HA and Mlf3-13Myc present in the cells after 2 h and 4 h of incubation at 37°C were also examined but not shown in this figure. Almost total disappearance of Vhs2-3HA protein was detected after 2 h of incubation at 37°C in both haploid and diploid cells.

Surprisingly, immunoblotting with anti-HA antibody demonstrated that Vhs2-3HA protein was present at 26°C but not after 2 h at 37°C. Although somewhat unexpected, this result is consistent with my previous observation that *mlf3* mutants are slightly more defective than *vhs2* mutants in polarized growth at 37°C (Figures 3.5 and 3.8).

Subcellular localization of Vhs2 and Mlf3

The localization pattern of a protein within a cell can provide a useful cue towards the function of that protein. A large number of budding yeast proteins involved in polarized growth localize at sites of active growth, (i.e., at the tip of a growing bud and at the bud neck of dividing cells). To determine if Vhs2 and Mlf3 exhibited a similar localization pattern, diploid cells (DBY1830) expressing GFP-Vhs2 or GFP-Mlf3 under the *ACT1* promoter (from plasmids pCC1658 and pCC1659, respectively) were cultured in synthetic complete medium (selecting for cells that maintained the plasmid) at 26°C and visualized using fluorescence microscopy. These two fusion proteins were functional since their expression complemented the Ts^- phenotype of *vhs2-Δ1::TRP1 mlf3-Δ1::Kan* cells (CCY1292-10C). Both, GFP-Vhs2 and GFP-Mlf3 appeared to be present throughout most part of the cell, being excluded from structures that were most likely vacuoles. Thus, GFP-Vhs2 and GFP-Mlf3 are probably cytoplasmic proteins. Subsequently, the genome-wide study of C-terminally GFP tagged proteins from *S. cerevisiae* also confirmed the cytoplasmic localization pattern for the Vhs2 and Mlf3 proteins (Huh et al., 2003).

Multi-copy suppressors of vhs2 mlf3 mutations

In order to gain further insight into the cellular function of Vhs2 and Mlf3, 59 proteins reported to function in budding yeast cell polarity, either directly or indirectly, were overproduced in *vhs2 mlf3* cells and their effect on the growth

phenotype of *vhs2 mlf3* cells was examined. To this end, a haploid *vhs2 mlf3* strain (CCY1292-10C) was transformed with 58 individual multi-copy plasmids, each carrying a different gene. Suspensions of transformants were spotted on YEPD agar and incubated at 37°C to determine whether an increased dosage of any of these genes could suppress or exacerbate the growth defect of *vhs2 mlf3* cells. 33 genes (including *ABP1*, *ACT5*, *BEM1*, *BEM2*, *BEM3*, *BUD5*, *CDC24*, *CDC42*, *CLA4*, *CYK2*, *ERF2*, *FKS2*, *LRG1*, *MGC1*, *MSB3*, *MSB4*, *PFY1*, *RGA1/DBM1*, *RHO3*, *RPI1*, *RSR1*, *SAC7*, *SIT4*, *SKM1*, *SLA1*, *SMY1*, *SPA2*, *SSN6*, *SWI6*, *TOS2*, *TUP1*, *ZDS1* and *ZDS2*) did not influence the temperature-sensitive growth defect of *vhs2 mlf3* cells. Increased expression of *STE20* (under the *ACT1* promoter on a CEN plasmid) also did not suppress this defect. The other 25 plasmids, however, were able to suppress the growth defect of *vhs2 mlf3* cells to varying degrees (Table 3.8). These plasmids expressed genes encoding components of the cell integrity pathway (*BCK1*, *BCK1-20*, *MID2*, *MKK1*, *MPK1/SLT2, RHO1*, *RHO2*, *PKC1* and *WSC1*,), G1 cyclins (*CLG1, CLN1*, *CLN2*, *PCL1* and *PCL2*), and proteins that regulate the transcription of G1 cyclin genes (*BCK2, PPZ2* and *SWI4*). In addition, increased dosage of *BNI1, GIC1*, *GIC2*, *MSB1* and *MSB2*, which are all involved in polarized growth, also suppressed the growth defect of *vhs2 mlf3* cells.

Table 3.8 Multi-copy suppressors of haploid *vhs2 mlf3* mutant cells.

Plasmid	Gene	Suppression at 37°C	
		YEPD	SD
B309	*BCK1*	++	-
p636	*BCK1-20*	+	-
pBH124	*BCK2*	+++	+
YEp352-BNI1	*BNI1*	++	-
YEp24-CDC28	*CDC28*	+++	+
p366	*CLG1*	+	+
YEp24-CLN1	*CLN1*	+++	+++
YEp24-CLN2	*CLN2*	+++	+++
pCC904	*GIC1*	+++	++
pCC967	*GIC2*	+	-
p1245	*MID2*	++	+
p594	*MKK1*	++	-
p582	*MPK1*	++	-
pPB191	*MSB1*	++	++
pPB207	*MSB2*	++	+
pBA531	*PCL1*	+++	++
pBA623	*PCL2*	+	-
p200	*PKC1*	+	+
p669	*PPZ2*	+	-
YEpU-RHO1	*RHO1*	++	+
YEpU-RHO2	*RHO2*	++	++
B305	*SLT2*	+	-
pCC75	*SSD1-v(1)*	+++	+++
B327	*SWI4*	+	-
p167	*WSC1*	+	+
pCC1606	*VHS2*	+++	++
pCC1635	*MLF3*	+++	++

Haploid *vhs2-Δ1::TRP1 mlf3-Δ1::kan* (CCY1292-10C) cells were transformed with multi-copy plasmids (except for p636 and pCC75, which were CEN plasmids). Suspension of cells from the transformants were spotted on YEPD agar and SD agar (supplemented with amino acids to maintain the plasmid) and incubated at 37°C for 2 days on YEPD agar and 3 days on SD agar before scoring. (-) indicates no suppression, (+) indicates mild suppression, (++) indicates moderate suppression and (+++) represents strong suppression of the growth defect of *vhs2 mlf3* cells.

Since the growth defect of haploid *vhs2 mlf3* cells is relatively modest on YEPD agar at 37°C, I also rechecked the growth of different *vhs2 mlf3* transformants on minimal supplemented medium. The growth defect of *vhs2 mlf3* cells was more pronounced on this medium. Clearly, not all multi-copy suppressors capable of complementing the growth defect of *vhs2 mlf3* cells on YEPD agar at 37°C were able to do so on minimal medium containing agar (Table 3.8).

The most robust suppressors identified from this experiment included *CLN1*, *CLN2*, *GIC1*, *PCL1* and *SSD1-v(1)* (Figure 3.14A). *SSD1* is a polymorphic locus in budding yeast. The *SSD1-v(1)* allele suppresses mutations that affect diverse cellular processes, including polarized growth, cell integrity, cell cycle progression, and growth at high temperatures (Kaeberlein et al., 2004; Kaeberlein and Guarente, 2002). It is noteworthy that *SSD1-v(1)* also suppresses the temperature-sensitivity of *gic1 gic2* cells (Chen et al., 1997; discussed in detail in Chapter 4).

The finding that increased dosage of *GIC1* (and to a lesser degree *GIC2*) could suppress the growth defect of *vhs2 mlf3* cells was intriguing. *VHS2* and *MLF3* themselves functioned as multi-copy suppressors of *gic1 gic2* mutations (Figure 3.1). Such a pattern of reciprocal suppression implied that Vhs2 and Mlf3 must function in a pathway that is redundant and parallel to that mediated by Gic1 and Gic2. Consistent with this interpretation, simultaneous deletion of *VHS2* and *MLF3* in a *gic1 gic2* mutant background exacerbated the temperature-sensitivity of *gic1 gic2* cells (Figure 3.14B). To understand this genetic interaction further, I examined whether any of the multi-copy plasmids that suppressed the growth defect of *vhs2 mlf3* cells could also suppress the growth defect of *gic1 gic2* cells. To this end, haploid *gic1 gic2* cells (CCY1024-3A) were transformed with plasmids expressing *BCK2*, *CLN1*, *MID2, PCL1*, or *WSC1*. Transformants were

incubated at different temperatures on YEPD agar. Increased dosage of *MID2, PCL1* and *WSC1* resulted in only slight improvement in the growth of *gic1 gic2* cells at 33°C (not shown). Increased dosage of *CLN2* has already been shown to raise the permissive growth temperature of *gic1 gic2* cells (Figure 3.1).

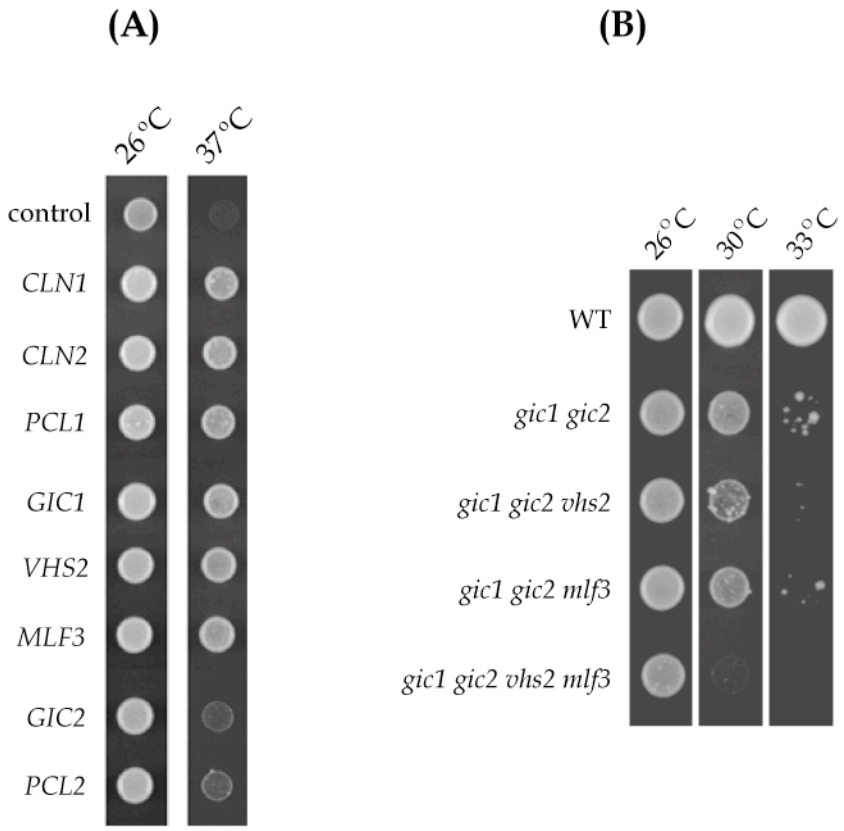

Figure 3.14 (A) Multi-copy plasmids expressing G1 cyclins and *GIC1* complement the growth defect of *vhs2 mlf3* cells. Suspensions of haploid *vhs2-Δ1::TRP1 mlf3-Δ1::kan* cells (CCY1292-10C) carrying different plasmids (see legend to Table 3.8) were spotted on YEPD agar and allowed to grow at the indicated temperatures for 2 days. Suppression by *SSD1-v(1)*-expressing CEN plasmid was equally impressive but not shown in this figure. **(B)** The mutant phenotype of *gic1 gic2* cells is exacerbated by additional mutations in *VHS2* and *MLF3*. The haploid strains used were DBY1829 (wild-type), CCY1726-18C (*gic1 gic2*), CCY1726-2B (*gic1 gic2 vhs2*), CCY1726-5B (*gic1 gic2 mlf3*) and CCY1726-4D (*gic1 gic2 vhs2 mlf3*).

The genetic interactions between *VHS2, MLF3*, *GIC1* and *GIC2* lead to speculations regarding how Vhs2 and Mlf3 might function in the polarization of the actin cytoskeleton. First, Vhs2 and Mlf3 might function in cooperation with the other effectors of Cdc42, such as Ste20 or Cla4. Second, Vhs2 and Mlf3 might function in a pathway that is independent of the signaling from Cdc42 GTPase to regulate the actin cytoskeleton. Consistent with the latter speculation is the

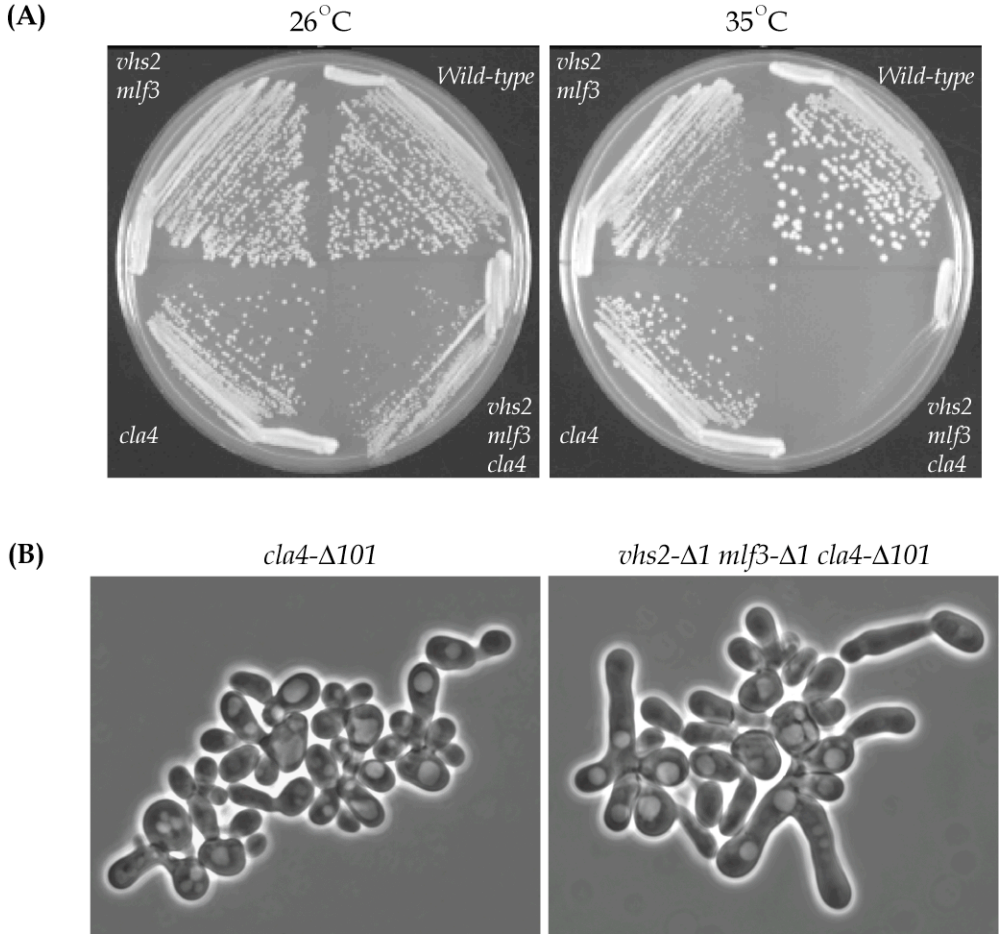

Figure 3.15 Deletion of *VHS2* and *MLF3* enhances the growth and morphological defect of *cla4* mutants. **(A)** Haploid congenic wild-type (DBY1829), *vhs2 mlf3* (CCY1368-12A), *cla4* (CCY1368-4C) and *vhs2 mlf3 cla4* (CCY1368-8C) cells were streaked out on YEPD agar and incubated at the indicated temperatures for 2 days. **(B)** *cla4* (CCY1368-12A) and *vhs2 mlf3 cla4* (CCY1368-8C) cells from exponentially growing YEPD cultures at 26°C were examined by phase-contrast microscopy. *vhs2 mlf3 cla4* cells were more branched and elongated than *cla4* single mutant cells.

synthetic genetic interaction between *vhs2 mlf3* and *cla4* mutations that I have identified. *vhs2 mlf3 cla4* triple mutant cells showed an exacerbation of the growth phenotype of *vhs2 mlf3* double mutant cells at 35°C (Figure 3.15A) as well as an enhancement in the elongated cell morphology of *cla4* single mutant cells at 26°C (Figure 3.15B).

The G1 cyclins associate with their Cdk partners to form functional Cdk-cyclin complexes and promote transition from G1 to S phase of the cell cycle (Lew and Reed, 1993). While Cln1 and Cln2 associate with Cdc28, the Pcl1 and Pcl2 cyclins bind to Pho85. One possible explanation for the observed suppression of the temperature-sensitive growth defect of *vhs2 mlf3* cells by increased dosage of *CLN1*, *CLN2* and *PCL1* is that *vhs2 mlf3* cells might be delayed in G1 to S transition at 37°C. If so, overproduction of G1 cyclins might facilitate the G1 to S transition in *vhs2 mlf3* cells, thus allowing them to grow at 37°C. However, *vhs2 mlf3* cells did not arrest exclusively as unbudded cells, as would be expected for a block in G1 to S transition (Figure 3.9B). In addition, the rate of cell cycle progression at 37°C, as measured by flow cytometry, was similar between haploid wild-type and *vhs2 mlf3* cells (Figure 3.16). Thus, the ability of the G1 cyclins to suppress the growth phenotype of *vhs2 mlf3* cells appeared to be distinct from their role in promoting G1 to S transition.

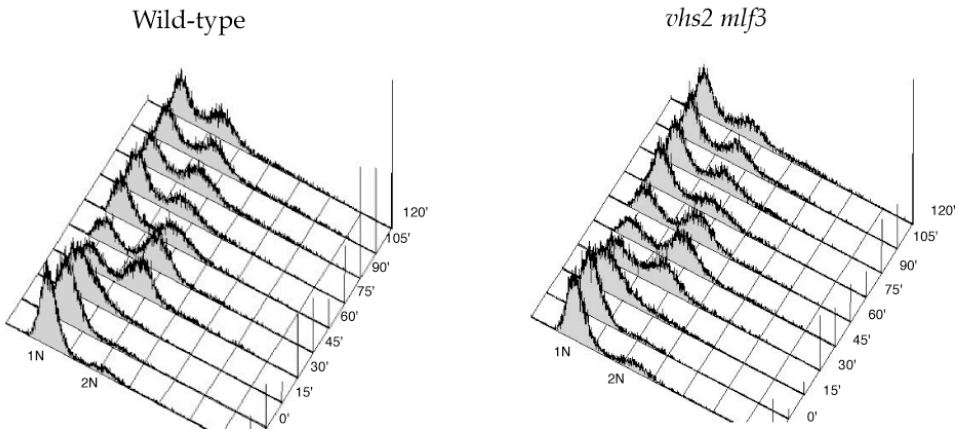

Figure 3.16 *vhs2 mlf3* cells progress through the cell cycle at the same rate as wild-type cells. Haploid wild-type (CCY1292-1A) and *vhs2 mlf3* (CCY1292-5B) cells were cultured in acidic YEPD (containing 0.1M citrate, pH 4.5) medium at 26°C to an OD_{600} of 0.3 - 0.4 and α-factor was added (10 μg/ml final concentration). After ~3 h of incubation at 26°C, when more than 90% of cells were arrested as unbudded cells, cultures were shifted to 37°C and a second dose of α-factor was added to maintain the cell cycle arrest. 2.5 h after temperature shift, cells were released from the arrest by being washed twice with water, resuspended in fresh YEPD medium and incubated at 37°C. Samples were taken at this time point (0 minute sample) and at every 15-minute interval thereafter and processed for flow cytometry.

cln1 cln2 pcl1 pcl2 mutants arrest in G1 stage of the cell cycle and are inviable (Lenburg and O'Shea, 2001). However, this defect can be rescued by 1 M sorbitol, suggesting that the primary defect in these quadruple mutant cells is not due to impaired G1 to S phase progression, but rather due a defect in cell wall biogenesis- or morphogenesis-related function (Lenburg and O'Shea, 2001). Recently, it has been suggested that a burst in G1 cyclin activity is required mainly for bud emergence and septin assembly instead of cell cycle progression (Moffat and Andrews, 2004). This additional function of G1 cyclins may provide an alternate plausible explanation for the ability of increased dosage of G1 cyclin genes to suppress the growth defect of *vhs2 mlf3* cells. As a reminder, *vhs2 mlf3*

cells are partially defective in polarization of the actin cytoskeleton (and thus budding) (Figure 3.9C) and mating projection formation (Figure 3.10).

Genetic interaction between VHS2/MLF3 and RVS161/RVS167

While Cln1 and Cln2 regulate polarity at least partly via regulation of Ste20 and Cla4 (Oda et al., 1999), the Pho85-Pcl1/2 complexes do so via the Rvs161 and Rvs167 proteins (Lee et al., 1998). Several lines of genetic evidence suggest that Pho85-Pcl/2-mediated regulation of actin cytoskeletal organization constitutes a functionally redundant pathway with that mediated by the Cdc42 GTPase (Lenburg and O'Shea, 2001; Moffat and Andrews, 2004). In light of the potential function of Vhs2 and Mlf3 in a pathway that is likely to be redundant to that mediated by the Cdc42 GTPase, the next question was to address whether Vhs2 and Mlf3 function in the Pcl1/2- mediated pathway of actin organization.

For this purpose, I carried out tetrad analysis to study potential genetic interactions between *VHS2, MLF3*, *RVS161* and *RVS167*. Indeed, the growth defect of *vhs2 mlf3* cells was exacerbated by a deletion mutation in *RVS161* or *RVS167* (Figure 3.17A). Although the enhanced temperature-sensitivity of *vhs2 mlf3 rvs161* cells is more severe than that of *vhs2 mlf3 rvs167* cells, it is of incomplete penetrance in nature. Out of 36 *vhs2 mlf3 rvs161* spores analyzed, only 25 showed the enhanced temperature-sensitivity. The different degrees to which the *rvs161* and *rvs167* mutations affect the growth phenotype of *vhs2 mlf3* cells are surprising, as Rvs167 and Rvs161 are thought to be dependent on each other for function (Lombardi and Riezman, 2001). Because of the incomplete penetrance of the growth phenotype of *vhs2 mlf3 rvs161* cells, I have chosen to focus on the *RVS167* gene in my studies.

Deletion of *RVS167* results in several polarity-related phenotypes, including increased sensitivity to salt, defects in endocytosis and actin cytoskeleton organization, and randomized budding in diploid cells

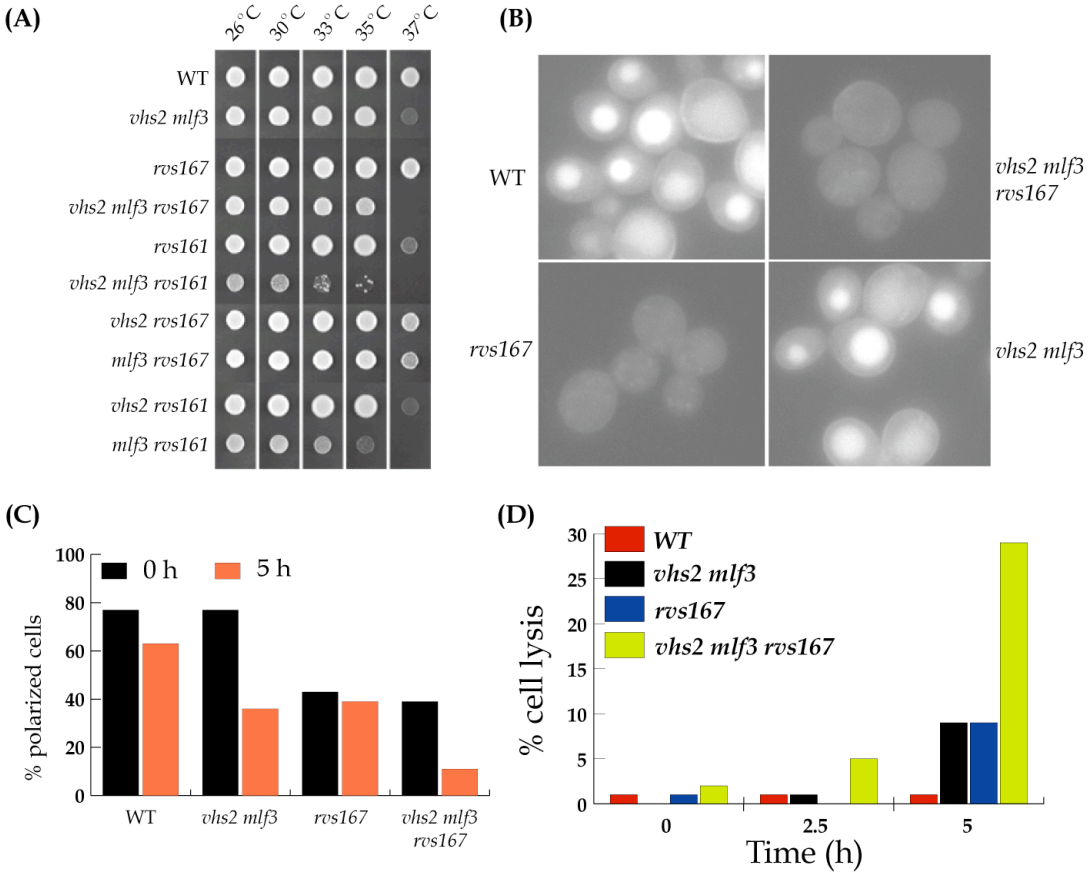

Figure 3.17 Genetic interaction between *VHS2, MLF3* and *RVS* genes. **(A)** Temperature-sensitive growth defect of haploid *vhs2 mlf3* cells is exacerbated by a deletion mutation in either *RVS161* or *RVS167*. Suspensions of cells (see below) were spotted on YEPD agar and allowed to grow at the indicated temperatures for 2 days. **(B)** At 26°C, haploid *vhs2 mlf3* cells do not exhibit defect in fluid-phase endocytosis, which was monitored by the uptake of Lucifer yellow (bright signal) into vacuoles. **(C)** Actin polarization and **(D)** cell lysis defects of *vhs2 mlf3* cells are enhanced by an *rvs167* mutation. Cells were cultured in YEPD medium at 26°C to ~0.5-0.7 X 10^7 cells/ml and shifted to 37°C for 5 h. For examining F-actin structures, cells were fixed and stained with rhodamine-phalloidin. For detecting cell lysis, equal volumes of cell culture and trypan blue solution (0.4% [w/v] stock concentration) were mixed and allowed to sit on the bench-top for 5 minutes. Cells that appeared blue (as observed by light microscopy) were considered lysed. ~200 cells from each sample were scored for rhodamine-phalloidin staining and trypan blue staining. The haploid strains used were CCY1292-1A (wild-type), CCY1292-5B (*vhs2 mlf3*), CCY1457-8B (*rvs167*), CCY1457-7C (*vhs2 mlf3 rvs167*), CCY1456-11B (*rvs161*), CCY1456-7A (*vhs2 mlf3 rvs161*), CCY1457-6C (*vhs2 rvs167*), CCY1457-2C (*mlf3 rvs167*), CCY1456-10D (*vhs2 rvs161*) and CCY1456-4B (*mlf3 rvs161*).

(Bauer et al., 1993; Desfarges et al., 1993; Munn et al., 1995; Sivadon et al., 1995; Sivadon et al., 1997a). Since *vhs2 mlf3* cells also exhibit actin cytoskeleton organization and cell lysis defects, I examined if the *rvs167* mutation exacerbates these defects of *vhs2 mlf3* cells. For this purpose, haploid wild-type, *vhs2 mlf3*, *rvs167* and *vhs2 mlf3 rvs167* cells were cultured in YEPD medium at 37°C for 5 h and stained with rhodamine-phalloidin or trypan blue. My results showed that the actin cytoskeleton organization and cell lysis defects of the *vhs2 mlf3* cells were exacerbated by the *rvs167* mutation (Figures 3.17C and 3.17D). It is noteworthy that *vhs2 mlf3* cells exhibited a primary actin cytoskeleton defect in unbudded cells and small-budded cells (Table 3.4; Figures 3.9C and 3.9D) whereas *vhs2 mlf3 rvs167* cells showed such a defect in all cell types. This suggested that Rvs167 must contribute to the process of actin organization during all stages of the cell cycle in the absence of Vhs2 and Mlf3.

Next, I examined if the endocytosis defect of *rvs167* cells was enhanced by deletion of *VHS2* and *MLF3*. Lucifer yellow uptake assays were carried out to examine fluid-phase endocytosis defect (Figure 3.17B). Wild-type cells showed uptake of this dye into their vacuoles. *vhs2 mlf3* mutant cells cultured at either 26°C or 37°C demonstrated uptake of lucifer yellow into vacuoles, indicating that there was no obvious defect in fluid-phase endocytosis in these cells. Most *rvs167* single mutant cells, however, failed to accumulate the dye even when cultured at 26°C. Therefore, it was not possible to measure if additional deletions of *VHS2* and *MLF3* in *rvs167* cells further enhanced this defect.

In order to further understand the synthetic sick interaction observed between *vhs2 mlf3* and *rvs161* or *rvs167* mutations, effects of increased dosage of *RVS161* and *RVS167* on the temperature-sensitive growth defect of *vhs2 mlf3* cells were examined. To this end, *vhs2 mlf3* cells (CCY1292-10C) were transformed with 2μ plasmids expressing *RVS161* (pCC1870) or *RVS167* (pCC1871). The

result of this experiment revealed that increased dosage of neither *RVS161* nor *RVS167* suppressed or exacerbated the growth property of *vhs2 mlf3* cells at temperatures ranging from 13°C or 37°C.

3.2.3 Functional Characterization of *MGC1* and *TOS2*

Mgc1 and Tos2 are proteins of 734 amino acids (~82 kDa) and 622 amino acids (~70 kDa), respectively. Comparison of the amino acid sequence of these two proteins using BLAST analysis revealed that the Mgc1 and Tos2 sequences share 34% identity and 47% similarity (Figure 3.18). Both proteins are predicted to contain a single transmembrane domain within their N-terminal region (residues 71-99 in Mgc1 and residues 37-64 in Tos2). The primary structure of Mgc1 differs from that of Tos2 in that it also contains putative signal peptide cleavage sites after residues 23 and 95. The sequence homology between Mgc1 and Tos2 suggests that these two proteins might have similar functions. Identification of both *MGC1* and *TOS2* as multi-copy suppressors of the phenotypic defects of *gic1 gic2* cells (Figures 3.1, 3.2 and 3.3) and the reported two-hybrid interactions of Mgc1 and Tos2 with other proteins of the Rho1- and Cdc42-GTPase pathways (Drees et al., 2001; Uetz et al., 2000; Figure 3.19) suggest that Mgc1 and Tos2 might participate in the process of polarized cell growth.

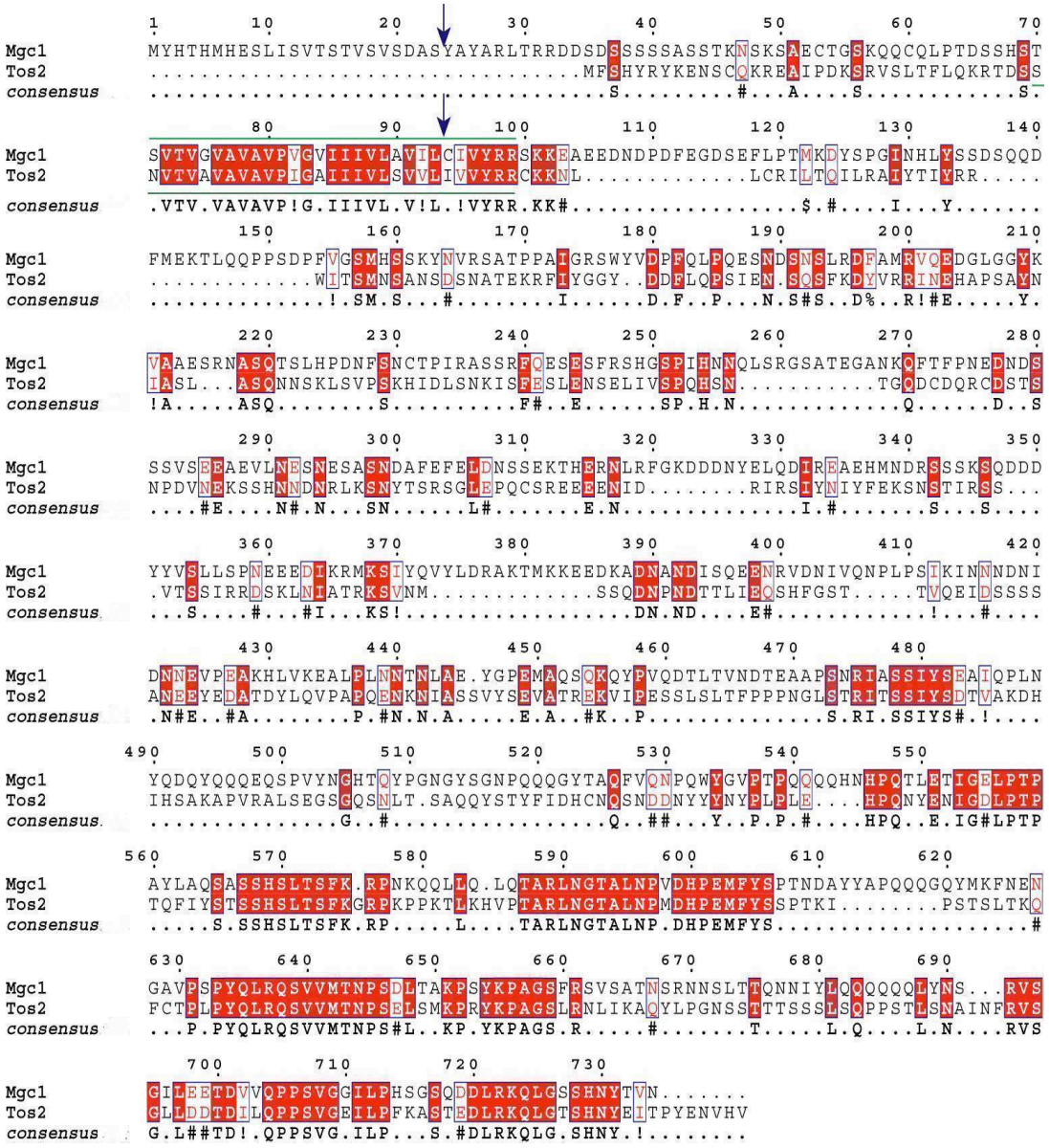

Figure 3.18 Alignment of the predicted sequences of Mgc1 (*YHR149C*) and Tos2 (*YGR221C*) using Multalin software (Corpet, 1988). Gaps are introduced for alignment purposes. Sequence identity and similarities are shown in red background and boxed, respectively. Note the presence of a putative transmembrane domain in Mgc1 and Tos2 (marked with green line) and putative signal peptide cleavage sites in the Mgc1 but not Tos2 sequence (blue arrows).

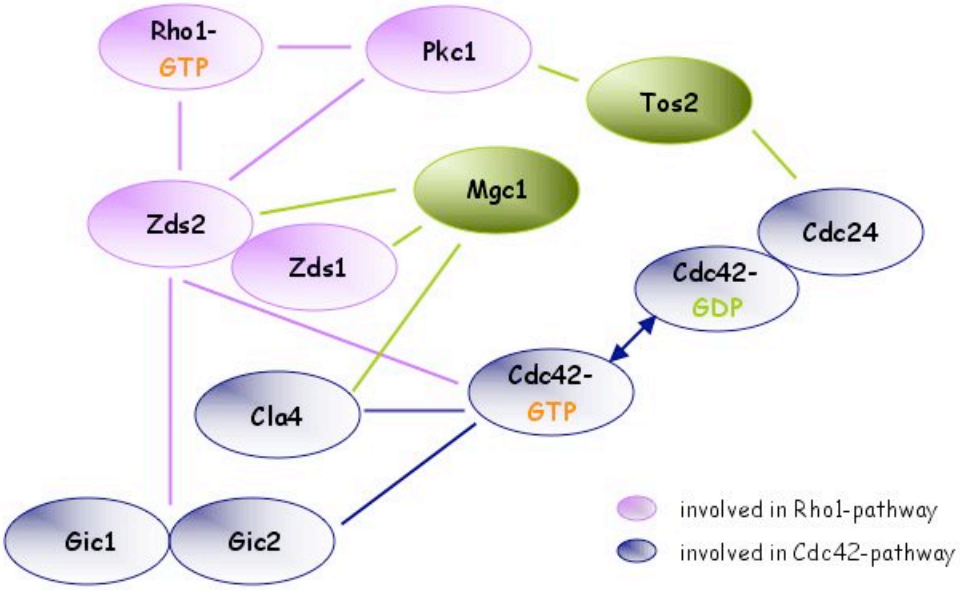

Figure 3.19 Reported two-hybrid interactions of Mgc1 and Tos2 with proteins that are known to interact with Rho1 and Cdc42 GTPases in the process of polarized growth in *S. cerevisiae* (Drees et al., 2001; Uetz et al., 2000).

Subcellular localization of Mgc1 and Tos2 proteins

Many budding yeast proteins that function primarily in the establishment and/or maintenance of the polarized actin cytoskeleton are localized at sites of active cell growth. To investigate if Mgc1 and Tos2 exhibit a similar subcellular localization pattern, diploid strains were constructed in which one chromosomal copy of either the *MGC1* or *TOS2* ORF was fused in frame at its 3′ end to a sequence encoding GFP. Examination of live diploid cells expressing the Mgc1-GFP fusion protein (CCY1830-74) by fluorescent microscopy revealed that the

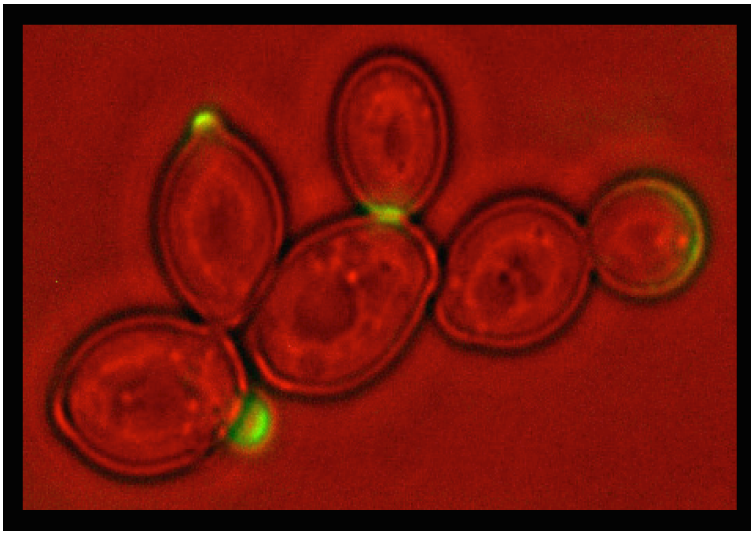

Figure 3.20 Localization of Mgc1-GFP (green) at sites of polarized growth. Diploid cells (CCY1830-74) expressing Mgc1-GFP were cultured in YEPD at 26°C and examined by fluorescent and nomarski microscopy. The fluorescent and nomarski images are merged in this figure.

cellular localization of Mgc1 is identical to that of Cdc42 and the Gic proteins. In unbudded cells, Mgc1 was either diffused throughout the cell cortex, or was focused at one end of the cell, the end from which the next bud would presumably emerge. In small-budded cells, Mgc1-GFP occupied the entire bud (cortex), whereas in medium-budded cells, Mgc1-GFP was localized as a cap along the distal end of the bud cortex. In large-budded cells, Mgc1 appeared to be re-polarized as a double ring structure at the bud-neck (Figure 3.20). Drees et al. (2001) reported that Tos2-GFP also localizes to similar sites of polarized growth. Together, the data on the subcellular localization of the Mgc1 and Tos2 reinforced the assumption that these proteins might function in the process of polarized cell growth.

Localization of Mgc1 in the absence of Gic1 and Gic2

Since *MGC1* and *TOS2* function as multi-copy suppressors of *gic1 gic2* cells and Mgc1, Tos2, Gic1 and Gic2 have similar localization patterns; I tested whether the localization of Mgc1 at sites of polarized growth was dependent on Gic1 and Gic2. For this purpose, the localization of Mgc1-GFP was examined in haploid *gic1-Δ1::LEU2 gic2-Δ2::TRP1* cells (CCY1502-1D). Since *gic1 gic2* mutant cells are mostly depolarized and unbudded at 37°C, it was not possible to determine the localization of Mgc1 at sites of polarized growth at that temperature. Therefore, the experiment was carried out at 26°C and 33°C, the permissive and semi-permissive growth temperatures of *gic1 gic2* mutant cells, respectively. Mgc1-GFP appeared to be present at sites of active growth in both wild-type and *gic1 gic2* cells at 26°C. After 4 h of incubation at 33°C, ~20-30% *gic1 gic2* cells appeared large, depolarized and unbudded. The localization of Mgc1-GFP seemed normal in the polarized *gic1 gic2* cells (not shown). Thus, the polarized localization of the Mgc1 protein appeared to be independent of Gic1 and Gic2.

Consequences of deletion mutations in MGC1 and TOS2

Growth defect

In order to obtain greater insight into the cellular function of the Mgc1 and Tos2 proteins, one chromosomal copy of the *MGC1* or *TOS2* gene was deleted in a diploid wild-type strain using PCR-mediated gene deletion technique (Longtine et al., 1998b). Tetrad analysis of the resulting heterozygous deletion strains carrying either the *mgc1-Δ1::kan* (CCY1830-72) or *tos2-Δ1::spHIS5* (CCY1830-67) mutation produced four viable spore colonies at 26°C, indicating that neither *MGC1* nor *TOS2* is essential for the viability of cells at this temperature. Neither *mgc1* nor *tos2* mutant cells demonstrated any

growth defect at temperatures ranging from 13°C to 37°C. Next, the effect of simultaneous deletion of *MGC1* and *TOS2* was determined. For this purpose, a haploid *mgc1-Δ1::kan* strain (CCY1151-1B) was crossed with a haploid *tos2-Δ1::spHIS5* strain (CCY1145-9D). Tetrad analysis of the resulting heterozygous diploid strain showed that haploid *mgc1-Δ1::kan tos2-Δ1::spHIS5* mutant progeny cells were also viable at 26°C and did not exhibit any growth defects at temperatures ranging from 13°C to 37°C.

Morphology defect

Very often the deletion of a particular gene may not result in a growth phenotype, yet it may alter the morphology of cells. For example, *cla4-Δ101* mutant cells grow well at 26°C but display a morphology that is indicative of hyperpolarized growth. To determine if the deletion of *MGC1* and *TOS2* caused any morphological changes, haploid wild-type (DBY1829), *mgc1-Δ1::kan* (CCY1151-1B), *tos2-Δ1::spHIS5* (CCY1145-1B) and *mgc1-Δ1::kan tos2-Δ1::spHIS5* (CCY1152-8B) cells were cultured in YEPD medium at 26°C, followed by an overnight subculture at 26°C or 37°C. Examination of cells by light microscopy indicated that there was no obvious defect in either the size or shape of *mgc1*, *tos2* or *mgc1 tos2* mutant cells. Also, the budding indices of the *mgc1*, *tos2* and *mgc1 tos2* mutant cells were comparable to that of the wild-type cells. Collectively, the absence of Mgc1 and Tos2 did not lead to any gross morphological abnormalities in cells.

Bud-site selection defect

The normal morphology of *mgc1*, *tos2* and *mgc1 tos2* mutant cells suggested that these cells might not have any obvious polarity-associated phenotypic defects. Indeed, examination of the bud-site selection pattern of

haploid *mgc1-Δ1::kan* (CCY1151-1B), *tos2-Δ1::spHIS5* (CCY1145-1B) and *mgc1-Δ1::kan tos2-Δ2::URA3* (CCY1176-1B) cells at 26°C revealed that, like wild-type cells (DBY1829), >98 % of these mutant cells budded axially and thus displayed no defect in the process of bud-site selection.

Sporulation efficiency

To examine if the loss of *MGC1* or *TOS2*, either singly or in combination, resulted in a sporulation defect, diploid wild-type (DBY1830), heterozygous *mgc1-Δ1::kan* (CCY1830-72), *tos2-Δ1::spHIS5* (CCY1830-67) and *mgc1-Δ1::kan tos2-Δ1::spHIS5* (CCY1151-1D X CCY1145-1B) strains as well as homozygous *mgc1-Δ1::kan* (CCY1151-1B X CCY1151-1D), *tos2-Δ1::spHIS5* (CCY1145-1B X CCY1145-9D) and *mgc1-Δ1::kan tos2-Δ1::spHIS5* (CCY1152-3B X CCY1152-5C) strains were induced to sporulate for 4 days at 26°C. The percentage of asci-forming cells was determined. All the strains tested sporulated at ~50% efficiency and the distribution of diads, triads and tetrads formed was comparable among the strains. This result indicated that the absence of Mgc1 and Tos2 did not impair the ability of budding yeast cells to undergo meiosis and sporulation.

Ability to form mating projections

To determine whether Mgc1 and Tos2 are specifically required in the process of polarized growth during mating, haploid *MATa* wild-type (DBY1828) and *mgc1-Δ1::kan tos2-Δ2::URA3* (CCY1176-1B) cells were cultured in YEPD (pH 4.5) medium at 26°C and α-factor was added to a final concentration of 4 or 8 μg/ml. Following 1 h of incubation at 26°C, a second dose of α-factor was added and the incubation was continued for one more h. Cells were then fixed with formaldehyde and the morphology of cells was examined by light microscopy. ~88-90% of both wild-type and *mgc1-Δ1::kan tos2-Δ2::URA3* cells arrested as

unbudded cells and formed mating projections. Further, the shape and size of the projections formed were comparable between the two strains, indicating that the combined absence of Mgc1 and Tos2 did not interfere with the ability of yeast cells to polarize during mating. This was further corroborated by the finding that the *mgc1-Δ1::kan*, *tos2-Δ1::spHIS5* and *mgc1-Δ1::kan tos2-Δ1::spHIS5* mutant cells did not exhibit altered sensitivity to α-factor.

Do mgc1 and/or tos2 mutations interact genetically with mutations in other genes involved in cell polarity?

Since deletion of *MGC1* and *TOS2* did not yield any phenotype characteristic of polarized cell growth defect, the phenotypic consequences of combining *mgc1* and/or *tos2* mutations with additional polarity-associated mutations were examined. The rationale was that the interaction of *mgc1* and/or *tos2* with mutation in polarity-related gene '*X*' would be manifested either as a suppression or an exacerbation in the growth phenotype of the '*x*' single mutant. Alternatively, if the '*x*' mutant did not have any growth defect to start with, its combination with the *mgc1* and/or *tos2* mutation(s) might result in a discernible growth defect. To this end, the interaction between *mgc1, tos2* and mutations in 28 other genes (*ACT1, BEM2, BEM3, BNI1, BNR1, BUD3, CDC10, CDC12, CDC24, CDC42, CLA4, CYC8, CYK2, DBM1/RGA1, GIC1, GIC2, MLF3, MSB3, MSB4, RGA2, RPI1, RSR1/BUD1, SCH9, SKM1, SPA2, SPO86, STE20* and *VHS2*) were investigated. With the exception of *cyk2*, mutations in none of these genes showed obvious genetic interaction with *mgc1* and *tos2*.

Suppression of cyk2 mutation by mgc1

Cyk2, a budding yeast homologue of Cdc15 in *S. pombe*, is thought to function as an adapter that links the actomyosin system with the primary septum synthesis machinery during cytokinesis (Vallen et al., 2000). Although Cyk2 contributes to the stability of the actomyosin ring during contraction (Lippincott and Li, 1998a), its primary role is in the process of septum formation that is necessary for cell separation after cytokinesis.

Cells carrying a deletion in *CYK2* exhibit a temperature-sensitive growth phenotype. These cells are multinucleate, with large and elongated buds. They fail to form septa between different cell bodies and accumulate as chains or clumps with their cytoplasm connected. Together, these phenotypic defects of *cyk2* mutant cells point towards the function of Cyk2 in cytokinesis (Lippincott and Li, 1998a; Vallen et al., 2000).

Study of the *cyk2* deletion mutant in the genetic background (*ssd1-d1*) of our laboratory strains revealed that the temperature-sensitive growth defect of *cyk2-Δ101::spHIS5* cells is variable with the experimental conditions. Tetrad analysis of the heterozygous diploid strain CCY1244 (made by crossing CCY1137-3B [carrying *CYK2* on a CEN plasmid] to CCY1176-11A and then allowing for the plasmid loss) carrying the *cyk2-Δ101::spHIS5* mutation invariably gave rise to tiny colonies for the haploid *cyk2* spores (Figure 3.21A). These cells exhibited poor growth on YEPD agar at 26°C to 37°C. However, if the spore colonies were allowed to grow for a longer period of time on the dissection plate, the growth defect of the *cyk2* mutant cells at 26°C was somewhat reduced at first and then disappeared over a period of time. Similar loss of the temperature-sensitive growth phenotype at 26°C was observed during repeated streaking of *cyk2* mutant cells on YEPD agar. Lippincott and Li (1998a) have also reported such abnormal growth behavior of *cyk2* cells.

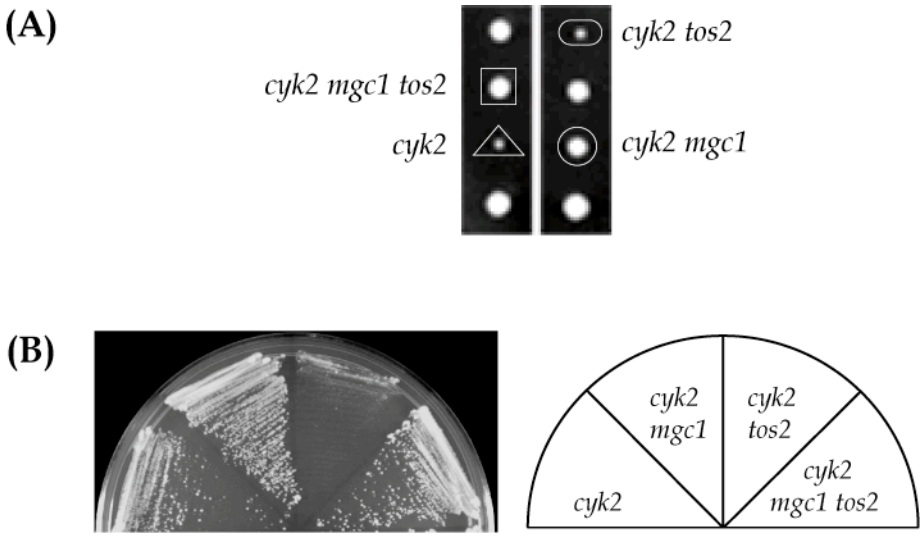

Figure 3.21 Deletion of *MGC1* suppresses the growth defect of *cyk2* cells. **(A)** Spore colonies bearing *cyk2-Δ101::spHIS5* (CCY1244-4D), *cyk2-Δ101::spHIS5 mgc1-Δ1::kan* (CCY1244-7C), *cyk2-Δ101::spHIS5 tos2-Δ2::URA3* (CCY1244-10D) and *cyk2-Δ101::spHIS5 mgc1-Δ1::kan tos2-Δ2::URA3* (CCY1244-17C) mutations on YEPD agar at 26°C. **(B)** Growth of the strains listed above on YEPD agar at 26°C. Note that *cyk2-Δ101::spHIS5* cells grew better than anticipated from the size of its spore colony shown in panel (A).

Investigation of the genetic interaction between *mgc1-Δ1::kan*, *tos2-Δ2::URA3* and *cyk2-Δ101::spHIS5* mutations revealed that like *cyk2* single mutant cells, *cyk2 tos2* double mutant cells also gave rise to tiny spore colonies and exhibited growth defects on YEPD agar at 26°C to 37°C (Figure 3.21A, not shown). However, *cyk2 mgc1* double mutant cells and *cyk2 mgc1 tos2* triple mutant cells consistently generated spore colonies of regular size. Furthermore, upon streaking on YEPD agar, these cells did not exhibit any growth defect at 26°C (Figure 3.21), thus suggesting that deletion of *MGC1* suppressed the growth defect of *cyk2* mutant cells. By extension, it meant that the absence of Mgc1 alleviated the requirement for Cyk2. Since Cyk2 plays a positive role in cytokinesis, Mgc1 may perform a negative regulatory role in this process.

Increased dosage of CYK2 does not affect growth of cells lacking Mgc1 and Tos2

To further dissect the genetic interaction described above, the effect of increasing the *CYK2* gene dosage in haploid wild-type (DBY1829), *mgc1-Δ1::kan* (CCY1176-10B), *tos2-Δ1::spHIS5* (CCY1145-12D) and *mgc1-Δ1::kan tos2-Δ1::spHIS5* (CCY1152-5C) cells was examined. Overexpression of *CYK2* from a 2μ plasmid (pCC1333) did not affect the growth at 26°C to 37°C or the morphology at 26°C of any of these cells.

Investigating the protein-protein interaction of Mgc1 and Tos2 with other proteins involved in polarized growth

In order to obtain stronger evidence about the putative function of Mgc1 and Tos2 in polarized cell growth, a two-hybrid interaction assay was used (Finley and Brent, 1994; detailed in Chapter 2) to examine whether Mgc1 and Tos2 associated with a panel of 'test' proteins that have recognized functions in polarized growth. A strain (EGY48) bearing a chromosomal *LEU2* reporter gene and a *LACZ* reporter gene on plasmid (pSH18-34) was co-transformed with two plasmids, one expressing a fusion of the LexA DNA-binding domain (BD) and the 'test' protein under the *ADH1* promoter, and the other expressing a fusion of the B42 trans-activation domain (AD) and Mgc1 (pCC1580) or Tos2 (pCC1581) under the *GAL1* promoter. Alternatively, in cases where the 'test' proteins were available as fusions to the B42 trans-activation domain, their interactions were tested against a fusion of LexA-BD and Mgc1 (pCC1551) or Tos2 (pCC1552). A list of all 'test' proteins examined is presented in Table 3.9. Since Mgc1 fused to either LexA-BD or B42-AD alone resulted in activation of the *LEU2* reporter gene, it was not possible to test whether Mgc1 demonstrated true interaction with any of the test proteins examined. Tos2, on the other hand, did not result in activation of the *LEU2* reporter gene when fused to the trans-activation or DNA binding domain. In fact, AD-Tos2 showed weak interactions with BD-Rho2^{C206S,}

^{C189S}, BD-Rho3^{C228S} and BD-Rsr1. It also exhibited considerably strong interactions with BD-Rho4, BD-Rho4^{C228S}, BD-Cdc42$^{G12V,\ C188S}$ and BD-Cdc42$^{Q16L,\ C188S}$. However, when the host strain (EGY48 with pSH18-34) used for this analysis was transformed with plasmids expressing each of these putatively

Table 3.9 List of fusion proteins used in two-hybrid assays against Mgc1 and Tos2.

Against BD-Mgc1 and BD-Tos2	Against AD-Mgc1 and AD-Tos2
PJG4-5 (AD)	pEG202 (BD)
AD-Mgc1	BD-Mgc1
AD-Tos2	BD-Tos2
AD-Bni1	BD-Bni1
AD-Cdc3	BD-Cdc3
AD-Cdc10	BD-Cdc10
AD-Cdc11	BD-Cdc11
AD-Cdc12	BD-Cdc12
AD-Gic1	BD-Rho1
AD-Gic2	BD-Rho1^{C206S}
AD-Gic1-2	BD-Rho2
AD-Gic1-3	BD-Rho2$^{C206S,\ C189S}$
AD-Gic1-Δ4	BD-Rho3
AD-Skm1	BD-Rho3^{C228S}
AD-Cla4	BD-Rho4
	BD-Rho4^{C228S}
	BD-Rsr1
	BD-Rsr1^{G12V}
	BD-Bem3
	BD-Cdc42
	BD-Cdc42^{C188S}
	BD-Cdc42$^{G12V,\ C188S}$
	BD-Cdc42$^{Q16L,\ C188S}$
	BD-Cdc42$^{D118A,\ C188S}$
	BD-Cdc42$^{T35A,\ C188S}$

positive interactors alone, significant activation of both *LEU2* and *LACZ* reporter genes was apparent. This observation indicated that the positive two-hybrid interactions seen with Tos2 might have been an artifact caused by the background activation of reporter genes by test protein fusions themselves. Thus, the attempt to identify physical interactors of Mgc1 and Tos2 by the two-hybrid assay was unsuccessful. However, Zds1, Zds2 and Cla4 were found to interact with Mgc1, and Pkc1 and Cdc24 were found to interact with Tos2 in two-hybrid assays, reported by Drees et al. (2001).

Phenotypic consequences of overproducing the Mgc1 and Tos2 proteins

As a next resort to understand the cellular role of Mgc1 and Tos2, I tested whether overproduction of these proteins, either individually or together, could change the behavior of wild-type cells. Gal^+ haploid strains were constructed in which a His3MX6-*pGAL1*-3HA cassette (Longtine et al., 1998b) was integrated immediately upstream of either the *MGC1* or *TOS2* ORF. In growth medium containing galactose as the sole carbon source, these strains overproduced Mgc1 or Tos2 that was tagged at its N-terminal end with the HA-epitope (Figure 3.22). It should be noted though that these N-terminal tags potentially might affect the functions of Mgc1 and Tos2, since both these proteins contain a putative transmembrane domain that may normally cooperate with an N-terminal signal sequence to target them to the membrane. The haploid stain overproducing HA-Mgc1 was crossed with a haploid strain overproducing HA-Tos2 to yield a progeny haploid strain that overproduced both HA-Mgc1 and HA-Tos2. Analysis of strains overproducing Mgc1 and Tos2, either singly or in combination, generated interesting phenotypes as described below.

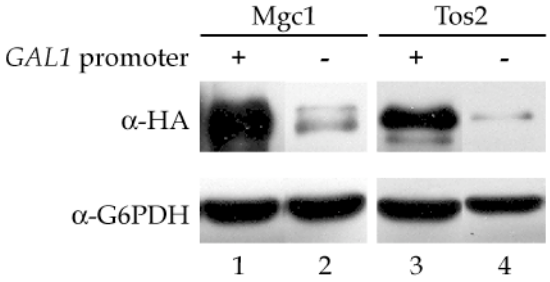

Figure 3.22 *MGC1* and *TOS2* expression from inducible *GAL1* promoter (+) compared to their native promoters (-). Haploid strains CCY1708-1A (containing *spHIS5-pGAL1-3HA-MGC1* integration in the chromosome) and CCY1709-2B (containing *spHIS5-pGAL1-3HA-TOS2* integration in the chromosome) were cultured 26°C in YEP-Raffinose (2%) to early- to mid-log phase. Galactose (4% final concentration) was added to the growth medium (to induce expression of *HA-MGC1* and *HA-TOS2*) and cultures were shifted to 37°C for 4 h. Total cell lysates were prepared, separated by 10% SDS-PAGE and immunoblotted with α-HA antibodies to detect HA-Mgc1 (lane 1) and HA-Tos2 (lane 3). For preparing the cell lysates from strains expressing *MGC1* and *TOS2* from their native promoters, strains CCY1165-1C (*MGC1-3HA::spHIS5*) and CCY1147-3A (*TOS2-3HA::spHIS5*) were cultured under similar conditions, except that the growth medium contained dextrose instead of raffinose and galactose. Mgc1-HA and Tos2-HA expressed from native promoters are shown in lanes 2 and 4, respectively. Immunoblotting with α-G6PDH antibody shows the amount of proteins loaded in different lanes.

Elongated bud and often 2-budded cell morphology

Microscopic examination of cells overproducing HA-Mgc1 or HA-Tos2 at 26°C for 6 h in YEP-galactose medium did not reveal any major alteration in their shape or size when compared to the control cells. However, when both proteins were simultaneously overproduced, ~12% of cells exhibited an elongated-bud morphology (Table 3.10). This abnormality was more pronounced at 37°C. After 6 h at 37°C, individual or simultaneous overproduction of HA-Mgc1 and HA-Tos2 resulted in even greater accumulation of cells with elongated buds. These unusually long buds often gave rise to a new bud without having itself undergone separation from the mother cell (Figure 3.23; Table 3.10). Many cells also had a second bud that emerged from the mother cell. Furthermore, the bud necks of many of these cells were often curved. Together, these phenotypic changes suggested that overproduction of HA-Mgc1 and HA-Tos2 results in a

defect in the switch from an apical to isotropic growth and a perturbation to the normal execution of cytokinesis.

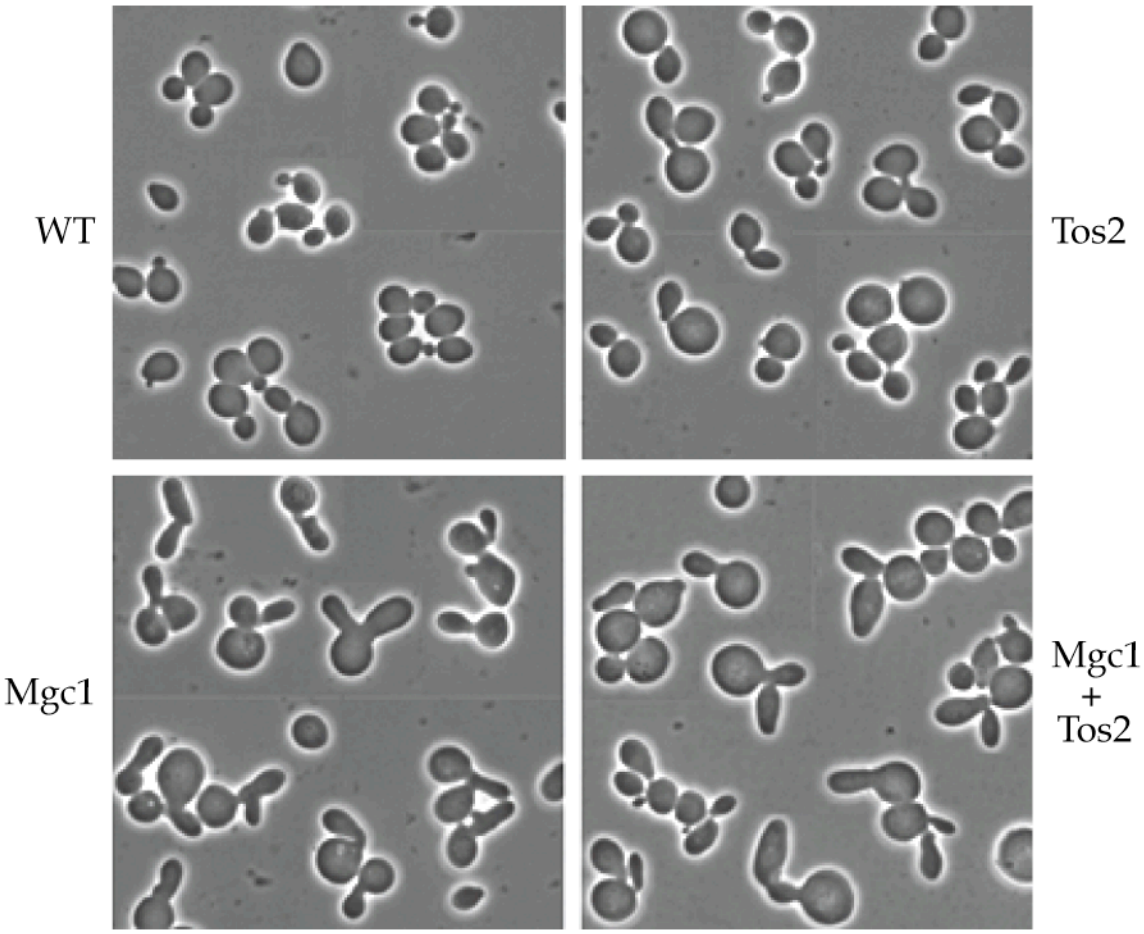

Figure 3.23 Morphological examination of haploid wild-type (CCY1710-3C) cells and cells overproducing HA-Mgc1 alone (CCY1708-1A), HA-Tos2 alone (CCY1709-2B) and both HA-Mgc1 and HA-Tos2 (CCY1710-7B). Cells were cultured at 26°C in YEP-Raffinose (2%) to early- to mid-log phase. Galactose was added (4% final concentration) to the growth medium (to induce expression of *HA-MGC1* and *HA-TOS2*) and cultures were incubated at 37°C for 6 h. Thereafter, cells were fixed with formaldehyde (3.7% final concentration) and examined by phase-contrast microscopy. Note the presence of cells with elongated buds and cells with 'bud from a bud' morphology in all except the wild-type samples.

Table 3.10 Morphological analysis of cells overproducing HA-Mgc1 and/or HA-Tos2

Growth condition	Protein overproduced	Unbudded (%)	Budded (%)			
			Single regular bud	Single Elongated bud	2 separate buds	'Bud from a bud'
26°C YEP-Raffinose	-	46	54	0	0	0
	HA-Mgc1	40	60	0	0	0
	HA-Tos2	45	55	0	0	0
	HA-Mgc1 + HA-Tos2	47	53	0	0	0
26°C YEP-Galactose for 6 h	-	49	51	0	0	0
	HA-Mgc1	41	56	3	0	0
	HA-Tos2	50	48	2	0	0
	HA-Mgc1 + HA-Tos2	45	43	12	0	0
37°C YEP-Galactose for 6 h	-	46	51	0	3	0
	HA-Mgc1	34	14	27	6	19
	HA-Tos2	46	38	10	3	3
	HA-Mgc1 + HA-Tos2	32	17	35	6	10

Haploid wild-type (CCY1710-3C) cells and cells that overproduced HA-Mgc1 alone (CCY1708-1A), HA-Tos2 alone (CCY1708-2B) or both HA-Mgc1 and HA-Tos2 (CCY1710-7B) were cultured in YEP-Raffinose (2%) medium to log phase and Galactose (4% final concentration) was added to the growth medium to induce overproduction of HA-Mgc1 and HA-Tos2. Cells were incubated further at 26°C or 37°C for 2, 4 and 6 h. At each time point, cells were fixed with formaldehyde (3.7%) and their morphology was examined using phase-contrast microscopy. For HA-Mgc1 overproducing cells, incubation at 37°C beyond 4 h resulted in a reduced fraction of cells with single elongated buds (not shown). This decrease was accompanied by a concomitant rise in the number of cells with 'bud from a bud' morphology. Also, a decrease in the population of unbudded cells in HA-Mgc1 overproducing cells is consistent with an increase in the population of cells with a potential cytokinesis defect.

Mislocalization of the Cdc3 septin

Septins (including Cdc3) form an hourglass structure (very often appearing as two closely apposed rings) at the mother-bud neck (Figure 1.7). They are essential for cytokinesis since they enable the recruitment of proteins that are required for cytokinesis to the mother-bud neck during later stages of the cell cycle. To understand why overproduction of Mgc1 and Tos2 causes a defect in cytokinesis, the localization of Cdc3-GFP septin was examined in cells overproducing these proteins.

Examination of cells cultured in YEP-galactose medium at 37°C for 6 h showed that ~99% of wild-type budded cells with Cdc3-GFP signal had the expected pattern of septin localization. In contrast, a large fraction of budded cells overproducing HA-Mgc1 and/or HA-Tos2 exhibited aberrantly organized and consequently mislocalized Cdc3-GFP under similar growth conditions

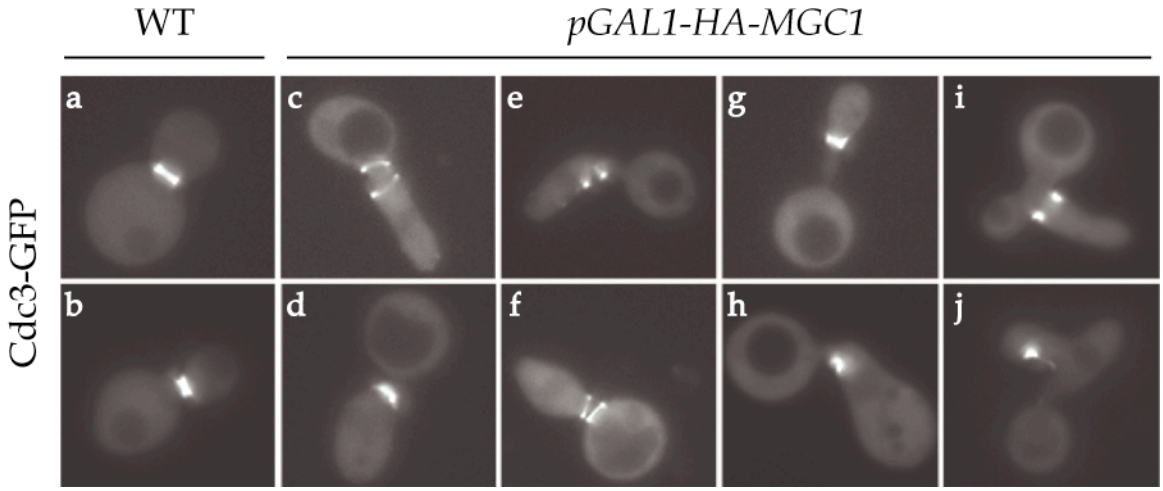

Figure 3.24 Aberrant localization of Cdc3-GFP due to overproduction of HA-Mgc1. Haploid wild-type (CCY1710-3C) cells and cells that overproduced HA-Mgc1 (CCY1708-1A) were transformed with the CEN plasmid pRS316-CDC3-GFP and cultured at 26°C to log phase in synthetic minimal media (supplemented with appropriate amino acids to maintain the plasmid) containing raffinose (2%). Galactose (4% final concentration) was then added and the cultures were incubated at 37°C for 6 h. Cells were immediately fixed with formaldehyde (1% final concentration) on ice for 10 minutes, washed once with ice-cold PBS and examined by fluorescent microscopy using an FITC filter.

Table 3.11 Aberrant localization of Cdc3-GFP in cells overproducing HA-Mgc1 and HA-Tos2.

Protein overproduced	% budded cells with Cdc3-GFP mislocalized
-	1
HA-Mgc1	47
HA-Tos2	14
HA-Mgc1 + HA-Tos2	26

Haploid wild-type (CCY1710-3C) cells and cells that overproduced HA-Mgc1 alone (CCY1708-1A), HA-Tos2 alone (CCY1708-2B) or both HA-Mgc1 and HA-Tos2 (CCY1710-7B) were transformed with the CEN plasmid pRS316-CDC3-GFP and cultured at 26°C to log phase in synthetic minimal media (supplemented with appropriate amino acids to maintain the plasmid) containing raffinose (2%). Galactose (4% final concentration) was then added and the cultures were incubated at 37°C for 6 h. Cells were immediately fixed with formaldehyde (1% final concentration) on ice for 10 minutes, washed once with ice-cold PBS and examined by fluorescent microscopy using an FITC filter. ~200 budded cells with Cdc3-GFP signal were scored for this analysis.

(Figure 3.24; Table 3.11). Interestingly, there was no uniform pattern of mislocalization of Cdc3-GFP in these cells. In many HA-Mgc1- or HA-Tos2-overproducing cells that had abnormal bud morphology, Cdc3-GFP was present either only towards the mother-side of the bud-neck (Figure 3.24, panel d) or only towards the daughter-side of the bud-neck (not shown). Cdc3-GFP was also found mislocalized away from the bud neck and towards the tip of the bud (Figure 3.24, panel f) or along only one side of the bud (Figure 3.24, panels e and h). Occasionally, the two rings of Cdc3-GFP were found to split asymmetrically

(Figure 3.24, panel f) or be separated much farther away from the bud-neck (Figure 3.24, panel c) than seen otherwise in the wild-type cells.

Since cells lacking Mgc1 and/or Tos2 (strains CCY1151-1B, CCY1145-1B and CCY1152-8B) had no morphological abnormalities, it was not surprising that Cdc3-GFP had a wild-type pattern of localization in these cells when cultured in YEPD medium at 37°C for 6 h. Taken together, the overproduction of Mgc1 and Tos2 interfered with the proper localization of Cdc3 (and likely also the other septins since the localization of the different septins is interdependent (Faty et al., 2002; Haarer and Pringle, 1987; Kim et al., 1991). This could at least partly explain the cytokinesis defect observed in these cells.

Localization of Mgc1 protein in cdc3-3 mutant

In order to examine if Mgc1 required an intact septin structure for its localization at sites of polarized growth, Mgc1-GFP was visualized in *cdc3-3* mutant cells. As in wild-type cells, Mgc1-GFP appeared at the bud tip and the cell cortex in *cdc3-3* cells. However, unlike in wild-type cells, Mgc1-GFP in this septin mutant was not exclusively restricted to sites of active growth. Instead, it was also unevenly distributed, often as patches, in the cytoplasm (Figure 3.25). The mislocalization of Mgc1-GFP was enhanced at 37°C, the restrictive temperature for *cdc3-3* cells. Furthermore, Mgc1-GFP was very frequently not seen at the bud neck region. When present at the bud neck, Mgc1-GFP often appeared as a dot instead of two rings.

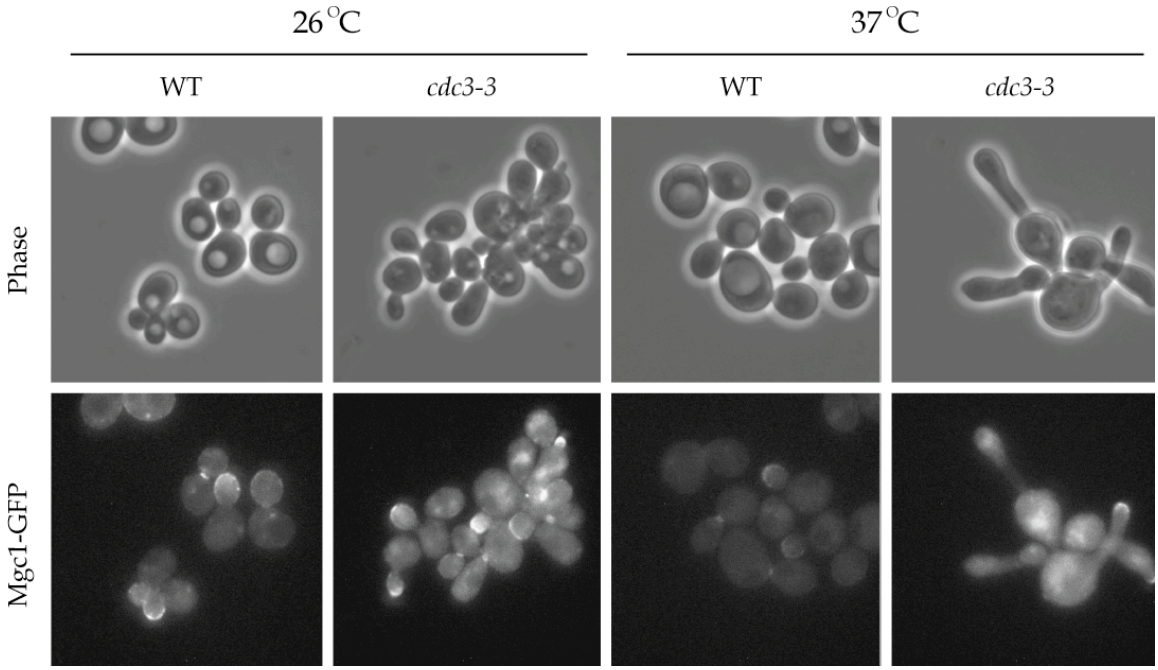

Figure 3.25 Localization of Mgc1-GFP in *cdc3-3* cells. Wild-type (CCY1154-2D) and *cdc3-3* (CCY1746-3A) cells expressing chromosomally integrated *MGC1-GFP* fusion were cultured in YEPD medium at 26°C to log phase and then shifted to 37°C for 4 h. Cells were immediately fixed with 1% formaldehyde on ice for 10 min., washed once with ice-cold PBS and examined by phase-contrast microscopy and fluorescent microscopy.

Re-polarization of the actin cytoskeleton at the bud neck

After actomyosin ring contraction, the re-orientation of the actin cytoskeleton to the mother-bud neck is necessary for septum formation and subsequent cell separation (Adams and Pringle, 1984). The septin scaffold plays an important role in this process of actin re-orientation. Since overproduction of HA-Mgc1 and HA-Tos2 resulted in the mislocalization of the Cdc3 septin, the next question was to address if overproduction of these proteins adversely affected the re-orientation of the actin cytoskeleton to the bud neck. To this end, I examined the actin cytoskeleton of cells overproducing either HA-Mgc1 and/or HA-Tos2. After 6 h incubation at 37°C in YEP-galactose medium, ~10% of the budded wild-type and HA-Tos2-overproducing cells showed actin-staining at

the mother-bud neck (regardless of the bud size), a slightly higher fraction (~14%) of budded cells overproducing HA-Mgc1 and HA-Tos2 together showed such an actin-staining pattern. Interestingly, a much higher fraction (27%) of budded cells overproducing HA-Mgc1 alone had the actin cytoskeleton polarized at the mother-bud neck. When carrying a bud of normal size and shape, most of these cells displayed the wild-type pattern of a tight double ring of actin patches at the bud neck. However, when the bud was unusually

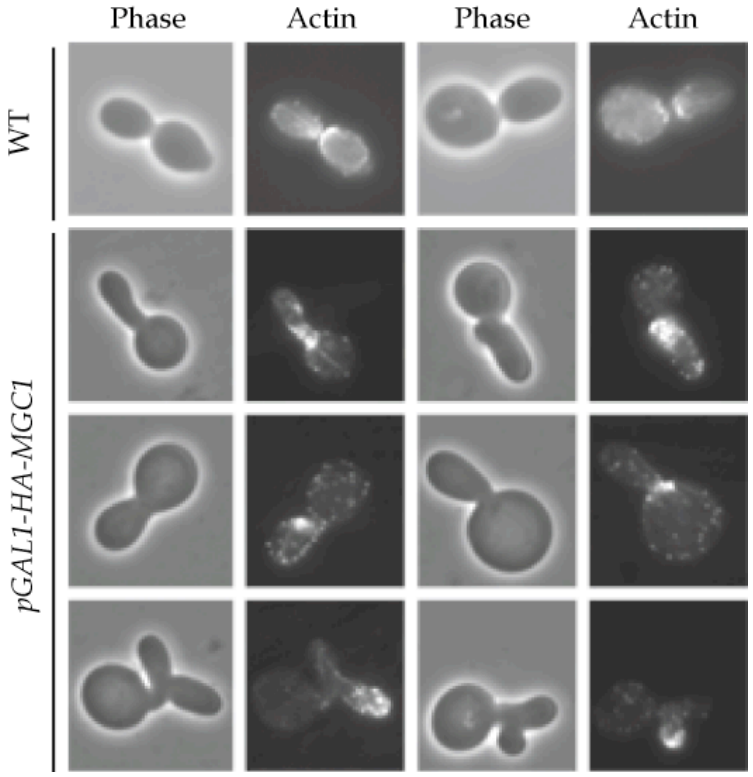

Figure 3.26 Abnormal organization of the actin cytoskeleton at the bud-neck of HA-Mgc1-overproducing cells. Haploid wild-type (CCY1710-3C) cells and cells overproducing HA-Mgc1 (CCY1708-1A) were cultured at 26°C to log phase in YEP-Raffinose (2%) medium. Galactose was then added (4% final concentration) and cultures were incubated at 37°C for 6 h. Cells were fixed with formaldehyde (3.7%), stained with rhodamine-phalloidin and examined by fluorescent microscopy. HA-Mgc1 overproducing cells in the bottom row are included to indicate normal apical polarization of the actin cytoskeleton in growing buds.

elongated, the actin-staining at the bud neck no longer appeared as a condensed doublet. Instead, it appeared fanned out and was often biased towards one side of the mother-bud neck (Figure 3.26; Table 3.12). This latter abnormality might occur as a consequence of the septin mislocalization.

Table 3.12 Distribution of the actin cytoskeleton at the mother-bud neck of cells with elongated buds.

Protein overproduced	Actin localization at the mother-bud neck of cells with elongated buds		
	None	Normal	Diffused
-	NA	NA	NA
HA-Mgc1	28	10	62
HA-Tos2	73	7	20
HA-Mgc1 + HA-Tos2	53	2	45

Haploid wild-type (CCY1710-3C), *pGAL1-HA-MGC1* (CCY1708-1A), *pGAL1-HA-TOS2* (CCY1708-2B) and *pGAL1-HA-MGC1* and *pGAL1-HA-TOS2* (CCY1710-7B) cells were cultured in YEP-Raffinose (2%) to early- to mid-log phase at 26°C. Galactose (4% final concentration) was added to the growth media and cultures were incubated at 37°C for 6 h. Cells were fixed with formaldehyde (3.7%), stained with rhodamine-phalloidin and examined by fluorescent microscopy. NA = not applicable since these cells did not form elongated buds.

Thus, the phenotypic characteristics of cells overproducing the Mgc1 and Tos2 proteins are indicative of an impaired cytokinesis in these cells. Together with the observation that *mgc1-Δ1::kan* partially suppresses the growth defect of *cyk2-Δ101::spHIS5* cells, these data suggest that Mgc1, and to a lesser degree Tos2,

may have a negative regulatory role in the process of cytokinesis in budding yeast.

3.3 DISCUSSION

In this chapter, I have described genes that were identified as multi-copy suppressors of *gic1 gic2* mutations. The goal of the multi-copy suppression screen was to identify components that function downstream of the Gic proteins or in a Gic-independent and redundant pathway of polarized growth.

3.3.1 Many multi-copy suppressors of *gic1 gic2* mutations are known to have functions in polarized growth

AXL2, *BNI1*, *CLN2, MSB1*, *MSB2*, *RSR1* and *STE20* are all known to participate directly or indirectly in polarized cellular morphogenesis in *S. cerevisiae*. Increased dosage of these genes suppresses the temperature-sensitive growth defect (Figure 3.1), the bud-site selection defect (Figure 3.2), and the actin organization defect (Figure 3.3) of *gic1 gic2* mutant cells to varying degrees. Furthermore, I subsequently also discovered that the *axl2*, *bni1*, *msb1* and *rsr1* mutations enhance the temperature-sensitive phenotype of *gic1 gic2* cells (see Chapter 4).

Since Gic1 and Gic2 localize at the presumptive bud-site before bud emergence, and *gic1 gic2* mutant cells exhibit a defect in bud-site selection (Chen et al., 1997), it is believed that the Gic proteins participate in the early establishment of polarized growth. Axl2 provides a cortical tag for axial bud-site selection in haploid cells (Roemer et al., 1996). Axl2 interacts with Bud5 and recruits it to the site of bud emergence (Kang et al., 2001). Since Bud5 is a GEF for the Rsr1 GTPase, Axl2 thus influence the activity of Rsr1. GTP-bound Rsr1 interacts with the upstream regulators of the actin cytoskeleton, including Cdc24 and Cdc42 (Park et al., 1997; Zheng et al., 1995). In light of such functions of Axl2 and Rsr1 in the process of bud-site selection and early polarity establishment, it

is not surprising that increased dosage of *AXL2* and *RSR1* suppresses the phenotypic defects of *gic1 gic2* mutant cells.

Cdc24 is a GEF for Cdc42 and GTP-bound Cdc42, in turn, associates with Gic1 and Gic2 (as well as other effectors, including Ste20). Since *MSB2* was originally identified as a multi-copy suppressor of the bud emergence defect of *cdc24* mutants (Bender and Pringle, 1992) and *MSB1* was identified as a multi-copy suppressor of both *cdc24* and *cdc42* mutants (Bender and Pringle, 1991; Bender and Pringle, 1989), it is not surprising increased dosage of *MSB2* or *MSB1* also suppresses the phenotypes of *gic1 gic2* mutant cells.

Like Gic1 and Gic2, Ste20 binds to Cdc42-GTP via its N-terminal CRIB domain (residues 334-369) (Eby et al., 1998) and functions as an effector of Cdc42 in the process of actin cytoskeletal organization. Binding of Cdc42 to the CRIB domain relieves the intra-molecular inhibition exerted by the CRIB domain on the C-terminal kinase domain of Ste20 (Lamson et al., 2002). Our screen identified a truncated form of *STE20* (*NΔ118-STE20*) as a multi-copy suppressor of *gic1 gic2* cells. Since full-length *STE20* expressed under the control of the relatively strong *ACT1* promoter does not suppress the temperature-sensitive growth defect of *gic1 gic2* cells, it is likely that *NΔ118-STE20* expressed from the multi-copy plasmid suppresses the *gic1 gic2* mutant phenotype due to an increase in Ste20-kinase activity. Although *NΔ118-STE20* carries an intact CRIB domain, it is possible that the absence of the N-terminal 118 residues results in a more 'open conformation' in the NΔ118-Ste20 protein, and thus activating its kinase activity.

In addition to its role in regulating G1 to S transition, the G1-cyclin Cln2 is involved in the polarization of the actin cytoskeleton during bud emergence and growth. While overproduction of Cln2 results in hyperpolarized growth, its simultaneous absence with additional G1 cyclins Cln1, Pcl1 and Pcl2 blocks bud

emergence (Espinoza et al., 1994; Measday et al., 1994). Cdc28-Cln1 and Cdc28-Cln2 complexes phosphorylate Ste20 (Oda et al., 1999) during the G1/S boundary of the cell cycle and facilitate the function of Ste20 in early apical bud growth (Oehlen and Cross, 1998). Thus, increased dosage of *CLN2* may have a similar effect as expression of *NΔ118-STE20*. However, the effects of increased dosage of *CLN2* on the suppression of the actin organization defect and the bud-site selection defect of *gic1 gic2* cells are fairly modest. One possible explanation for this could be the lack of the concomitant increase in the dosage of an additional gene that is required for the Cln2-mediated polarized growth (e.g., *CDC28*).

Bni1 is a component of the 12S polarisome complex that is comprised of Sph1, Spa2, Pea2 and Bud6/Aip3 (Sheu et al., 1998). It is directly involved in the nucleation of actin filaments (Evangelista et al., 1997; Pruyne et al., 2002; Sagot et al., 2002). Several evidences support a functional link between Gic1, Gic2 and the polarisome. Deletion of *GIC2* results in lethality of *bni1*, *bud6* and *spa2* mutants (Jaquenoud and Peter, 2000). Gic2 also interacts physically with Bud6 (Jaquenoud and Peter, 2000) and Spa2 (Erfei Bi, personal communication). Localizations of Bni1 and Bud6 at the incipient bud site depend on activated Cdc42 and Gic2 but not the actin cytoskeleton (Jaquenoud and Peter, 2000). It is possible that Gic1, Gic2 and Bni1 (and other polarisome proteins) form a module that transduces signal from GTP-bound Cdc42 to the actin cytoskeleton. In this context, Bni1 may function downstream of Gic1 and Gic2 and thus may explain why increased dosage of *BNI1* can suppress the phenotypic defects of *gic1 gic2* cells.

3.3.2 *SSN6* and *TUP1* as multi-copy suppressors of *gic1 gic2* mutations

In addition to the genes with known polarity-related functions, increased dosage of *SSN6* and *TUP1,* which encode subunits of a transcriptional repressor

complex (Smith and Johnson, 2000), also partially suppresses the *gic1 gic2* mutations (Figure 3.1). While increased dosage of both *SSN6* and *TUP1* reduces the bud-site selection defect (Figure 3.2), only increased dosage of *SSN6* results in the suppression of the actin organization defect of *gic1 gic2* cells (Figure 3.3). In an independent study in our laboratory, a two-hybrid interaction between Gic1 and Ssn6 has been identified (unpublished). Thus, it appears that at least some function of Gic/Gic2 and Ssn6/Tup1 might closely overlap. However, the significance of the interactions between these proteins is not clear yet. It is possible that Ssn6/Tup1 complex may have a more direct role in regulating polarized cell growth than previously conceived. Alternatively, it is also possible that Gic1 and Gic2 may somehow participate in a signaling process that modulates the transcriptional repression activities of the Ssn6-Tup1 complex. This latter speculation is consistent with the reported localization of a fraction of Gic1 in the nucleus of some cells (Chen et al., 1997). However, if Gic1 does have a role in transcriptional regulation, this is unlikely its only role in the nucleus, since it has been reported recently that Gic1 and Gic2 also function in the regulation of mitotic exit (Hofken and Schiebel, 2004).

3.3.3 Multi-copy suppressors of *gic1 gic2* mutations with previously unknown functions

VHS2/MLF3 and *MGC1/TOS2* are two pairs of structurally related genes that have no previously reported polarity-related function. They were also identified as multi-copy suppressors of the phenotypic defects of *gic1 gic2* mutants.

VHS2/MLF3 and organization of the actin cytoskeleton

VHS2 and *MLF3* are non-essential genes. However, simultaneous deletion of both genes results in a mild temperature-sensitive growth phenotype at 37°C that is exacerbated in diploid cells (Figure 3.5). The growth defect is

accompanied by an accumulation of large and round cells at this temperature (Figure 3.8). Although *vhs2 mlf3* cells do not arrest exclusively as unbudded cells, a significant enrichment of unbudded cells with depolarized actin cytoskeleton is seen in these mutant cells (Figure 3.9, B and C). There are two possible explanations for this observation. First, *vhs2 mlf3* cells spend a longer time in G1 than wild-type cells. Second, *vhs2 mlf3* cells may transit through G1 at a wild-type pace but are partially defective in the process of apical polarization of the actin cytoskeleton. The first explanation is likely not true because no major differences in the rate of cell cycle progression (Figure 3.16) was observed between wild-type and *vhs2 mlf3* mutant cells when these cells were released into the cell cycle after a transient arrest in late G1 by α-factor treatment. The second explanation, on the other hand, is supported by the observation that the process of mating projection formation is sub-optimal in *vhs2 mlf3* cells cells (Figure 3.10). Furthermore, a large fraction of small-budded *vhs2 mlf3* cells have an abnormal pattern of actin localization in that their buds are largely devoid of cortical actin patches (Figure 3.9, A and C). Together, such abnormal patterns of actin localization in *vhs2 mlf3* cells strongly indicate that Vhs2 and Mlf3 participate in the organization of the actin cytoskeleton and thus in polarized cell growth. The diffused cytoplasmic localization of Vhs2 and Mlf3 suggests that these proteins are unlikely to be stably associated components of the actin cytoskeleton.

Cell lysis in the absence of Vhs2 and Mlf3

I show here that *vhs2 mlf3* cells exhibit a cell wall defect (Figure 3.12A) and undergo cell lysis at the restrictive temperature (Figure 3.12B). Normal polarized growth requires that the polarized actin cytoskeleton direct the secretory machinery to deposit cell wall synthesis/modifying enzymes to sites of active cell growth. The importance of the coordination between these processes is evident since ~27% of SBF target genes are those involved in cell wall biogenesis

and polarized growth-related functions (Iyer et al., 2001). In addition, cellular response to environmental stress conditions requires the function of an active cell integrity pathway, which constitutes the Rho1-Pkc1-MAP kinase cascade (described in Chapter 1). Mutants in this pathway demonstrate a cell lysis phenotype that can be rescued by the presence of an osmotic stabilizer in the growth medium (Heinisch et al., 1999). The cell lysis defect of *vhs2 mlf3* mutant cells can also be rescued partially by the presence of 1 M sorbitol in the growth medium (Figures 3.5, 3.7 and 3.12B). For two reasons, it does not seem likely that Vhs2 and Mlf3 function directly as part of the cell integrity pathway. First, mutants defective in the cell integrity pathway lyse (and thus die) at the small-budded stage, whereas *vhs2 mlf3* cells accumulate as large and round cells. Second, the onset of the actin depolarization defect appears earlier than the onset of the cell lysis defect. Thus, the latter defect may occur as a consequence of the former, possibly because a compromise in the actin cytoskeleton organization in *vhs2 mlf3* mutant cells leads to inefficient polarized secretion of cell wall synthesis/modifying enzymes at sites of active growth, thus resulting in cell lysis.

Vhs2 and Mlf3 are functionally redundant with Gic1 and Gic2

I have shown that increased dosage of *GIC1* (and to a much lesser degree *GIC2*) can ameliorate the growth defect of *vhs2 mlf3* mutant cells at 37°C (Figure 3.14A). Since increased dosage of *VHS2* or *MLF3* also suppresses the phenotypic defects of *gic1 gic2* double mutant cells (Figures 3.1, 3.2 and 3.3), the observed pattern of reciprocal suppression indicates that Vhs2 and Mlf3 likely function in a pathway that is distinct from but redundant with that mediated by Gic1 and Gic2. This conclusion is further supported by the observation that deletion of *VHS2* and *MLF3* exacerbates the growth defect of *gic1 gic2* cells (Figure 3.14B) and the morphological defects of *cla4* cells (Figure 3.15). Several other differences

between Vhs2/Mlf3 and Gic/Gic2 also underscore this interpretation. First, Gic1 and Gic2 are localized at sites of polarized growth, whereas both Vhs2 and Mlf3 are cytoplasmic. Second, haploid *gic1 gic2* cells (Chen et al., 1997), but not *vhs2 mlf3* cells (Table 3.5), exhibit defect in the process of bud-site selection. Third, *vhs2 mlf3* cells exhibit cell lysis defect (Figure 3.12B) and their temperature-sensitive growth defect can be rescued by sorbitol (Figure 3.5), whereas *gic1 gic2* mutant cells do not show obvious cell lysis phenotype and their temperature-sensitive growth defect cannot be rescued by sorbitol (not shown). However, both *gic1 gic2* and *vhs2 mlf3* mutant cells exhibit a defect in actin cytoskeleton polarization, and it is likely that this common function serves as the basis for the observed reciprocal suppression.

The connection between VHS2/MLF3 and G1-cyclin genes

Increased dosage of each of the G1 cyclin genes *CLN1*, *CLN2* and *PCL1* ameliorates the growth defect of *vhs2 mlf3* cells (Figure 3.14A). Since *vhs2 mlf3* cells do not arrest in G1 phase of the cell cycle, it is the likely that the polarity-related function of Cln1, Cln2 and Pcl1 is responsible for suppression. While Cln1 and Cln2 complex with Cdc28 to phosphorylate and regulate the Cdc42 effector Ste20 (Oda et al., 1999), Pcl1 complexes with Pho85 to regulate Rvs161 and Rvs167 (Lee et al., 1998).

VHS2 and MLF3 interact genetically with RVS genes

The Cdk Pho85 complexes with Pcl1 or Pcl2 to phosphorylate the Rvs proteins and thus regulates the actin cytoskeleton (Lee et al., 1998). This pathway is functionally redundant with that mediated by the Cdc42 GTPase (Lenburg and O'Shea, 2001; Moffat and Andrews, 2004). One way to explain the synthetic interaction of the *vhs2 mlf3* mutations with the *gic1 gic2* and the *cla4* mutations as well as the ability of increased *PCL1* dosage to suppress the growth defect of *vhs2*

mlf3 cells is that *VHS2* and *MLF3* function in the Pho85-Pcl1/2-mediated pathway of actin organization. Several lines of observation argue against this possibility. First, deletion of either *RVS161* or *RVS167* exacerbates the temperature-sensitive growth defect of *vhs2 mlf3* cells (Figure 3.17A). Second, the actin organization and cell lysis defects caused by the *rvs167* and *vhs2 mlf3* mutations are additive (Figure 3.17C and 3.17D). Third, the bud-site selection defect of *rvs167* diploid cells (Sivadon et al., 1995) is much stronger than that of *vhs2 mlf3* diploid cells (Table 3.6). Fourth, unlike *rvs161* and *rvs167* cells, *vhs2 mlf3* mutant cells do not exhibit any defect in fluid-phase endocytosis (Figure 3.17B). Thus, Vhs2 and Mlf3 likely regulate the actin cytoskeleton and polarized growth through a pathway that is distinct from those mediated by the Rvs proteins and the Gic proteins.

MGC1/TOS2 and polarized cell growth

Increased dosage of either *MGC1* or *TOS2* suppresses the temperature-sensitive growth defect (Figure 3.1), bud-site selection defect (Figure 3.2) and actin organization defect (Figure 3.3) of *gic1 gic2* mutant cells. Both *MGC1* and *TOS2* are non-essential genes. Deletion of *MGC1* and *TOS2*, either singly or in combination, does not produce any phenotype that would be indicative of a defect in polarized growth. However, several lines of evidence suggest that Mgc1 and Tos2 do function in the process of polarized cell growth. Like Cdc42, Gic1 and Gic2, Mgc1 is localized at sites of polarized growth (Figure 3.20). Tos2 also exhibits a similar subcellular localization pattern (Drees et al., 2001). Mgc1 and Tos2 also exhibit two-hybrid interactions with components of the Rho1- and Cdc42-mediated pathways of cell polarity (Drees et al., 2001; Uetz et al., 2000). Expression profiling studies have identified *GIC1* and *GIC2* as targets of the SBF transcription factor complex and *MGC1* and *TOS2* as targets of the related MBF transcription factor complex (Iyer et al., 2001), thus suggesting that the

expression of *MGC1* and *TOS2* is temporally coordinated with that of *GIC1* and *GIC2*.

Morphological and cytological consequences of Mgc1 and/or Tos2 overproduction

Overexpression of *MGC1* and *TOS2*, individually or together, culminates in cells that are hyperpolarized and have elongated buds. This phenotype is especially pronounced at 37°C (Figure 3.23). Overproduction of Mgc1 and Tos2 might interfere with the switch from apical to isotropic growth. Further, these cells often have an extra bud, which may emerge from the mother cell or more frequently from another bud (Figure 3.23). This phenotype is indicative of a cytokinesis defect. Aberrant localization of the Cdc3 septin (and likely other septins) in the morphologically abnormal cells that overproduce Mgc1 and/or Tos2 (Figure 3.24) can explain at least partly the cytokinesis defect observed in these cells. Since the septin scaffold is required for re-polarization of actin at the mother-bud neck at the time of cytokinesis, mislocalization of Cdc3 may also be the cause for the abnormal patterns of actin localization near the bud neck in these cells (Figure 3.26). It would be very interesting to see if the formation and positioning of the septum occurs normally in cells overproducing Mgc1 and Tos2.

Our laboratory has previously reported a synthetic lethal interaction between the *gic1 gic2* and *cla4* mutations and an exacerbated cytokinesis defect in the *gic1 gic2 cla4* triple mutant relative to the *cla4* single mutant (Chen et al., 1997). Recently, Cla4 has been implicated to have a role in septin collar formation (Schmidt et al., 2003; Versele and Thorner, 2004). Mgc1 interacts with Cla4 in the two-hybrid assay (Uetz et al., 2000). Although *MGC1* and *TOS2* do not exhibit synthetic genetic interaction with *CLA4*, it would be interesting to check the effect of Mgc1 overproduction in *cla4* mutant background.

Suppression interaction between mgc1 and cyk2 mutations

The suppression of the growth defect of *cyk2* mutant cells by the deletion of *MGC1* (Figure 3.21) suggests that Mgc1 and Cyk2 perform antagonistic functions in the cell. In light of the positive role of Cyk2 in cytokinesis, this genetic interaction suggests an inhibitory function of Mgc1 in cytokinesis. This is consistent with the cytokinesis defect observed upon overproduction of Mgc1. I discuss three models to interpret the genetic interaction between the *mgc1* and *cyk2* mutations (Figure 3.27).

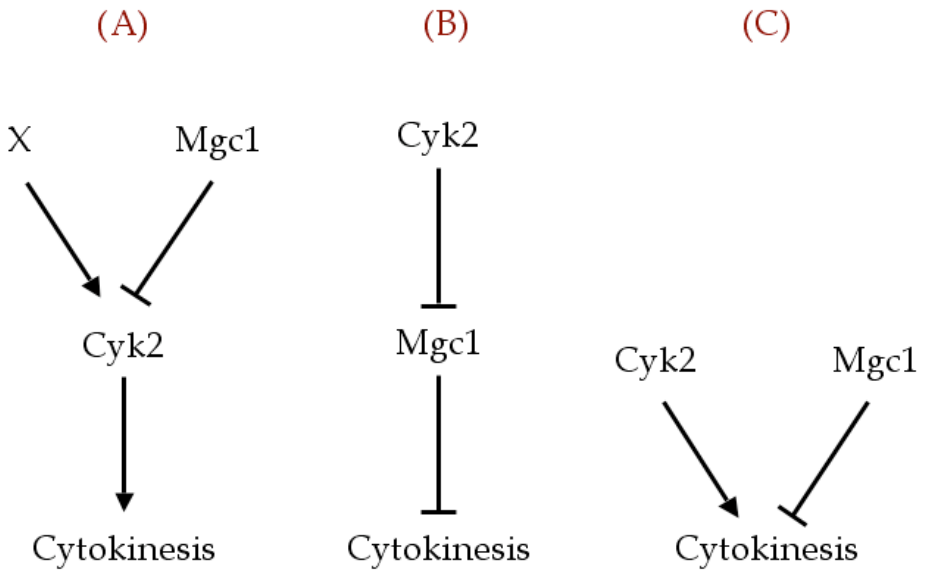

Figure 3.27 Genetic models to explain the functional relationship between Cyk2 and Mgc1 in cytokinesis.

In the first model, Mgc1 negatively regulates Cyk2, a positive regulator of cytokinesis. In wild-type cells, this inhibitory effect of Mgc1 may be limited either because of a relatively greater abundance of Cyk2 or due to the

counteracting function of an upstream activator (X) of Cyk2. This model can explain the cytokinesis defect observed upon overproduction of Mgc1. According to this model, *cyk2* single mutant and *mgc1 cyk2* double mutant should exhibit a similar growth phenotype. However, the observation was opposite. Therefore, based on the epistatic relationship, this model cannot hold true.

In the second model, Cyk2 positively regulates cytokinesis via inhibition of Mgc1, a negative regulator of cytokinesis. This model explains why overproduction of Mgc1 results in cytokinesis defect. It also explains why the absence of Cyk2 results in cytokinesis and growth defects, and why the loss of Mgc1 from *cyk2* cells alleviates this growth defect.

In the third model, Cyk2 and Mgc1 function independently to regulate cytokinesis in a positive and negative manner, respectively. This model can also explain the observed cytokinesis defect upon Mgc1 overproduction and the suppression of the growth defect of *cyk2* cells by deletion of *MGC1*.

In summary, the work described in this chapter primarily focuses on the study of four previously uncharacterized genes that can suppress the phenotypic growth defects of *gic1 gic2* cells. Analysis of Vhs2 and Mlf3 revealed that they function in a pathway that influences both actin cytoskeleton organization and cell wall integrity. Analysis of Mgc1 and Tos2 implicates them as negative regulators of cytokinesis. The mechanistic details of how these proteins participate in their proposed cellular function to facilitate polarized cell growth remains to be elucidated.

CHAPTER 4

Mutations that exacerbate the phenotype of *gic1 gic2* cells

4.1 BACKGROUND

The *S. cerevisiae* genome is marked by a high degree of functional redundancy between genes. Around 80% of the ~6,200 predicted genes in budding yeast are non-essential and as a result the genome is buffered from the phenotypic consequences of genetic perturbations (Hartman et al., 2001). For this reason, it is difficult to unveil the functions of a large number of non-essential genes by using a reverse genetics approach.

Synthetic lethal screens have been traditionally used to identify genes with redundant functions. In this genetic approach, a specific mutant is typically used as the starting strain for screening second-site mutations that enhance the phenotype of the original mutant. Two genes show a synthetic lethal interaction if the combination of the two mutations, neither by itself lethal, causes cell death. Synthetic lethal relationships may occur for genes acting in a single biochemical pathway or for genes within two distinct pathways if one process functionally compensates for the defects in the other (Guarente, 1993). Many genes involved in cell polarity (Bender and Pringle, 1991; Wang and Bretscher, 1997), secretion (Chen and Graham, 1998), DNA repair (Mullen et al., 2001) and numerous other processes have been identified using synthetic lethal screens.

To enable high-throughput synthetic lethal analyses, a method called synthetic genetic array (SGA) analysis has been developed by Dr. Charles Boone's group at the Univeristy of Toronto, Canada (Tong et al., 2001). In this method, a systematic array of ~4,700 haploid mutants, each carrying a deletion of a non-essential gene, is assembled. The deletion mutant in query is mated with every single mutant in the array. Sporulation and meiotic recombination is then

induced in each of the resultant diploid and the haploid progenies containing double mutations are analyzed for their ability to grow. The SGA methodology and examples of such an analysis are shown schematically in Figures 4.1 and 4.2, respectively.

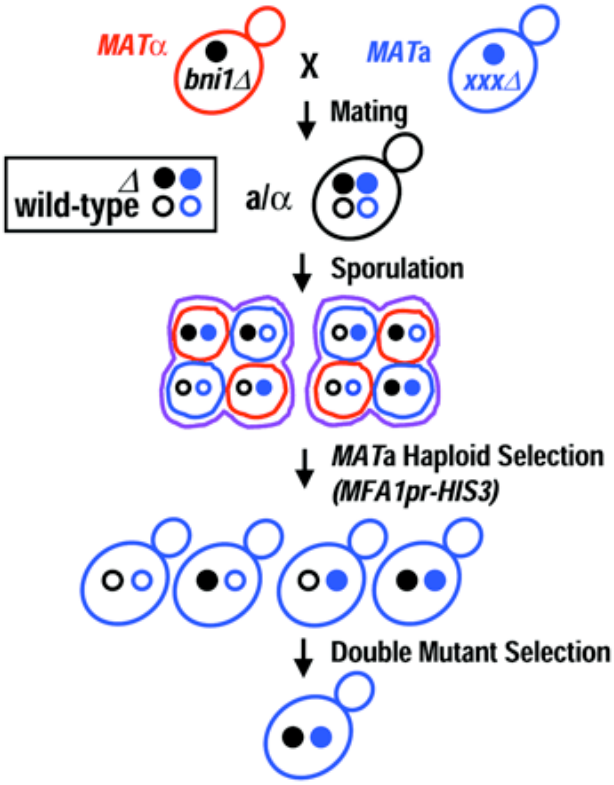

Figure 4.1 Synthetic genetic array methodology. **(i)** A *MATα* strain carrying a query mutation (e.g., *bni1*) linked to a dominant selectable marker, such as the nourseothricin-resistance marker (*natMX*) that confers resistance to the antibiotic nourseothricin, and an *MFA1pr-HIS3* reporter is crossed to an ordered array of *MATa* viable yeast deletion mutants, each carrying a gene deletion mutation linked to a kanamycin-resistance marker (*kanMX*). Growth of resultant heterozygous diploids is selected for on medium containing nourseothricin and kanamycin. **(ii)** The heterozygous diploids are induced to undergo sporulation during which tetrads are formed. **(iii)** Haploid meiotic spore progenies are transferred to synthetic medium lacking histidine, which allows for selective germination of *MATa* meiotic progenies because these cells express the *MFA1pr-HIS3* reporter specifically. **(iv)** *MATa* meiotic progenies are transferred to medium that contains both nourseothricin and kanamycin, which then selects for growth of double-mutant meiotic progeny. (Source: Tong et al., 2001).

As mentioned earlier, neither *GIC1* nor *GIC2* is an essential gene. In the absence of both genes, cells exhibit a temperature-sensitive growth phenotype but are still viable at $\leq$ 30°C. This implies that there must be other proteins in the cell that compensate for the loss of Gic1 and Gic2 at permissive temperatures. If this is indeed the case, then loss of these 'other' proteins should further compromise the growth defect of *gic1 gic2* double mutant cells and should yield a synthetic growth phenotype. With this rationale in mind, we set up collaboration with the Boone laboratory and performed an SGA analysis using *gic1 gic2* double mutations as the query. We anticipated that this screen would identify genes that function in Gic-independent pathways of actin cytoskeleton organization. Additionally, such analyses would also shed light upon previously unappreciated functions of the Gic proteins outside the range of actin organization.

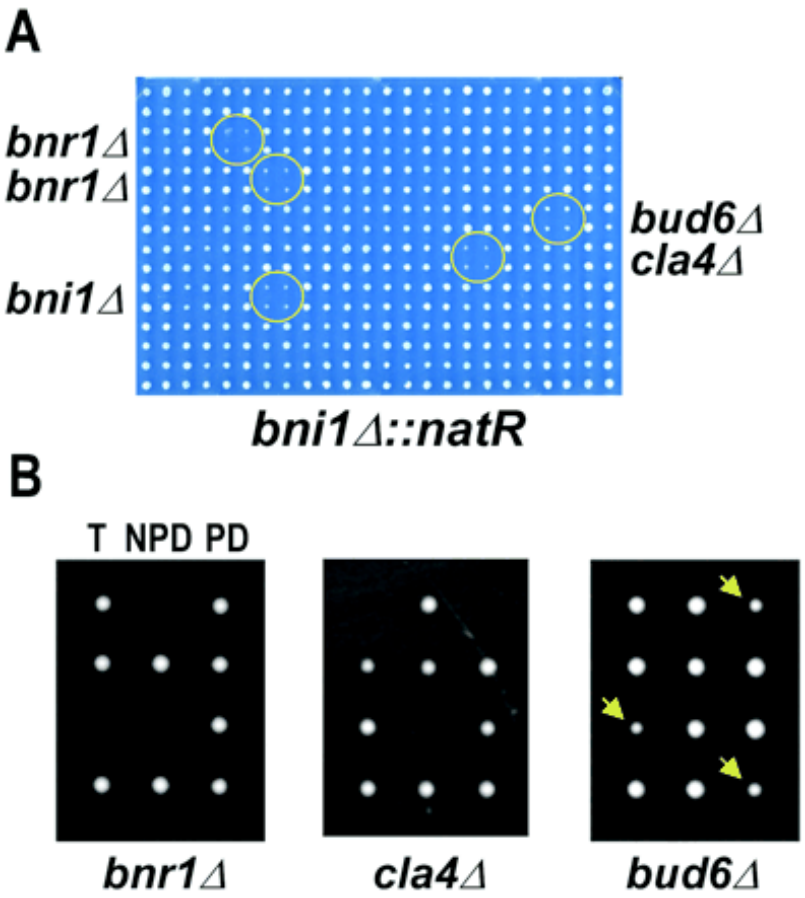

Figure 4.2 Final double-mutant array and tetrad analysis for SGA. Shown is an example of synthetic lethal analysis with *bni1* mutant as the query **(A)** *bni1::natR* cells were crossed to a test array containing 96 deletion mutants, each arrayed in quadruplicate in a square pattern. *bnr1* was duplicated within the array. The final array that selects for growth of the *bni1* double mutants is shown. Synthetic lethal/sick interactions lead to the formation of residual colonies (yellow circles) that were relatively smaller than the equivalent colony on the wild-type control plate. Synthetic lethal/sick interactions were scored with *bnr1*, *cla4*, and *bud6*. When the query mutation was identical to one of the gene deletions within the array, double mutants could not form because haploids carry a single copy of each allele; therefore, *bni1* appeared synthetic lethal with itself. **(B)** Tetrad analysis of meiotic progeny derived from diploid cells heterozygous for *bni1* and either *bnr1*, *cla4*, or *bud6*. Tetratypes (T) contain one double-mutant spore; nonparental ditypes (NPD) contain two double-mutant spores; and parental ditypes (PD) lack double-mutant spores. The spores were micromanipulated onto distinct positions on the surface of agar medium and then allowed to germinate to form a colony. *bni1 bnr1* and *bni1 cla4* double mutants are inviable and therefore fail to form a colony, whereas *bni1 bud6* double mutants showed a synthetic slow growth (sick) phenotype (yellow arrows). The genetic make-up of the double mutants was inferred by replica plating the colonies to medium containing nourseothricin, which selects for growth of *bni1::natR* cells, and kanamycin, which selects for growth of the *bnr1*, *cla4*, and *bud6* gene-deletion mutants. (Source: Tong et al., 2001).

4.2 RESULTS

The gic1-Δ3::natR gic2-Δ3::URA3 strain used for SGA bears an SSD1-v(1) allele

Since SGA analysis is typically carried out using yeast deletion mutants created in the Research Genetics strain background, a *gic1-Δ3::natR gic2-Δ3::URA3* strain (CCY1446-1A) was created in the same genetic background (see Chapter 2 for details). The *gic1 gic2* double mutants that were generated previously in our laboratory strain background exhibit a Ts^- growth defect at ≥33°C. In contrast, *gic1 gic2* double mutants generated in the Research Genetics strain background showed growth defect only at 37°C. Further, this defect was restricted mainly to the double mutant cells of α-mating-type (see below).

Our laboratory has previously reported that commonly used laboratory yeast strains carry either an *ssd1-d* (*d* for death) or *SSD1-v(1)* (*v* for viable) allele on their chromosomes (Kim et al., 1994). Although the molecular basis for the difference between the two alleles of *SSD1* is unknown, phenotypes of many mutants, including *sit4* (Sutton et al., 1991), *bck1* (Costigan et al., 1992), *slt2* (Mazzoni et al., 1993), *cln1*, *cln2* (Cvrckova and Nasmyth, 1993) and *bem2* (Kim et al., 1994), are suppressed by the *SSD1-v(1)* allele. It has also been shown that the Ts^- phenotype of *gic1 gic2* cells can be suppressed partially by *SSD1-v(1)* on a CEN plasmid (Chen et al., 1997). Since most of the strains used in our laboratory, including the *gic1 gic2* strains described in the previous chapter, contain the *ssd1-d* allele, one possible explanation for the lack of severity in the Ts^- growth defect seen for the *gic1-Δ3::natR gic2-Δ3::URA3* strain could be that it carried an *SSD1-v(1)* allele.

To address this possibility, a haploid *bem2-101 ssd1-d* strain (CCY471-13C, Ts^- at 37°C) was crossed with a haploid wild-type strain of Research Genetics background (Y3656). If the Research Genetics strain carried an *ssd1-d* allele, the prediction would be that all *bem2-101* progenies obtained from the above diploid

would exhibit Ts- growth defect at 37°C. However, if it carried the *SSD1-v(1)* allele, only ~50% of the *bem2-101* progenies would exhibit a similar growth defect at 37°C. Indeed, tetrad analysis showed that out of 24 *bem2-101* spores, only 12 were Ts- at 37°C, suggesting the latter possibility to be true. Thus, the Research Genetics strain background likely carries an *SSD1-v(1)* allele, which may account for the less severe Ts- growth defect seen in the *gic1-Δ3::natR gic2-Δ3::URA3* strain used for the SGA analysis. By extension, we hypothesized that the synthetic sick phenotype of the potential *gic1 gic2 x* triple mutants (where *x* represents the gene identified in SGA) would be much more severe if it were to be recapitulated in the *ssd1-d* allele-bearing genetic background of most of our laboratory strains.

The growth defect of gic1-Δ3::natR gic2-Δ3::URA3 cells is affected by their mating-type

During the construction of the *gic1-Δ3::natR gic2-Δ3::URA3* strain (detailed in Chapter 2), I observed that all *MATα gic1-Δ3::natR gic2-Δ3::URA3* cells were Ts- at 37°C, whereas *MATa gic1-Δ3::natR gic2-Δ3::URA3* cells did not show any obvious growth defect at that temperature. During subsequent tetrad analyses, this observation was quantitatively supported. ~80% of *MATα gic1-Δ3::natR gic2-Δ3::URA3* haploid cells (n=70) were Ts- at 37°C, whereas ~81% of *MATa gic1-Δ3::natR gic2-Δ3::URA3* haploid cells (n=88) were Ts+ at 37°C. The *GIC1* and *GIC2* genes are not located on Chromosome III and therefore are not linked to the *MAT* locus. There could at least be two possible explanations for these observations. First, a suppressor mutation that is tightly linked to *MATa* may suppress the Ts- phenotype of *gic1-Δ3::natR gic2-Δ3::URA3* cells. Second, mating-type-specific gene expression may affect the temperature-sensitivity of *gic1-Δ3::natR gic2-Δ3::URA3* cells.

To address these possibilities, I first tested whether the putative suppressor in *MATa gic1-Δ3::natR gic2-Δ3::URA3* cells is dominant or recessive.

To this end, four *MATα gic1-Δ3::natR gic2-Δ3::URA3* strains (CCY1551-1B, CCY1551-5C, CCY1551-3B and CCY1551-8B; all Ts^- at 37°C) were crossed with four *MATa gic1-Δ3::natR gic2-Δ3::URA3* strains (CCY1551-3C, CCY1551-12A, CCY1551-2D and CCY1551-11B; all Ts^+ at 37°C) in different combinations, and the 16 resulting diploids were tested for their ability to grow at 37°C. All but one of these diploids (CCY1551-5C X CCY1551-12A) showed growth phenotype at 37°C, suggesting that if there is a suppressor in *MATa gic1-Δ3::natR gic2-Δ3::URA3* cells, it is of recessive nature. Tetrad analyses of one of the diploids described above (CCY1551-8B X CCY1551-2D, [Cross CCY1583]) revealed that all 14 *MATα gic1-Δ3::natR gic2-Δ3::URA3* haploids tested were Ts^- at 37°C, whereas none of the 14 *MATa gic1-Δ3::natR gic2-Δ3::URA3* haploids tested showed a similar growth defect.

To determine whether the variations in the temperature-sensitivity of *gic1 gic2* cells was due to differences in mating-type or a recessive suppressor mutation that is tightly linked to the mating-type locus, I carried out a mating-type switching experiment.

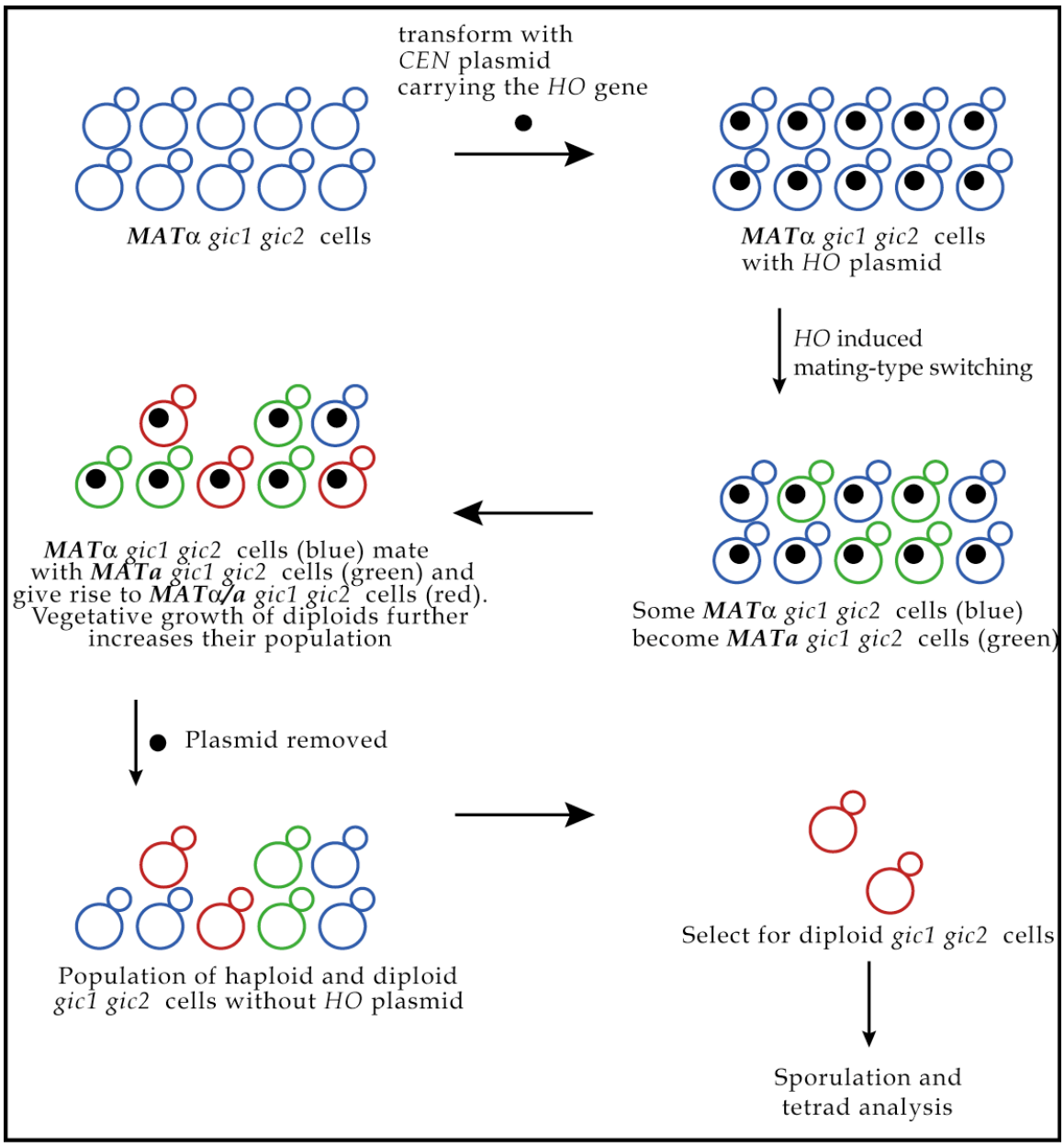

Figure 4.3 Experimental design for determining whether the phenotype is linked to the mating-type of cells. The result of tetrad analysis would show cosegregation of the phenotype with mating-type if the mating-type is the cause of the phenotype. Otherwise, all meiotic progenies will exhibit identical phenotype independent of their mating-type.

MATα gic1-Δ3::natR gic2-Δ3::URA3 cells (CCY1551-8B) were transformed with a plasmid (pCC1872, CEN) bearing the *HO* gene. Transformants would undergo mating -type switching to yield *MATa gic1-Δ3::natR gic2-Δ3::URA3* cells. The *MATa* and *MATα gic1-Δ3::natR gic2-Δ3::URA3* cells within the transformant colony would mate and become diploids. After plasmid loss and subsequent induction of sporulation in such diploids, all four meiotic products should remain Ts^- at 37°C if a recessive mutation that is tightly linked to the mating-type locus (but not the mating-type locus itself) was responsible for suppressing the Ts^- phenotype of *MATa gic1 gic2* cells. Instead, I found that only the two *MATα* meiotic products of each tetrad (n=8) remained Ts^- at 37°C, thus indicating that the mating-type locus itself dictates the Ts^- phenotype of *gic1 gic2* cells.

Mutations in several cellular pathways show synthetic interaction with *gic1 gic2* mutations

The *MATα gic1-Δ3::natR gic2-Δ3::URA3* strain CCY1446-1A was used as a query in SGA analysis against an array of all the non-essential genes in *S. cerevisiae*. At the end of three rounds of SGA analysis, 72 genes were tentatively identified by Amy Tong (in Charlie Boone's laboratory) as those required for the normal growth of *gic1 gic2* cells at the otherwise permissive growth temperature of 30°C (Table 4.1). The distribution of these synthetic lethal/sick interactors, based on their functions listed in the Yeast Protein Database, is shown in Figure 4.4.

Table 4.1 Synthetic interactors of *gic1 gic2* identified by SGA analysis. These interactors are categorized according to their annotated functions.

Cellular Function	Gene	ORF	Count of Hits [a]
Cell polarity	*AXL2*	*YIL140W* ▤	2
	BEM4	*YPL161C*	1
	BNI1	*YNL271C*	1
	BOI1	*YBL085W*	1
	BUD6	*YLR319C* ◉	3
	CLA4	*YNL298W*	3
	MSB1	*YOR188W*	2
	MSB3	*YNL293W*	3
	NBP2	*YDR162C*	1
	PEA2	*YER149C*	3
	RSR1	*YGR152C* ✶	1
	RVS161	*YCR009C*	1
	SPA2	*YLL021W*	3
		YGR151C ✶	1
Cell cycle control	*SSD1*	*YDR293C*	3
	SWI4	*YER111C*	2
Cell structure	*CAP1*	*YKL007W*	1
	CAP2	*YIL034C*	1
Cell wall organization and biogenesis	*FKS1*	*YLR342W*	1
	HOC1	*YJR075W*	1
	ROM2	*YLR371W* ◆	2
	SMI1	*YGR229C* ◇	3
Chromatin/chromosome structure	*EST2*	*YLR318W* ◉	1
	HIR1	*YBL008W*	1
	SIF2	*YBR103W*	1
	TOP3	*YLR234W* ▲	1
Energy generation	*CEM1*	*YER061C*	1
	ILM1	*YJR118C*	2

Table 4.1 contd.

Cellular Function	Gene	ORF	Count of Hits [a]
Lipid metabolism	*LAS21*	*YJL062W*	3
	OPI3	*YJR073C*	
	SUR4	*YLR372W* ◆	1
	SUR7	*YML052W*	1
Meiosis	*SPO21*	*YOL091W*	1
		YLR235C ▲	1
		YPL144W	1
Nuclear membrane organization and biogenesis	*NEM1*	*YHR004C*	2
Other metabolism	*SPE2*	*YOL052C*	1
Pol II transcription	*IKI3*	*YLR384C*	1
	SEF1	*YBL066C*	1
Protein degradation	*PRE9*	*YGR135W*	1
Protein modification	*KIN4*	*YOR233W*	1
Protein synthesis	*RPL34B*	*YIL052C*	1
	RPS10B	*YMR230W*	1
	RPS26B	*YER131W*	1
Recombination	*SOH1*	*YGL127C*	1
Small molecule transport	*PMR1*	*YGL167C*	2
Transport	*HSE1*	*YHL002W*	1
		YDR119W	1

Table 4.1 contd.

Cellular Function	Gene	ORF	Count of Hits [a]
Vesicular transport	*DID2*	*YKR035W-A*	1
	DRS2	*YAL026C*	3
	ERV14	*YGL054C*	2
	PDR17	*YNL264C*	1
	RIC1	*YLR039C*	3
	SEC66	*YBR171W*	1
	SEM1	*YDR363W-A*	2
	VPS17	*YOR132W*	2
	VPS21	*YOR089C*	1
	YPT6	YLR262C	1
Vacuolar organization and biogenesis	*VAM10*	*YOR068C*	1
	VID22	*YLR373C* ◆	2
Unknown	*HUR1*	*YGL168W*	3
		YBR077C	3
		YEL067C	1
		YGR011W	1
		YGR228W ◇	3
		YIL141W ▤	1
		YJL211C	1
		YLR374C ◆	1
		YML057C-A	1
		YMR124W	2
		YPL205C	1
		YPR045C	1

[a] A total of three rounds of SGA analysis were carried out. The numbers indicate the number of rounds in which the candidate gene showed synthetic interaction with *gic1 gic2*.
- Like symbols in column 3 denote neighboring open reading frames. *YGR151C, YGR228W, YIL141W, YLR235C and YLR374C* are currently annotated as dubious ORFs in the *Saccharomyces* Genome Database. These ORFs are either completely or partially embedded within *RSR1, SMI1, AXL2, TOP3* and *VID22*, respectively.

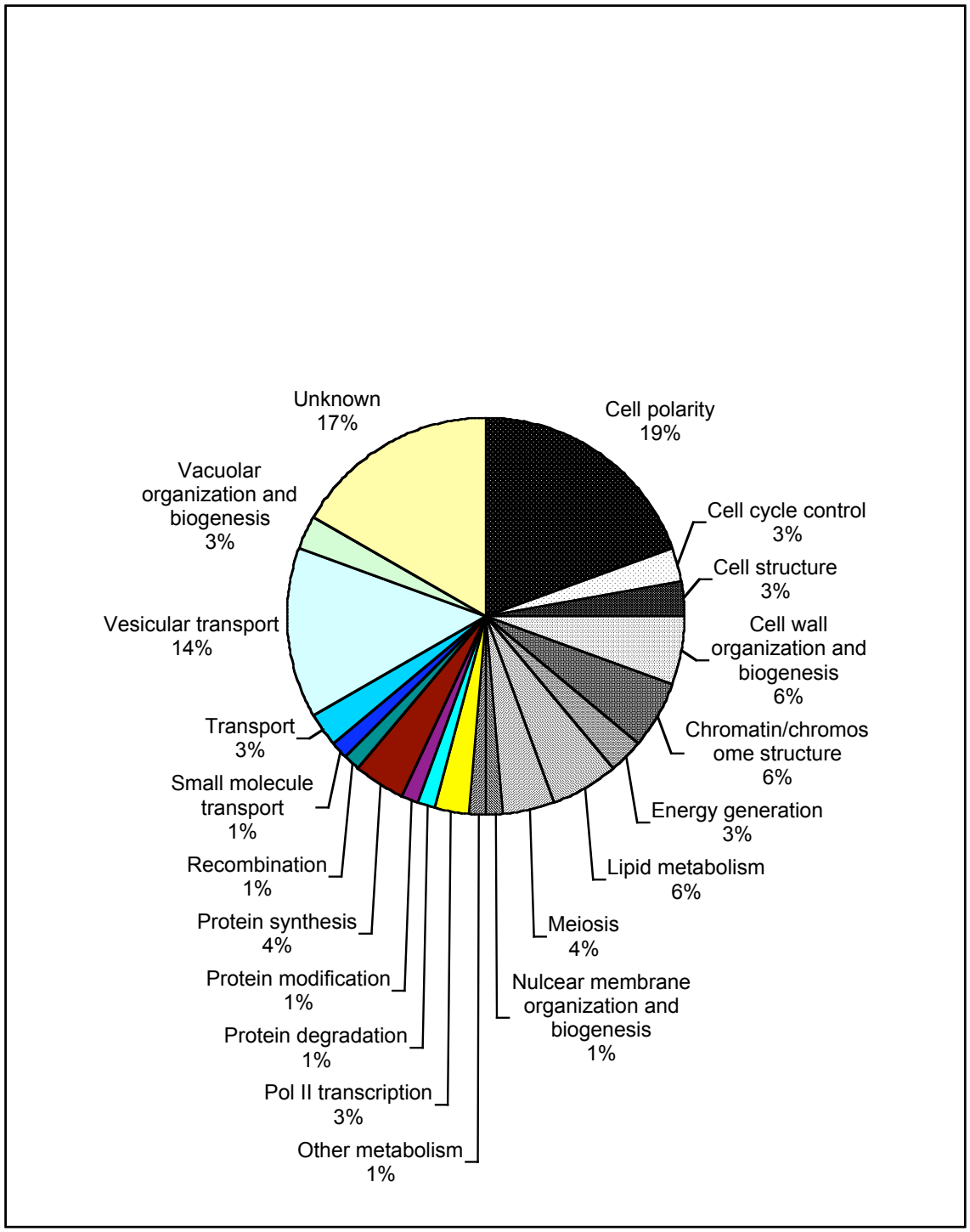

Figure 4.4 Distribution of synthetic interactors of *gic1 gic2* identified by SGA analysis based on their function (listed in the Yeast Protein Database).

SGA relies on assessing the synthetic phenotype of double mutants (or in this case triple mutants) that are formed as a result of meiotic recombination. Thus, deletion mutations that are genetically linked to the query mutation form double mutants at a reduced frequency and may thus be mistakenly identified as genetic interactors of the query mutation. Table 4.2 shows the list of such putative false positive synthetic interactors identified in this study.

Table 4.2 List of candidate genes identified as synthetic interactors of *gic1 gic2*, which are genetically linked to *GIC1* (*YHR061C*) or *GIC2* (*YDR309C*).

Gene	ORF
Unknown	*YHR045W*
SMF2	*YHR050W*
CPR2	*YHR057C*
FYV4	*YHR059W*
GIC1	*YHR061C*
SSZ1	*YHR064C*
CPR5	*YDR304C*
HNT2	*YDR305C*
Unknown	*YDR306C*
Unknown	*YDR307W*
GIC2	*YDR309C*
SUM1	*YDR310C*
SSF2	*YDR312W*

SGA is a very rapid and efficient technique to obtain a global view of genetic interactions. However, when the result of SGA is double-checked by traditional tetrad analysis, ~20-50% SGA interactions appear to be false-positives. These discrepancies may arise partly due to differences in the growth conditions used (minimal medium for SGA vs. rich medium for tetrad analysis).

Furthermore, mutations that lower the mating, sporulation or germination efficiency below a particular threshold level may also be incorrectly scored as genetic interactors. Thus, it is necessary to confirm the result of SGA analysis by using a more classical genetic technique such as tetrad analysis (Tong et al., 2001).

Validation of the SGA analysis result by tetrad analyses

I carried out tetrad analyses to determine which of the 72 mutations listed in Table 4.1 indeed interact genetically with *gic1 gic2*. For this purpose, haploid deletion mutants were first obtained by dissecting the corresponding heterozygous deletion mutants from the Research Genetics deletion strain collection. Each haploid deletion strain was then crossed with a haploid *gic1 gic2* strain. Dissection of tetrads from heterozygous *gic1 gic2 x* triple mutant (where *x* is one of the 72 putative interactor genes) strains generated haploid *gic1 gic2 x* haploid progeny cells, which were assessed for their growth phenotype. The summary of this analysis is presented in Table 4.3. The candidate genes that were confirmed as positive synthetic interactors of *gic1 gic2* mutations are listed in Table 4.4 and their distribution based on known functions is shown in Figure 4.5.

Table 4.3 Summary of genetic interactions between *gic1 gic2* and SGA interactors, examined by tetrad analyses.

A	B	C	D	E	F
AXL2	*RSR1*	*CEM1*	*FKS1*	*HIR1*	*BEM4*	*RPL34B*
BNI1	*SEC66*	*HUR1*	*KIN4*	*YBR077C*	*BOI1*	*RPS26B*
BUD6	*SMI1*	*LAS21*	*PMR1*	*YJL211C*	*DID2*	*SIF2*
CAP1	*SPA2*	*YPL205C*	*RPS10B*		*DRS2*	*SOH1*
CAP2	*SSD1*		*SEF1*		*HOC1*	*TOP3*
CLA4	*SUR4*		*SPE2*		*IKI3*	*YLR235C*
ERV14	*SUR7*		*SPO21*		*OPI3*	
EST2	*SWI4*		*YDR119W*		*PDR17*	
HSE1	*VAM10*		*YEL067C*		*ROM2*	
ILM1	*VPS17*		*YGR011W*		*RVS161*	
MSB1	*YGR151C*		*YPR045C*		*SEM1*	
MSB3	*YGR228W*				*VID22*	
NBP2	*YLR374C*				*VPS21*	
NEM1	*YMR124W*				*YIL141W*	
PEA2	*YPL144W*				*YML057C-A*	
PRE9	*YPT6*					
RIC1						

A. Positive synthetic interaction seen.

B. Seemingly positive synthetic interaction but inconclusive because very few *gic1 gic2 x* triple mutants were tested.

C. No synthetic genetic interaction seen.

D. Mutations in these genes appear to suppress the growth defect of *gic1 gic2* cells.

E. Heterozygous diploids containing mutations in *GIC1 GIC2* and these genes resulted in very poor spore viability, thus precluding tetrad analysis.

F. These haploid deletion strains were either inviable or not available and thus could not be tested.

Table 4.4 Candidate genes confirmed by tetrad analysis as positive synthetic interactors of *gic1 gic2* mutations.

Function*	Genes
Cell Polarity	*AXL2, BNI1, BUD6, CLA4, MSB1, MSB3, NBP2, PEA2, RSR1, SPA2, YGR151C*
Cell cycle control	*SSD1, SWI4*
Cell structure	*CAP1, CAP2*
Cell wall organization and biogenesis	*SMI1*
Chromatin/chromosome structure	*EST2*
Energy generation	*ILM1*
Lipid metabolism	*SUR4, SUR7*
Meiosis	*YPL144W*
Nuclear membrane organization and biogenesis	*NEM1*
Protein degradation	*PRE9*
Transport	*HSE1*
Vesicular transport	*ERV14, RIC1, SEC66, VPS17, YPT6*
Vacuolar organization and biogenesis	*VAM10*
Unknown	*YGR228W, YLR374C, YMR124W*

* as listed in the Yeast Protein Database

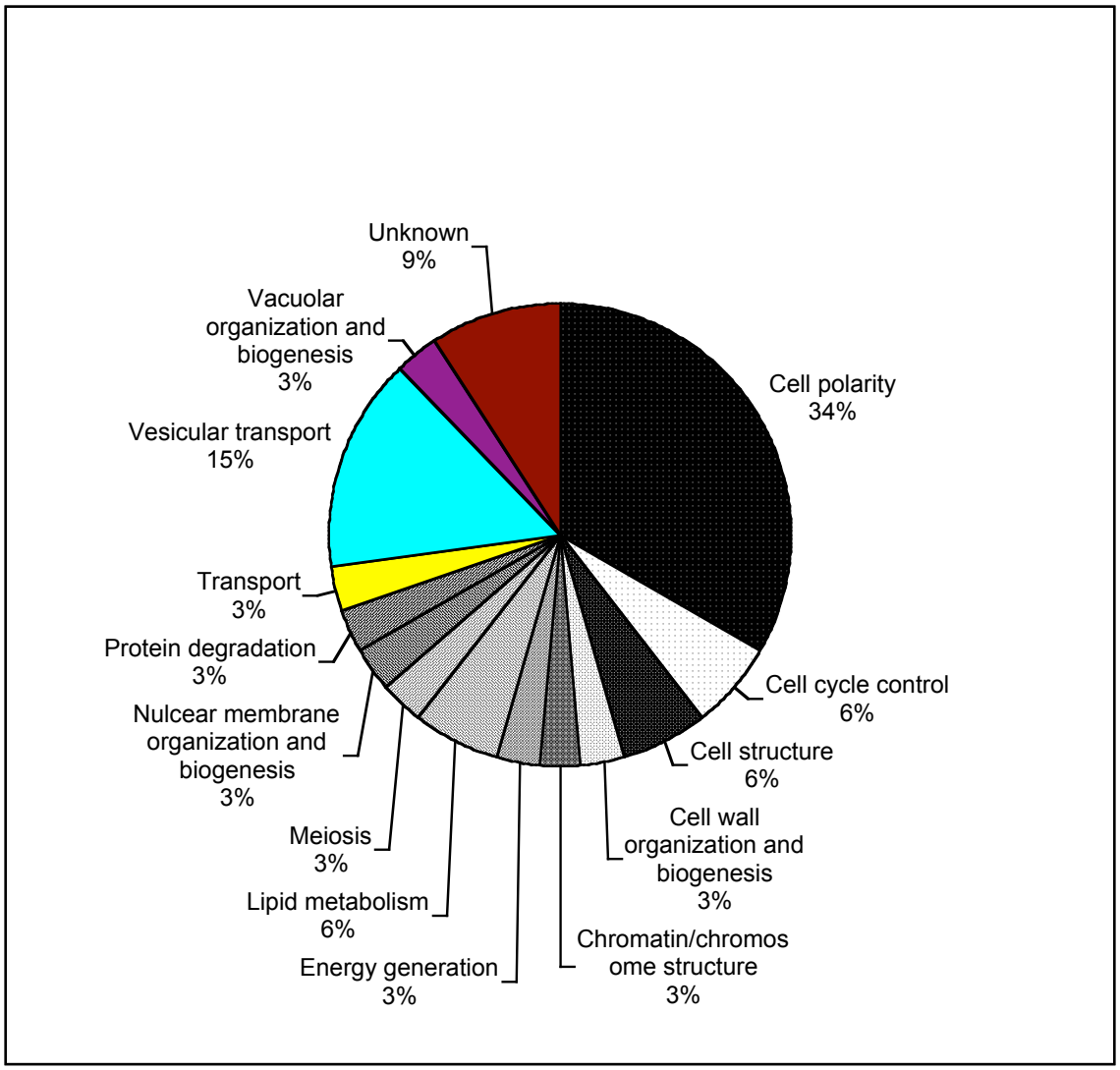

Figure 4.5 Distribution of synthetic interactors of *gic1 gic2* confirmed positive by tetrad analysis, based on their functions listed in the Yeast Protein Database.

Mutations in SGA identified genes produce synthetic sick growth phenotype when combined with mutations in *GIC1* and *GIC2*

Of the 72 candidate genes identified by SGA analysis, I have confirmed that 33 genes indeed show positive synthetic interaction in combination with *gic1 gic2* mutations. The growth phenotypes of many such *gic1 gic2 x* triple mutants on YEPD agar are shown in Figure 4.6. None of these interactions are truly 'synthetic lethal'. Instead, most of them are synthetic sick to varying degrees. However, I expect at least some of these genetic interactions to be more severe in yeast strains that carry the *ssd1-d* allele instead of the *SSD1-v(1)* allele present in the strains shown in Figure 4.6. For example, *gic1 gic2 cla4 ssd1-d* cells are known to be inviable at 26°C (Chen et al., 1997).

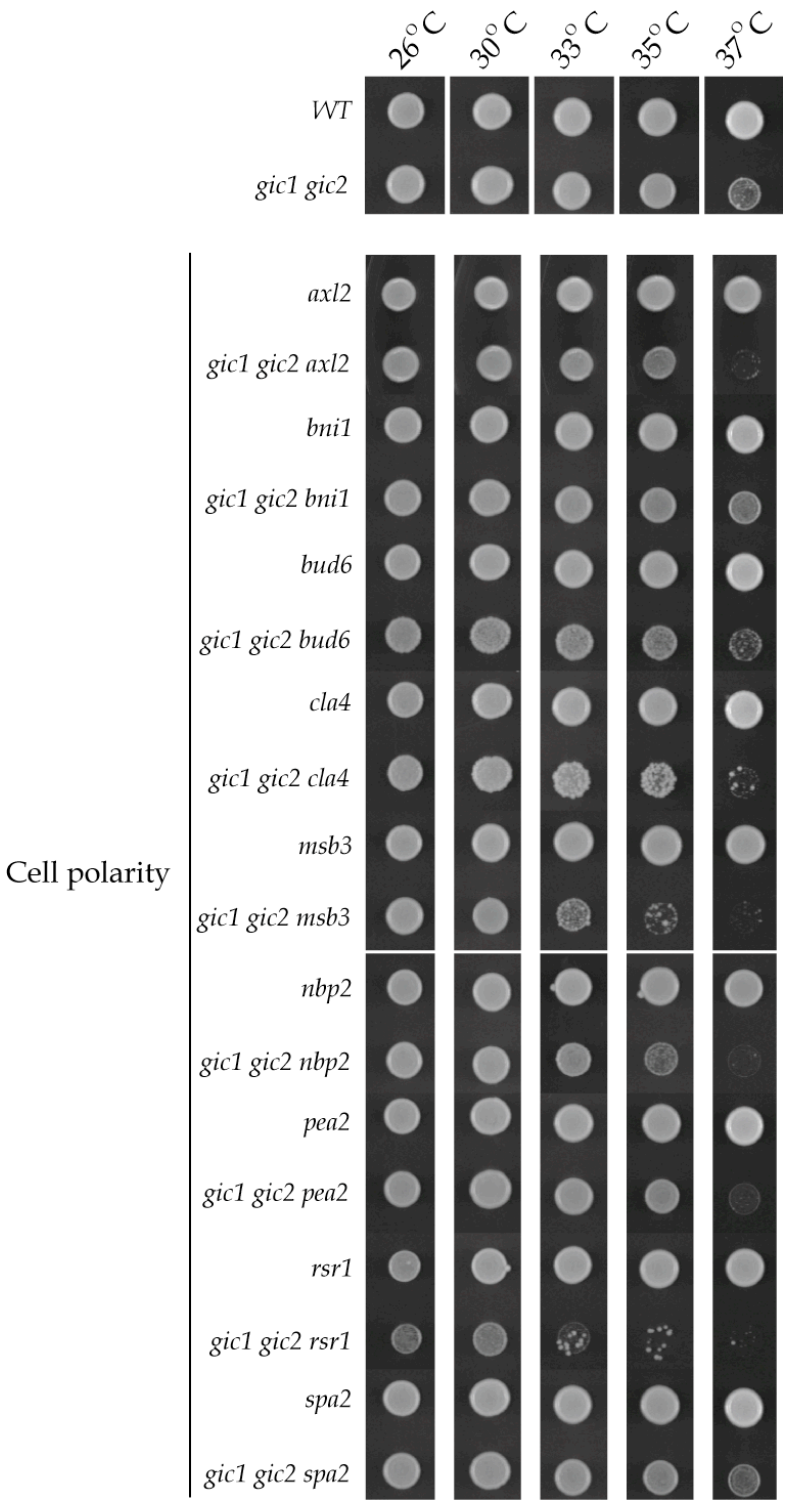

Figure 4.6 Synthetic sick phenotypes of *gic1 gic2 x* triple mutants

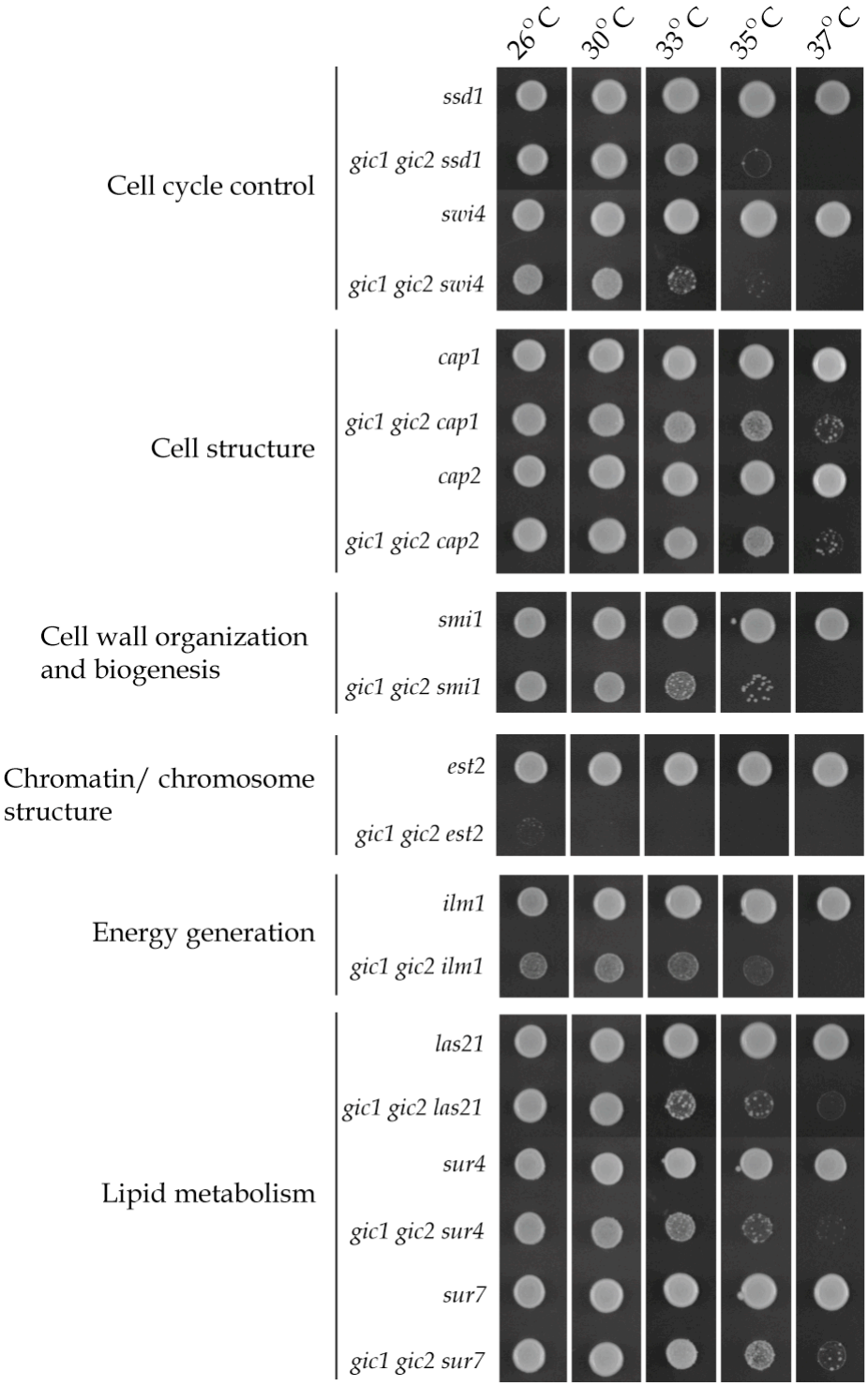

Figure 4.6 (contd.) Synthetic sick phenotypes of *gic1 gic2 x* triple mutants

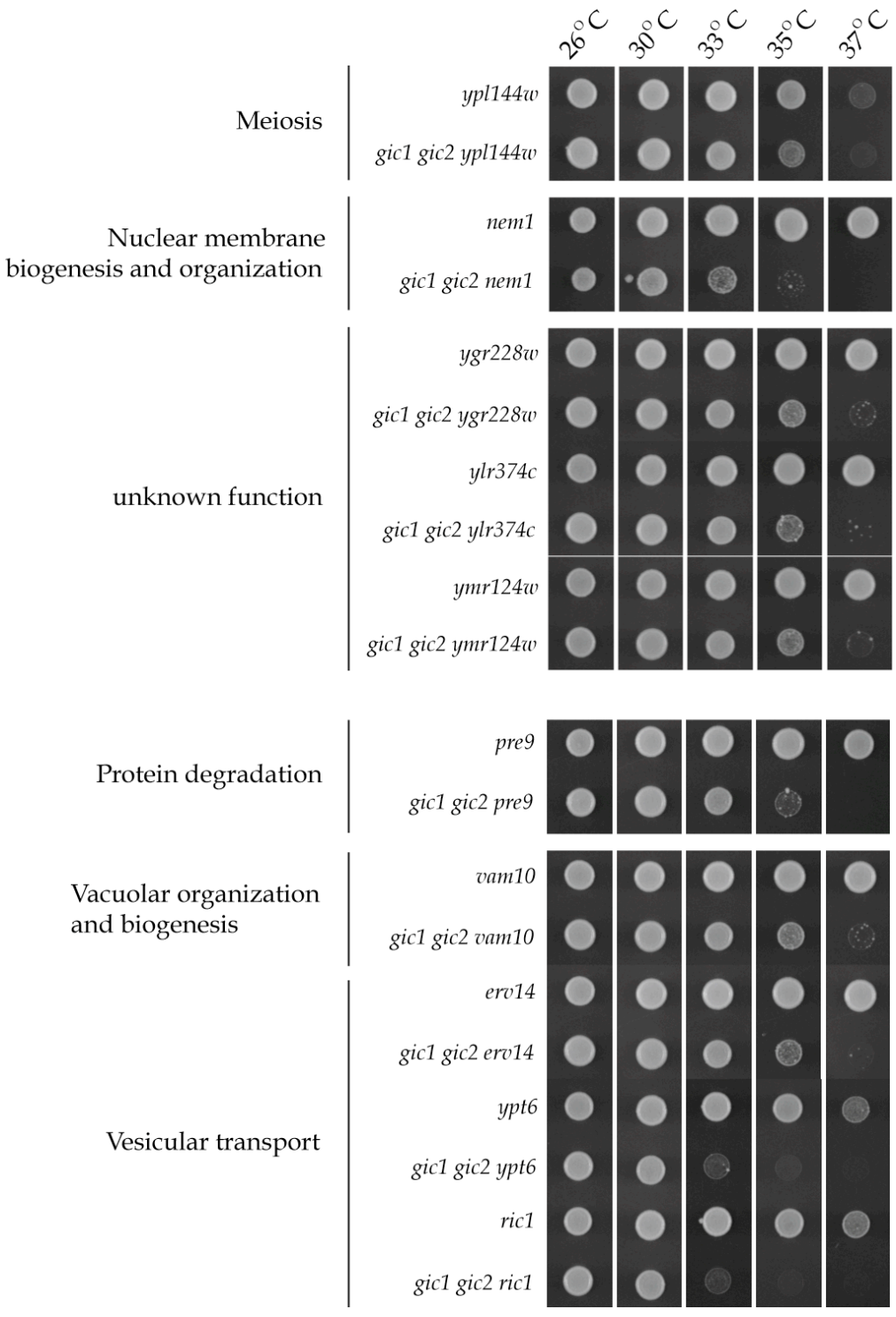

Figure 4.6 (contd.) Synthetic sick phenotypes of *gic1 gic2 x* triple mutants

Figure 4.6 Synthetic sick phenotypes of *gic1 gic2 x* triple mutants (where *x* is a variable mutation from the SGA). Suspensions of cells with different genotypes were spotted on YEPD and allowed to grow for 2 days at indicated temperatures.

Notes:

(1) Scoring of spore colonies revealed that *gic1 gic2 swi4* triple mutants also exhibit cold-sensitivity at 13°C. *swi4* and *gic1 swi4* cells showed normal growth whereas *gic2 swi4* cells were moderately sick at 13°C.

(2) Scoring of spore colonies revealed that *gic1 ypl144w* double mutants (2 out of 4) and *gic2 ypl144w* double mutants (2 out of 4) were also Ts- at 37°C.

(3) Scoring of spore colonies revealed that *gic1 gic2 bni1* triple mutants are variably sick either at all temperatures, at ≥33°C only or at ≥35°C only. The strain used for this experiment exhibited growth defect at ≥33°C. However, when cells were frozen and subsequently restreaked for use in this experiment, the severity of the growth defect was lost. Similar observation was made for *gic1 gic2 spa2* triple mutants, which were sick at ≥35°C, but apparently grew well after being frozen and restreaked for use in this experiment.

(4) Scoring of spore colonies revealed that *gic1 gic2 est2* triple mutants were sick at ≥35°C. These cells were frozen and subsequently restreaked for use in this experiment. The severe growth defect seen in this figure could possibly be due to the senescent phenotype of delayed inviability normally observed in *est2* cells.

(5) Synthetic sick phenotypes for *gic1 gic2 msb1* (Ts- at ≥35°C), *gic1 gic2 hse1* (Ts- at ≥35°C), *gic1 gic2 sec66*, (Ts- at ≥35°C), *gic1 gic2 vps17* (Ts- at ≥35°C), and *gic1 gic2 ygr151c* (Ts- at ≥33°C) are not shown.

(6) The ORF *YGR151C* is annotated as a dubious ORF in the *Saccharomyces* Genome Database and is entirely embedded within another ORF, *YGR152C*, which encodes Rsr1. Since mutation in *rsr1* is confirmed to show synthetic interaction with *gic1 gic2*, it is likely that the interaction seen in *gic1 gic2 ygr151c* cells is actually due to *gic1 gic2 rsr1*. Likewise, *YGR228W* is annotated as a dubious ORF and is embedded within the *SMI1* ORF. Therefore, the *gic1 gic2 ygr228w* interaction may actually be due to *gic1 gic2 smi1* interaction.

The strains used for this experiment include CCY1518-1A (wild-type), CCY1551-8B (*gic1 gic2*), CCY1590-3B (*axl2*), CCY1608-6A (*gic1 gic2 axl2*), CCY1601-10C (*bni1*), CCY1601-11C (*gic1 gic2 bni1*), CCY1602-1C (*bud6*), CCY1602-5A (*gic1 gic2 bud6*), CCY1594-3B (*cla4*), CCY1603-7A (*gic1 gic2 cla4*), CCY1595-3B (*msb3*), CCY1604-6D (*gic1 gic2 msb3*), CCY1618-2B (*nbp2*), CCY1661-3A (*gic1 gic2 nbp2*), CCY1596-4A (*pea2*), CCY1605-3A (*gic1 gic2 pea2*), CCY1606-5B (*rsr1*), CCY1606-11A (*gic1 gic2 rsr1*), CCY1598-1D (*spa2*), CCY 1609-5A (*gic1 gic2 spa2*), CCY1599-1A (*ssd1*), CCY1607-2D (*gic1 gic2 ssd1*), CCY1635-1B (*swi4*), CCY1651-2A (*gic1 gic2 swi4*), CCY1516-1D (*cap1*), CCY1585-4B (*gic1 gic2 cap1*), CCY1517-2C (*cap2*), CCY1586-6C (*gic1 gic2 cap2*), CCY1532-1A (*smi1*), CCY1569-5D (*gic1 gic2 smi1*), CCY1617-1B (*est2*), CCY1642-8D (*gic1 gic2 est2*), CCY1523-1D (*ilm1*), CCY1554-4A (*gic1 gic2 ilm1*), CCY1525-3C (*las21*), CCY1556-5A (*gic1 gic2 las21*), CCY1662-1C (*sur4*), CCY1662-1A (*gic1 gic2 sur4*), CCY1533-3C (*sur7*), CCY1561-8B (*gic1 gic2 sur7*), CCY1548-2C (*ypl144w*), CCY1567-1C (*gic1 gic2 ypl144w*), CCY1649-16C (*nem1*), CCY1649-13B (*gic1 gic2 nem1*), CCY1542-1C (*ygr228w*), CCY1574-6B (*gic1 gic2 ygr228w*), CCY1546-4A (*ylr374c*), CCY1575-2B (*gic1 gic2 ylr374c*), CCY1627-1D (*ymr124w*), CCY1652-2A (*gic1 gic2 ymr124w*), CCY1559-21B (*pre9*), CCY1559-1C (*gic1 gic2 pre9*), CCY1547-4A (*vam10*), CCY1587-7C (*gic1 gic2 vam10*), CCY1625-1C (*erv14*), CCY1643-4B (*gic1 gic2 erv14*), CCY1571-14A (*ypt6*), CCY1571-5D (*gic1 gic2 ypt6*), CCY1530-8A (*ric1*) and CCY1654-4B (*gic1 gic2 ric1*).

With the exception of the *pea2* (CCY1596-4A), *nbp2* (CCY1618-2B), *gic1 gic2 rsr1* (CCY1606-11A), *gic1 gic2 ypl144w* (CCY1567-1C), and *gic1 gic2 ymr124w* (CCY1652-2A) strains, all strains used in this experiment were *MAT*α.

4.3 DISCUSSION

Synthetic interactors of *gic1 gic2* mutations that function in the polarized growth process

Many of the mutations that interact synthetically with *gic1 gic2* define genes, which are implicated in processes that encompass polarized growth, including regulation of the actin cytoskeleton. *AXL2*, *BNI1*, *BUD6*, *CAP1*, *CAP2*, *CLA4*, *MSB1*, *MSB3*, *PEA2*, *RSR1*, *SMI1, SPA2* and *SWI4* have well documented functions in polarized growth (see Introduction). *ILM1, NBP2*, *PRE9, SUR4* and *SUR7* have also been linked to polarized growth, although how they do so is less clear.

Nbp2 was originally identified as a Nap1 binding protein that is involved in the process of nucleosome assembly (Shimizu et al., 2000). However, *nbp2* mutation also exhibits synthetic lethal interactions with mutations in *BNI1*, *CAP1*, *CAP2* and *SMI1* (Tong et al., 2001). All of these four genes are involved in polarized growth and they have also been identified as synthetic interactors of *gic1 gic2* mutations in this study. *PRE9*, encodes the only non-essential subunit of the 20S proteasome (Velichutina et al., 2004). *pre9* mutation is synthetic lethal with *cla4* (Goehring et al., 2003). *ILM1* is implicated in energy metabolism (Entian et al., 1999). *ilm1* mutation is synthetic lethal with *chs3*, *chs4*, *fks1* and *smi1* (Tong et al., 2004). All four of these mutations affect the process of cell wall biosynthesis (Douglas et al., 1994; Hong et al., 1994; Shaw et al., 1991; Trilla et al., 1997).

Some of the genes involved in lipid metabolism also appear to have roles in the control of polarized growth. For example, Sur4 is an endoplasmic reticular protein (David et al., 1998) that is known to have a fatty acid elongase activity and is involved in sphingolipid biosynthesis (Oh et al., 1997). Mutation in *SUR4* suppresses mutation in *RVS161*, which is involved in the process of actin organization (Balguerie et al., 2002). Similarly, *SUR7*, which encodes an integral

membrane protein (Navarre et al., 2002) that is involved in maintaining the normal sphingolipid content of the yeast plasma membrane (Young et al., 2002). It also functions as a multi-copy suppressor of *rvs167* mutation (Sivadon et al., 1997b). One speculation to explain the potential link between lipid metabolism and polarized growth could be that intermediates of sphingolipid metabolism may serve as cellular signals and modulate the yeast actin cytoskeleton.

Gic1 and Gic2 may functionally interact with multi-protein complexes

If the *gic1 gic2* mutations exhibit synthetic genetic interaction with a mutation that inactivates one subunit of a multiprotein complex, it is likely that the *gic1 gic2* mutations would interact similarly with other mutations that inactivate other subunits of this complex, assuming that inactivation of any single subunit leads to inactivation of the entire complex. A common pattern of genetic interaction would also be expected for mutations that inactivate different steps of a functional pathway. Results from my SGA analysis are consistent with these expectations.

The polarisome complex

Bni1, Spa2, Pea2 and Bud6 constitute a 12S polarisome complex that is believed to function as an apical scaffold for keeping Cdc24-Cdc42 complex clustered at sites of polarized growth (Pruyne and Bretscher, 2000b). The available literature suggests that the polarisome links Rho-type GTPase signaling to actin filament assembly. In this context, the formin, Bni1, appears to play a central role as it binds to the activated Rho-type GTPases Cdc42, Rho1, Rho3, and Rho4 as well as to the other components of the polarisome, such as Bud6 and Spa2 (Evangelista et al., 1997; Kohno et al., 1996). Bni1 directly participates in the nucleation of actin filaments (Pruyne et al., 2002; Sagot et al., 2002) and the binding of Bud6 to Bni1 is important for this process (Moseley et al., 2004).

Polarized docking sites for Bni1 and Bud6 are provided by the other polarisome components, such as Spa2 and Pea2, which also localize at sites of active growth (Fujiwara et al., 1998; Sheu et al., 1998; Valtz and Herskowitz, 1996). In this manner, polarisome proteins are required for the apical organization of actin.

In the absence of polarisome proteins, buds grow as spheres rather than as ellipsoids. Bud elongation during filamentous growth is blocked, and mating projections are depolarized, resulting in short, broadened projections (Amberg et al., 1997; Chenevert et al., 1994). Polarisome mutants also exhibit widened mother-bud necks, suggesting that initial bud emergence is improperly focused in these mutants, and occurs from a larger area of the cell surface than in wild-type cells (Zahner et al., 1996). Thus, polarisome proteins apparently have important roles during early periods of apical growth.

None of the genes encoding polarisome proteins is essential. However, mutation in each showed synthetic growth interaction with *gic1 gic2* double mutations (Figure 4.6 and Figure 4.6 legend note#3). Jaquenoud et al. (2000) previously reported synthetic interaction of *gic2* with *bni1*, *bud6* and *spa2*. However, I did not observe any synthetic interaction between the polarisome mutants and *gic1* or *gic2* single mutants. Like polarisome proteins, Gic1 and Gic2 are known to be specifically required at the time of bud emergence. Synthetic interactions of *gic2* with *bni1*, *bud6* and *spa2*, as well as co-fractionation of Gic2 with Bud6 and Spa2 (Jaquenoud and Peter, 2000) and direct binding of Gic1 to Bud6 (Jaquenoud and Peter, 2000) and Spa2 (Erfei Bi, personal communication) suggest that the Gic proteins interact with polarisome proteins. Furthermore, activated Cdc42 and the Gic proteins are required for the localization of Bni1 and Bud6 at the incipient bud site (Jaquenoud and Peter, 2000). Taken together, Gic1 and Gic2 seem to collaborate intimately with the polarisome proteins during polarized cell growth and they may serve as adapters to link activated Cdc42 to the polarisome complex.

The Ric1-Rgp1-Ypt6 complex

Ypt6 is a homolog of mammalian Rab6 GTPase (Li and Warner, 1996). It functions with Ric1 and Rgp1 to regulate the retrograde pathway of transport from endosomes to the trans-Golgi network (Bensen et al., 2001). Ric1 and Rgp1 bind to each other at 1:1 stoichiometry and they function as a GEF to catalyze nucleotide exchange on the Ypt6 GTPase, thus activating it at the Golgi membrane. Accordingly, both Ric1 and Rgp1 localize to the late Golgi compartment. Ypt6 also localizes to the same cellular compartment in a Ric1- and Rgp1-dependent manner (Siniossoglou et al., 2000). Besides their similar localization pattern, deletions of *RIC1* and *YPT6* generate the same phenotype and *ric1Δ ypt6Δ* double mutant does not exhibit an additive phenotype (Bensen et al., 2001). Furthermore, a 2μ *YPT6*-plasmid can complement the defect of *ric1Δ* mutant but not vice-versa. Taken together, it is clear that Ric1, Rgp1 and Ypt6 function intimately together.

The *gic1 gic2* mutations showed positive synthetic interaction with both *ric1* and *ypt6* mutations (Figure 4.6), suggesting that the functions of Ric1/Ypt6 and Gic1/2 may overlap closely. One way to interpret this result is to speculate that the Gic proteins, like Ric1, Rgp1 and Ypt6, may have direct or indirect role in the retrograde pathway of transport from endosome to the trans-Golgi network.

An alternate way to interpret this result is to propose that Ric1 and Ypt6 may be involved in the process of actin organization. In support of this conjecture, both *ypt6Δ* and *ric1Δ* are known to be synthetic lethal with *imh1Δ* (Siniossoglou et al., 2000; Tsukada et al., 1999). *IMH1* encodes a non-essential Golgi-associated coiled-coil protein that is involved in vesicular transport. Recently, Imh1 has been purified in a complex that contains Bni1 and several components of the Arp2/3 complex (Ho et al., 2002). Since Bni1 and the Arp2/3 complex are involved in the process of actin filament assembly (Goode and

Rodal, 2001; Pruyne et al., 2002; Sagot et al., 2002), it is plausible that Imh1 may also participate in the actin organization process. By extrapolation of their synthetic genetic interaction with *IMH1*, *RIC1* and *YPT6* may also function in the actin-related process. Results of other SGA analyses show that *ric1Δ* is synthetic lethal with *bud14Δ* and *rga1Δ*, whereas *ypt6Δ* is synthetic lethal with *bni1Δ*, *bud14Δ* and *bem4Δ* (Tong et al., 2001; Tong et al., 2004). Since Bem4, Bni1, Bud14 and Rga1 are all involved in processes related to polarized growth, these interactions further support the idea that Ric1 and Ypt6 may function in polarized growth.

Table 4.5 Common synthetic interactors of *gic1 gic2*, *ypt6* and *ric1* mutations.

	gic1 gic2[a]	*ric1*	*ypt6*
bni1	✓	-	✓*
erv14	✓	✓	✓
est2	✓	✓	✓
nbp2	✓	✓	✓
nem1	✓	✓	✓
opi3	✓	✓	✓
smi1	✓	✓	✓
vam10	✓	✓	✓

*(Tong et al., 2001)
[a] interaction identified in this study
Other interactions are reported in Tong et al. (Tong et al., 2004).

In addition to its role in the retrograde transport, Ric1 is also implicated in vacuolar biogenesis. *ric1Δ* cells demonstrate vacuolar fragmentation (Siniossoglou et al., 2000). Like *ric1*, mutations in *VAM10* and *ERV14*, both of

which are implicated in vacuolar organization and biogenesis (Kato and Wickner, 2003; Powers and Barlowe, 2002), also show synthetic interactions with *gic1 gic2* cells. Finally, several synthetic interactors of *gic1 gic2* mutants identified from this study are also identified as synthetic lethal interactors of *ypt6* and *ric1* mutations (Table 4.5) and further underscore the potential significance of the genetic interaction between the *GIC*s, *YPT6* and *RIC1* discovered in this study. It is noteworthy that the stability and function of Ric1 and Rgp1, are interdependent (Siniossoglou et al., 2000), yet the *rgp1* mutation did not show up as a synthetic interactor of *gic1 gic2* in our SGA analysis. Neither did *rgp1* show synthetic interactions with the other synthetic interactors of *gic1 gic2*, *ric1* and *ypt6* mutations listed in Table 4.5.

In summary, the identification of synthetic interactors of *gic1 gic2* mutations appear to function in many diverse processes and suggest that Gic1 and Gic2 may link the signaling from Cdc42 GTPase to different cellular activities, such as actin filament assembly, cell wall biosynthesis, vesicular transport, secretion, organelle biogenesis, etc., all of which may need to be executed in unison during polarized growth.

Following up this study

Further experiments are clearly needed to comprehend the functional significance of the genetic interactions described above. Recapitulating the positive synthetic interactions in our laboratory strain background bearing an *ssd1-d* allele should yield stronger phenotypes. It is very likely that at least some of these interactions will be truly synthetic lethal in the *ssd1-d* background (e.g., *gic1 gic2 cla4*). Further, the morphological defect exhibited by *gic1 gic2 ssd1-d* cells is also more dramatic than that observed for *gic1 gic2 SSD1-v(1)* cells. Thus, morphological examination of *gic1 gic2 x* cells will further point to the functional pathway that is likely compromised in the combined absence of the *GIC1*, *GIC2*

and *X* genes. Localization of X proteins in *gic1 gic2* background and the converse experiment of studying Gic1 or Gic2 localization in *x* mutant background will also be a reasonable approach to gain further insights into the basis of these synthetic interactions observed.

Although the potential functional connections between Gic1, Gic2 and Ypt6, Ric1 discussed above are based mainly on genetic and circumstantial evidences and are thus speculative at this time, they certainly warrant further investigation. To this end, one can ask if the Gic proteins are involved in the process of vesicular trafficking by examining *gic1 gic2* cells for the mutant phenotypes demonstrated by *ric1* and *ypt6* mutants, such as partial mislocalization of vacuolar carboxypeptidase Y and mislocalization of late Golgi protein Kex2 to the vacuole. Alternately, *ric1* and *ypt6* cells can be examined for bud-site selection defect and/or actin polarization defect that are typical of polarity mutants. The interaction between the *GIC*s and *RGP1*, a third member of the *RIC1/YPT6* pathway must be checked. The positive genetic and cytological leads should then provide a premise for testing the biochemical interaction between the Gic proteins and components of the Ric1-Ypt6 complex. As suggested for the polarisome function, Gic1 and Gic2 proteins may have an adapter-like role for the establishment of Ric1-Ypt6 complex or for coordinating the activity of this complex with that of Cdc42 GTPase. To address this possibility, one can ask if the Ric1-Ypt6 complex formation and function is dependent on the presence of Gic proteins.

CHAPTER 5

Summary and conclusions

Gic1 and Gic2 function as effectors of the Cdc42 GTPase. Both of these proteins bind to the GTP-bound form of Cdc42 via their CRIB domain and mediate the organization of the actin cytoskeleton during periods of polarized cell growth. However, the molecular mechanism underlying their function is unclear. The main objectives of this thesis were to obtain greater insight into the function of Gic1 and Gic2 as well as to further explore the process of polarized growth. To address these objectives, I used two genetic approaches - multi-copy suppression screen and genome-wide synthetic genetic array analysis - to identify functionally interacting partners of Gic1 and Gic2.

5.1 MULTI-COPY SUPPRESSORS OF *gic1 gic2* MUTATIONS

The goal for the multi-copy suppressor screen was to identify genes that function downstream of Gic1 and Gic2 or in a parallel pathway that is functionally redundant with that mediated by Gic1 and Gic2. Analyses of the suppressor genes that complement the phenotypic defects of the *gic1 gic2* mutants revealed that many of them are genes that have well-recognized functions in polarized cell growth. Interestingly, two pairs of structurally related genes including *VHS2-MLF3* and *MGC1-TOS2* that have no previously known functions were also identified from the screen. The major findings from the functional characterization studies of these four genes are as follows.

VHS2 and *MLF3* function together in the process of polarized growth primarily via their role in the organization of the actin cytoskeleton. This conclusion is based on the morphological and actin cytoskeleton organization defects observed in *vhs2 mlf3* cells. I have shown that *VHS2* and *MLF3* are functionally redundant with *GIC1* and *GIC2*. This conclusion is based on the

reciprocal suppression of growth defect observed when the dosage of either member of one gene pair is increased in cells that lack the other gene pair. The temperature-sensitive growth defect caused by the deletion of either gene pair is additive since cells lacking all four genes are more temperature-sensitive. The phenotypic defects of *vhs2 mlf3* mutant are not identical to those of *gic1 gic2* mutant. For example, *vhs2 mlf3* cells show cell lysis defect that can be rescued by 1 M sorbitol, whereas *gic1 gic2* cells do not exhibit cell lysis and the growth defect of *gic1 gic2* cells cannot be rescued by 1 M sorbitol. On the other hand, *vhs2 mlf3* cells do not show obvious bud-site selection defect that is seen in *gic1 gic2* cells. Therefore, it is likely that polarized organization of the actin cytoskeleton is a common function shared by *VHS2-MLF3* and *GIC1-GIC2*, and this common function is likely the basis for the reciprocal suppression seen between these genes.

The Pho85-Pcl1/2-Rvs-mediated pathway of actin organization is parallel to that mediated by the Cdc42 GTPase (Lenburg and O'Shea, 2001; Moffat and Andrews, 2004). If Vhs2 and Mlf3 are not part of the linear pathway mediated by Gic1 and Gic2, are they part of the Pho85-Pcl1/2-Rvs-mediated pathway of actin organization? My genetic studies showed that the *rvs161* and *rvs167* mutations exacerbate the growth defect of *vhs2 mlf3* cells. This result suggested that the function of Vhs2-Mlf3 and that of the Pho85-Pcl1/2-Rvs-mediated pathway might be redundant. Since *pho85*, *pcl1*, *pcl2*, *rvs161* and *rvs167* mutants exhibit endocytosis defect and bud-site selection defects, whereas *vhs2 mlf3* cells do not exhibit any such defects, it may be the common function of Vhs2-Mlf3 and the Pho85-Pcl1/2-Rvs-mediated pathway in the organization of actin cytoskeleton that is responsible for the genetic interaction observed between *vhs2 mlf3* and *rvs* mutations. Consistent with this idea, the actin organization defect of *vhs2 mlf3* cells is exacerbated by the deletion of *RVS167*. The proposed redundancy between the Vhs2/Mlf3- and Pho85-Pcl1/2-Rvs-mediated pathways for actin

cytoskeleton organization is also consistent with the result that overexpression of *PCL1* can complement the growth defect of *vhs2 mlf3* cells.

Since *vhs2 mlf3* cells exhibit cell wall defect and undergo cell lysis, most likely as a consequence of the actin organization defect, it is reasonable to speculate that Vhs2 and Mlf3 function in a process that coordinates polarized actin cytoskeleton with polarized secretion of cell wall material. Further experiments that show alteration in the cell wall structure and occurrence of cell lysis at sites of active growth in *vhs2 mlf3* cells can support this hypothesis.

Functional characterization of Mgc1 and Tos2 revealed that both these proteins localize at sites of polarized growth (i.e., at the bud tip and at the site of cell division). The role of Mgc1 and Tos2 in apical polarization is evident from the observation that overexpression of either gene results in cells with elongated buds. Additionally, Mgc1 and Tos2 also have a negative function in cytokinesis. This conclusion is based on the observation that overexpression of either gene results in cells with a 'bud from a bud' morphology where the first bud fails to separate from its mother cell. Mislocalization of septin and less than perfect re-polarization of the actin cytoskeleton at the bud neck in such morphologically abnormal cells further supports the role of Mgc1 and Tos2 in cytokinesis. Finally, the genetic interaction observed between *MGC1* and *CYK2*, which is involved in cytokinesis, is consistent with the finding that *MGC1* has a role in cytokinesis.

Although the function of Gic1 and Gic2 in cytokinesis is not well defined, the synthetic lethal interaction between *gic1 gic2* and *cla4* mutations where the cytokinesis defect of *cla4* single mutation is exacerbated (Chen et al., 1997), together with the reported 2-hybrid interactions of both Gic1 and Gic2 with Cla4 and the Cdc12 septin (Drees et al., 2001) imply that Gic1 and Gic2 also function in cytokinesis.

5.2 MUTATIONS THAT ENHANCE THE GROWTH DEFECT OF *gic1 gic2* CELLS

The goal of the synthetic genetic array analysis was to identify genes whose function(s) overlaps with that of *GIC1* and *GIC2*. These genes might function in *GIC*-independent pathways of polarized growth or they might participate in other cellular processes that have not been associated with *GIC1* and *GIC2*. Consistent with this reasoning, many genes (*AXL2*, *BNI1*, *BUD6*, *CAP1*, *CAP2*, *CLA4, MSB1*, *MSB3, PEA2*, *RSR1*, *SMI1, SPA2* and *SWI4*) that have well documented functions in polarized growth were identified from this screen. In addition, other genes (*ILM1, NBP2*, *PRE9, SUR4* and *SUR7*) that have been indirectly linked to polarized cell growth were also identified in this study. Further analyses of the synthetic interaction of *gic1 gic2* with mutations in these genes should clarify the role of these genes in polarized growth.

Interestingly, genes involved in vacuolar organization and biogenesis (e.g., *ERV14* and *VAM10*) as well as those involved in retrograde transport from endosomes to the trans-Golgi network (e.g., *RIC1* and *YPT6*) were also identified in this screen. Several synthetic interactors of *gic1 gic2* mutations identified in the present study (including *erv14*, *est2*, *nbp2*, *nem1*, *opi3*, *smi1* and *vam10*) have also been found as synthetic interactors of *ric1* and *ypt6* mutations (Tong et al., 2001; Tong et al., 2004). Together, this implies that the functions of *GIC1-GIC2* and *RIC1-YPT6* might overlap very closely. Although the evidences are circumstantial, they point to a potentially strong functional link between *GIC1-GIC2* and *RIC1-YPT6*. It is plausible that *RIC1* and *YPT6* may have a more direct role in actin organization via their functional interaction with *GIC1* and *GIC2*. Conversely, it is also possible that *GIC1* and *GIC2* may have a previously unappreciated role in vesicular transport via their functional interaction with *RIC1* and *YPT6*. Further analyses of the synthetic interactions found in this study

will clarify potential links between the Cdc42 signaling pathway and diverse cellular processes, including actin cytoskeleton organization, cell wall biogenesis, vesicular transport, secretion and organelle biogenesis. All of these processes need to be executed coordinately during polarized cell growth.

References

Adamo, J. E., Moskow, J. J., Gladfelter, A. S., Viterbo, D., Lew, D. J., and Brennwald, P. J. (2001). Yeast Cdc42 functions at a late step in exocytosis, specifically during polarized growth of the emerging bud. J Cell Biol *155*, 581-592.

Adams, A. E., Johnson, D. I., Longnecker, R. M., Sloat, B. F., and Pringle, J. R. (1990). CDC42 and CDC43, two additional genes involved in budding and the establishment of cell polarity in the yeast Saccharomyces cerevisiae. J Cell Biol *111*, 131-142.

Adams, A. E. M., and Pringle, J. R. (1984). Relationship of actin and tubulin distribution in wild-type and morphogenetic mutant *Saccharomyces cerevisiae*. J Cell Biol *98*, 934-945.

Albert, S., and Gallwitz, D. (1999). Two new members of a family of Ypt/Rab GTPase activating proteins. Promiscuity of substrate recognition. J Biol Chem *274*, 33186-33189.

Albert, S., and Gallwitz, D. (2000). Msb4p, a protein involved in Cdc42p-dependent organization of the actin cytoskeleton, is a Ypt/Rab-specific GAP. Biol Chem *381*, 453-456.

Altman, R., and Kellogg, D. (1997). Control of mitotic events by Nap1 and the Gin4 kinase. J Cell Biol *138*, 119-130.

Amberg, D. C., Zahner, J. E., Mulholland, J. W., Pringle, J. R., and Botstein, D. (1997). Aip3p/Bud6p, a yeast actin-interacting protein that is involved in morphogenesis and the selection of bipolar budding sites. Mol Biol Cell *8*, 729-753.

Andrews, B., and Measday, V. (1998). The cyclin family of budding yeast: abundant use of a good idea. Trends Genet *14*, 66-72.

Ayscough, K. R., Stryker, J., Pokala, N., Sanders, M., Crews, P., and Drubin, D. G. (1997). High rates of actin filament turnover in budding yeast and roles for actin in establishment and maintenance of cell polarity revealed using the actin inhibitor latrunculin-A. J Cell Biol *137*, 399-416.

Aznar, S., Fernandez-Valeron, P., Espina, C., and Lacal, J. C. (2004). Rho GTPases: potential candidates for anticancer therapy. Cancer Lett *206*, 181-191.

Balguerie, A., Bagnat, M., Bonneu, M., Aigle, M., and Breton, A. M. (2002). Rvs161p and sphingolipids are required for actin repolarization following salt stress. Eukaryot Cell *1*, 1021-1031.

Balguerie, A., Sivadon, P., Bonneu, M., and Aigle, M. (1999). Rvs167p, the budding yeast homolog of amphiphysin, colocalizes with actin patches. J Cell Sci *112 (Pt 15)*, 2529-2537.

Barral, Y., Mermall, V., Mooseker, M. S., and Snyder, M. (2000). Compartmentalization of the cell cortex by septins is required for maintenance of cell polarity in yeast. Mol Cell *5*, 841-851.

Barral, Y., Parra, M., Bidlingmaier, S., and Snyder, M. (1999). Nim1-related kinases coordinate cell cycle progression with the organization of the peripheral cytoskeleton in yeast. Genes Dev *13*, 176-187.

Bauer, F., Urdaci, M., Aigle, M., and Crouzet, M. (1993). Alteration of a yeast SH3 protein leads to conditional viability with defects in cytoskeletal and budding patterns. Mol Cell Biol *13*, 5070-5084.

Bender, A. (1993). Genetic evidence for the roles of the bud-site-selection genes BUD5 and BUD2 in control of the Rsr1p (Bud1p) GTPase in yeast. Proc Natl Acad Sci U S A *90*, 9926-9929.

Bender, A., and Pringle, J. (1991). Use of a screen for synthetic lethal and multicopy suppressee mutants to identify two new genes involved in morphogenesis in *Saccharomyces cerevisiae*. Mol Cell Biol *11*, 1295-1305.

Bender, A., and Pringle, J. R. (1989). Multicopy suppression of the *cdc24* budding defect in yeast by *CDC42* and three newly identified genes including the *ras*-related gene *RSR1*. Proc Natl Acad Sci USA *86*, 9976-9980.

Bender, A., and Pringle, J. R. (1992). A ser/thr-rich multicopy suppressor of a *cdc24* bud emergence defect. Yeast *8*, 315-323.

Bensen, E. S., Yeung, B. G., and Payne, G. S. (2001). Ric1p and the Ypt6p GTPase function in a common pathway required for localization of trans-Golgi network membrane proteins. Mol Biol Cell *12*, 13-26.

Bi, E., Chiavetta, J. B., Chen, H., Chen, G. C., Chan, C. S., and Pringle, J. R. (2000). Identification of novel, evolutionarily conserved Cdc42p-interacting proteins and of redundant pathways linking Cdc24p and Cdc42p to actin polarization in yeast. Mol Biol Cell *11*, 773-793.

Bi, E., Maddox, P., Lew, D. J., Salmon, E. D., McMillan, J. N., Yeh, E., and Pringle, J. R. (1998). Involvement of an actomyosin contractile ring in Saccharomyces cerevisiae cytokinesis. J Cell Biol *142*, 1301-1312.

Bon, E., Recordon-Navarro, P., Durrens, P., Iwase, M., Toh, E. A., and Aigle, M. (2000). A network of proteins around Rvs167p and Rvs161p, two proteins related to the yeast actin cytoskeleton. Yeast *16*, 1229-1241.

Breton, A. M., and Aigle, M. (1998). Genetic and functional relationship between Rvsp, myosin and actin in Saccharomyces cerevisiae. Curr Genet *34*, 280-286.

Breton, A. M., Schaeffer, J., and Aigle, M. (2001). The yeast Rvs161 and Rvs167 proteins are involved in secretory vesicles targeting the plasma membrane and in cell integrity. Yeast *18*, 1053-1068.

Bretscher, A. (2003). Polarized growth and organelle segregation in yeast: the tracks, motors, and receptors. J Cell Biol *160*, 811-816.

Brown, J. L., Jaquenoud, M., Gulli, M. P., Chant, J., and Peter, M. (1997). Novel Cdc42-binding proteins Gic1 and Gic2 control cell polarity in yeast. Genes Dev *11*, 2972-2982.

Burridge, K., and Wennerberg, K. (2004). Rho and Rac take center stage. Cell *116*, 167-179.

Butty, A. C., Perrinjaquet, N., Petit, A., Jaquenoud, M., Segall, J. E., Hofmann, K., Zwahlen, C., and Peter, M. (2002). A positive feedback loop stabilizes the guanine-nucleotide exchange factor Cdc24 at sites of polarization. Embo J *21*, 1565-1576.

Cabib, E., Drgonova, J., and Drgon, T. (1998). Role of small G proteins in yeast cell polarization and wall biosynthesis. Annu Rev Biochem *67*, 307-333.

Carlson, M., and Botstein, D. (1982). Two differentially regulated mRNAs with different 5' ends encode secreted with intracellular forms of yeast invertase. Cell *28*, 145-154.

Carroll, C. W., Altman, R., Schieltz, D., Yates, J. R., and Kellogg, D. (1998). The septins are required for the mitosis-specific activation of the Gin4 kinase. J Cell Biol *143*, 709-717.

Casamayor, A., and Snyder, M. (2002). Bud-site selection and cell polarity in budding yeast. Curr Opin Microbiol *5*, 179-186.

Caviston, J. P., Longtine, M., Pringle, J. R., and Bi, E. (2003). The role of Cdc42p GTPase-activating proteins in assembly of the septin ring in yeast. Mol Biol Cell *14*, 4051-4066.

Chang, F., and Peter, M. (2003). Yeasts make their mark. Nat Cell Biol *5*, 294-299.
Chant, J. (1999). Cell polarity in yeast. Annu Rev Cell Dev Biol *15*, 365-391.

Chant, J., and Herskowitz, I. (1991). Genetic control of bud site selection in yeast by a set of gene products that constitute a morphogenetic pathway. Cell *65*, 1203-1212.

Chant, J., Mischke, M., Mitchell, E., Herskowitz, I., and Pringle, J. R. (1995). Role of Bud3p in producing the axial budding pattern of yeast. J Cell Biol *129*, 767-778.

Chant, J., and Pringle, J. R. (1995). Patterns of bud-site selection in the yeast Saccharomyces cerevisiae. J Cell Biol *129*, 751-765.

Chen, C. Y., and Graham, T. R. (1998). An arf1Delta synthetic lethal screen identifies a new clathrin heavy chain conditional allele that perturbs vacuolar protein transport in Saccharomyces cerevisiae. Genetics *150*, 577-589.

Chen, G. C., Kim, Y. J., and Chan, C. S. (1997). The Cdc42 GTPase-associated proteins Gic1 and Gic2 are required for polarized cell growth in Saccharomyces cerevisiae. Genes Dev *11*, 2958-2971.

Chenevert, J., Valtz, N., and Herskowitz, I. (1994). Identification of genes required for normal pheromone-induced cell polarization in Saccharomyces cerevisiae. Genetics *136*, 1287-1296.

Christianson, T. W., Sikorski, R. S., Dante, M., Shero, J. H., and Hieter, P. (1992). Multifunctional yeast high-copy-number shuttle vectors. Gene *110*, 119-122.

Colwill, K., Field, D., Moore, L., Friesen, J., and Andrews, B. (1999). In vivo analysis of the domains of yeast Rvs167p suggests Rvs167p function is mediated through multiple protein interactions. Genetics *152*, 881-893.

Corpet, F. (1988). Multiple sequence alignment with hierarchical clustering. Nucleic Acids Res *16*, 10881-10890.

Costigan, C., Gehrung, S., and Snyder, M. (1992). A synthetic lethal screen identifies SLK1, a novel protein kinase homolog implicated in yeast cell morphogenesis and cell growth. Mol Cell Biol *12*, 1162-1178.

Cross, F., Hartwell, L. H., Jackson, C., and Konopka, J. B. (1988). Conjugation in Saccharomyces cerevisiae. Annu Rev Cell Biol *4*, 429-457.

Cross, F. R. (1990). Cell cycle arrest caused by CLN gene deficiency in Saccharomyces cerevisiae resembles START-I arrest and is independent of the mating-pheromone signalling pathway. Mol Cell Biol *10*, 6482-6490.

Cvrckova, F., De Virgilio, C., Manser, E., Pringle, J. R., and Nasmyth, K. (1995). Ste20-like protein kinases are required for normal localization of cell growth and for cytokinesis in budding yeast. Genes Dev *9*, 1817-1830.

Cvrckova, F., and Nasmyth, K. (1993). Yeast G1 cyclins CLN1 and CLN2 and a GAP-like protein have a role in bud formation. Embo J *12*, 5277-5286.

David, D., Sundararabu, S., and Gerst, J. E. (1998). Involvement of long chain fatty acid elongation in the trafficking of secretory vesicles in yeast. J Cell Biol *143*, 1167-1182.

Desfarges, L., Durrens, P., Juguelin, H., Cassagne, C., Bonneu, M., and Aigle, M. (1993). Yeast mutants affected in viability upon starvation have a modified phospholipid composition. Yeast *9*, 267-277.

Di Como, C. J., Chang, H., and Arndt, K. T. (1995). Activation of CLN1 and CLN2 G1 cyclin gene expression by BCK2. Mol Cell Biol *15*, 1835-1846.

Douglas, C. M., Foor, F., Marrinan, J. A., Morin, N., Nielsen, J. B., Dahl, A. M., Mazur, P., Baginsky, W., Li, W., el-Sherbeini, M., and et al. (1994). The

Saccharomyces cerevisiae FKS1 (ETG1) gene encodes an integral membrane protein which is a subunit of 1,3-beta-D-glucan synthase. Proc Natl Acad Sci U S A *91*, 12907-12911.

Drees, B. L., Sundin, B., Brazeau, E., Caviston, J. P., Chen, G.-C., Guo, W., Kozminski, K. G., Lau, M. W., Moskow, J. J., Tong, A., *et al.* (2001). A protein interaction map for cell polarity development. J Cell Biol *154*, 549-571.

Drgonova, J., Drgon, T., Roh, D. H., and Cabib, E. (1999). The GTP-binding protein Rho1p is required for cell cycle progression and polarization of the yeast cell. J Cell Biol *146*, 373-387.

Drgonova, J., Drgon, T., Tanaka, K., Kollar, R., Chen, G. C., Ford, R. A., Chan, C. S., Takai, Y., and Cabib, E. (1996). Rho1p, a yeast protein at the interface between cell polarization and morphogenesis. Science *272*, 277-279.

Drubin, D. G., and Nelson, W. J. (1996). Origins of cell polarity. Cell *84*, 335-344.

Dulic, V., Egerton, M., Elguindi, I., Raths, S., Singer, B., and Riezman, H. (1991). Yeast endocytosis assays. Methods Enzymol *194*, 697-710.

Eby, J. J., Holly, S. P., van Drogen, F., Grishin, A. V., Peter, M., Drubin, D. G., and Blumer, K. J. (1998). Actin cytoskeleton organization regulated by the PAK family of protein kinases. Curr Biol *8*, 967-970.

Eitzen, G., Thorngren, N., and Wickner, W. (2001). Rho1p and Cdc42p act after Ypt7p to regulate vacuole docking. Embo J *20*, 5650-5656.

Entian, K. D., Schuster, T., Hegemann, J. H., Becher, D., Feldmann, H., Guldener, U., Gotz, R., Hansen, M., Hollenberg, C. P., Jansen, G., *et al.* (1999). Functional analysis of 150 deletion mutants in Saccharomyces cerevisiae by a systematic approach. Mol Gen Genet *262*, 683-702.

Epp, J. A., and Chant, J. (1997). An IQGAP-related protein controls actin-ring formation and cytokinesis in yeast. Curr Biol *7*, 921-929.

Espinoza, F. H., Ogas, J., Herskowitz, I., and Morgan, D. O. (1994). Cell cycle control by a complex of the cyclin HCS26 (PCL1) and the kinase PHO85. Science *266*, 1388-1391.

Etienne-Manneville, S., and Hall, A. (2002). Rho GTPases in cell biology. Nature *420*, 629-635.

Evangelista, M., Blundell, K., Longtine, M. S., Chow, C. J., Adames, N., Pringle, J. R., Peter, M., and Boone, C. (1997). Bni1p, a yeast formin linking cdc42p and the actin cytoskeleton during polarized morphogenesis. Science *276*, 118-122.

Evangelista, M., Klebl, B. M., Tong, A. H., Webb, B. A., Leeuw, T., Leberer, E., Whiteway, M., Thomas, D. Y., and Boone, C. (2000). A role for myosin-I in actin assembly through interactions with Vrp1p, Bee1p, and the Arp2/3 complex. J Cell Biol *148*, 353-362.

Fankhauser, C., Reymond, A., Cerutti, L., Utzig, S., Hofmann, K., and Simanis, V. (1995). The S. pombe cdc15 gene is a key element in the reorganization of F-actin at mitosis. Cell *82*, 435-444.

Faty, M., Fink, M., and Barral, Y. (2002). Septins: a ring to part mother and daughter. Curr Genet *41*, 123-131.

Finley, R. L., Jr., and Brent, R. (1994). Interaction mating reveals binary and ternary connections between Drosophila cell cycle regulators. Proc Natl Acad Sci U S A *91*, 12980-12984.

Flescher, E. G., Madden, K., and Snyder, M. (1993). Components required for cytokinesis are important for bud site selection in yeast. J Cell Biol *122*, 373-386.

Friesen, H., Murphy, K., Breitkreutz, A., Tyers, M., and Andrews, B. (2003). Regulation of the yeast amphiphysin homologue Rvs167p by phosphorylation. Mol Biol Cell *14*, 3027-3040.

Fujimura, H.-a. (1998). *Saccharomyces cerevisiae MLF3/YNL074C* gene, encoding a serine-rich protein of unknown function, determines the level of resistance to the novel immunosuppressive drug leflunomide. Biochim Biophys Acta *1442*, 415-418.

Fujita, A., Oka, C., Arikawa, Y., Katagai, T., Tonouchi, A., Kuhara, S., and Misumi, Y. (1994). A yeast gene necessary for bud-site selection encodes a protein similar to insulin-degrading enzymes. Nature *372*, 567-570.

Fujiwara, T., Tanaka, K., Mino, A., Kikyo, M., Takahashi, K., Shimizu, K., and Takai, Y. (1998). Rho1p-Bni1p-Spa2p interactions: implication in localization of

Bni1p at the bud site and regulation of the actin cytoskeleton in Saccharomyces cerevisiae. Mol Biol Cell *9*, 1221-1233.

Gao, X. D., Albert, S., Tcheperegine, S. E., Burd, C. G., Gallwitz, D., and Bi, E. (2003). The GAP activity of Msb3p and Msb4p for the Rab GTPase Sec4p is required for efficient exocytosis and actin organization. J Cell Biol *162*, 635-646.

Gietz, D., St Jean, A., Woods, R. A., and Schiestl, R. H. (1992). Improved method for high efficiency transformation of intact yeast cells. Nucleic Acids Res *20*, 1425.

Gimeno, C. J., Ljungdahl, P. O., Styles, C. A., and Fink, G. R. (1992). Unipolar cell divisions in the yeast S. cerevisiae lead to filamentous growth: regulation by starvation and RAS. Cell *68*, 1077-1090.

Gladfelter, A. S., Bose, I., Zyla, T. R., Bardes, E. S., and Lew, D. J. (2002). Septin ring assembly involves cycles of GTP loading and hydrolysis by Cdc42p. J Cell Biol *156*, 315-326.

Goehring, A. S., Mitchell, D. A., Tong, A. H., Keniry, M. E., Boone, C., and Sprague, G. F., Jr. (2003). Synthetic lethal analysis implicates Ste20p, a p21-activated potein kinase, in polarisome activation. Mol Biol Cell *14*, 1501-1516.

Goldstein, A. L., and McCusker, J. H. (1999). Three new dominant drug resistance cassettes for gene disruption in Saccharomyces cerevisiae. Yeast *15*, 1541-1553.

Goode, B. L., and Rodal, A. A. (2001). Modular complexes that regulate actin assembly in budding yeast. Curr Opin Microbiol *4*, 703-712.

Guarente, L. (1993). Synthetic enhancement in gene interaction: a genetic tool come of age. Trends Genet *9*, 362-366.

Gyuris, J., Golemis, E., Chertkov, H., and Brent, R. (1993). Cdi1, a human G1 and S phase protein phosphatase that associates with Cdk2. Cell *75*, 791-803.

Haarer, B. K., and Pringle, J. R. (1987). Immunofluorescence localization of the Saccharomyces cerevisiae CDC12 gene product to the vicinity of the 10-nm filaments in the mother-bud neck. Mol Cell Biol *7*, 3678-3687.

Harrison, J. C., Zyla, T. R., Bardes, E. S., and Lew, D. J. (2004). Stress-specific activation mechanisms for the "cell integrity" MAPK pathway. J Biol Chem *279*, 2616-2622.

Hartman, J. L. t., Garvik, B., and Hartwell, L. (2001). Principles for the buffering of genetic variation. Science *291*, 1001-1004.

Heinisch, J. J., Lorberg, A., Schmitz, H. P., and Jacoby, J. J. (1999). The protein kinase C-mediated MAP kinase pathway involved in the maintenance of cellular integrity in Saccharomyces cerevisiae. Mol Microbiol *32*, 671-680.

Helliwell, S. B., Schmidt, A., Ohya, Y., and Hall, M. N. (1998). The Rho1 effector Pkc1, but not Bni1, mediates signalling from Tor2 to the actin cytoskeleton. Curr Biol *8*, 1211-1214.

Ho, Y., Gruhler, A., Heilbut, A., Bader, G. D., Moore, L., Adams, S. L., Millar, A., Taylor, P., Bennett, K., Boutilier, K., *et al.* (2002). Systematic identification of protein complexes in Saccharomyces cerevisiae by mass spectrometry. Nature *415*, 180-183.

Hofken, T., and Schiebel, E. (2004). Novel regulation of mitotic exit by the Cdc42 effectors Gic1 and Gic2. J Cell Biol *164*, 219-231.

Holly, S. P., and Blumer, K. J. (1999). PAK-family kinases regulate cell and actin polarization throughout the cell cycle of *Saccharomyces cerevisiae*. J Cell Biol *147*, 845-856.

Hong, Z., Mann, P., Brown, N. H., Tran, L. E., Shaw, K. J., Hare, R. S., and DiDomenico, B. (1994). Cloning and characterization of KNR4, a yeast gene involved in (1,3)-beta-glucan synthesis. Mol Cell Biol *14*, 1017-1025.

Huang, D., Moffat, J., and Andrews, B. (2002). Dissection of a complex phenotype by functional genomics reveals roles for the yeast cyclin-dependent protein kinase Pho85 in stress adaptation and cell integrity. Mol Cell Biol *22*, 5076-5088.

Huh, W. K., Falvo, J. V., Gerke, L. C., Carroll, A. S., Howson, R. W., Weissman, J. S., and O'Shea, E. K. (2003). Global analysis of protein localization in budding yeast. Nature *425*, 686-691.

Imai, J., Toh-e, A., and Matsui, Y. (1996). Genetic analysis of the Saccharomyces cerevisiae RHO3 gene, encoding a rho-type small GTPase, provides evidence for a role in bud formation. Genetics *142*, 359-369.

Irazoqui, J. E., Gladfelter, A. S., and Lew, D. J. (2003). Scaffold-mediated symmetry breaking by Cdc42p. Nat Cell Biol *5*, 1062-1070.

Iyer, V. R., Horak, C. E., Scafe, C. S., Botstein, D., Snyder, M., and Brown, P. O. (2001). Genomic binding sites of the yeast cell-cycle transcription factors SBF and MBF. Nature *409*, 533-538.

Jaquenoud, M., Gulli, M. P., Peter, K., and Peter, M. (1998). The Cdc42p effector Gic2p is targeted for ubiquitin-dependent degradation by the SCFGrr1 complex. Embo J *17*, 5360-5373.

Jaquenoud, M., and Peter, M. (2000). Gic2p may link activated Cdc42p to components involved in actin polarization, including Bni1p and Bud6p (Aip3p). Mol Cell Biol *20*, 6244-6258.

Jensen, S., Geymonat, M., Johnson, A. L., Segal, M., and Johnston, L. H. (2002). Spatial regulation of the guanine nucleotide exchange factor Lte1 in Saccharomyces cerevisiae. J Cell Sci *115*, 4977-4991.

Johnson, D. I. (1999). Cdc42: An essential Rho-type GTPase controlling eukaryotic cell polarity. Microbiol Mol Biol Rev *63*, 54-105.

Johnson, D. I., and Pringle, J. R. (1990). Molecular characterization of CDC42, a Saccharomyces cerevisiae gene involved in the development of cell polarity. J Cell Biol *111*, 143-152.

Jones, J. S., and Prakash, L. (1990). Yeast Saccharomyces cerevisiae selectable markers in pUC18 polylinkers. Yeast *6*, 363-366.

Kaeberlein, M., Andalis, A. A., Liszt, G. B., Fink, G. R., and Guarente, L. (2004). Saccharomyces cerevisiae SSD1-V confers longevity by a Sir2p-independent mechanism. Genetics *166*, 1661-1672.

Kaeberlein, M., and Guarente, L. (2002). Saccharomyces cerevisiae MPT5 and SSD1 function in parallel pathways to promote cell wall integrity. Genetics *160*, 83-95.

Kamada, Y., Qadota, H., Python, C. P., Anraku, Y., Ohya, Y., and Levin, D. E. (1996). Activation of yeast protein kinase C by Rho1 GTPase. J Biol Chem *271*, 9193-9196.

Kamei, T., Tanaka, K., Hihara, T., Umikawa, M., Imamura, H., Kikyo, M., Ozaki, K., and Takai, Y. (1998). Interaction of Bnr1p with a novel Src homology 3 domain-containing Hof1p. Implication in cytokinesis in Saccharomyces cerevisiae. J Biol Chem *273*, 28341-28345.

Kang, P. J., Sanson, A., Lee, B., and Park, H. O. (2001). A GDP/GTP exchange factor involved in linking a spatial landmark to cell polarity. Science *292*, 1376-1378.

Karpova, T. S., McNally, J. G., Moltz, S. L., and Cooper, J. A. (1998). Assembly and function of the actin cytoskeleton of yeast: relationships between cables and patches. J Cell Biol *142*, 1501-1517.

Kato, M., and Wickner, W. (2003). Vam10p defines a Sec18p-independent step of priming that allows yeast vacuole tethering. Proc Natl Acad Sci U S A *100*, 6398-6403.

Kawasaki, R., Fujimura-Kamada, K., Toi, H., Kato, H., and Tanaka, K. (2003). The upstream regulator, Rsr1p, and downstream effectors, Gic1p and Gic2p, of the Cdc42p small GTPase coordinately regulate initiation of budding in Saccharomyces cerevisiae. Genes Cells *8*, 235-250.

Keleher, C. A., Redd, M. J., Schultz, J., Carlson, M., and Johnson, A. D. (1992). Ssn6-Tup1 is a general repressor of transcription in yeast. Cell *68*, 709-719.

Kim, H. B., Haarer, B. K., and Pringle, J. R. (1991). Cellular morphogenesis in the Saccharomyces cerevisiae cell cycle: localization of the CDC3 gene product and the timing of events at the budding site. J Cell Biol *112*, 535-544.

Kim, Y. J., Francisco, L., Chen, G. C., Marcotte, E., and Chan, C. S. (1994). Control of cellular morphogenesis by the Ip12/Bem2 GTPase-activating protein: possible role of protein phosphorylation. J Cell Biol *127*, 1381-1394.

Kohno, H., Tanaka, K., Mino, A., Umikawa, M., Imamura, H., Fujiwara, T., Fujita, Y., Hotta, K., Qadota, H., Watanabe, T., *et al.* (1996). Bni1p implicated in cytoskeletal control is a putative target of Rho1p small GTP binding protein in Saccharomyces cerevisiae. Embo J *15*, 6060-6068.

Kozma, R., Ahmed, S., Best, A., and Lim, L. (1995). The Ras-related protein Cdc42Hs and bradykinin promote formation of peripheral actin microspikes and filopodia in Swiss 3T3 fibroblasts. Mol Cell Biol *15*, 1942-1952.

Lamson, R. E., Winters, M. J., and Pryciak, P. M. (2002). Cdc42 regulation of kinase activity and signaling by the yeast p21-activated kinase Ste20. Mol Cell Biol *22*, 2939-2951.

Lechler, T., Shevchenko, A., and Li, R. (2000). Direct involvement of yeast type I myosins in Cdc42-dependent actin polymerization. J Cell Biol *148*, 363-373.

Lee, J., Colwill, K., Aneliunas, V., Tennyson, C., Moore, L., Ho, Y., and Andrews, B. (1998). Interaction of yeast Rvs167 and Pho85 cyclin-dependent kinase complexes may link the cell cycle to the actin cytoskeleton. Curr Biol *8*, 1310-1321.

Lee, K. S., Hines, L. K., and Levin, D. E. (1993). A pair of functionally redundant yeast genes (PPZ1 and PPZ2) encoding type 1-related protein phosphatases function within the PKC1-mediated pathway. Mol Cell Biol *13*, 5843-5853.

Lee, P. R., Song, S., Ro, H. S., Park, C. J., Lippincott, J., Li, R., Pringle, J. R., De Virgilio, C., Longtine, M. S., and Lee, K. S. (2002). Bni5p, a septin-interacting protein, is required for normal septin function and cytokinesis in Saccharomyces cerevisiae. Mol Cell Biol *22*, 6906-6920.

Lenburg, M. E., and O'Shea, E. K. (2001). Genetic evidence for a morphogenetic function of the Saccharomyces cerevisiae Pho85 cyclin-dependent kinase. Genetics *157*, 39-51.

Levin, D. E., Bowers, B., Chen, C. Y., Kamada, Y., and Watanabe, M. (1994). Dissecting the protein kinase C/MAP kinase signalling pathway of Saccharomyces cerevisiae. Cell Mol Biol Res *40*, 229-239.

Lew, D. J., and Reed, S. I. (1993). Morphogenesis in the yeast cell cycle: regulation by Cdc28 and cyclins. J Cell Biol *120*, 1305-1320.

Li, B., and Warner, J. R. (1996). Mutation of the Rab6 homologue of Saccharomyces cerevisiae, YPT6, inhibits both early Golgi function and ribosome biosynthesis. J Biol Chem *271*, 16813-16819.

Li, R. (1997). Bee1, a yeast protein with homology to Wiscott-Aldrich syndrome protein, is critical for the assembly of cortical actin cytoskeleton. J Cell Biol *136*, 649-658.

Li, R., Zheng, Y., and Drubin, D. G. (1995). Regulation of cortical actin cytoskeleton assembly during polarized cell growth in budding yeast. J Cell Biol *128*, 599-615.

Lila, T., and Drubin, D. G. (1997). Evidence for physical and functional interactions among two Saccharomyces cerevisiae SH3 domain proteins, an adenylyl cyclase-associated protein and the actin cytoskeleton. Mol Biol Cell *8*, 367-385.

Lippincott, J., and Li, R. (1998a). Dual function of Cyk2, a cdc15/PSTPIP family protein, in regulating actomyosin ring dynamics and septin distribution. J Cell Biol *143*, 1947-1960.

Lippincott, J., and Li, R. (1998b). Sequential assembly of myosin II, an IQGAP-like protein, and filamentous actin to a ring structure involved in budding yeast cytokinesis. J Cell Biol *140*, 355-366.

Lippincott, J., Shannon, K. B., Shou, W., Deshaies, R. J., and Li, R. (2001). The Tem1 small GTPase controls actomyosin and septin dynamics during cytokinesis. J Cell Sci *114*, 1379-1386.

Lombardi, R., and Riezman, H. (2001). Rvs161p and Rvs167p, the two yeast amphiphysin homologs, function together in vivo. J Biol Chem *276*, 6016-6022.

Longtine, M. S., and Bi, E. (2003). Regulation of septin organization and function in yeast. Trends Cell Biol *13*, 403-409.

Longtine, M. S., Fares, H., and Pringle, J. R. (1998a). Role of the yeast Gin4p protein kinase in septin assembly and the relationship between septin assembly and septin function. J Cell Biol *143*, 719-736.

Longtine, M. S., McKenzie III, A., DeMarini, D. J., Shah, N. G., Wach, A., Brachat, A., Philippsen, P., and Pringle, J. R. (1998b). Additional modules for versatile and economical PCR-based gene deletion and modification in *Saccharomyces cerevisiae*. Yeast *14*, 953-961.

Macara, I. G. (2004). Parsing the polarity code. Nat Rev Mol Cell Biol *5*, 220-231.

Madaule, P., Axel, R., and Myers, A. M. (1987). Characterization of two members of the rho gene family from the yeast Saccharomyces cerevisiae. Proc Natl Acad Sci U S A *84*, 779-783.

Madden, K., and Snyder, M. (1998). Cell polarity and morphogenesis in budding yeast. Annu Rev Microbiol *52*, 687-744.

Madhani, H. D., and Fink, G. R. (1998). The control of filamentous differentiation and virulence in fungi. Trends Cell Biol *8*, 348-353.

Madhani, H. D., Galitski, T., Lander, E. S., and Fink, G. R. (1999). Effectors of a developmental mitogen-activated protein kinase cascade revealed by expression signatures of signaling mutants. Proc Natl Acad Sci U S A *96*, 12530-12535.

Marston, A. L., Chen, T., Yang, M. C., Belhumeur, P., and Chant, J. (2001). A localized GTPase exchange factor, Bud5, determines the orientation of division axes in yeast. Curr Biol *11*, 803-807.

Martin, H., Mendoza, A., Rodriguez-Pachon, J. M., Molina, M., and Nombela, C. (1997). Characterization of SKM1, a Saccharomyces cerevisiae gene encoding a novel Ste20/PAK-like protein kinase. Mol Microbiol *23*, 431-444.

Matsui, Y., and Toh, E. A. (1992). Yeast RHO3 and RHO4 ras superfamily genes are necessary for bud growth, and their defect is suppressed by a high dose of bud formation genes CDC42 and BEM1. Mol Cell Biol *12*, 5690-5699.

Matsui, Y., and Toh-e, A. (1992). Isolation and characterization of two novel ras superfamily genes in Saccharomyces cerevisiae. Gene *114*, 43-49.

Mazzoni, C., Zarov, P., Rambourg, A., and Mann, C. (1993). The SLT2 (MPK1) MAP kinase homolog is involved in polarized cell growth in Saccharomyces cerevisiae. J Cell Biol *123*, 1821-1833.

Measday, V., Moore, L., Ogas, J., Tyers, M., and Andrews, B. (1994). The PCL2 (ORFD)-PHO85 cyclin-dependent kinase complex: a cell cycle regulator in yeast. Science *266*, 1391-1395.

Measday, V., Moore, L., Retnakaran, R., Lee, J., Donoviel, M., Neiman, A. M., and Andrews, B. (1997). A family of cyclin-like proteins that interact with the Pho85 cyclin-dependent kinase. Mol Cell Biol *17*, 1212-1223.

Moffat, J., and Andrews, B. (2003). Ac'septin' a signal: kinase regulation by septins. Dev Cell *5*, 528-530.

Moffat, J., and Andrews, B. (2004). Late-G1 cyclin-CDK activity is essential for control of cell morphogenesis in budding yeast. Nat Cell Biol *6*, 59-66.

Moseley, J. B., Sagot, I., Manning, A. L., Xu, Y., Eck, M. J., Pellman, D., and Goode, B. L. (2004). A conserved mechanism for Bni1- and mDia1-induced actin assembly and dual regulation of Bni1 by Bud6 and profilin. Mol Biol Cell *15*, 896-907.

Mulholland, J., Preuss, D., Moon, A., Wong, A., Drubin, D., and Botstein, D. (1994). Ultrastructure of the yeast actin cytoskeleton and its association with the plasma membrane. J Cell Biol *125*, 381-391.

Mullen, J. R., Kaliraman, V., Ibrahim, S. S., and Brill, S. J. (2001). Requirement for three novel protein complexes in the absence of the Sgs1 DNA helicase in Saccharomyces cerevisiae. Genetics *157*, 103-118.

Muller, O., Johnson, D. I., and Mayer, A. (2001). Cdc42p functions at the docking stage of yeast vacuole membrane fusion. Embo J *20*, 5657-5665.

Munn, A. L., Stevenson, B. J., Geli, M. I., and Riezman, H. (1995). end5, end6, and end7: mutations that cause actin delocalization and block the internalization step of endocytosis in Saccharomyces cerevisiae. Mol Biol Cell *6*, 1721-1742.

Muñoz, I., Simón, E., Casals, N., Clotet, J., and Ariño, J. (2003). Identification of multicopy suppressors of cell cycle arrest at the G1-S transition in *Saccharomyces cerevisiae*. Yeast *20*, 157-169.

Navarre, C., Degand, H., Bennett, K. L., Crawford, J. S., Mortz, E., and Boutry, M. (2002). Subproteomics: identification of plasma membrane proteins from the yeast Saccharomyces cerevisiae. Proteomics *2*, 1706-1714.

Nelson, W. J. (2003). Adaptation of core mechanisms to generate cell polarity. Nature *422*, 766-774.

Nishizawa, M., Kawasumi, M., Fujino, M., and Toh-e, A. (1998). Phosphorylation of sic1, a cyclin-dependent kinase (Cdk) inhibitor, by Cdk including Pho85 kinase is required for its prompt degradation. Mol Biol Cell *9*, 2393-2405.

Nobes, C. D., and Hall, A. (1995). Rho, rac, and cdc42 GTPases regulate the assembly of multimolecular focal complexes associated with actin stress fibers, lamellipodia, and filopodia. Cell *81*, 53-62.

Oda, Y., Huang, K., Cross, F. R., Cowburn, D., and Chait, B. T. (1999). Accurate quantitation of protein expression and site-specific phosphorylation. Proc Natl Acad Sci U S A *96*, 6591-6596.

Oehlen, B., and Cross, F. R. (1994). Signal transduction in the budding yeast Saccharomyces cerevisiae. Curr Opin Cell Biol *6*, 836-841.

Oehlen, L. J., and Cross, F. R. (1998). Potential regulation of Ste20 function by the Cln1-Cdc28 and Cln2-Cdc28 cyclin-dependent protein kinases. J Biol Chem *273*, 25089-25097.

Oh, C. S., Toke, D. A., Mandala, S., and Martin, C. E. (1997). ELO2 and ELO3, homologues of the Saccharomyces cerevisiae ELO1 gene, function in fatty acid elongation and are required for sphingolipid formation. J Biol Chem *272*, 17376-17384.

Ozaki, K., Tanaka, K., Imamura, H., Hihara, T., Kameyama, T., Nonaka, H., Hirano, H., Matsuura, Y., and Takai, Y. (1996). Rom1p and Rom2p are GDP/GTP exchange proteins (GEPs) for the Rho1p small GTP binding protein in Saccharomyces cerevisiae. Embo J *15*, 2196-2207.

Park, H.-O., Bi, E., Pringle, J. R., and Herskowitz, I. (1997). Two active states of the Ras-related Bud1/Rsr1 protein bind to different effectors to determine yeast cell polarity. Proc Natl Acad Sci USA *94*, 4463-4468.

Powers, J., and Barlowe, C. (2002). Erv14p directs a transmembrane secretory protein into COPII-coated transport vesicles. Mol Biol Cell *13*, 880-891.

Pringle, J. R., Preston, R. A., Adams, A., Stearns, T., Drubin, D., Haarer, B. K., and Jones, E. (1989). Fluorescence microscopy methods for yeast. Methods Cell Biol *31*, 357-435.

Pruyne, D., and Bretscher, A. (2000a). Polarization of cell growth in yeast. J Cell Sci *113 (Pt 4)*, 571-585.

Pruyne, D., and Bretscher, A. (2000b). Polarization of cell growth in yeast. I. Establishment and maintenance of polarity states. J Cell Sci *113 (Pt 3)*, 365-375.

Pruyne, D., Evangelista, M., Yang, C., Bi, E., Zigmond, S., Bretscher, A., and Boone, C. (2002). Role of formins in actin assembly: nucleation and barbed-end association. Science *297*, 612-615.

Pruyne, D. W., Schott, D. H., and Bretscher, A. (1998). Tropomyosin-containing actin cables direct the Myo2p-dependent polarized delivery of secretory vesicles in budding yeast. J Cell Biol *143*, 1931-1945.

Qadota, H., Python, C. P., Inoue, S. B., Arisawa, M., Anraku, Y., Zheng, Y., Watanabe, T., Levin, D. E., and Ohya, Y. (1996). Identification of yeast Rho1p GTPase as a regulatory subunit of 1,3-beta-glucan synthase. Science *272*, 279-281.

Raclavsky, V. (1998). Signalling towards cell wall synthesis in budding yeast. Acta Univ Palacki Olomuc Fac Med *141*, 7-16.

Rajavel, M., Philip, B., Buehrer, B. M., Errede, B., and Levin, D. E. (1999). Mid2 is a putative sensor for cell integrity signaling in Saccharomyces cerevisiae. Mol Cell Biol *19*, 3969-3976.

Ram, A. F. J., Wolters, A., Hoopen, R. T., and Klis, F. M. (1994). A new approach for isolating cell wall mutants in *Saccharomyces cerevisiae* by screening for hypersensitivity to Calcofluor White. Yeast *10*, 1019-1030.

Richardson, H. E., Wittenberg, C., Cross, F., and Reed, S. I. (1989). An essential G1 function for cyclin-like proteins in yeast. Cell *59*, 1127-1133.

Richman, T. J., Sawyer, M. M., and Johnson, D. I. (1999). The Cdc42p GTPase is involved in a G2/M morphogenetic checkpoint regulating the apical-isotropic switch and nuclear division in yeast. J Biol Chem *274*, 16861-16870.

Ridley, A. J., and Hall, A. (1992). The small GTP-binding protein rho regulates the assembly of focal adhesions and actin stress fibers in response to growth factors. Cell *70*, 389-399.

Ridley, A. J., Paterson, H. F., Johnston, C. L., Diekmann, D., and Hall, A. (1992). The small GTP-binding protein rac regulates growth factor-induced membrane ruffling. Cell *70*, 401-410.

Roberts, R. L., and Fink, G. R. (1994). Elements of a single MAP kinase cascade in Saccharomyces cerevisiae mediate two developmental programs in the same cell type: mating and invasive growth. Genes Dev *8*, 2974-2985.

Roemer, T., Madden, K., Chang, J., and Snyder, M. (1996). Selection of axial growth sites in yeast requires Axl2p, a novel plasma membrane glycoprotein. Genes Dev *10*, 777-793.

Rose, M. D., Winston, F., and Hieter, P. (1990). Methods in Yeast Genetics (Cold Spring Harbor, NY, Cold Spring Harbor Laboratory Press).

Sagot, I., Rodal, A. A., Moseley, J., Goode, B. L., and Pellman, D. (2002). An actin nucleation mechanism mediated by Bni1 and profilin. Nat Cell Biol *4*, 626-631.

Sambrook, J., Fritsch, E.F. & Maniatis, T. (1989). Molecular Cloning: A Laboratory Manual, 2nd Ed edn (Cold Spring Harbor, NY, Cold Spring Harbor Laboratory Press).

Sanders, S. L., and Herskowitz, I. (1996). The BUD4 protein of yeast, required for axial budding, is localized to the mother/BUD neck in a cell cycle-dependent manner. J Cell Biol *134*, 413-427.

Satterwhite, L. L., and Pollard, T. D. (1992). Cytokinesis. Curr Opin Cell Biol *4*, 43-52.

Schmidt, A., and Hall, M. N. (1998). Signaling to the actin cytoskeleton. Annu Rev Cell Dev Biol *14*, 305-338.

Schmidt, M., Bowers, B., Varma, A., Roh, D. H., and Cabib, E. (2002). In budding yeast, contraction of the actomyosin ring and formation of the primary septum at cytokinesis depend on each other. J Cell Sci *115*, 293-302.

Schmidt, M., Varma, A., Drgon, T., Bowers, B., and Cabib, E. (2003). Septins, under Cla4p regulation, and the chitin ring are required for neck integrity in budding yeast. Mol Biol Cell *14*, 2128-2141.

Seshan, A., Bardin, A. J., and Amon, A. (2002). Control of Lte1 localization by cell polarity determinants and Cdc14. Curr Biol *12*, 2098-2110.

Shapiro, L., McAdams, H. H., and Losick, R. (2002). Generating and exploiting polarity in bacteria. Science *298*, 1942-1946.

Shaw, J. A., Mol, P. C., Bowers, B., Silverman, S. J., Valdivieso, M. H., Duran, A., and Cabib, E. (1991). The function of chitin synthases 2 and 3 in the Saccharomyces cerevisiae cell cycle. J Cell Biol *114*, 111-123.

Sheu, Y. J., Santos, B., Fortin, N., Costigan, C., and Snyder, M. (1998). Spa2p interacts with cell polarity proteins and signaling components involved in yeast cell morphogenesis. Mol Cell Biol *18*, 4053-4069.

Shimizu, Y., Akashi, T., Okuda, A., Kikuchi, A., and Fukui, K. (2000). NBP1 (Nap1 binding protein 1), an essential gene for G2/M transition of Saccharomyces cerevisiae, encodes a protein of distinct sub-nuclear localization. Gene *246*, 395-404.

Simon, M. N., De Virgilio, C., Souza, B., Pringle, J. R., Abo, A., and Reed, S. I. (1995). Role for the Rho-family GTPase Cdc42 in yeast mating-pheromone signal pathway. Nature *376*, 702-705.

Singer-Kruger, B., and Ferro-Novick, S. (1997). Use of a synthetic lethal screen to identify yeast mutants impaired in endocytosis, vacuolar protein sorting and the organization of the cytoskeleton. Eur J Cell Biol *74*, 365-375.

Siniossoglou, S., Peak-Chew, S. Y., and Pelham, H. R. (2000). Ric1p and Rgp1p form a complex that catalyses nucleotide exchange on Ypt6p. Embo J *19*, 4885-4894.

Sivadon, P., Bauer, F., Aigle, M., and Crouzet, M. (1995). Actin cytoskeleton and budding pattern are altered in the yeast rvs161 mutant: the Rvs161 protein shares common domains with the brain protein amphiphysin. Mol Gen Genet *246*, 485-495.

Sivadon, P., Crouzet, M., and Aigle, M. (1997a). Functional assessment of the yeast Rvs161 and Rvs167 protein domains. FEBS Lett *417*, 21-27.

Sivadon, P., Peypouquet, M. F., Doignon, F., Aigle, M., and Crouzet, M. (1997b). Cloning of the multicopy suppressor gene SUR7: evidence for a functional relationship between the yeast actin-binding protein Rvs167 and a putative membranous protein. Yeast *13*, 747-761.

Smith, R. L., and Johnson, A. D. (2000). Turning genes off by Ssn6-Tup1: a conserved system of transcriptional repression in eukaryotes. Trends Biochem Sci *25*, 325-330.

Sohrmann, M., and Peter, M. (2003). Polarizing without a c(l)ue. Trends Cell Biol *13*, 526-533.

Sutton, A., Immanuel, D., and Arndt, K. T. (1991). The SIT4 protein phosphatase functions in late G1 for progression into S phase. Mol Cell Biol *11*, 2133-2148.

Takizawa, P. A., DeRisi, J. L., Wilhelm, J. E., and Vale, R. D. (2000). Plasma membrane compartmentalization in yeast by messenger RNA transport and a septin diffusion barrier. Science *290*, 341-344.

Tong, A. H., Drees, B., Nardelli, G., Bader, G. D., Brannetti, B., Castagnoli, L., Evangelista, M., Ferracuti, S., Nelson, B., Paoluzi, S., *et al.* (2002). A combined experimental and computational strategy to define protein interaction networks for peptide recognition modules. Science *295*, 321-324.

Tong, A. H., Evangelista, M., Parsons, A. B., Xu, H., Bader, G. D., Page, N., Robinson, M., Raghibizadeh, S., Hogue, C. W., Bussey, H., *et al.* (2001). Systematic genetic analysis with ordered arrays of yeast deletion mutants. Science *294*, 2364-2368.

Tong, A. H., Lesage, G., Bader, G. D., Ding, H., Xu, H., Xin, X., Young, J., Berriz, G. F., Brost, R. L., Chang, M., *et al.* (2004). Global mapping of the yeast genetic interaction network. Science *303*, 808-813.

Trilla, J. A., Cos, T., Duran, A., and Roncero, C. (1997). Characterization of CHS4 (CAL2), a gene of Saccharomyces cerevisiae involved in chitin biosynthesis and allelic to SKT5 and CSD4. Yeast *13*, 795-807.

Tsukada, M., Will, E., and Gallwitz, D. (1999). Structural and functional analysis of a novel coiled-coil protein involved in Ypt6 GTPase-regulated protein transport in yeast. Mol Biol Cell *10*, 63-75.

Uetz, P., Giot, L., Cagney, G., Mansfield, T. A., Judson, R. S., Knight, J. R., Lockshon, D., Narayan, V., Srinivasan, M., Pochart, P., *et al.* (2000). A comprehensive analysis of protein-protein interactions in *Saccharomyces cerevisiae*. Nature *403*, 623-627.

Vallen, E. A., Caviston, J., and Bi, E. (2000). Roles of Hof1p, Bni1p, Bnr1p, and Myo1p in cytokinesis in *Saccharomyces cerevisiae*. Mol Biol Cell *11*, 593-611.

Valtz, N., and Herskowitz, I. (1996). Pea2 protein of yeast is localized to sites of polarized growth and is required for efficient mating and bipolar budding. J Cell Biol *135*, 725-739.

Velichutina, I., Connerly, P. L., Arendt, C. S., Li, X., and Hochstrasser, M. (2004). Plasticity in eucaryotic 20S proteasome ring assembly revealed by a subunit deletion in yeast. Embo J *23*, 500-510.

Verna, J., Lodder, A., Lee, K., Vagts, A., and Ballester, R. (1997). A family of genes required for maintenance of cell wall integrity and for the stress response in Saccharomyces cerevisiae. Proc Natl Acad Sci U S A *94*, 13804-13809.

Versele, M., and Thorner, J. (2004). Septin collar formation in budding yeast requires GTP binding and direct phosphorylation by the PAK, Cla4. J Cell Biol *164*, 701-715.

Vojtek, A. B., and Cooper, J. A. (1995). Rho family members: activators of MAP kinase cascades. Cell *82*, 527-529.

Wang, T., and Bretscher, A. (1997). Mutations synthetically lethal with tpm1delta lie in genes involved in morphogenesis. Genetics *147*, 1595-1607.

Watanabe, Y., Takaesu, G., Hagiwara, M., Irie, K., and Matsumoto, K. (1997). Characterization of a serum response factor-like protein in Saccharomyces cerevisiae, Rlm1, which has transcriptional activity regulated by the Mpk1 (Slt2) mitogen-activated protein kinase pathway. Mol Cell Biol *17*, 2615-2623.

Wedlich-Soldner, R., Altschuler, S., Wu, L., and Li, R. (2003). Spontaneous cell polarization through actomyosin-based delivery of the Cdc42 GTPase. Science *299*, 1231-1235.

Wodarz, A. (2002). Establishing cell polarity in development. Nat Cell Biol *4*, E39-44.

Wu, C., Lytvyn, V., Thomas, D. Y., and Leberer, E. (1997). The phosphorylation site for Ste20p-like protein kinases is essential for the function of myosin-I in yeast. J Biol Chem *272*, 30623-30626.

Yamochi, W., Tanaka, K., Nonaka, H., Maeda, A., Musha, T., and Takai, Y. (1994). Growth site localization of Rho1 small GTP-binding protein and its involvement in bud formation in Saccharomyces cerevisiae. J Cell Biol *125*, 1077-1093.

Young, M. E., Karpova, T. S., Brugger, B., Moschenross, D. M., Wang, G. K., Schneiter, R., Wieland, F. T., and Cooper, J. A. (2002). The Sur7p family defines novel cortical domains in Saccharomyces cerevisiae, affects sphingolipid metabolism, and is involved in sporulation. Mol Cell Biol *22*, 927-934.

Zahner, J. E., Harkins, H. A., and Pringle, J. R. (1996). Genetic analysis of the bipolar pattern of bud site selection in the yeast Saccharomyces cerevisiae. Mol Cell Biol *16*, 1857-1870.

Zhang, X., Bi, E., Novick, P., Du, L., Kozminski, K. G., Lipschutz, J. H., and Guo, W. (2001). Cdc42 interacts with the exocyst and regulates polarized secretion. J Biol Chem *276*, 46745-46750.

Zheng, Y., Bender, A., and Cerione, R. A. (1995). Interactions among proteins involved in bud-site selection and bud-site assembly in Saccharomyces cerevisiae. J Biol Chem *270*, 626-630.

Ziman, M., O'Brien, J. M., Ouellette, L. A., Church, W. R., and Johnson, D. I. (1991). Mutational analysis of CDC42Sc, a Saccharomyces cerevisiae gene that encodes a putative GTP-binding protein involved in the control of cell polarity. Mol Cell Biol *11*, 3537-3544.

Ziman, M., Preuss, D., Mulholland, J., O'Brien, J. M., Botstein, D., and Johnson, D. I. (1993). Subcellular localization of Cdc42p, a Saccharomyces cerevisiae GTP-binding protein involved in the control of cell polarity. Mol Biol Cell *4*, 1307-1316.

VITA

Meghal Kanaiyalal Gandhi was born in Mumbai, India on June 1, 1971, the daughter of Mradula Gandhi and Kanaiyalal Gandhi. She received her Bachelor of Science degree in Food and Nutrition from University of Mumbai, Mumbai in 1991, followed by a Master of Science degree in Food and Nutrition from the same university in 1993. Thereafter, she worked as a lecturer at the University of Mumbai, Mumbai until August 1996, when she entered the Graduate school of the University of Texas at Austin.

Permanent address: 3/521-B, Narayan Villa, R. P. Masani Road, Matunga, Mumbai-400 019.

This dissertation was typed by the author.